1-1-2017

Development of Phenotypic Drug Discovery Models for Tropical Parasitic Diseases

Surendra Kumar Jain
University of Mississippi

DEVELOPMENT OF PHENOTYPIC DRUG DISCOVERY MODELS FOR TROPICAL PARASITIC DISEASES

A dissertation
presented in partial fulfillment of the requirements
for the degree of Doctor of Philosophy
in Pharmaceutical Sciences
in the Department of Biomolecular Sciences
Division of Pharmacology
School of Pharmacy
The University of Mississippi

by

SURENDRA K. JAIN

December 2017

ABSTRACT

Malaria and visceral leishmaniasis are major killer parasitic diseases. These diseases though occur primarily in tropical countries; economic burden and overall health impacts of malaria and leishmaniasis are global. The emergence of drug-resistant and more-virulent strains of the pathogens has further amplified the problems. New drug discovery approaches primarily rely on *in vitro* and *in vivo* models of the disease. The pathogens causing leishmaniasis and malaria are intracellular. Leishmania parasite grows as amastigotes in macrophages cells, and malaria parasite grows within the hepatocytes or erythrocytes. The intracellular forms of the pathogens are responsible for the pathophysiology of the diseases. New phenotypic cell-based models have been developed for leishmaniasis and malaria, those have been employed for *in vitro/in vivo* screening for new drug discovery.

A parasite-rescue and transformation assay was developed for macrophage-internalized *Leishmania donovani* amastigotes. The assay has been applied for high-throughput screening of a library of plants' fractions. Two fluorescent transgenic cell lines of *L. donovani* were developed with mCherry and Citrine reporter genes by stable transfection approach. The transgenic cell lines have shown stable and constitutive expression of the fluorescent reporter proteins. The *in vitro* screening methods were developed with the transgenic leishmania cells employing flow-cytometric and fluorescent microscopy analyses.

Analysis of parasitemia and intra-erythrocytic growth of the parasite are hallmarks of

malaria research. A flow-cytometric assay, based on staining of the malaria parasites with LDS-751, a fluorescent cell-permeant nucleic acid stain, was developed for parasitemia analysis. Staining of malaria-infected RBCs may be performed directly without additional processing. Selective staining of malaria-infected erythrocytes by LDS-751 was confirmed with fluorescent microscopy. The method has been applied for flow-cytometric analysis of parasitemia in mice blood infected with *Plasmodium berghei* and human blood infected with *P. falciparum*. The utility of this developed method was established for both *in vitro* and *in vivo* antimalarial drug screenings.

Establishment of the new phenotypic assay will expedite the process of new drug discovery against the tropical parasitic diseases. These assays would also have utility for understanding biology, virulence, and pathogenesis of malaria and leishmania pathogens.

DEDICATION

This work is dedicated to my wife, daughter, siblings, and parents. Without their continuous support, encouragement, and inspiration I would not have accomplished, what I accomplished today.

ACKNOWLEDGMENTS

Acknowledgement is a pleasant segment. It gives me the delight to express my gratitude towards people who have helped me fare through the expedition of my Ph.D. Program. At the outset, I wish to express my deepest gratitude and sincere thanks to Dr. Babu Tekwani, Research Professor of Pharmacology and Principal Scientist, National Center for Natural Products Research (NCNPR), School of Pharmacy, University of Mississippi for accepting me as a student and providing me the opportunity to work under his guidance. His kind attention, care & continuous encouragement have been a source of inspiration throughout the project. His constant support and patience in guiding me throughout the work helped me to complete the project.

I want to express my profound and sincere gratitude and thank my dissertation and original research proposal committee members, Dr. Kristie Willett, Dr. Ziaeddin Shariat-Madar, Dr. Samir A. Ross, Dr. Ameeta Agarwal, Dr. Christopher R. McCurdy and Dr. Deborah Gochfeld for their suggestion, guidance and their valuable time. I am thankful to Dr. Larry Walker and Dr. Ikhlas Khan, Directors of the NCNPR, for providing me necessary research facilities and resources.

I thank Dr. Rafael balaña fouce and Dr. Rosa Reguera (Department of Biomedical Sciences, Universidad de León, León, Spain) for providing the plasmid constructs and their valuable support and suggestion during the development of the transgenic parasite. I also thank Dr. Kip Guy (St. Jude Children's Research Hospital, Department of Chemical Biology and Therapeutics) and his team for development of natural products fractions library and Dr. Melisa

Jacob for her effort to provide me the fractions library. I thank Dr. Ilias Mohammad and Dr. Xing Cong Li for further analysis of the active plant fractions. I thank Dr. Shabana Khan and Mr. John Trott for helping with *Plasmodium falciparum* culture.

I am thankful to Dr. Narayan D Chaurasiya and Dr. Jagrati Jain for helping me in some experiments of this work. I am thankful to Ms. Jennifer Michael and Ms. Sherrie Gussow for their administrative support. I would like to thank the University Library and the Science Library for their extensive collections, as without them my research would have been a tough task.

I am thankful to the graduate students, faculty, and staff of the School of Pharmacy. The constant support, encouragement, and love that I got from them have made my stay at the School of Pharmacy a memorable one. I would always cherish the time spent with my fellow graduate students and thank them for all the help and support.

Lastly, I would like to thank my parents, sibling, wife, and daughter whose constant source of inspiration stood behind me to give every kind of support and help.

LIST OF ABBREVIATIONS

BCECF-Am	29,79bis-(2-carboxyethyl)-5-(and-6)carboxyfluorescein, acetoxymethyl ester
MTT	3-(4,5-dimethylthiazol-2-yl)-2,5-diphenyltetrazolium bromide
APAD	3-acetylpyridine NAD
ACD	Acid citrate dextrose
AMQ	Amodiaquine
ART	Artemisinin
AHTS	Automated High Throughput Systems
BSD	Blasticidin S
BMM	Bone marrow-derived macrophages
CQ	Chloroquine
CTN	Citrine
Citrine-Ld	Citrine transgenic *Leishmania donovani*
CTN-HYG	Citrine-Hygromycin
CL	Cutaneous leishmaniasis
DIC	Differential interference contrast
DIA	Digital image analysis
DIAM	Digital images analysis method
DMSO	Dimethyl sulfoxide
DPBS	Dulbecco's phosphate-buffered saline

ESI-MS	Electrospray Ionization Mass Spectrometer
EGFP	Enhanced green fluorescent protein
ELISA	Enzyme-linked immunosorbent assay
ELSD	Evaporative Light Scanning Detector
FBS	Fetal bovine serum
FCA	Flow cytometric analysis
FITC	Fluorescein isothiocyanate
FACS	Fluorescence-activated cell sorter
FSC	Forward Scatter
GFP	Green fluorescent protein
HBSS	Hank’s balanced salt solution
HSC	Hematopoietic stem cells
HTS	High throughput screening
HYG	Hygromycin
IACA	Image Analysis and Direct-Counting Assay
IM	Image Mining
IVIS	In Vivo Imaging System
iPFP	Infrared fluorescent proteins
IACUC	Institutional Animal Care and Use Committee
IVM	Intravital microscopy imaging

kDa	Kilo Dalton
kDNA	Kinetoplast DNA
LDH	Lactate dehydrogenase
LDS-751	Laser dye styryl–751
LEM	Leishmania
LEXSY	Leishmania expression system
LPG	lipophosphoglycan
mN	Macrophage nucleus
CHR	mCherry
mCherry-Ld	mCherry transgenic *L. donovani*
CHR-BSD	mCherry-Blasticidin
MMV	Medicines for Malaria Venture
MOBOT	Missouri Botanical Garden
NTD	Neglected tropical diseases
NBT	Nitroblue tetrazolium
NHP	Non-human primate
NOD	Non-obese diabetic
ONP	o-nitrophenol
ONPG	o-nitrophenyl-β-D-galactopyranoside
ORFs	Open reading frames

pN	Parasite nucleus
PRT	Parasite rescue and transformation
PBMC	Peripheral blood monocyte cells
PEC	Peritoneal exudate cells
PMA	Phorbol 12-myristate 13-acetate
PBS	Phosphate buffered saline
PDA	PhotoDiode Array
PKH2-GL	PKH2 Green Fluorescent General cell linker
pf HRP-II	*Plasmodium falciparum* histidine-rich protein-II
PCR	Polymerase chain reaction
PI	Propidium iodide
RDTs	Rapid diagnostic tests
RBCs	Red blood cells
RFP	Red fluorescent protein
RFU	Relative fluorescence units
rDNA	Ribosomal DNA
rRNA	Ribosomal RNA
SCID	Severe combined immunodeficiency
SSC	Side Scatter
SDS	Sodium dodecyl sulfate

TXR	Texas-Red
UPLC	Ultra-performance liquid chromatography
VL	Visceral leishmaniasis
WBCs	White blood cells
WT-Ld	Wild-type *L. donovani*
WHO	World health organization

TABLE OF CONTENT

LIST OF TABLES

LIST OF FIGURES

FIGURE PAGE

CHAPTER I

CURRENT DRUG DISCOVERY MODELS FOR VISCERAL LEISHMANIASIS AND MALARIA

1.1. INTRODUCTION

Tropical diseases refer to the diseases, which are more prevalent in tropical regions of the world. These include mostly infectious diseases such as leishmaniasis, malaria, Chagas disease, African trypanosomiasis, schistosomiasis, onchocerciasis, filariasis, and dengue, that epidemic in the hot and humid environment of tropical areas

Malaria, leishmaniasis, Chagas disease and African trypanosomiasis are caused due to the infections with protozoan parasitic pathogens. These protozoan parasitic diseases are responsible for high mortality and morbidity, globally affecting more than 500 million people (WHO, 2016). Protozoan parasites namely, *Plasmodium spp*., *Leishmania spp*. and *Trypanosoma spp.*, are more prevalent in tropical and subtropical countries, causing heavy loss of lives and reduced working abilities (Dupouy-Camet, 2004). Despite heavy burden to humanity due to the diseases caused by the parasitic protozoa, very few antiparasitic drugs have been developed in the last few years (Simon, 2016). The Recent involvement of some nonprofit and public-private partnership organizations for the development of strategies to treat and control malaria and other neglected diseases, namely leishmaniasis, sleeping sickness and Chagas' disease, has generated the unprecedented interest of several laboratories and pharmaceutical companies in new, antiparasitic drug discovery programs (Tekwani and Walker, 2006). Neglected tropical diseases (NTDs), are a

group of 17 diseases including leishmaniasis, sleeping sickness and Chagas' disease that are found primarily among the poorest people in 149 countries and territories. According to recent World Health Organization (WHO) estimates, more than 2 billion people are at risk of contracting an NTD, of whom more than 1 billion people are afflicted with one or more. Roughly 534,000 people are believed to be killed by an NTD annually. If we include the annual deaths because of malaria (438,000), that makes the total deaths 1 million because of NTD and malaria (WHO, 2016). Vaccines are still not available for malaria and other neglected diseases, namely leishmaniasis, sleeping sickness and Chagas' disease. So cure of these diseases mainly depends on drug treatments.

Visceral leishmaniasis (VL) and malaria are the primary focus of the work reported in this dissertation. There are only a few drugs available for the treatment of malaria and leishmaniasis. Most of them are toxic and going out of the market because of resistance development. Toxicity and emerging resistance against current antileishmanial and antimalarial drugs necessitate the discovery of new drugs and drug leads. Drug discovery approaches for both the diseases are based on the availability of *in vitro* and *in vivo* screening models that help in selections of novel pharmacophores from natural products and synthetic compounds libraries. As both leishmania and malaria parasite exist in the intracellular forms in the human host, it is significantly challenging to analyze the growth of the intracellular parasites (Fidock et al., 2004; Sereno et al., 2007). Maintaining *in vitro* cultures for intracellular forms of these parasites are complex. The host and parasite cells have to be maintained together, and growth of parasite inside the host cells may be analyzed by different techniques. Currently available technologies have severe limitations and are labor intensive. Simpler technologies, which yield reproducible results, are desperately needed. Current status of available *in vitro* and *in vivo* screening models for visceral leishmaniasis and

malaria is presented here.

1.2. VISCERAL LEISHMANIASIS

Leishmania donovani, a protozoan parasite, is the causative agent of visceral leishmaniasis (VL). VL is fatal if left untreated. It is highly endemic in the Indian subcontinent and East Africa. An estimated 200,000 to 400,000 new cases of VL occur worldwide each year. Over 90% of new cases occur in 6 countries: Bangladesh, Brazil, Ethiopia, India, South Sudan and Sudan (WHO Expert Committee on the Control of the Leishmaniases. Meeting (2010 : Geneva) and World Health Organization., 2010).

1.2.1. TREATMENT OF VISCERAL LEISHMANIASES: LIMITATIONS AND PROBLEMS WITH CURRENT THERAPEUTIC OPTIONS

The choice of drugs available to treat leishmaniasis is already limited, and even these suffer from limited efficacy and significantly high toxicities at therapeutic doses **(Table 1.1)**. A few of the first line treatment drugs, namely Sodium stibogluconate, have already lost their utility due to increasing multiple drug resistance (Croft et al., 2006b). Use of the pentavalent antimony compounds sodium stibogluconate (SSG), and meglumine antimonite has remained the mainstay of treatment of VL (Tiuman et al., 2011). However, in several areas where leishmaniasis has developed refractoriness against antimonials, the treatment option has been shifted mainly to the use of amphotericin B (Croft et al., 1991). Both antimonials and amphotericin B have to be administered parenterally, are highly toxic, and require a long duration of treatment (Croft et al., 2006b). Lipid formulations of amphotericin B, however, have greatly reduced the toxicity of the drug, allowing administration of large doses and shortening the treatment period (Croft and

Olliaro, 2011). However, the high cost of treatment and the requirement for administration of the drug under supervised hospitalization have limited its use in endemic areas and for routine treatments (Croft and Olliaro, 2011). Recently, miltefosine, an alkyl phospholipid derivative, which was originally developed as an anticancer agent, has been approved as the first orally active drug for the treatment of visceral leishmaniasis in India. At a dose of approximately 2.5 mg/kg/day for 28 days, miltefosine is > 90% curative for visceral disease in India and cutaneous disease in Colombia (Dorlo et al., 2012). Miltefosine causes reversible gastrointestinal disturbances and renal toxicity. The teratogenic nature of this drug prevents its use in pregnant women and other young females not following contraceptive measures (Dorlo et al., 2012). The antileishmanial potential of paromomycin, an antibacterial/antiprotozoal aminoglycoside, was discovered as early as the 1960's. The drug remained neglected due to unavailability of suitable formulations and discontinuation of its production. Injectable paromomycin was equally effective to amphotericin B for the treatment of visceral leishmaniasis in India in phase III clinical trials (Sundar et al., 2007). The antifungal azole compounds are promising antileishmanial agents. However, the results of the treatment of VL with antifungal azole drugs have been highly variable. Pentamidine isethionate, an aromatic diamidine was previously used as a second line treatment for leishmaniasis as a parenteral drug, but in later trials, pentamidine failed to produce a satisfactory cure (Croft and Olliaro, 2011). Use of pentamidine for treatment of visceral leishmaniasis has been discontinued, due to limited efficacy and other toxicity concerns with this drug (Tiuman et al., 2011). Thus the armamentarium of drugs for the treatment of VL is severely limited and underscores the need for discovery of new antileishmanial drugs with proven clinical efficacy and broader utility for oral treatment of VL. The major clinical drugs with their mode of action, their primary source, available toxicity and the important remarks are given in **Table 1.1**. The structures are given in **Figure 1.1**.

Table 1.1: The drugs presently used for treatment of visceral leishmaniasis. *Adapted from (Croft and Olliaro, 2011).

Drug Name	**Mode of Action**	**Primary Therapeutic Use**	**Toxicity**	**Remarks**
Sodium Stibogluconate	Multiple Pathways	Leishmaniasis	Pancreatitis, Cardiac toxicity	Drug resistance
Amphotericin B	Ergosterol pathway	Antifungal	Severe Kidney damage	Severe Toxicity, Liposomal Formulations
Pentamidine	Multiple Pathways	Pneumonia (PCP)	Insulin- Dependent diabetes mellitus.	Drug resistance
Miltefosine	Lipid metabolism, Apoptotic effect	Anticancer	Teratogenicity	Drug resistance High Cost
Paromomycin		Antibiotic		Drug resistance
Azole	Ergosterol pathway	Antifungal	Cardiac problems	Suboptimal efficacy

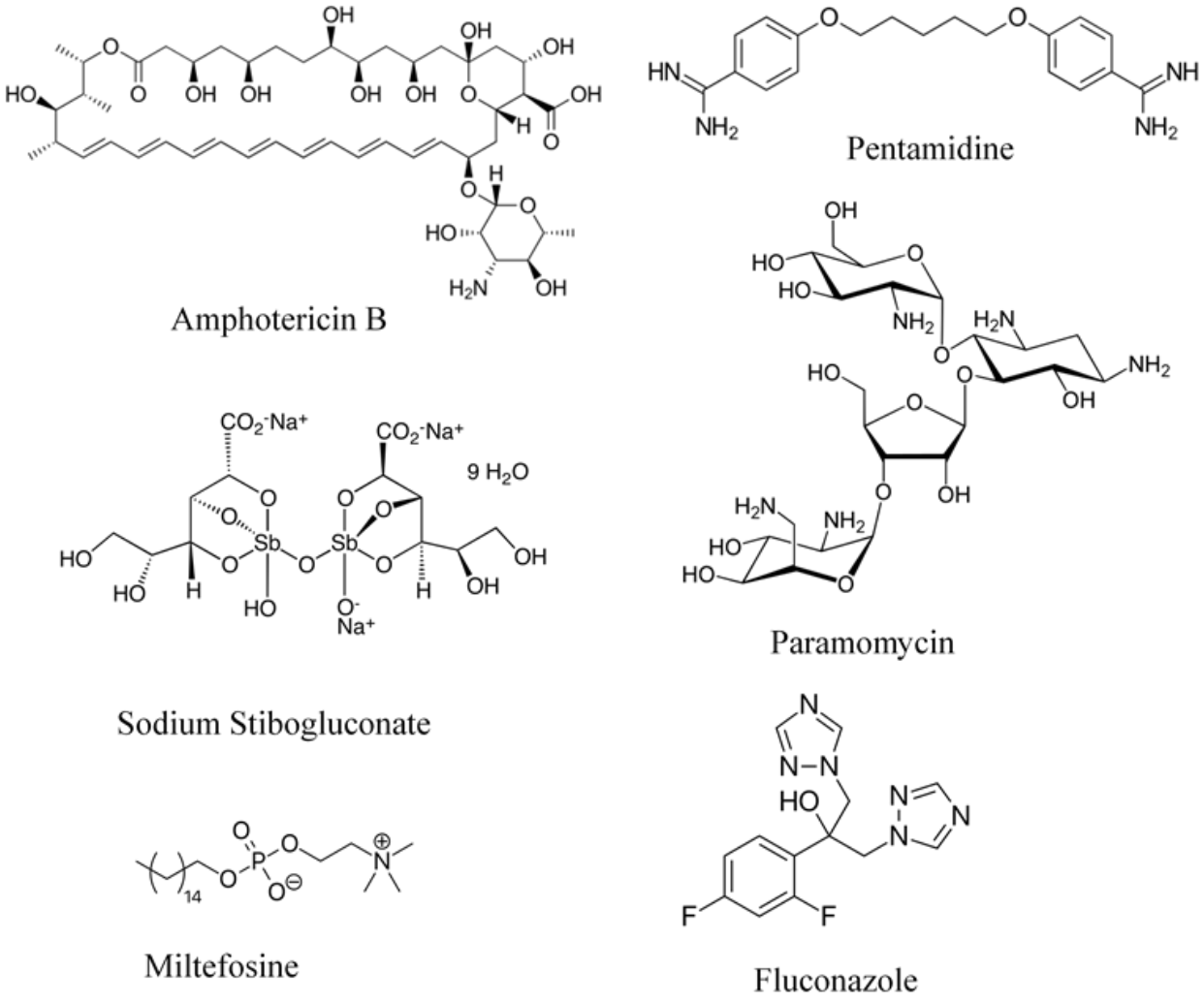

Figure 1.1: The chemical structures of clinical available antileishmanial drugs.

1.2.2. ANTILEISHMANIAL DRUGS CURRENTLY UNDER CLINICAL DEVELOPMENT FOR VISCERAL LEISHMANIASIS.

1.2.2.1. NITROIMIDAZOLES

1.2.2.1.a. FEXINIDAZOLE

Fexinidazole is believed to act as a prodrug that requires enzyme-mediated reduction by nitroreductases to generate cytotoxic species that cause DNA, lipid and protein damage (Raether and Hanel, 2003). As the genomes of leishmania parasites contain a homologous nitroreductase gene, a study to assess the leishmanicidal activity and preclinical profile of fexinidazole was done. In vivo sensitivity of *L. donovani* to the drug was excellent with five single daily doses of 200 mg/ kg in BALB/c mice suppressing infection by 98.4%.Lower doses of the drug were also effective in treating the murine model of infection, with the ED50 and ED90 estimated at 12 and 57 mg/ kg, respectively (Wyllie et al., 2012). Overexpression of the leishmanial homolog of this nitroreductase in *L. donovani* increased sensitivity to fexinidazole sulfone by 19-fold indicating that nitroreductase played a crucial role in activation of fexinidazole and its metabolites in *L. donovani* (Wyllie et al., 2012). Phase 1study of fexinidazole in healthy male volunteers has been completed (ClinicalTrial, 2012, 2014). A phase II proof of concept trial to determine the efficacy of fexinidazole at the daily dose of 1800 mg (3 tablets) once a day for four days continued by 1200mg (2 tablets) once a day for six days in VL patients in Sudan is recruiting patients (ClinicalTrial, 2013).

1.2.2.1.b. Pretomanid (PA-824)

Pretomanid (PA-824) is a bicyclic nitroimidazole-like molecule. (S)-PA- 824 showed

antileishmanial activity against both developmental stages of the parasite, with EC50 of 0.9± 0.1 and 4.9± 0.3μM against promastigotes and intracellular amastigotes, respectively (Patterson et al., 2013). The efficacy of both (R)- and (S)-PA-824 was assessed in a mouse model of VL. Dosing with (R)-PA-824 (99.9% suppression) at this concentration proved to be superior to treatment with sodium stibogluconate (41.9% suppression) and miltefosine (68.7% suppression) (Patterson et al., 2013). A phase 1 study was done in 58 healthy male volunteers using single oral doses (50, 250, 500, 750, 1,000, 1,250, or 1,500 mg) or multiple doses of 200, 600 and 1,000 mg of (S)- PA-824 each day for 7 days (Ginsberg et al., 2009). PA-824 was well tolerated following oral doses once daily for up to 7 days, and pharmacokinetic parameters were consistent with a once-a-day regimen.

1.2.2.2. QUINOLINE DERIVATIVES

1.2.2.2.a. 8-AMINOQUINOLINES

Sitamaquine (WR- 6026) is an 8-aminoquinoline analog discovered by the Walter Reed Army Institute of Research (WRAIR, USA) being developed as an oral treatment for VL. Sitamaquine was shown to be 708 times more active than meglumine antimoniate (Glucantime®) against *L. donovani* in hamsters (Kinnamon et al., 1978). The first phase 2 study was done in Kenya in 16 patients at a dose of 0.75-1.00mg/kg for 2-4 weeks with 50% cure rate for 28-day treatment with 1mg/kg (Sherwood et al., 1994). Final cure in Brazilian patients (primary efficacy outcome) was achieved in 92 of 106 (87%) overall and 25 of 31 (81%), 24 of 27 (89%), 23 of 23 (100%), and 20 of 25 (80%) patients at doses of 1.5, 1.75, 2.0, or 2.5 mg/ kg/day sitamaquine, respectively (Jha et al., 2005). Recent data suggest that sitamaquine accumulate in Leishmania parasites (Lopez-Martin et al., 2008). However, its molecular targets remain unknown yet. The short elimination half-life of sitamaquine is preventing a rapid resistance emergence(Loiseau et

al., 2011). The selection of a sitamaquine-resistant clone of *L. donovani* in the laboratory and the phase II clinical trials pointing out some adverse effects such as methemoglobinemia and nephrotoxicity are considered for a further development decision (Jha et al., 2005).

1.3. *IN VITRO* PHENOTYPIC MODELS FOR ANTILEISHMANIAL SCREENING

Phenotypic parasite culture-based *in vitro* screening and *in vivo* preclinical evaluation are the hallmarks of new antileishmanial drug discovery (Gupta and Nishi, 2011; Reguera et al., 2014; Sereno et al., 2007). Different methods have been reported for phenotypic cell-based screening assays for leishmania. These assays differ regarding the type of parasite forms employed, the complexity of the experimental protocol and the methods used for evaluation of growth and proliferation of the parasite cells in culture. *L. donovani* cycles between phagolysosomes of mammalian macrophages and alimentary tract of sand flies (Herwaldt, 1999). During its life-cycle, the parasite exists in two forms. 'Amastigotes' found in the mammalian host and 'Promastigotes,' which grow in the sandfly host, which is also the vector for transmission of leishmaniasis. Amastigotes are ovoid, non-motile, intracellular stages; promastigotes are elongated, motile, extracellular stages. Promastigotes are injected into the skin of the mammalian host by the bite of the infected female sandfly. Promastigotes selectively invade macrophage cells and transform into the intracellular amastigotes. The parasite remains in amastigote form for the duration of the mammalian phase of the life cycle. Sandflies feed on an infected mammal host and ingest amastigotes during blood feeding. The amastigotes transform into promastigotes for the vector phase of the life cycle (**Figure 1.2**). The phenotypic screening assays employing promastigotes as well as amastigotes forms of the parasite have been described.

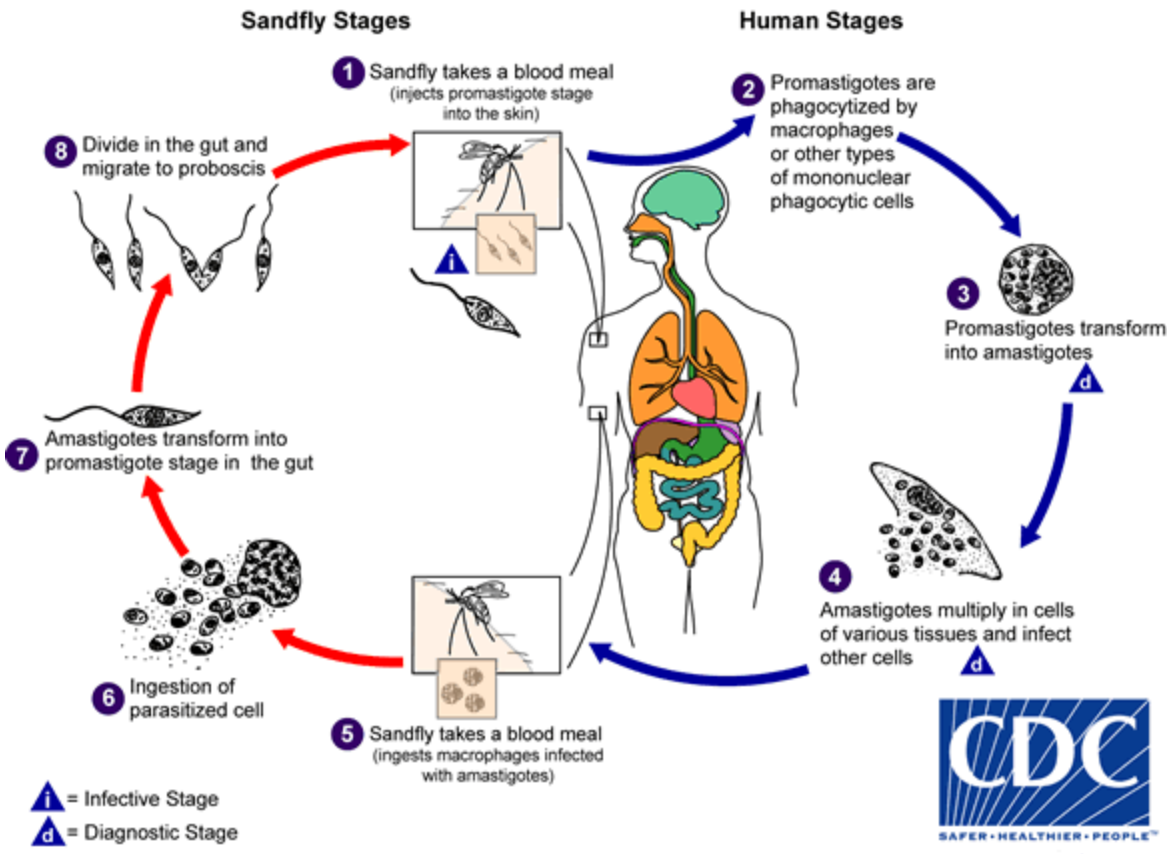

Figure 1.2: Life cycle of *Leishmania donovani* parasite. **(***Leishmania donovani* life cycle by Center for Disease Control and Prevention). 1- The sandflies inject the promastigotes during blood meals. 2- Promastigotes are phagocytized by macrophages cells. 3,4-Progmastigotes transform in these cells into the amastigotes., which multiply by simple division and proceed to infect other mononuclear phagocytic cells. 5,6- Sandflies become infected by ingesting infected cells during blood meals. 7,8- In sandflies, amastigotes transform into promastigotes, develop in the gut, and migrate to the proboscis.

Figure adapted from https://www.cdc.gov/parasites/leishmaniasis/biology.html

1.3.1. PROMASTIGOTES-BASED PHENOTYPIC SCREENING ASSAYS

The leishmania promastigotes grown in simple media have been used as the test parasite to screen potential antileishmanial agents. Simplicity and potential for automation of the promastigotes-based assay account for its wide popularity. The promastigotes are a culture in vitro in the medium at 21 to 27^{o}C. The promastigotes are treated in vitro with the test drugs and compounds for 48 to 72 h. The growth of prokaryotes is analyzed by different cell viability indicators, e.g., AlamarBlue, MTT (Dutta et al., 2005; Kulshrestha et al., 2013; Manda et al., 2014). The technique is simple and easily applicable for high-throughput screening (Gupta and Nishi, 2011). However, the metabolism and physiological conditions for culture and growth of promastigote differ from those of amastigote (host stage of the parasite). Because of these metabolic and physiological differences, screening data obtained from *in vitro* promastigote screening may not reflect activity against intracellular amastigotes (Sereno et al., 2007). Promastigotes grow at a lower temperature (21-27°C), while amastigotes in human host grow at 37^{o}C. Intracellular amastigotes grow within the macrophage phagolysosomes, the amastigotes face the acidic environment of phagolysosomal vacuoles, while promastigotes growth at neutral pH (Vermeersch et al., 2009). Due to these problems, use of promastigotes culture for in vitro antileishmanial screening has lesser value than the screening against intracellular amastigotes.

1.3.2. AXENIC AMASTIGOTES-BASED PHENOTYPIC SCREENING ASSAYS

Axenic amastigotes are the leishmania cells in amastigote forms adapted to grow in the medium *in vitro* by providing the optimum temperature of 30^{o}C and acidic 5.5 pH (Zakai et al., 1999). The in vitro screening with axenic amastigotes culture has several advantages. The test is directed against the amastigotes (host stage of the parasite). The axenic amastigotes are easy to

manipulate in *in vitro* culture. The growth analysis (Rahman et al., 2011) is of axenic amastigote can be performed with simple cellular growth indicators. Axenic amastigotes-based screening is simple and inexpensive. Axenic amastigotes system for drug screening has been used earlier (Callahan et al., 1997; Doyle et al., 1991). Several investigators used different methods for evaluating activity of compound against axenic amastigotes such as viability of cell population with a 3-(4-5 dimethyl-thiazol–2–yl)–2, diphenyl tetrazolium bromide, thiazole blue (MTT) based method (Ganguly et al., 2006; Sereno and Lemesre, 1997), determining ornithine decarboxylase activity or using a fluorescent dye like propidium iodide (PI) and fluorescence-activated-cell-sorter (FACS)(Sereno et al., 2005; Vergnes et al., 2005). Several Leishmania parasites expressing reporter genes have been selected, and the capacity of some of them to be used in axenic amastigote drug screening protocol has been assessed. Axenic *L. infant* amastigotes with Luciferase expressing DNA transformed and showed its utility in high throughput screening for new antileishmanial drugs (Sereno et al., 2001). A rapid fluorescent assay using AlamarBlue for screening drugs on axenic amastigotes of *L. donovani* and *L. tropica* was done recently (Shimony and Jaffe, 2008). However, the assay is semi – predictive, it neither test for penetration of the compound into the host cell nor for activity in the peculiar environment of the macrophage phagolysosome(Gupta and Nishi, 2011). Axenic amastigotes may have different metabolic processes than intracellular amastigotes. As this parasite grows in medium with 5.5 pH, there are chances that compounds may get precipitated at acidic pH. These assays do not have same pathophysiological environmental as in human host. So any compounds active here may not be active in human macrophage cells internalized amastigote form.

1.3.3. INTRACELLULAR AMASTIGOTES-BASED PHENOTYPIC SCREENING

ASSAYS

Amastigotes growing inside the phagolysosomal vacuoles of macrophage cells represent the pathophysiology of leishmaniasis disease (Handman, 1999). These intracellular amastigotes are the real target for the antileishmanial drug candidate. For the discovery of new antileishmanial drug candidate, there is a need for screening compounds libraries against intracellular growth and proliferation of the amastigotes in the host cells. The intracellular amastigotes-macrophage phenotypic assays also have application for evaluation of infectivity of clinical and laboratory isolates of leishmania cells. These assays offer significant challenges compared to the simple promastigotes/axenic amastigotes assays (a) regarding selection of appropriate host cells (b) individual variations in host cell populations (c) variable infectivity of pathogen-cells and susceptibility of the host-cells, (d) long-term maintenance of the host-parasite cell cultures and (e) quantitative/qualitative monitoring of intracellular growth of the parasites. Recent advancements in *vitro* cell culture methods, availability of a variety of primary and culture-derived host cells, high-throughput sensitive/quantitative cell-imaging technologies and development of transgenic parasite cells with stable constitutive expression of reporter genes have addressed these challenges.

1.3.3.1. THE HOST CELLS

Macrophages are the primary host target cells during the leishmaniasis disease condition in mammalian hosts. Assay for intracellular amastigotes requires host macrophages cells, which can be infected with the leishmania cells and development growth and proliferation of intracellular amastigotes (Handman, 1999). Primary macrophages cells can be obtained from various sources like peritoneal exudate cells (PEC), peripheral blood monocyte cells (PBMC), and bone marrow-derived macrophages (BMM)(Alexander et al., 1999; Maia et al., 2007). Mice are injected with

3.0 ml of 3% thioglycollate medium intraperitoneally to obtain PECs. After three days of injecting thioglycollate medium, the peritoneal exudates cells were harvested with 5ml of ice-cold phosphate buffer saline (PBS). PBMC are obtained by Ficoll-Hypaque fractionation of the heparinized blood, washed with Hank's balanced salt solution (HBSS-Sigma H6136) and re-suspended in warm RPMI-1640 medium. BMM is harvested from both femur and tibia of the individual mouse by washing with RPMI (Maia et al., 2007). These differentiated primary macrophages collected from various sources such as mice and rats are non-dividing in nature, but these cell preparations may not have homogeneous cell populations (Croft et al., 2006a). There are several human macrophage cells lines are available namely, THP1 (human monocytic leukemia cell line) (Sodji et al., 2014), U937 (pro-monocytic, human myeloid leukemia cell line)(Abdullah et al., 1999) and HL-60 (acute promyelocytic leukemia cell line)(Chen et al., 2009). There are several mice macrophage cell lines are available namely, J774 (Alexander et al., 1999) and RAW 264.7 cells (Kolodziej and Kiderlen, 2005). The cultured cells lines have a homogenous population of macrophages cells. However, the assays, which use dividing host cells, must ensure that the confounding effects of drug activity on both parasite and host cells number are considered. Out of different monocyte cell lines, differentiated THP1 cells forms a non-dividing monolayer, like primary cells and have complete characteristics of macrophage cells and offer an attractive alternative to primary isolated macrophages (Croft et al., 2006a; Jain et al., 2012).

1.3.3.2. THE PARASITE CELLS FOR INFECTION OF THE HOST CELLS

There are more than 30 species for the genus leishmania. However, for screening purpose *L. donovani* or *L. infant* used for visceral leishmaniasis and *L. major, L. tropica, L. mexicana, L. brazilensis* are used for cutaneous leishmaniasis (CL) drug screening (Gupta and Nishi, 2011).

Particularly for visceral leishmaniasis, *L. infantum* parasite has been used for promastigote screening as well as intracellular amastigote screening using macrophage cell line and other primary macrophages cells (Abamor, 2017; Maia et al., 2007). Several in vivo studies have been done using *L. infantum* in mice (Cajueiro et al., 2017), golden hamster host (de Almeida et al., 2017; Rouault et al., 2017) and dogs (Albuquerque et al., 2017). Similarly, *L. donovani* parasite has been used for promastigote screening as well as intracellular amastigote screening using macrophage cell lines and other primary macrophages cells (Abdullah et al., 1999; Manda et al., 2014). Several in vivo studies have been done using *L. donovani* in mice (Amit et al., 2017), golden hamster host (Rouault et al., 2017) and dogs (Jambulingam et al., 2017).

Metacyclic promastigotes **(Figure 1.3)** are the infective stage of the parasite. Parasite acquires the metacyclic stage at the stationary phase of *in vitro* culture. Metacyclic promastigotes are highly mobile, cylindrical and are highly infective to macrophages cells (Jain et al., 2012).

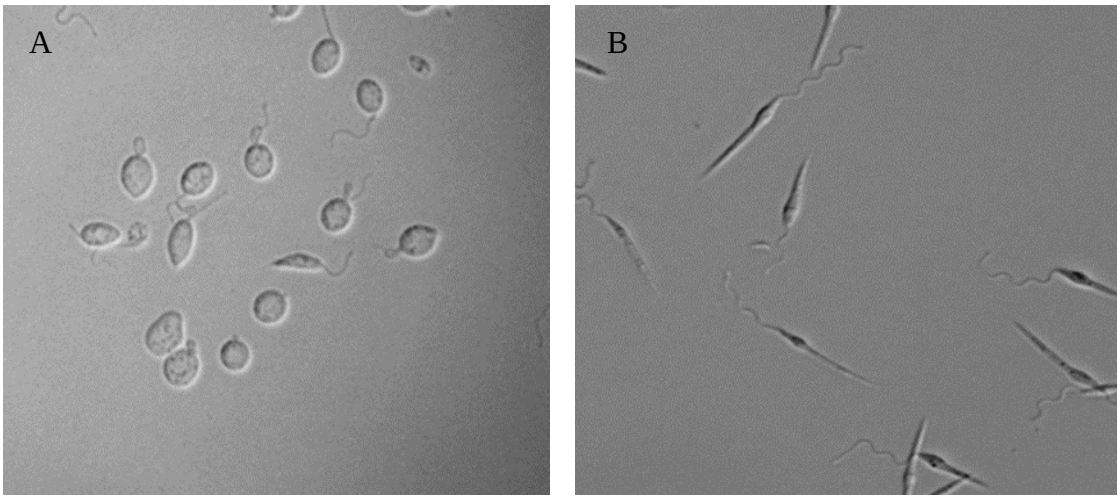

Figure 1.3: Procyclic and metacyclic forms of *Leishmania donovani* promastigotes. Image collected in phase contrast microscopy. (A) Procyclic promastigotes are short and ellipsoid with short flagellum and are only weakly motile (B) Metacyclic promastigotes are long cylindrical forms with a long flagellum, which are highly motile.

1.4. METHODS FOR INTRACELLULAR AMASTIGOTES GROWTH ANALYSIS

Intracellular amastigotes assays are complex assays that require both host cells (macrophages cells) and leishmania parasites cells. Several kinds of macrophages can be selected as host cells for screening purposes (Section 1.2.3.1.). Macrophages cells seeded in plates and incubated overnight at 37ºC 5%CO2 incubator. Some monocytic cell lines (THP1cells) require Phorbol Myristate Acetate (PMA) treatment to differentiate them into full macrophages cells (Jain et al., 2016a; Jain et al., 2012). Once the macrophages cells adhere to the plate surface, metacyclic leishmania promastigotes parasites are allowed to infect these macrophages cells. Different macrophages cells have specific infectivity for different leishmania parasites. There is a need for rigorous standardization of ratio of macrophage to parasite ratio (multiplicity of infection) to get an optimum infectivity(Jain et al., 2012). The infected macrophages cells are treated with test compounds for 48 h to 96 h. After test compounds treatment the growth of intracellular amastigotes is measured with one of the following methods.

1.4.1. MICROSCOPIC METHOD

This approach involves infection of the host macrophage cells with leishmania promastigotes or amastigotes. The infected macrophage cells are stained with nucleic acid stains (e.g., Giemsa, SYBR Green I). The infected macrophages are treated with the standard drugs and the test compounds. The anti-leishmanial activity of the test drugs/compounds is measured either by comparing the ratio of some amastigote nuclei to macrophages cell nuclei or by comparing percentages of infected cells (**Figure 1.4**). Classical microscopic evaluation based on manual direct cell and parasite counting is labor intensive. The absence of automation limits the utility of this assay. The classical microscopic methods have been modified to digital image-analysis

methods. In these methods, the images of nucleic acid stained infected macrophage cells are captured with a microscope and the counting of amastigote nuclei and macrophages cell nuclei done with the help of ImageJ software (Gupta and Nishi, 2011; Neal and Croft, 1984).

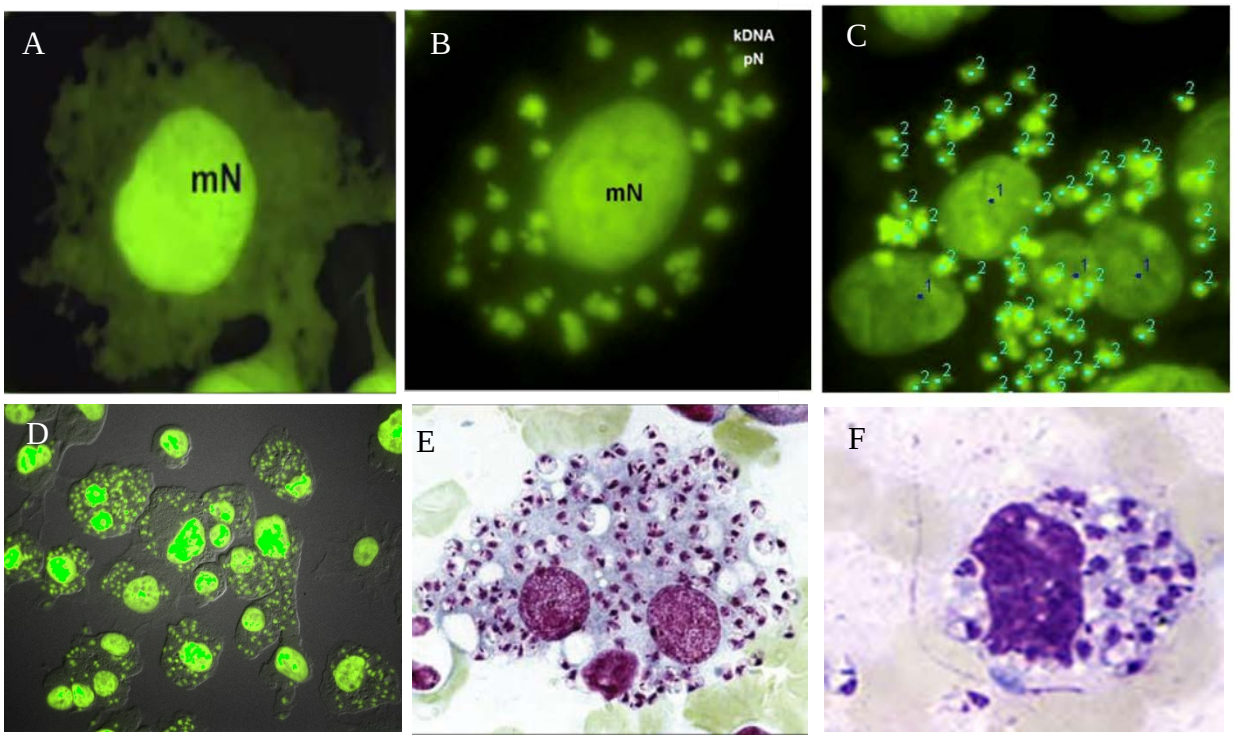

Figure 1.4: Infection of macrophage cells with *L. donovani* and their analysis with fluorescent microscopy. A- Uninfected differentiated THP1 cell; B- *L. donovani* amastigote infected THP1 cell; C-digital differential counting of amastigotes and THP1 cells with the help of ImageJ software; D to F- *L. donovani* amastigotes infected THP1 cells (big green nuclei with gray cell membrane). Images A to C are stained with SYBR Green I and image collected in Fluorescein isothiocyanate (FITC) filter of a fluorescent microscope. Image D is stained with SYBR Green I and image collected in differential interference contrast (DIC) with FITC filter of a fluorescent microscope. Image E (Imani et al., 2014) and F (https://www.cdc.gov/leishmaniasis/index.html) are stained with Giemsa and image collected in the light microscope. (mN- Macrophage nucleus; kDNA-Kinetoplast DNA; pN-Parasite nucleus).

1.4.2. IMAGE-BASED MICROSCOPIC HIGH CONTENT SCREENING

Microscopic imaging-based technologies represent powerful tools for the primary and secondary screening of drug compounds, as these methodologies have high throughput screening capability and also offer important information related to the infectious pathogen and the target host cell and organ. Therefore, the imaging-based high content screening methodologies have great potential for elaborating a more biology-driven environment for compound discovery *in vitro* as well as in vivo studies. A high content analysis for wild-type of *L. donovani* has been developed using Draq5 nuclear staining. This method involves rigorous analysis using Image Mining (IM) software and computing the Voronoi diagram (Siqueira-Neto et al., 2012). Another high content method was developed for *L. donovani* using Hoechst staining using intravital microscopy imaging (IVM) technique through confocal microscopy (Forestier et al., 2015).

1.4.3. FLOW CYTOMETRIC ASSAYS

The fluorescent dyes and monoclonal antibodies have also been employed for analysis of the leishmania infected macrophages by flow cytometry. BCECF-Am (29,79bis-(2-carboxyethyl)-5-(and-6)carboxyfluorescein, acetoxymethyl ester), SYTO 17, PKH2-GL (PKH2 Green Fluorescent General cell linker), propidium iodide, and acridine orange have tested for their capacity to monitor leishmania infection in a U-937 host cell model (Abdullah et al., 1999). This method could not be used to monitor infection for longer periods. The incubation of the infected macrophage cells with the test compounds/drugs ranges from two to four days, which makes this technique imperfect for the intracellular screening purposes (Sereno et al., 2007). Several Leishmania-specific monoclonal antibodies have been used with analysis of infected-macrophages by flow-cytometry. Specific monoclonal antibody against the leishmania lipophosphoglycan

(LPG) has been used for flow-cytometry based analysis (Di Giorgio et al., 2000; Guinet et al., 2000). These antibody-based assays allowed the accurate assessment of the activity of standard and test compounds against intracellular amastigote. However, the antibody-based immunostaining methods are time-consuming and are not cost effective for large screening. The antibody-immunostaining-based methods may have limited use for large-scale high-throughput screening programs. This approach may not differentiate between live and dead intracellular amastigotes (Di Giorgio et al., 2000; Sereno et al., 2007). The compounds with cytostatic actions against leishmania amastigotes may not show activity in these assays.

1.4.4. TRANSGENIC LEISHMANIA CELLS WITH REPORTER GENES

The externally inserted genes, which are expressed into the readily measurable phenotypic proteins that can be differentiated easily from the background of endogenous proteins are termed as reporter-genes. Introduction of such exogenous genes facilitate the measuring of the growth of the transgenic cells or microbes population and may be applied for the screening of antimicrobial agents. The transgenic cells carrying a reporter gene can be developed by either an episomal transfection of recombinant plasmids with the copy of reporter gene or after integration of reporter gene on a defined locus of the genome, generally the rDNA locus, of the target cells. There are several leishmania transgenic parasites were developed with different reporter genes including fluorescent protein reporter genes (green fluorescent protein (GFP), mCherry protein, Infra-red fluorescent) and catalytically enzymes reporter genes (β–galactosidase, β–lactamase, Luciferase)(Gupta and Nishi, 2011; Sereno et al., 2007). Fluorescent protein reporter genes have an advantage over catalytic reporter genes, as transgenic cells with fluorescent reporter gene do not require cofactors or substrates since the protein is intrinsically fluorescent.

1.4.4.1. GREEN FLUORESCENT PROTEIN (GFP)

GFP is a fluorescent protein, which originates from the *Aequorea victoria* (jellyfish). GFP based assays offer simplicity, time-dependent growth monitoring with low cost compared to classical non-reporter gene assays and enhanced biosafety in vivo animal models. Transgenic Leishmania spp cells with GFP have been developed by both episomal transfection or by stable transfection and applied for drug screening studies (Dube et al., 2009; Singh et al., 2009). The transgenic GFP leishmania cells do not express GFP fluorescence protein, which may not be sufficient for measurement with a spectrofluorometric reader. The GFP transgenic leishmania cells may not be suitable for application for the assays with fluorescence measurements. A multimeric form of GFP was engineered and expressed in Leishmania promastigotes to increase the intensity of the fluorescence in transgenic parasites (Chan et al., 2003). Stably transfected leishmania parasite was developed in which the GFP reporter gene was integrated downstream of the 18 S rRNA gene promoters within the genome of the parasite (Singh et al., 2009).

1.4.4.2. RED FLUORESCENT PROTEIN (RFP)

The GFP produces significant fluorescence and is extremely stable, but the excitation wavelength of the light required for GFP is close to the ultraviolet range. Exposure of leishmania cells to this light may damage the cells and affect their viability. In contrast, Red-fluorescence labeled parasites have excitation maxima in the safe region. Transgenic *L. major* Red Fluorescent Protein 1 (RFP)-expressing strain found helpful in identification of the site of sandfly bites has been identified in vivo in a mouse model (Peters et al., 2008; Ribeiro-Gomes et al., 2012). Transgenic *L. infantum* cells with expression of RFP have been employed to report the recruitment

of neutrophils and their role in non-ulcerative forms of leishmaniasis (Thalhofer et al., 2011). Recently, a transgenic leishmania parasite with an expression of mCherry (A modified form of RFP) has been developed and implemented for *in vitro* and *in vivo* screening (Calvo-Alvarez et al., 2012). A transgenic cell line of *L. amazonensis* was generated by chromosomal integration of the fluorescent DSRED2 molecule. A High Content Analysis assay was developed based on the use of homogeneous populations of primary mouse macrophages hosting transgenic fluorescent DSRED2 *L. amazonensis* amastigotes. This multi-parametric assay helped in monitors the parasitic load of fluorescent DSRED2 amastigotes-hosting macrophage cultures (Aulner et al., 2013).

1.4.4.3. INFRARED FLUORESCENT PROTEIN

The fluorescence with an emission spectrum in the visible region has low tissue penetration (Shcherbo et al., 2007). A new fluorescent protein with the emission spectrum of near infrared region has been discovered from the bacteriophytochrome of *Deinococcus radiodurans* (Chernov et al., 2017; Shcherbakova et al., 2015). The infrared fluorescent proteins (iRFPs) have advantages over the fluorescent reporter proteins with better tissue penetration capacity of the light emitted from the iRFPs. The emission spectrum of this protein is in the near infrared region, and the emitted fluorescence is free of any background interference derived from organs or tissues (Shu et al., 2009). The fluorescent iRFPs have been successfully applied to image the in vivo infection of the adenovirus serotype 5 in mouse liver (Calvo-Alvarez et al., 2015). More recently, a new infrared fluorescent protein (iRFP) from the photosynthetic bacterium *Rhodopseudomonas palustris* has been engineered with more penetration capacity (Ref). Recently, (Calvo-Alvarez et al., 2015) Have reported generation of two strains of *L. infantum* strains, which stably overexpress the IFP 1.4 and

iRFP reporter genes. The bio-photonic properties of the transgenic *L. infantum* cells were compared for promastigote and amastigote stages. The constructs for transfection were engineered with the regulatory sequences of genes (A2, AMASTIN, and HSP70 II), which are differentially expressed in the leishmania amastigotes, to improve the fluorescence emission of the selected reporter in intracellular amastigotes. The transgenic leishmania strain, which carries the iRFP gene under the control of the *L. infantum* HSP70 II downstream region (DSR), showed selective and high expression of iRFP in leishmania amastigotes. Application of this strain for phenotypic screening using *ex vivo* splenocytes from infrared-infected BALB/c mice was also reported (Calvo-Alvarez et al., 2015).

1.4.4.4. β-GALACTOSIDASE

The β-galactosidase is an enzyme that hydrolyzes the colorless substrate o-nitrophenyl-β-D-galactopyranoside (ONPG) to o-nitrophenol (ONP), which is yellow. Transgenic Leishmania promastigote expressing β-galactosidase were developed and utilized in drug screening procedures (Okuno et al., 2003). B-Galactosidase presents the advantage of colorimetric detection. However, some common drawbacks including its large size (the monomer is 116 kDa), expensive substrate and the endogenous expression of β-galactosidase by some mammalian cell types including macrophages, hinder the use of these transgenic parasites for general drug screening purpose, particularly for intracellular amastigote screening and in vivo screening(Buckner and Wilson, 2005; Campbell, 2004).

1.4.4.5. β–LACTAMASE

The β–lactamase is an enzyme that hydrolyzes the colorless substrate nitrocefin to a

chromogenic cephalosporin, a colored product. This product can be colorimetrically measured at 490 nm. The β–lactamase is a smaller sized protein than β–galactosidase. Two transgenic leishmania parasites cells lines, *L. major* and *L. amazonensis*, with the β-lactamase reporter gene, were developed (Campbell, 2004). The transgenic leishmania cells were developed through stable transfection, in which β-lactamase gene was integrated into ribosomal RNA (rRNA) region of the genome, thereby allowing for high-level of stable expression of the enzyme. The activity of some standard antileishmanial drugs was evaluated on the transgenic intracellular amastigotes, which demonstrate that this method could be used for phenotypic drug screening procedures (Zlokarnik et al., 1998).

1.4.4.6. LUCIFERASE

Luciferase is an enzyme found in fireflies that catalyze the conversion of luciferin to oxyluciferin, which produces luminescence. The luminescence is produced because the reaction product oxyluciferin remains in an electronically excited state. The reaction releases a photon of light as oxyluciferin goes back to the ground state. Various transgenic leishmania parasites (*L. donovani, L. infantum, L. major*) cell lines expressing luciferase have been developed (Ashutosh et al., 2005; Roy et al., 2000). The high sensitivity of the assay and the absence of background activity in the host cell are important advantages of the luciferase assays. Recently, a transgenic cell line of *L. amazonensis* expressing firefly luciferase has been used to monitor leishmania infection in real time, through imaging analysis. The advantage of this methodology relies on the capacity to perform experiments on live cells, making the analysis faster and more accurate since the viability of both the parasites within the host cells is monitored (Sereno et al., 2007).

1.4.4.7. TRANSGENIC LEISHMANIA CELL MODELS: ADVANTAGES AND DISADVANTAGES FOR PHENOTYPIC SCREENING

The transgenic leishmania cells lines with stable and constitutive expression of reporter proteins have provided valuable tools for phenotypic screening and new antileishmania drug discovery. These models have been extensively applied for large-scale high-throughput, and high-content screenings (Aulner et al., 2013; De Rycker et al., 2013) The intracellular transgenic parasite cells can be monitored by digital image analysis, by flow-cytometry or chemiluminescence reader, based on the nature of the reporter gene.

The construction of transgenic leishmania models requires the application of drug-resistance markers for selection of transgenic cells. The transgenic cells were grown with a contact pressure of the selection drug for maintenance of episomal expression of the reporter genes. If the reporter gene is expressed, episomally the relative expression of the reporter protein may depend on the number of copies of the transfected plasmid, rather than on the activity of the drug (Buckner and Wilson, 2005). In case of stable transfections and genetic integration, the use of selection-drug may not be necessary once the integration of reporter gene into the leishmania genome and stable expression of the reporter protein are confirmed. The assays based on transgenic parasites with luciferase reporter gene required substrate and cell lysis buffer, which makes the assays expensive for large-scale screening (Calvo-Alvarez et al., 2015; Roy et al., 2000). Growth analysis methods of intracellular amastigotes with their advantages and disadvantages are summarized in **Table 1.2**.

Table 1.2. Macrophage internalized leishmania amastigotes models for phenotypic screening: the approaches for evaluation of intracellular growth and proliferation of leishmania amastigotes

Type of Assay	**Method**	**Advantages**	**Disadvantages**
Classical microscopic evaluation	Nuclear staining of infected macrophage cells	Gold Standard Reliable	Labor intensive Time consuming Low Throughput Human Bias
Advanced Digital-Image analysis based assays	Analysis of digital images of the intracellular leishmania amastigotes [fluorescent probe staining/Immuno-staining/Transgenic leishmania cells]	Can be automated Multi-parametric High throughput Screening High-content analysis	Costly instrumentation Limited facility
Flow cytometric assays	Antibodies-based analysis	Specific, Less background signal	Sensitivity issues
Transgenic leishmania-Reporter gene assays	Transfections of reporter gene	Live imaging Live growth analysis	Require drug selection for episomal expression. Relative expression of the reporter gene may depend on the copy number of the transfected plasmid. Altered physiological properties of the parasite

1.5. IN VIVO ASSAYS FOR ANTILEISHMANIAL SCREENING

Animals with the similar pathological responses as observed in humans after infection of leishmania parasite could be selected for *in vivo* anti-leishmanial studies. In visceral leishmania parasites reside in deep organs like spleen or liver. So in animal models for visceral leishmaniasis, parasites must be able to invade in macrophages cells, transform there to amastigotes and must be able to reside in deep organs like spleen and liver. There are several animal models available for visceral leishmaniasis to research various aspects including host-parasite interactions, pathogenesis, biochemical changes, prophylaxis, and maintenance of parasites and evaluation of antileishmanial activity of drug leads. These *in vivo* experiments include the intravenous parasite inoculation, compounds dosing, preparation of impression smears of weighed livers, staining of slides and analyzing the parasitemia and other host-parasite interactions (Garg and Dube, 2006; Gupta and Nishi, 2011).

Although none of the animal models accurately reproduce what happens in humans during visceral leishmaniasis, there are several animal models developed with their advantages and disadvantages. Several animals like BALB/c mice, Syrian golden hamster, dogs, and monkeys (squirrel, vervet, and Indian languor) were developed as an experimental host for VL. Besides evaluating drug activity, a suitable animal host for leishmania parasite is very important for other studies including host-parasite interactions, immunological changes, pathogenesis, biochemical changes, and prophylaxis. Animal models help to evaluate the antileishmanial activity with other significant information like bioavailability, absorption, distribution, metabolism, excretion, and maximum tolerated dose that help in determining the route, treatment dose, duration of dosing, therapeutic window and the toxicity of new leishmanicidal lead. Ideally, a drug should have an invasive route of administration (administered orally), should be effective in a small dose with a

shorter course of action (around a week) and should not have any toxicity, even at higher doses.

1.5.1. RODENT MODELS

Rodents are the preferred choice for primary *in vivo* experiments, and several rodent models were adopted for antileishmanial drug screening. Rodents are comparatively smaller in size. So they are cheaper, require less maintenance and area, require less quantity of testing compound and are easy to handle during experiments. Common rodent models for visceral leishmaniasis include BALB/c mice and Syrian golden hamsters (Oliveira, 2004). These rodent models of leishmaniasis have been extensively used to evaluate the pharmacological effects of anti-leishmanial efficacy, toxicity profiling, host-pathogen interaction and pathogenesis of the disease. These are available as inbred strains that in help in generation reproducible results with less variation.

Mice are susceptible to different species of Leishmania parasite. Inbred strains of mice have been used widely for both *L. donovani* susceptible, resistant and intermediate strains (Barbosa Junior et al., 1987). The infection of Leishmania parasite in different mouse strain needs to be characterized to ensure that the test compounds are tested for their effect appropriately. Athymic (with $Foxn1^{nu}$ mutation) and SCID (with $Prkdc^{scid}$ mutation) mice provide a model for treatment of VL in immunosuppressed cases (Croft et al., 2006a).

1.5.1.1. MICE MODEL

The BALB/c mouse is a most common strain with reproducible levels of infection (Parasitemia) when the amastigote or metacyclic promastigote inoculum is administered intravenously. Initially, all BALB/c mice divided into groups with five mice in each group and

infected intravenously with *L. donovani* parasite. The test compounds are prepared in different doses and dosed to mice orally, intraperitoneally, or intravenously at day 7 of post-infection for five consecutive days (day 7 to day 11). All infected mice are sacrificed at day 14 of post-infection. Spleen and liver were collected from all mice and weighed. During the whole experiment, mice of all group are observed for change in weight and behavior. Impression smears are collected on slides from spleen and liver of each mice. Slides with smears are fixed with methanol and stained with Giemsa. The total number of leishmania amastigotes are counted in per 500 liver cells with the help of a microscope. The parasitemia of each treated mice liver smears is compared with liver smears of untreated mice (Gupta and Nishi, 2011).

1.5.1.2. RAT MODEL

Mastomys albicandatus (the African white-tailed rat) also investigated for in vivo maintenance (Mikhail and Mansour, 1973)and long-term experiments with *L. donovani* and *L. Brazilians*. *Sigmodon hispidus* (The cotton rat) is also a good susceptible animal host for *L. donovani* (De Lima et al., 2002). The Leishmania infection sustained in this host for 3-4 months after the appearance of initial clinical symptoms. *Mastomys natalensis* (Natal multi-mammate Rat) was also used to develop the experimental model for visceral leishmaniasis using *L. donovani* as a parasite (Nolan and Farrell, 1987). The experimental procedures for rat animal models are similar to mice models. Here the rat is able to sustain the parasite for longer duration then mice and is a better model for long-term studies (Gupta and Nishi, 2011).

1.5.1.3. HAMSTER MODEL

Mesocricetus auratus (The Syrian golden hamster) established a good model for VL and

which provides a synchronous infection in the liver and spleen that can develop into a chronic non-curable disease that is similar to human VL (Farrell, 1976; Gifawesen and Farrell, 1989). It reproduces the clinical and pathological features of human disease such as a progressive increase in visceral parasite burden, cachexia, massive splenomegaly, hyper-gammaglobulinemia, and ultimately death (Gifawesen and Farrell, 1989).

Most VL studies involve intravenous, intracardiac or intraperitoneal inoculations of rodents (Melby et al., 1998) with 10^6 to 10^8 parasites; however, VL has also been induced via intradermal inoculation, a route considered much closer to natural infection (Osorio et al., 2012). More recently, a new hamster model of progressive leishmaniasis was developed by natural transmission of the parasites via bites by vector sand flies (Aslan et al., 2013). Parasitemia is reported in tissues by monitoring parasites in spleen, liver and bone marrow by limiting dilution cultures or by imprinting smears with splenic biopsy (Melby et al., 2001).

Several methods have been developed using hamster as a model for VL. Classically, the pre-treatment parasitic burden was assessed by a splenic biopsy that helps to carry the similar parasitic load by the same experimental animal. This method comes with the disadvantages of its inability to assess the delayed action of drugs. Later this technique was modified for repeated spleen biopsies on the same animal at different intervals of day 7, 14, and 28, thus making it suitable for studying the long-acting and delayed action drug in the model(Gupta and Nishi, 2011). The advantage is that biopsy is possible to monitor pre- and post-treatment infection status and all antileishmanials are active against liver as well as spleen parasites. Golden hamster is the best experimental model to study VL, because it reproduces the clinical and pathogenesis of the disease, as seen in humans and dogs (Oliveira, 2004).

Recently level of infection was accessed by real-time imaging of golden hamster model

with the help of virulent transgenic *L. donovani* that stably express a reporter luciferase and compared with the real-time RT-PCR to quantify both Leishmania and host transcripts(Rouault et al., 2017).

1.5.1.4. REAL-TIME IMAGING OF A MURINE LEISHMANIASIS MODEL

Episomally transfected Leishmania parasite with enhanced green fluorescent protein, and stably transfected infrared fluorescent Leishmania parasite strains are enabling in vivo real-time fluorescence imaging to analyze the time-dependent progression of Leishmania infection in parasitized tissues. Level of fluorescence correlated with the number of Leishmania parasites in the tissue and that demonstrated the real-time efficacy of a test compound or vaccine. There are several advantages of this approach over the classical microscopic based approach. Here the change in the level of infection could be analyzed in real time manner without scarifying the animal. These include improvements in sensitivity and the ability to acquire real-time data on progression and spread of the infection.

1.5.2. DOG MODEL

Wild canines and dogs are the main reservoirs of zoonotic visceral leishmaniasis caused by *L. infantum* in the Mediterranean area, Middle-East, Asian countries and Latin America. The role of dogs as the main reservoir of visceral leishmaniasis has led to an increased interest in developing dogs and canine as an animal model for VL(Alvar et al., 2004). Canine visceral leishmaniasis is a multi-systemic disease with variable clinical signs. Dogs have been developed as an experimental model for Leishmania infections in the 1990s using *L. donovani, L. infantum* or *L. chagasi*. Dogs are important laboratories models because they reproduce the natural infection

similar to human infection(Ciaramella et al., 1997). German shepherd dogs are reported to give better results than beagles, but some workers claim highly successful infection rate with mixed breeds. The level of infection is accessed by spleen or liver biopsies (Baneth et al., 2008).

1.5.3. NON-HUMAN PRIMATE (NHP) MODEL

There are several observations in rodent models those are not relevant to human hosts due to several physiological and anatomical differences. However, non-human primates have similarities to humans in anatomy, immunology, and physiology. So they are valuable primate models for biomedical research. They are expensive laboratory animals that are difficult to obtain and to handle. Furthermore, the institutional animal committee also hinder the use of primates because of ethical reasons in biomedical research. So, only a few laboratories worldwide are working on primate model, especially for a neglected disease like visceral leishmaniasis. Availability of a non-human primate model for visceral leishmaniasis would facilitate the study of different aspects of this disease and would accelerate the development of vaccines and testing of new drug candidates.

Monkeys are normally used for the final preclinical studies for safety and efficacy of any new drug candidate or newly developed vaccines (Gupta and Nishi, 2011; Loria-Cervera and Andrade-Narvaez, 2014). Anti-leishmanial screening has been performed in owl and squirrel monkeys. Initially, the effort has been made to develop an infection in New and Old World monkeys and demonstrated that *Aotus trivirgatus* (owl monkeys) and *Saimiri sciureus* (squirrel monkey) developed an acute and fulminated, but short-lived, infection (Chapman and Hanson, 1981; Chapman et al., 1983). Attempts were also made to establish VL in *Presbytis entellus* (Gray langur) showed that this species was highly susceptible to single intravenous inoculation of

hamster-spleen-derived *L. donovani* amastigotes, which invariably produced consistent and progressive acute fatal infection, leading to death between 110 to 150 days post-infection. The infected animals presented all the immunopathological clinic features as observed in human VL. The Indian languor has also been used for preclinical evaluation of potential antileishmanial drugs and vaccine (Gupta and Nishi, 2011; Loria-Cervera and Andrade-Narvaez, 2014).

1.6. MALARIA

Malaria is another deadly parasitic disease and major global health challenge. An estimated 3.4 billion people continue to be at risk of malaria. According to a recent estimate by the World Health Organization (WHO), there had been 212 million cases of malaria globally in 2016, which caused 429 000 deaths (WHO, 2016). Malaria is caused by the protozoan parasites of *Plasmodium* genus. *P. falciparum* is a fatal species of malaria. Another species, *P. vivax* has a broad geographic distribution as it can grow at low temperature in female Anopheles mosquito vector, can persist at higher altitudes and in colder climates (Beck-Johnson et al., 2013). Additionally, *P. vivax* forms a dormant liver stage called hypnozoites, increases its survival, acts as a potential inventory of infection, activates months after primary infection when the conditions are optimum and cause relapse (Judith Recht, 2014). The first synthetic drug chloroquine (CQ) was discovered in the 1940s (Goldsmith, 1946). CQ helped in malaria treatment and eradicated throughout the world (Hoekenga, 1952). However, the therapeutic efficacy of CQ for malaria parasite was diminished due to the occurrence of CQ resistance (Da Silva and Lopes, 1964; Montgomery, 1964; Sandosham, 1963). Due to the lack of potent alternative drug for treatment of CQ-resistant malaria parasite, the number of deaths increased to 2–3-fold in the 1980s (Trape, 2001). Since then, several amino quinolones derivatives were developed, but the parasites developed the similar resistance

against most of the amino quinolones derivative. Several alternative drugs like sulfadoxine, pyrimethamine (SP) (Simpson et al., 1972) and artemisinin (Bruce-Chwatt, 1982) emerged later as the first-line of treatment for malaria. However, several cases of parasite resistance were reported for these new drugs also (Hurwitz et al., 1981; Meshnick, 1998). These conditions of emerging resistance alarm the further possibility of an increase in malaria fatalities (**Table 1.3**). There is an urgent need for better alternative treatment for malaria and necessitate the discovery of new drugs and drug leads.

Table 1.3. Available treatments for malaria. Adopted from (Antony and Parija, 2016)

Chemical class	**Name of drug**	**Mode of Action**	**Primary Therapeutic Use**	**Status of resistance**
4-Aminoquinolines	Chloroquine, Amodiaquine,	Accumulation in digestive vacuole of parasite	Treatment of Non severe falciparum	Yes
Amino alcohols	Mefloquine, Halofantrine, Lumefantrine	Accumulation in digestive vacuole of parasite	Multidrug resistance falciparum	Yes
8-Aminoquinolines	Primaquine	Not precisely known	Infection of vivax and ovale. Prevent relapse. Gametocytocidal agent	Yes
Naphthoquinone	Atovaquone	Target cytochrome bc1 complex		Yes
Artemisinin and derivative	Artesunate Artemether Artemisinin		Chloroquine resistance falciparum	Yes

1.6.1. LIFE CYCLE OF MALARIA PARASITE

When the female *Anopheles mosquito* bites a human host, it injects sporozoites into the bloodstream. These sporozoites travel through the bloodstream to the liver. In all plasmodium species these sporozoites are rapidly taken up by the liver cells, and there they get converted to schizont and eventually to merozoites. Merozoites attack to healthy red blood cells where the asexual reproduction occurs. In red blood cells (RBCs), merozoites reproduce and eventually rupture the cells and produce more merozoites which in turn going to infect other RBCs leading to massive destruction of RBCs. A small percentage of merozoites differentiate into gametocytes, which are taken up by the mosquito during another subsequent blood feeding. In mosquito, these gametocytes convert to sporozoites (**Figure 1.5**).

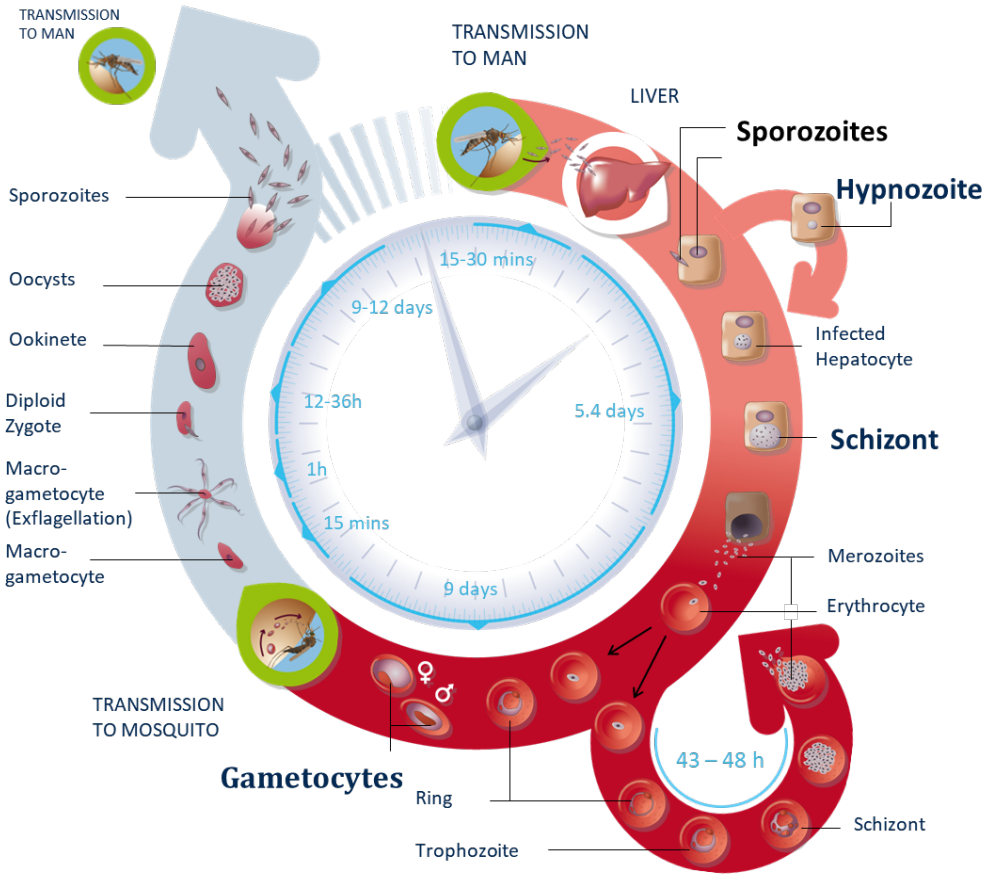

Figure 1.5: The life cycle of the malaria parasite. When the female Anopheles mosquito bites a human host, it injects sporozoites into the bloodstream. These sporozoites travel in the bloodstream to the liver. In all plasmodium species these sporozoites are rapidly taken up by the liver cells, and there they get converted to schizont and eventually to merozoites. Merozoites attack to healthy red blood cells where the asexual reproduction occurs. In RBCs, merozoites reproduce and eventually rupture the cells and producing more merozoites which in turn going to infect other RBCs leading to massive destruction of RBCs. A small percentage of merozoites differentiate into gametocytes, which are taken up by the mosquito during another subsequent blood feeding. In mosquito, these gametocytes convert to sporozoites. Figure collected from Medicine for Malaria Venture (MMV) (Delves et al., 2012).

There are many challenges in malaria control, particularly diagnosis and treatment of malaria. The majority of malaria cases worldwide rely on clinical diagnosis to define the type of treatment (Landier et al., 2016). Diagnosis of malaria is based on the confirmation of malaria parasites in RBCs of patients. New antimalarial drug discovery approaches rely on *in vitro* screening of compound libraries against malaria parasite culture and further activity assessment of lead compounds in vivo animal models. *In vitro* and *in vivo* antimalarial screening methods are based on malaria parasitemia analysis which is the ratio of infected RBCs to total RBCs.

1.6.2. METHODS FOR INTRAERYTHROCYTIC MALARIA PARASITE GROWTH ANALYSIS

1.6.2.1. MICROSCOPIC PARASITEMIA ANALYSIS

The microscopic parasitemia method with the help of Giemsa stain was developed in 1904 (Shute and Maryon, 1963). Since that time it remains as the official gold standard for malaria diagnosis (Makler et al., 1998). Although microscopy is the time consuming and laborious method, most of the clinical laboratories depend on microscopy for confirmation of malaria and species identification. Microscopy is the major method for malaria diagnosis in the clinical laboratories as well as malaria parasitemia analysis in antimalarial screenings (Makler et al., 1998). An infected mice blood smear slide stained with Geimsa is given in **Figure 1.6.** However, the microscopic analysis has some potentials problem in all clinical diagnosis as well as laboratory parasitemia analysis. Significant misdiagnosis of false positives (7–36%), false negatives (5–18%), and wrong identification (13–15%) have been reported in shortcomings in the diagnosis of malaria in the United Kingdom (Milne et al., 1994) and Thailand (Beadle et al., 1994; Fix et al., 1988). A high

frequency of technical errors (e.g., wrong pH in staining solution or a poor quality film) was also reported. Therefore, microscopy is an imperfect ‘Gold Standard’ diagnostic methodology (Collier and Longmore, 1983; Makler et al., 1998).

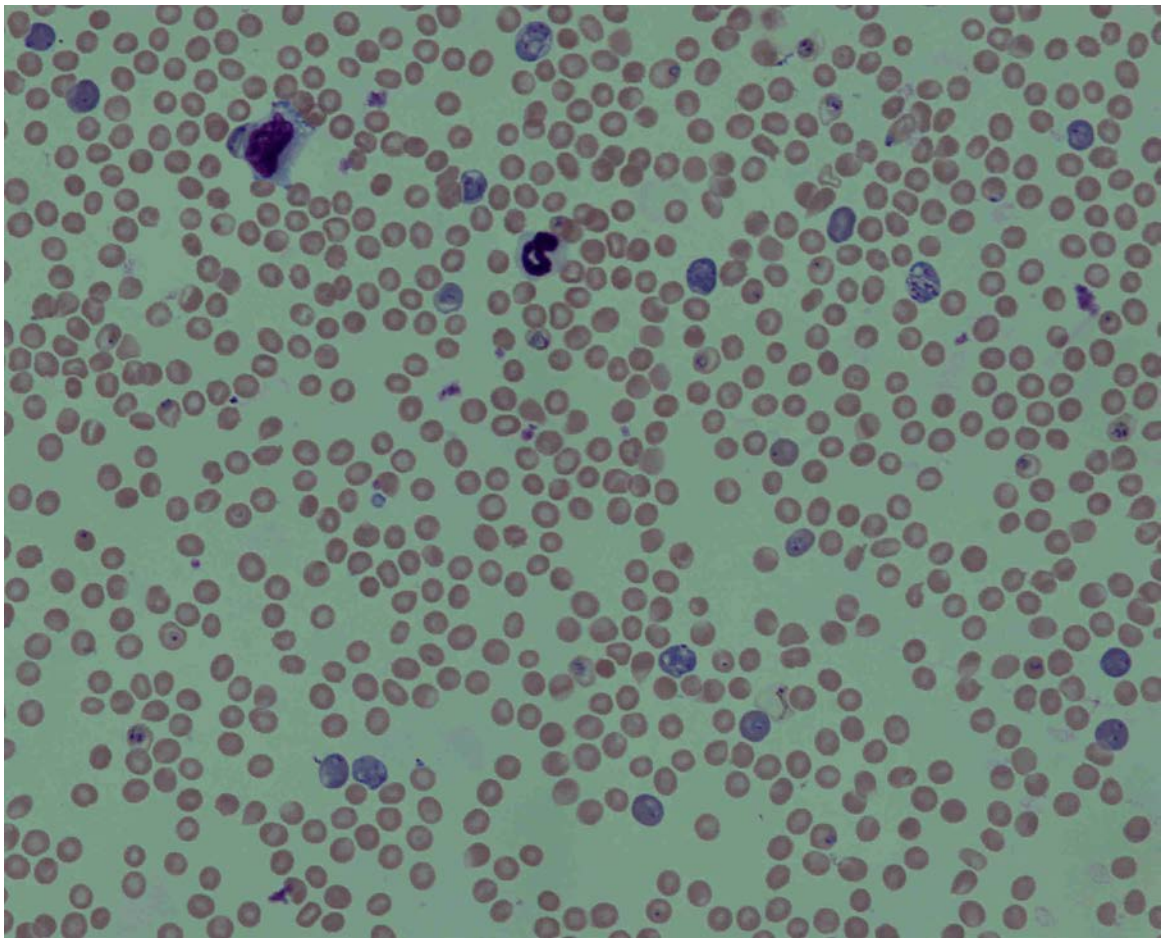

Figure 1.6: Blood smear slides prepared from *P. berghei* infected swiss webster albino mice. The slide is fixed with methanol and stained with Giemsa. The image has been collected by Nikon 90i eclipse light microscope. RBCs identified here as pink cells. The parasite nuclei as well as white blood cells (WBCs) nuclei identified as purple colored.

1.6.2.2. RADIOACTIVE SUBSTRATE INCORPORATION ASSAY

The malaria parasitemia analysis method based on incorporation of radioactive substrates, such as [3H] isoleucine, [3H] hypoxanthine, and [3H] ethanolamine to measure parasitic growth was developed as an alternative to laborious and time-consuming microscopic assays (Desjardins et al., 1979).

These assays are widely used, accurate, and reliable, and this method could be used for high throughput screening purposes. However, these assays are very expensive, involve multiple processing steps and require special handling and waste disposal procedures. Thus, these radioactive assays are functional in only a few labs with radioactive research facilities and not in the field of diagnosis. These assays are also not convenient for detection of parasite stage-specific effects. Here incorporation of H3 purine from radioactive hypoxanthine could be possible in other blood cells like WBC and lymphocyte, which leads to a higher background. Also, hypoxanthine uptake does not measure parasitemia directly, as its incorporation is dependent on DNA synthesis which only occurs in the later stages of the parasite life cycle (Yayon et al., 1983). So radioactive incorporation is directly proportional to further growth of the malaria parasite. Also, the DNA synthesis, in turn, is dependent on the growth rate of the parasite strain being observed.

1.6.2.3. *P. FALCIPARUM* LACTATE DEHYDROGENASE (Pf LDH)

There are some more methods developed for monitoring malaria growth based on the enzymatic activity of parasite's lactate dehydrogenase (pLDH) (Beadle et al., 1994). The lactate dehydrogenase enzyme of several Plasmodium species can use 3-acetylpyridine NAD (APAD) as a coenzyme in the reaction leading to the formation of pyruvate from lactate (Sherman 1961; Kaushal et al. 1993) and the measurement of this parasite lactate dehydrogenase (pLDH) has been

presented as an easy and rapid method for the diagnosis of malaria in humans (Makler & Hinrichs 1993; Makler et al. 1993). Here the malaria parasite interacts with Malstat reagent (0.21% v/v Triton -100, 222mM L-(+)-Lactic acid, 54.5mM Tris, 0.166mM 3-acetylpyridine adenine dinucleotide (APAD) The spectrophotometric assessment of LDH activity is facilitated by adding nitroblue tetrazolium (NBT), phenazine ethosulfate PES to the Malstat reagent. As APADH is formed, the NBT is reduced and forms a formazan product that is blue and can be detected visually and measured at 650 nm. This metabolic changes can be detected by a plate reader. So assays can be applied for high throughput screening. However, there is a low degree of concordance between LDH-based assay and standard microscopy-based determinations of parasitemia (Jelinek et al., 1996; Knobloch and Henk, 1995).

1.6.2.4. *P. FALCIPARUM* HISTIDINE-RICH PROTEIN-II (Pf HRP-II)

The enzyme-linked immunosorbent assay (ELISA)-based methods that use monoclonal antibodies to *Plasmodium falciparum* histidine-rich protein-II (pf HRP-II) have begun to be widely used in recent years due to their ease of use. PfHRP-II is found in the parasitophorous vacuole or the parasite cytoplasm, and the protein actively facilitates the polymerization of toxic heme, resulting from the degradation of host hemoglobin to form a non-toxic hemozoin (Sullivan et al., 1996). PfHRP-II has multiple repeats of AHHAAD, with AHH and AHHAA and the presence of repetitive B-cell epitopes; this enables the detection of the protein by multiple antibodies, increasing the sensitivity of methods detecting the protein (Wellems & Howard, 1986; Panton et al.,1989). PfHRP2-based rapid diagnostic tests (RDTs) are the most widely used of the RDTs and have been utilized in low- and high-density malaria zones in both pregnant women and non-pregnant individuals for the diagnosis of mild and paediatric severe malaria (Mueller et al., 2007;

Hopkins et al., 2007, 2008; Houze´ et al., 2009; Laurent et al., 2010; Abba et al., 2011; Hendriksen et al., 2011; Kattenberg et al., 2011, 2012b; Kyabayinze et al., 2011; Aguilar et al., 2012).

This assay has sensitive and specificity. However, PfHRP-II based assay is expensive. The PfHRP-II based rapid diagnostic tests are not useful for the prediction of parasite responses to treatments because of the persistence of the PfHRP-II antigen in the peripheral blood circulation after parasite clearance (Tjitra et al., 2001; Houze´ et al., 2009).

1.6.2.5. SYBR GREEN 1 ASSAY

SYBR Green I is a nucleic acid stain and has been used to monitor the presence of DNA in biochemical matrices. As the RBCs do not have DNA and intraerythrocytic stage of parasite development is the primary target of antimalarial drugs, assays based on SYBR green I am helpful for high-throughput screening for new antimalarial therapies. In the assay, SYBR green with RBC lysis buffer is used to expose the parasite DNA and bind with SYBR green I to generate the fluorescence. Here, the fluorescence correlated with the growth of intraerythrocytic malaria parasites. These assays could be applied for automation to develop high throughput screening systems. However, there assay come with high fluorescent background signals.

1.6.2.6. FLOW CYTOMETRIC ASSAYS

Several new methods of malaria diagnosis and parasitemia analysis have been developed based on flow cytometry. These methods can be applied to automation and high throughput parasitemia analysis, but no technique can yet be used for routine clinical diagnosis or automated screening. Most of the flow cytometric methods have taken advantage of the absence of DNA in uninfected RBCs and presence of parasite DNA in malaria-infected RBCs. This intraerythrocytic

malaria parasite could be detected by flow cytometry by staining with nucleic acid-binding fluorescent dyes. Different fluorescent dyes, such as Hoechst 33258(van Vianen et al., 1990), SYTO-9(Izumiyama et al., 2009), SYTO-61(Fu et al., 2010), Ethidium bromide(Staalsoe et al., 1999), Propidium iodide(Pattanapanyasat et al., 1997), Acridine orange(Hare, 1986), 4,6-diamidino-2-phenylindole (Baniecki et al., 2007), YOYO-1 (Campo et al., 2011; Xie et al., 2007), SYBR Green I (Izumiyama et al., 2009) recently have been considered for the determination of parasitemia *in vitro* cultures of *Plasmodium falciparum* by FCM. Some dyes such as YOYO-1(Xie et al., 2007), SYTO-16 (Jimenez-Diaz et al., 2009) and SYBR Green I (Somsak et al., 2012)have been recently employed for the determination of parasitemia in *in vivo* blood samples from *Plasmodium berghei* infected mice. The parasitemia analysis directly from human or mice blood samples is particularly difficult because blood samples have a mixed population of erythrocytes, neutrophils, leukocytes, monocytes, and reticulocytes. Because of this mixed population, all fluorescence detection methods for parasitemia have high backgrounds. Mixed cell populations of blood samples could be separated in Forwarding Scatter (FSC)/Side Scatter (SSC) dot plot. However, still, it is not possible to separate reticulocyte and erythrocyte populations in FSC/SSC dot plot(Terstappen and Levin, 1992; Wiczling and Krzyzanski, 2008). Reticulocytes remain a big problem in malaria parasitemia analysis in blood samples that come with high background and sometimes give a false signal of parasitemia. Reticulocytes have RNA. Thus the effect of reticulocytes could be neutralized by treatment of blood samples with RNase. If the fluorescent nucleic acid dye is not cell permeant, then permeabilization is required. So most of the methods based on flow cytometric analysis of parasitemia in blood samples have steps of cells fixation, permeabilization, RNase treatments, nucleic acid dye staining and complex flow cytometric analysis (Jimenez-Diaz et al., 2009; Xie et al., 2007). Each step added the chances of error and

loss of samples, which in also increases the duration of parasitemia analysis and required a higher volume of blood sample.

1.6.2.7. REPORTER GENE ASSAYS

1.6.2.7.a. GREEN FLUORESCENCE PROTEIN

Green fluorescent protein (GFP)-expressing *P. berghei* (NK65 stain and ANKA stain) have been produced and detected in the red blood cells, cultured liver cells, and midgut and salivary glands of the mosquito(Franke-Fayard et al., 2004; Frischknecht et al., 2004; Sanchez et al., 2004). Initially, *P. berghei* lines were constructed that expresses GFP under control of the regulatory sequences of the *P. berghei* dihydrofolate reductase-thymidylate synthase (*pbdhfr-ts*) gene (de Koning-Ward et al., 2000). However, these *P. berghei* lines have several disadvantages including the relatively low level of expression of GFP and the lack of expression in certain stages or the episomal nature of the introduced GFP (de Koning-Ward et al., 1998). The GFP gene is integrated into the genome in the c-ribosomal-RNA gene unit (c-rRNA), which is not essential for parasite development (van Spaendonk et al., 2001). This stably *P. berghei* GFP parasite showed similar growth characteristics as wild-type *P. berghei* and the use of this parasite is demonstrated as a reference line for visualization, investigation of parasite-host interactions and confirming phenotypes of mutant parasites in co-infection studies(Franke-Fayard et al., 2004; Sanchez et al., 2004). Previous studies using GFP-expressing malaria parasites revealed how malaria parasites moved in the skin and invaded blood vessels during their migration to the liver(Amino et al., 2006; Jin et al., 2007). However, the fluorescence emitted by GFP was not strong enough to observe these parasites from outside of the animal.

1.6.2.7.b. LUCIFERASE

To overcome the drawback of GFP parasite, researchers have developed transgenic parasites that express luciferase; transgenic *P. berghei* expressing luciferase was initially developed(Franke-Fayard et al., 2006; Ploemen et al., 2009), followed by transgenic *P. yoelii* expressing luciferase(Miller et al., 2013; Mwakingwe et al., 2009). Not only the blood stage, but also the liver stage in the development of malaria parasites could be observed these transgenic malaria parasites, and the liver was confirmed as the first organ that malaria parasites reached, entered, and increased in *in vivo* imaging of animal models.

Transgenic luciferase *P. berghei* parasite has been successfully used to study sequestration during blood-stage infection in mice. However, the transgenic luciferase *P. yoelii* is commonly used to study the efficacy of agents against liver stages, because its sporozoites infect the hepatocytes efficiently and develop large numbers of liver-stage parasites (Tarun et al., 2006). *P. yoelii* has also been used extensively for immunology and vaccine studies because it is thought to better mimic in experimental animals the immune response to human malaria (Khan and Vanderberg, 1991). After inoculation, *P. yoelii* sporozoites result in the release of a high number of merozoites into the blood. Because of that, the partial therapeutic effects of drugs could not accurately measure by analysis of the infected state (Mwakingwe et al., 2009).

8-week-old mice were inoculated intravenously with 2 X 10^5 red blood cells infected with transgenic luciferase *P. yoelii* to infect the naive mice. Five mice are included in each infection group. Luciferase activity is measured using an intensified charged coupled device video camera of the In Vivo Imaging System (IVIS). WT- and luciferase *P. yoelii* infected animals were intravenously injected through the tail with 200µl of D-1uciferin sodium salt (100 mg/kg of body weight) dissolved in PBS. Luciferin is allowed to distribute systemically for 3 min. The infected

animals are anesthetized with the use of isofluorane. Anesthetized animals were placed in the camera chamber of IVIS 100 system, and a bioluminescence signal is acquired for 5 min. Bioluminescence measurements produced by the IVIS 100 system are expressed as a pseudocolor on a gray background, with red denoting the highest intensity and blue the lowest. A region of interest is outlined and analyzed by use of Living Image (with the help of Igor Pro (version 4.02A; WaveMetrics) software to quantify luminescence. Images of mice infected by mosquito bites are displayed with the minimal signal set at 4000 photons (Franke-Fayard et al., 2006; Ploemen et al., 2009).

1.7. *IN VITRO* MODELS FOR MALARIA

In vitro antimalarial screens for compound activity, which constitute a key component of a critical path for an antimalarial drug discovery program, are based on the ability to culture *P. falciparum in vitro* in human erythrocytes. Typically, the parasite was grown erythrocytes with 2 to 6% hematocrit in RPMI 1640 medium supplemented with 0.23% sodium bicarbonate, 0.006% Amikacin, 10% A+ human serum, A+ human erythrocytes (6% hematocrit), and 0.027% hypoxanthine in 25-mm^2 culture flasks. Culture flasks are kept in an environment of 5% O2, 5% CO_2, and 90% N_2 and at 37°C. The medium is changed after every 48 h. For adaptation of the *P. falciparum* culture growing in the medium with human serum.The medium is changed every 48 h, and the parasite was subcultured with fresh RBCs after every 6 to 7 days (Singh et al., 2007).

Multiple drug-resistant (W2, Indochina, stain) and drug-sensitive (D6, Sierra Leone, stain) of *P. falciparum* isolate from around the world have now been culture-adapted and can be obtained from the Malaria Research and Reference Reagent Resource Center. The appropriate dilutions of the drugs are prepared in DMSO or RPMI-1640 medium and added to the cultures of *P. falciparum*

(2% hematocrit, 2% parasitemia) set up in clear, flat-bottomed, 96-well plates. The plates are placed in the humidified incubator with 90% N2, 5% CO2 and 5% O2 gas mixture and 37ºC. The cultures plates are incubated at 37°C for 48–120 h (Sahu et al., 2014). Parasitemia of the treated infected RBCs can be analyzed by several methods and then compared with untreated infected RBCs as a positive control and uninfected RBCs as a negative control. *In vitro* screening of malaria comes with several advantages. These screenings are precise and efficient for big compounds libraries. Thousands of compounds can be screened rapidly in few months. It is easier to studies drug combinations effects like synergism or antagonism. *In vitro* screening come with a better assessment of the intrinsic activity of a drug. Intro screenings also with several limitations. Drugs acting through active metabolite cannot be studied in *in vitro* settings. Pharmacokinetic effects cannot be studied *in vitro* studies. There is also a possibility that the toxic compounds also come out as false positives in *in vitro* screening. Active compounds in *in intro* screening lack the clinical correlation (Kalra, 2006).

1.8. *IN VIVO* MODELS FOR MALARIA

Animal models of malaria are important tools for antimalarial drug discovery (Fidock et al. 2004). Animal models are integrated systems in which the antimalarial efficacy of drugs is assessed in pathophysiological conditions of real disease. There are several factors contributed to the efficacy, e.g., absorption, distribution, metabolism and excretion, toxicity and antimalarial activity. Both pharmacokinetic and pharmacodynamics of antimalarial drugs may be different in animal models and humans because of dissimilarity in anatomy, physiology, and susceptibility to the different malaria parasite. However, many pharmacological interactions between drugs and parasites are independent of the host involved. So, animal models allow an investigation into the

in vivo pharmacological properties of drugs and their combinations.

1.8.1. RODENT MODEL

The mouse model is the most often used malaria drug discovery model because of its versatility, accessibility, and requirement of low amounts of compound. There are four Plasmodium species adapted to grow in mice that includes *P. berghei*, *P. yoelii*, *P. chabaudi* and *P. vinckei* (Bhattacharjee et al., 2007; Chong et al., 2006; Cosledan et al., 2008; Jain et al., 2004; Jimenez-Diaz et al., 2014; Kelly et al., 2009). Out of these four, the *P. berghei* is the most widely used species in antimalarial drug discovery program. The progression of the disease in mice ranges between lethal infections to a self-limited disease that depends on the strain of Plasmodium species and also on the murine genetic background. The choice of Plasmodium species is based on their susceptibility to test the drug in rodent hosts(Jimenez-Diaz et al., 2014). The Plasmodium spp. of rodents have biological cycles of about 24 h, which is a major difference from the classical human pathogens(Sanni et al., 2002). However, the rodent-adapted parasites species can reproduce the full cycle of malaria in mammals (Scheller et al., 1994). Even though, the evaluation of new drugs leads is performed with parasites that show significant evolutionary divergence from *P. falciparum* and *P. vivax* in these models (Prugnolle et al., 2008). The choice of Plasmodium species also depends on the genetic similarity at the level of the molecular target. For example, *P. yoelii* was chosen to test 4-pyridones because of the high sequence homology with *P. falciparum* for the target cytochrome bc1, which is a key protein in the mitochondrial respiratory chain (Yeates et al., 2008). On the other hand, diamidines have been tested in the *P. vinckei* model because *P. berghei* is almost insensitive to these drugs (Angulo-Barturen et al., 2008). *P.chabaudi* and *P. vinckei* generate a high level of parasitemia and produce synchronous infections enabling studies on

parasite stage specificity. Also, *P.chabaudi* and *P. vinckei* are more sensitive than *P. berghei* to iron chelators and lipid biosynthesis inhibitors (Wengelnik et al., 2002).

1.8.1.1. ANTIMALARIAL EFFICACY TEST

Two different assays are typically employed to access the efficacy of any test drug. One is the Thompson test, and another is Peters' suppressive 4-day test (Peters and Robinson, 1999). In the Thompson test, *P. berghei* pre-infected mice are treated with a drug for three days and the survival time of a group of treated mice is compared to a group of vehicle-treated controls. In the Peters' 4-day test, the administration of test drug starts from day one, just after one to three hours after infection with *P. berghei* infected erythrocytes and the resulting parasitemia is measured on the fifth day that is 24 h after the last dose administration and compared to vehicle-treated controls. This is the most widely used preliminary test, in which the efficacy of a compound is assessed by comparison of blood parasitemia and mouse survival time in treated and untreated mice. On day 0, mice are injected with the Plasmodium parasite-infected erythrocytes intravenously or intraperitoneally into an experimental group (five each). The group of vehicle-treated mice is compared with the test drug-treated group. For a positive control of reference antimalarial drug, a group of chloroquine also compared with the group of test drug treatment. The drugs are prepared at required concentration, as a solution or suspension and administered 2-4 h post infection by appropriate routes (Orally, intraperitoneally, and intravenously). On day 1 to 3, the experimental groups are treated again (with the same dose and same route) as on day 0. On day 4, 24 h after the last dose (i.e., 96 h post-infection), blood smears from all animals are prepared with Giemsa stain. Parasitemia is determined microscopically by counting four fields of approximately 100 erythrocytes per field. For low parasitemia (<1%), up to 4000 erythrocytes have to be counted.

The difference between the mean value of the control group (taken as 100%) and those of the experimental groups is calculated and expressed as percent reduction or suppression. For slow acting drugs, additional smears should be taken on days 5 and 6, to determine parasitemia from which the activity is calculated accordingly. Untreated control mice typically die within two weeks after infection. For treated mice, the survival-time is recorded and the mean survival time for treated group compared with untreated and reference antimalarial drug-treated groups. If no parasitemia appears in mice until day 28 of post-infection, they are considered cured.

1.8.1.2. ONSET/RECRUDESCENCE TEST

In the ‘onset/recrudescence test,' mice are administered with single dose of the test compound on day 3 of postinfection, subcutaneously. Control mice receive the suspension vehicle alone. Blood smears are prepared at intervals of 12 h, 24h and then daily until day 33, Giemsa stained and assessed for parasitemia. Results are expressed regarding the rapidity of onset of action, time to onset of recrudescence, increase of parasitemia and duration of survival (in days). Compounds are also tested for prophylactic activity by administrating them before infection, followed by a daily examination of smears (Kalra, 2006).

1.8.1.3. CAUSAL PROPHYLAXIS AND RESIDUAL ACTIVITY TEST (HILL’S TEST)

In this model, mice are inoculated with *P. yoelii* (N67 strain) sporozoites from *Anopheles stephensi* mosquitos. Sporozoites are harvested from mosquitos at 8-11 days after the infected blood meal. Whole mosquitoes are grounded with Tyrode’s Ringer solution and centrifuged to remove the debris. Each mouse receives approximately 10^4-10^5 sporozoites intravenously in a total volume of 0.2ml. For a compound to be considered as prophylactic, it must pass through four

different phases.(Ager, 1984; Kalra, 2006)

Phase 1 (Protective effect): This is the basic procedure that involves evaluation of causal prophylactic activity of the test drug in mice. Test drug is administered in infected mice 3h after the sporozoites inoculation. During the 14 day period, blood smears are taken until 2% parasitemia is achieved. If no parasitemia appeared until 14 days, the test drug is considered protective (Kalra, 2006).

Phase 2 (Residual activity): Test drug is then tested for residual activity against blood stage parasites by administrating a single dose of the test drug 48 h before inoculation of 10^4 trophozoites intravenously. If the time interval to reach 2% parasitemia is similar to that of the control group (untreated group), then it is considered that no residual activity has occurred (Kalra, 2006).

Phase 3 (Reconfirmation of Residual activity): Test drug with the possibility of prolonged residual activity is tested by inoculation of sporozoites followed by the administration of drug after 3 h. After an additional 48 h, 0.2 ml blood is removed from each mouse and injected intraperitoneally into a clean (new) mouse. Blood smears from recipient mice are examined for a 14 day period or until parasite appears. If less than 50% of the recipient mice develop parasitemia, then test drugs considered with residual activity. A compound has no residual activity of 75% or more recipient mice develop an infection (Kalra, 2006).

Phase 4: Mice are injected intravenously with 10^4 trophozoites 48 h after the compound administration to determine if the intra-erythrocytic plasmodium parasites are still viable. After an additional 3-4 h, 0.2ml of blood collected and injected to clean (new) recipient mice. Blood smears are taken and the time interval to reach 2% parasitemia is compared with control mice. If the time interval is similar, it reflects that no permanent damage has been done to the parasites and thus no residual activity is present (Kalra, 2006).

1.8.1.4. SPORONOICIDAL ACTIVITY TESTING

Here, albino mice are inoculated with *P. yoelii* nigeriensis N 67 parasite (10^7 infected red blood cells)) on day 0. Female *Anopheles stephensi* mosquitoes are placed in containers (about 25 mosquitos per container) and fed with 4% sucrose for the first five days after hatching. They are kept at a constant temperature of 24ºC and 75% humidity. After five days, mosquitos are starved for 24 h. On third-day post infection in mice, mosquitoes which were starved for 24 h are allowed to feed on mice. Before mosquitoes are allowed to feed, the presence of mature gametocytes is confirmed on blood smear of mice. The mice are then anesthetized with a single dose of 60 mg/kg of sodium pentobarbitone i.p. and laid on top of mosquito containers, so that the mosquitos can feed on them through the membrane covering of mosquito container for about 30 min. On the seventh day after the blood feed, a sample of each batch of mosquitos is removed and dissected. Midguts are examined for plasmodium parasites oocysts. The mean count for each batch is calculated. It is dissolved in 4% sucrose and *fed ad libitum* to the insects following the blood meal to determine the inhibitory effects of a test drug on oocyst development. Usually, a batch of 10 surviving mosquitos for each drug concentration and each control is sufficient to provide data from which the level of drug activity can be calculated from a comparison of mean oocyst counts in treated and control batches (Ager, 1984; Kalra, 2006).

1.8.2. HUMANIZED MOUSE MALARIA MODEL

Humanized mice are the mice that express human genes and comprise human tissues (Siu and Ploss, 2015). Humanized mice models often employ mutations and genetically deficient backgrounds which maintain the immunocompromised status of mice and further enable

engraftment with human cells and tissues (Kaushansky et al., 2014). These models are important tools to understand the biology, and development of malaria and may have potential in the development of antimalarials drugs and vaccines (Kaushansky et al., 2014; Siu and Ploss, 2015). The blood and liver stages of human malaria infection are compartmentalized in nature, and thus independent studies can be done for each stage. The blood and liver stage can be replicated in a human erythroid and liver chimeric mouse respectively. Also, a dual engraftment of erythroid/liver would allow replicate the complete Plasmodium life cycle in vivo (Siu and Ploss 2015).

1.8.2.1. BLOOD STAGE MODEL

As mentioned earlier, human erythroid chimeric mice are used to replicate *Plasmodium* asexual blood stage infection. In the present, there are two ways to generate human erythroid chimeric mice infection 1) to infuse human RBCs and 2) to transplant hematopoietic stem cell (Vaughan et al., 2012). The most effective and successful method to generate a human erythroid chimeric mouse is to engraft human RBCs in immuno-deficient mice (Siu and Ploss, 2015). The severe combined immunodeficiency (SCID) mice contain a point mutation in the Prkdc kinase (PrkdcSCID), which hampers with the development and functions of B and T lymphocytes. Thus, these SCID mice accept xenogenic grafts of human RBCs and are used to establish *P. falciparum* asexual blood-stage infection for up to 2 weeks (Tsuji et al., 1995). The non-obese diabetic (NOD) mice background is often used with SCID mice further facilitate the engraftment of human RBCs (Siu and Ploss, 2015; Vaughan et al., 2012).

Another model that would support asexual blood infection of *Plasmodium* is through transplant of hematopoietic stem cells (HSCs) in the bone marrow of mice. Practically, this model has produced limited success. To produce human hematolymphoid mice, SCID mice are

transplanted with HSCs isolated from human fetal tissues, human peripheral blood, or human bone marrow (Rongvaux et al., 2013; Strowig et al., 2011).

1.8.2.2. LIVER STAGE MODEL

The human liver chimeric mice are generated by injecting human primary adult hepatocytes in Xeno recipient SCID mice. To further boost the growth of human hepatocyte, the liver injury is induced in the mice (Billerbeck et al., 2013; Siu and Ploss, 2015). The SCID mice expressing urokinase-type plasminogen activator transgene (UPA) using the albumin promoter (Alb) (SCID Alb-UPA) are the well-distinguished human liver chimeric mice model. The cells which do not contain the toxic urokinase-type plasminogen activator transgene, for example, engrafted human hepatocytes get a selective advantage to grow. This humanized mouse model is successfully used to engraft human hepatocytes with almost 90% engraftment (Sandgren et al., 1991). Importantly, this model is shown to maintain *P. falciparum* infection effectively (Sacci et al., 2006).

1.8.3. NON-HUMAN PRIMATE (NHP) MODELS

Aotus trivirgatus (Owl monkey) and the *Saimiri sciureus* (squirrel monkey) have served as experimental models for antimalarial drug research. Primate models are more advanced animal models than rodent models. NHP models have utility for re-confirmation of rodent efficacy results with a more clear prediction of drug effect in humans and evaluating the efficacy against malaria. These primate hosts are primarily used for screening of antimalarial drugs. *A. trivirgatus* is one of the WHO recommended a model for studies in malaria research, and these are the only models which can sustain malarial infection caused by human malaria parasites, *P. falciparum* and *P. vivax*

and rhesus malaria parasite *P. cynomolgi*. The progression of *P. vivax* infection in this primate model is similar to *P. vivax* infection in man. The same model could evaluate the prophylactic, schizonticidal, and hypnozoitocidal effect of test drug (Peters, 1987).

The NHP *in vivo* experiments started with young, tuberculin-negative rhesus monkeys (3.5 to 6 kg). The infected female anopheles mosquitos are ground in a 1:1 mixture of saline and normal monkey serum to initiate the infection in monkey. The debris is removed by light centrifugation. The sporozoites are counted, and each primate inoculated intravenously with approximately 500,000 sporozoites in 2 ml of fluid. The suspension of drug in water is prepared and administered with the help of stomach tube once daily, starting the day before infection and up to day 8. Blood smears are prepared, and parasitemia analyzed daily until 46 weeks. At the end of 6 weeks, if the animals are still negative, they are rechallenged with another inoculum to check their susceptibility to infection (Kalra, 2006; Peters, 1987).

All the animals become infected during 4-6 weeks of the period are treated with test compounds as soon as the parasitemia level reaches 0.1 to 0.5%.The infected animals receive seven daily oral doses of the drug and blood smear slides are prepared and analyzed daily during and after the treatment up to 30 days. If the animals found negative for malaria parasite, they examined twice weekly until they parasite relapse. If the parasites are not cleared by the drug during the primary treatment, the animals are given seven daily doses of 5mg/kg of chloroquine. If no relapse follows chloroquine administration, it indicates that the test drug has destroyed the hypnozoites. When no relapse occurs within 8-12 weeks, the animals are splenectomized. Failure to develop further parasitemia within four weeks of this procedure indicates that the animals are radically cured since, in 99% of those that are not splenectomized, the infection relapses within three weeks of splenectomy (Fidock et al., 2004; Kalra, 2006).

A particularly valuable model for the study of hypnozoites has been established with the simian parasite *P. cynomolgi* in *Macaca mulatta* (rhesus monkeys), enabling efficacy tests of drugs against the dormant liver stages(Deye et al., 2012; Dow et al., 2011).

The rhesus macaque *P. knowlesi* infection model remains a preferred model used to study Plasmodium liver stages since it approximates the *P. falciparum* course of infection in young children and adults and parallels *P. falciparum* in having a longer liver stage duration of parasite development, in contrast to the rodent malaria parasites. The animal model for *P. falciparum* infection in the *Aotus* spp. monkey host is suboptimal because cycles of transmission through sporozoites are unreliably maintained and the availability of *Aotus spp.* monkeys are also low(Galinski et al., 2017; Hobbs et al., 2014; Pasini et al., 2016).

This close relatedness between human and non-human primate hosts and between human and simian Plasmodium parasites makes non-human primates models of choice for human malaria for the biomedical research community. The main simian Plasmodium parasites infecting Old World primates include *P. knowlesi*, *P. coatneyi*, *P. fragile*, *P. cynomolgi*, P. inui, *P. fieldi*, and *P. simiovale*, in South East Asia, as well as *P. gonderi* in Africa, while simian Plasmodium parasites infecting New World primates comprise *P. brasilianum* and *P. simium* in South America (Galinski, 2012). Simian Plasmodium parasites sharing similarities with human parasites were reported at the beginning of the 20th century (Coatney, 1971). Deciphering the evolutionary history of Plasmodium parasites and their primate hosts' restrictions is a matter of intensive research, to determine the origin of human Plasmodium parasites and when they emerged (Beignon et al., 2014).

Infections with *P. coatneyi*, a simian malaria species that is closely related to *P. knowlesi* (Singh and Daneshvar, 2013; Vargas-Serrato et al., 2003), mirror the biology and pathogenesis of

falciparum malaria, with severe forms of pathology including anemia. A procedure was established to measure the turnover of in vivo biotinylated RBCs in rhesus macaque (*Macaca mulatta)* to study mechanisms of the onset and recovery of anemia (Moreno et al., 2013). These macaques had been experimentally infected for the first time (i.e., when malaria naïve) with *P. coatneyi* infected RBCs and, then again, while partially immune, nine months after curative anti-malarial drug treatment (Fonseca et al., 2016). This model also permits the quantification of the production of newly generated RBCs and of the different processes leading to the removal of RBCs in the absence or presence of a *P. coatneyi* infection in malaria naïve or semi-immune rhesus macaque (Fonseca et al., 2016; Teja-Isavadharm et al., 2016). The model can be employed as a tool for predicting and exploring disease severity and evaluating host-directed interventions. This capability includes the study of other species of Plasmodium that cause malaria in primates, each with their unique blood-stage biology and pathogenic characteristics (Fonseca et al., 2016).

Several species of New World Monkeys belonging to the genus *Aotus* and *Saimiri* are susceptible to infection by the five species mentioned above (Collins, 2002b). *P. falciparum, P. vivax,* and *P. malariae* require a process of adaptation in vivo to grow reproducibly in New World monkeys. Also, splenectomy is often necessary to obtain significant parasitemias and production of infective gametocytes (Collins, 2002a, b). Conversely, *P. knowlesi*, a natural parasite of monkeys, readily infects *Aotus, Saimiri* and Rhesus monkeys (*Macaca mulatta*). As a major advantage of nonhuman primates, all stages of the biological cycle of the human parasites can be reproduced for drug evaluation by choosing appropriate host-parasite pairs (Collins, 2002a; Stewart, 2003). Nonetheless, the use of monkey models is quite limited due to ethical concerns and experimental complexity because highly specialized facilities are required (Jimenez-Diaz et al., 2014).

Macaques are the natural host of *P. cynomolgi*, a malaria parasite that has a biological cycle similar to *P. vivax* and can infect humans (Coatney et al., 1961; Jimenez-Diaz et al., 2014). *P. cynomolgi* has a cycle of maturation in the blood of 48 h with reticulocytes being the preferred cells for malaria of infection. The blood-stage infection is self- limited but presents characteristic relapses (Kocken et al., 2009). *P. cynomolgi* is also noteworthy as it can also form hypnozoites upon liver infection. All these characteristics make *P. cynomolgi* an interesting surrogate model for *P. vivax* infection (Jimenez-Diaz et al., 2014). Different models for malaria drug discovery are summarized in **Table 1.4**.

Table 1.4: Models for malaria drug discovery. Table adapted from Jimenez-Diaz et al., 2014 (Jimenez-Diaz et al., 2014). The intensity is defined in + sign. Single + is lowest and +++++ is the highest intensity.

	In vitro	Rodent	Humanized mouse	Non-human primates
Plasmodium spp.	*P. falciparum* (Chloroquine sensitive and resistance strains)	*P. berghei, P. yoelii, P. chabaudi, P. vinckei*	*P. falciparum*	*P. falciparum, P. vivax, P. malariae, P. ovale,* and *P. knowlesi*, are infectious for both Old and new World Monkey. *P. cynomolgi* infectious in New World monkeys
Parasite cycle stage for assay	Blood stage only	Full cycle Gametocyte	Blood stage Liver stage Gametocyte	Full cycle. *P. cynomolgi* for hypnozoite stage
Parasite maintenance	*In vitro*	In vivo passage	*In vitro/in vivo* passage	*In vitro/in vivo* passage
Host immunity	Not applied	Immuno-deficient Immuno-competent	Immuno-deficient	Immunocompetent
Complexity	+	++	+++	+++++
Facilities	+	++	+++	+++++
Accessibility	++++	++++	+++	Highly restricted
Animal handling	No animal handling	+	++++	++
Cost	+	++	+++	+++++

1.9. CONCLUDING REMARKS

Visceral leishmaniasis is one of manifestation of leishmaniasis with very high mortality and morbidity. Several phenotypic cells-based *in vitro* models are available for antileishmanial screening. Intracellular amastigotes represent the pathophysiological scenario of leishmaniasis diseases. Screening against intracellular amastigotes is more logical for *in vitro/ex vivo* antileishmanial drug discovery than promastigotes or axenic amastigotes form of parasites. Screening assays for intracellular amastigotes are complex as they require both host and parasite cells. THP1 cells can be differentiated to form a monolayer of macrophage cells and are most appropriate host cells with non-dividing nature as of cells with homogeneous cell population. Similarly, several *in vivo* models are available for antileishmanial screening, based on rodents (mice, Hamster), dogs and non-human primate animals as the host for the leishmania parasite. Both *in vitro* and *in vivo* antileishmanial screenings assays rely on growth analysis the intracellular amastigotes. The currently available *in vitro/ex vivo* screening methods have significant limitations and shortcomings, which should be addressed by developing better phenotypic better models. In case of visceral leishmaniasis, the parasite penetrates into the visceral organs. Analysis of growth of leishmania parasite in internal visceral organs becomes challenging. Generation of stably transfected transgenic parasite cell lines with a strong and sustained expression of reporter proteins which can monitor in the deep visceral organs with minimal background interference.

Similarly, malaria is a fatal disease if left untreated and is a major cause of deaths globally. Several screening assays are available for *in vitro* antimalarial screening based on *P. falciparum* cultures maintained in human erythrocytes. Most of the currently employed assays are complex as the parasite grows inside the erythrocytes through multiple developmental stages. Several *in vivo* experimental animal models have been developed with rodent and non-human primates host

animals and different species of the malaria parasite. Both *in vitro* and *in vivo* models rely on the intra-erythrocytic growth analysis of the malaria parasite. Most of the current lab and even clinical diagnostic centers for malaria around the world rely on microscopy for observing the malaria parasite in the blood sample. Several other parasitemia analysis methods have been developed, but most of these models have significant limitations. To accelerate the antimalarial drug discovery research, there is a significant need for the development of methods for parasitemia analysis, which are robust, cost-effective and can be applied for automated high-throughput screening.

The research project have addresses the critical need for development and standardization of novel models and assays for phenotypic screening for visceral leishmaniasis and malaria. The project includes the development of high throughput screening assay against intracellular amastigotes of *L. donovani* which is the causative agent of visceral leishmaniasis. The utility of the developed assay was confirmed by applying the developed assay for high throughput screening for a big natural product fraction library. Furthermore, the two new transgenic *L. donovani* parasites, one with a citrine reporter gene and another with the mCherry reporter gene were developed by stable transfection method. The developed transgenic parasite was utilized as promastigote and intracellular screening models. The project also includes the development of a noble method for malaria parasite-infected red blood cells analysis based on LDS-751 nucleic acid staining. The method was implemented here in *in vitro* and *in vivo* settings of antimalarial screening assays. These newly developed assay will contribute significantly to accelerating the current search for noble pharmacophores with antileishmanial and antimalarial activity. The new models will also have important applications in understanding biology, virulence, and pathogenesis of malaria and leishmania pathogens, host-parasite interactions and *in vitro/in vivo* screening for new drug discovery.

CHAPTER II

DEVELOPMENT OF AN IN VITRO MACROPHAGE CELLS INTERNALIZED LEISHMANIA AMASTIGOTES ASSAY AND SCREENING OF A NATURAL PRODUCTS LIBRARY

2.1. INTRODUCTION

Leishmania donovani, the causative agents of visceral leishmaniasis (VL), are intracellular parasitic protozoa that cycle between phagolysosomes of mammalian macrophages and alimentary tract of sand flies (Chang and Fong, 1983). New antileishmanial drug discovery approaches primarily rely on the availability of suitable *in vitro* and *in vivo* screening models. *In vitro* promastigotes (Mikus and Steverding, 2000) and axenic amastigotes assays (Callahan et al., 1997) have been used for anti-leishmanial drug screening. However, the promastigotes-based assays may not be appropriate due to significant cellular, physiological, biochemical and molecular differences in comparison to intracellular amastigotes. Macrophage-internalized amastigotes are responsible for pathophysiological conditions of leishmaniasis (Croft et al., 2006a). Therefore, the assays based on intracellular macrophage-amastigotes are more appropriate for *in vitro* screening. Screening based on intracellular amastigotes gives essential information on the capacity of the drugs to target intracellular microorganisms (Sereno et al., 2007). Macrophage-amastigotes models are complex, as they require host macrophages cells and parasite (Leishmania spp.) cells. Quantitative analysis of viability, growth, and proliferation of leishmania amastigotes within

macrophages cells is challenging. Differentiated nondividing THP1 cells make an attractive alternative to primary macrophage cells and can be used for assaying the anti-leishmanial activity of different compounds against intracellular amastigotes (Croft et al., 2006a). Currently available macrophage-amastigote assays have several limitations. Classical microscopic assays, based on the microscopic counting of amastigotes/cell are labor-intensive. Further, the absence of automation limits the utility of this assay.

To overcome above demerits and limitations of the available macrophage-amastigote assays, we have developed a parasite rescue and transformation (PRT) assay with differentiated THP1 cells infected *in vitro* with *L. donovani* for screening pure compounds and natural products extracts (Jain et al., 2012). The assay involves the following steps: (1) terminal differentiation of THP1 cells to non-dividing macrophages, (2) infection of macrophages with *L. donovani* metacyclic promastigotes, (3) treatment of infected cells with test drugs, (4) controlled lysis of the infected macrophages, (5) release/rescue of amastigotes and (6) transformation of live amastigotes to promastigotes (7) quantitative analysis of growth of promastigotes.

The assay was optimized using detergent treatment for controlled lysis of *Leishmania*-infected THP1 cells to achieve almost complete rescue of viable intracellular amastigotes with minimal effect on their ability to transform into promastigotes. Different macrophage:promastigotes ratios were tested to achieve maximum infection. Quantification of the infection was performed through the transformation of living, rescued *Leishmania* amastigotes to promastigotes and evaluation of their growth by an AlamarBlue fluorometric assay in 96-well microplates. This protocol has been optimized for 384 well plates, and its applicability as high throughput assay has been established by the screening a natural products fractions library. Further, the assay was modified for simultaneity evaluation of the test samples for THP1

cytotoxicity (Jain et al., 2016b).

The use of natural products for treatment and cure of diseases has its roots in pre-historic times (Newman and Cragg, 2012). Despite significant advancement in synthetic medicinal chemistry, the natural products remain to be the unmatched source of drugs with novel pharmacophore structures (Cragg and Newman, 2013). Most of the currently available drugs have their genesis, directly or indirectly, from natural products. Amphotericin B used for the treatment of leishmaniasis originates from natural source *Streptomyces nodosus*, a filamentous bacterium. Several new assays were up-graded to 384 well format and applied for screening of a natural products fractions library generated by high throughput fractionation (Rocha et al., 2005; Sen and Chatterjee, 2011; Tu et al., 2010).

A natural products library of 13584 plant fractions obtained from 958 plant extracts was developed. Fractions were generated using a high throughput preparative fractionation (HTPF) of plant-extracts, coupled with a collection of UPLC-MS-ELSD-PDA data for each fraction. This UPLC-MS-ELSD-PDA data for each fraction will be helpful in identification of novel pharmacophores with potent leishmanicidal activity against intracellular amastigotes. This natural products library of plant fraction was utilized in high throughput screening against intracellular amastigotes with the help of parasite rescue and transformation assay.

2.2. HYPOTHESIS

The internalized leishmania amastigotes rescued by controlled lysis of the infected host macrophage cells transformed into cell-free promastigotes forms. The numbers and growth of transformed promastigotes correlate with the numbers of live amastigotes rescued from the leishmania infected macrophages cells.

2.3. OBJECTIVES

Purpose of this study to develop an in vitro method for screening against macrophage internalized *L. donovani* amastigotes. THP1 cells, terminally differentiated into adherent macrophages, were employed as the host cells. The transformed THP1 cells were infected with *L. donovani* promastigotes. The infected THP1 cells were treated with the test compounds. The macrophage internalized amastigotes were rescued by controlled lysis. Live amastigotes were transformed to promastigotes. The growth of promastigotes was analyzed by AlamarBlue assay. The library of natural products fractions were screened, and outcome of hits for any particular target was further evaluated.

2.4. MATERIALS AND METHODS.

2.4.1. *L. DONOVANI* PROMASTIGOTE CULTURE

Promastigote culture *L. donovani* (S1 strain) in RPMI 1640 medium supplemented with 10% fetal bovine serum (FBS) is maintained at the 26^{o}C incubator.

2.4.2. THP1 CELLS CULTURE

THP1 cell culture in RPMI medium supplemented with 10% FBS was maintained at 37^{o}C in 5% CO_2 incubator.

2.4.3. DIFFERENTIATION OF THP1 CELLS

A 3-days old culture of THP1 cells in the exponential phase was diluted with RPMI medium to 2.5 X 10^5 cells/mL. Phorbol 12-myristate 13-acetate (PMA) was added to the cell suspension to achieve a final concentration of 25 ng/mL (Jain et al., 2016a). The final concentration of PMA was standardized with different concentrations ranges from 10ng/mL to 100ng/mL. No toxicity was observed at any PMA concentrations in this range. PMA concentration of 25 ng/mL concentration was selected for differentiation of 100% THP1 cells. THP1 cells treated with PMA were seeded onto clear flat-bottom experimental plates (50,000 cells/well in 96 wells plate or 12,500 cells/well for 384 wells plate) or chamber slides (50,000 cells/well in 16 well chamber slides). Plates/chamber slides were incubated in a 5% CO_2 incubator at 37ºC for at least 12 h for differentiation of the THP1 cells to adherent macrophages. After overnight incubation, the medium from each well was discarded, and adherent cells were gently washed at least twice with serum-free RPMI1640 medium.

2.4.4. PARASITE RESCUE AND TRANSFORMATION (PRT) ASSAY

2.4.4.1. INFECTION OF DIFFERENTIATED THP1 CELLS WITH *L. DONOVANI*

The plates/chamber slides with differentiated THP1 cells were washed with serum-free medium. The *L. donovani* promastigotes culture was harvested at the stationary phase (metacyclic infective stage) and diluted to a density of 5X10^6 cells/mL in RPMI1640 medium with 4% FBS. The 100 µL (96 well plate) of promastigotes were added over serum-free medium in plates. The final density of promastigote parasite remained 2.5X10^6, parasites/mL in plates (5X10^5

parasites/well). The THP1 cells were infected with promastigotes in the ratio of 1:10. Plates with THP1 cells with promastigotes were incubated at 37^{o}C with 5% CO2 for 24 h to allow the promastigote parasite to infect the THP1 cells and transform to amastigotes. Plates were washed after 24 h with serum-free medium to remove external (non-internalized) parasites.

2.4.4.2. TREATMENT OF INFECTED THP1 CELLS WITH TEST DRUGS

Standard antileishmanial drugs amphotericin B, pentamidine and miltefosine, were selected for testing against intracellular amastigotes by both PRT assay and compare with digital image analysis assay. Stock solutions of the drugs/test compounds were prepared in water or dimethyl sulfoxide (DMSO). Each drug/compound was tested at six different concentrations. The standard drugs and test compounds were serially diluted in a fresh 96-well plate with RPMI-1640 medium with 4% FBS. The drugs/test compound concentrations were prepared in 2 times of the final concentrations. The serially diluted samples (100µl) were transferred to the experimental plate over 100µl serum-free medium. The plates were incubated at 37^{o}C and 5% CO_2 for 48 h. The plates were washed again with serum-free RPMI medium. The infected THP1 cells control without drugs were set up simultaneously in each plate/chamber slide.

2.4.4.3. CONTROLLED LYSIS AMASTIGOTES-INFECTED MACROPHAGES

The serum-free medium was removed from plates **(Figure 2.1A)** and infected THP1 cells were treated with 0.05% sodium dodecyl sulfate (SDS) in serum-free RPMI medium for 30 seconds (20µL/well). The plate was shaken for 30 sec duration **(Figure 2.1B).** The 0.05% Sodium dodecyl

sulfate (SDS) in serum-free RPMI medium diluted with the RPMI medium with 10% FBS (180µl/well). After treatment of all wells for controlled SDS lysis, the plates were transferred to an incubator at 26ºC for 48 h. This allowed transformation of rescued live amastigotes to promastigotes.

2.4.4.4. QUANTITATIVE ANALYSIS OF TRANSFORMED PROMASTIGOTES

After a 48 h incubation at 26°C, the rescued live amastigotes were transformed into promastigotes **(Figure 2.1D)**. AlamarBlue (10 µL) was added to each well, and the plates were incubated at 26ºC for overnight. The plates were read for standard fluorescence on a Fluostar Galaxy fluorimeter (BMG Lab Technologies) at 544 nm excitation, 590nm emission. The dose-response curved was prepared with XLfit software, and IC50 (concentration of the test compound causing 50% inhibition of growth) IC90 (concentration of the test compound causing 90% inhibition of growth) were computed.

2.4.5. THE DIGITAL IMAGE ANALYSIS (DIA) ASSAY

2.4.5.1. INFECTION OF THP1 CELLS WITH *L. DONOVANI* AND TREATMENTS WITH TEST DRUGS

The chamber slides with differentiated THP1 Cells were washed with serum-free medium infected with the *L. donovani* promastigotes as described in section 2.4.4. Chamber slides with infected THP1 cells were treated with test samples or standard drugs (Amphotericin B and

Pentamidine) at different concentrations for 48 h.

2.4.5.2. FLUORESCENT MICROSCOPE IMAGING AND IMAGE ANALYSIS

The chamber slides were washed with serum-free RPMI medium. The plastic well inserts were peeled off from the glass slides. The slides with infected THP1 cells were fixed by immersing the slides in methanol for 30 sec, dried under air flow and stained with 5 X SYBR Green I (prepared in water from the stock of 10,000X) for 15 minutes in a dark chamber at room temperature. The slides were washed to remove the extra stain and dried for 30 min under airflow. A full glass coverslip was placed over the stained slide with the mounting medium. The images of the control, infected and treated THP1 cells were collected with a Nikon 90i eclipse fluorescent microscope in FITC and DIC filters. The macrophage nuclei and parasite nuclei were counted with the help of ImageJ software **(Figure 2.3)**. The infectivity in particular sample images was calculated as

$$\text{Infectivity} = \frac{\text{Number of amastigotes nuclei counted}}{\text{Number of THP1 cells nuclei counted}} \times 100$$

The dose-response curves were generated with XLfit software for computation of IC_{50} and IC_{90} values.

2.4.6. STANDARDIZATION OF THP1 CELLS TO PARASITES RATIO

The THP1 cells to parasites ratio to determine the sensitivity of the assay was Standardized. Low parasites numbers/infection may compromise with sensitivity and selectivity of the screening. To acquire an optimum infection in THP1 cells, the ratio of THP1 cells to infecting promastigote

parasite were standardized in 96 well plates and 16 well chamber slides. The plates/chamber slides with differentiated THP1 Cells were washed with serum-free medium and 100µl of medium remain left over the cells. These differentiated THP1 cells infected with *L. donovani* promastigotes in different ratios of THP1 cells to parasites (1:1.25, 1:2.5, 1:5 and 1:10). The *L. donovani* promastigotes culture was harvested at the stationary phase (metacyclic infective stage) and diluted to a density of $5X10^6$ parasites/mL in RPMI1640 medium with 4% FBS. The promastigotes parasite were further serially diluted (1:1) from $5X10^6$ parasites/mL. The 100µl of serially diluted promastigotes were added over serum-free medium in separate wells of plates or chamber slides. The number THP1 cells/ well remained constant (50,000cells/mL). Plates/chamber slides with THP1 cells with promastigote were incubated at 37ºC in 5% CO2 incubator for 24 h. Plates/chamber slides were washed after 24 h with serum-free medium to remove external (uninfected) parasites and added with RPMI medium with 2% FBS. The plates/chamber slides were incubated for 48 h. The plates were washed again with serum-free RPMI medium and treated accordingly for PRT assay, and chamber slides were fixed with methanol and stained with 5X SYBR green for 15 min for digital image analysis assay.

2.4.7. STANDARDIZATION OF CONTROLLED CELL LYSIS

Controlled lysis of the THP1 cells was to achieve maximum/complete THP1 cells lysis without significantly affecting the viability of the rescued amastigote parasites. Infected THP1 cells were achieved by following the previous protocols (2.4.4.). Different detergents such as Tween 20, Tween 80, Triton X-100, NP-40 and SDS at different concentrations (0.5 and 0.05) and different durations of treatment (from 10sec to 60 sec) **(Figure 2.2)** were tested for control lysis

of *L. donovani* amastigotes infected THP1 cells. The effect of detergent was diluted immediately after the treatment time with RPMI medium with 10% FBS.

2.4.8. PLANT MATERIALS

Most of all samples were collected by botanists at Missouri Botanical Garden (MOBOT) in St. Louis, Missouri and some are collected by Elray Nixon. All the information NP ID, Sample Name, Sample Code, Genus, Species, Family, Source Common Name, Plant Part, Geographical Location, Collector, Collector number, Collection Reference and MOBOT Link for every extract have been mentioned in the compound library. Bulk plant samples are dried and frozen in the field and freeze dried at the University of Mississippi before extracting.

2.4.9. EXTRACTS PREPARATIONS

Extracts were prepared in National Center for Natural Products Research at the University of Mississippi by Dr. Melisa Jacob and his team. Extraction of the sample by was done by Dionex ASE 300. Extraction was done in 100% methanol. Each sample was placed in a specific ASE cell and extracted at 1500psi, at 40^{o}C for three times with 10-minute static time/Extraction. 100% volume get flushed out. Moreover, ASE cells purged for 120 Seconds. After extraction, all extract was dried and weighed and then dissolved in DMSO at a concentration of 20mg/mL.

2.4.10. FRACTIONATION OF EXTRACTS

Fractionation of the plant extracts was done in Chemical Biology and Therapeutics, St. Jude Children Research Hospital, Memphis Tennessee, by Dr. Kip Guy and his team. Natural products fractions library was generated using AHTS from various plant extracts (Tu et al., 2010; Tu and Yan, 2012). UPLC-MS-ELSD-PDA data were obtained with a Waters Acquity UPLCMS system (Waters Corp., Milford, MA, USA). An Acquity UPLC BEH C18 column (2.1 × 50 mm, 1.7 μm) was used. The mobile phase consisted of H_2O containing 0.1% HCOOH and CH_3CN or MeOH. The total run time for each analysis was 3.0 min. Ionization and detection of natural products were carried out on a Waters SQ mass spectrometer using both the positive and negative ESI modes. The capillary voltage was set at 3.4 kV. The extractor voltage was 2 V. Nitrogen was used as the nebulizing gas, and the source temperature was set at 130 °C. The scan range was m/z 130-1400. Data processing was performed automatically with OpenLynx by extracting all graphics information, such as retention times and UV and ELSD peak areas, and converted to text to allow transfer to a database for storage and analysis. Each 384-well plate could be analyzed in 20 h (Yang et al., 2014).

2.4.11. HIGH-THROUGHPUT PRT AND THP1 CELLS CYTOTOXICITY ASSAYS

The THP1 treated with PMA were seeded for differentiation in clear flat bottom 384 wells plates. Duplicate plates were set up, one each for leishmania and THP1 cytotoxicity assays. In one plate THP1 cells were infected with *L. donovani* promastigotes. After 24 h non-internalized promastigotes were washed off with serum-free RPMI1640 medium with the help of Aquamax 4000 microplate washer and left with 25μL/well of serum-free medium in plates. The test samples (plant extracts fractions) were diluted in separate plates in RPMI medium with 4% FBS. The test

samples (25 µL each) were transferred to the experimental plates with infected THP1 cells for antileishmanial assay and uninfected THP1 cells for cytotoxicity assay. The plates were placed in a CO_2 incubator at 37ºC for 48 h. After 48 h the plates were washed with serum-free RPMI medium with Aquamax 4000 microplate washer. Infected THP1 cells were subjected to controlled lysis with 0.05% SDS solution for 30 sec to rescue live amastigotes. The amastigotes were allowed 48 h to transform into promastigotes. Growths of leishmania promastigotes and THP1 cells were quantified with AlamarBlue (see section 2.4.4.).

2.4.12. HIGH-THROUGHPUT THP1 CELLS CYTOTOXICITY ASSAY

384 plates with differentiated THP1 cells (follow the method of section 2.4.3.) were washed at least twice with serum-free RPMI1640 medium. The 25µl of RPMI medium with 4% FBS were added over 25µl of serum-free medium and incubated the plates back to 37ºC with 5% CO2 for 24 h. Plates were washed serum-free medium. 25 µl of Plant fractions, diluted in daughter plates in RPMI medium with 4% FBS and transferred into experimental plates with THP1 cells. Cytotoxicity of Active fractions was performed at range from 10ug/mL to 0.0032ug/mL. The plate was incubated in a 5% CO_2 incubator at 37ºC for 48hr. After 48 of treatment, AlamarBlue was added to the plates, and the plates were incubated back in a 5% CO_2 incubator at 37ºC for overnight and read on a BMG Fluostar microplate reader (BMG Lab Technologies) at an excitation wavelength of 544 nm and an emission wavelength of 590 nm. Each compound was tested in duplicates at six concentrations, IC50 and IC90 values were computed from the dose-response curves developed by XLfit software.

2.5. RESULTS

2.5.1. COMPARATIVE ANALYSIS OF DIGITAL IMAGE ASSAY AND PRT ASSAY

A quantitative analysis was done for both Digital-Image-Analysis-Direct-Counting-Assay and PRT Assay for 24, 48, 72 and 96 h post standard antileishmanial drug treatment. In the direct counting method, level of infection of *L. donovani* infected macrophages (THP1 cells) was calculated by the amastigotes (determined by counting amastigotes nuclei)/100 transformed THP1 cells (determined by counting THP1 cell nuclei) **(Figure 2.6)** is a more accurate measure to analyze the effect of different standard or test compounds than the percentage of infected THP1 cells, as reported in some previous papers (Sereno et al., 2007), because this number is directly related to overall effect of compounds either through a decrease in number of parasites in macrophage cells or total removal of parasite from the macrophage cells. Infection was calculated from digital images of infected THP1 cells treated with different standard drugs at different dilutions for various time intervals **(Figure 2.6 and Table 2.1)**. The read-out for the Digital-Image-Analysis-Direct-Counting-Assay was amastigotes infection/100 transformed THP1 cells, while the read-out for the Parasite- Rescue-Transformation-Assay was relative fluorescence units (RFU), which is directly proportional to the number of live Leishmania amastigotes rescued from the infected macrophages and transform into promastigotes. The AlamarBlue assay is routinely used for Leishmania promastigotes anti-leishmanial drug screening.

2.5.2. CONTROLLED LYSIS OF INFECTED DIFFERENTIATED THP1 CELLS

The assay was initially standardized and optimized for controlled lysis of Leishmania-

infected THP1 cells. The objective was to optimize the conditions for detergent treatment, which yield almost complete lysis of THP1 cells with minimal effect on the viability of the rescued amastigotes. Treatment with NP-40 (**Figure 2.2A**) and Triton X-100 (**Figure 2.2B)** lysed the infected THP1 cells; however, it also influenced the viability and transformation of the rescued amastigotes. Treatment with Tween 20 (**Figure 2.2C**) and Tween 80 (**Figure 2.2D**) did not cause optimal lysis of THP1 cells resulting in an incomplete rescue of amastigotes as indicated by low numbers of transformed promastigotes. Treatment with 0.05% SDS for 30 sec **(Figure 2.2E)** yielded almost complete lysis of Leishmania-infected THP1 cells and did not affect viability and transformation of rescued amastigotes. Further optimization showed that treatment of cells with 0.05% SDS for 20-30 sec yielded the highest rescue of viable Leishmania amastigotes (**Figure 2.2F**). Because of the better yield of rescued parasite and maximum lysis of THP1 cell membrane, in subsequent experiments, treatment with 0.05% SDS for 30 sec was used. **Figure 2.1** depicts a microscopic view of the complete control lysis protocol. Intact THP1 cells infected with Leishmania amastigotes can be seen in **Figure 2.1A**. **Figure 2.1B** shows lysis of the THP1 cells after detergent treatment. **Figure 2.1C** shows rescued Leishmania amastigotes, which have been partially transformed into promastigotes and **Figure 2.1D** shows the almost complete transformation of amastigotes into promastigotes and their subsequent proliferation. The growth of these transformed promastigotes can be quantitatively monitored with the addition of AlamarBlue and measurement of fluorescence on a microplate reader. Procedure for SDS treatment was same for single or multiple plates. In multiple plates, SDS treatment was implemented column by column with a multichannel pipette. Serum-free medium was removed from all eight wells of one column of the plate, and 20 µl of 0.05% SDS was added to 8 wells of the same column and diluted after 30 sec with RPMI-1640 with 10% FBS. During initial

standardization of the assay, the plates were checked under the microscope for non-internalized promastigotes. A minimum of five items of washing was necessary for removal of parasites before step 5 of treatment of infected macrophage cells with standard compounds and three items of washing were necessary before step 7 of SDS treatment. Thus, the cells were washed eight times, and no visible non-internalized promastigotes remained before control lysis of infected THP1 cells.

2.5.3. DIGITAL IMAGE ANALYSIS AND DIRECT COUNTING

The digital images of Leishmania-infected THP1 cells were captured on Nikon Eclipse 90i fluorescent microscope after staining with SYBR Green I. Both macrophage nuclei and intracellular Leishmania nuclei with characteristic kinetoplast DNA were observed under the fluorescent filters **(Figure 2.3)**. Further, the images of infected THP1 cells were also captured under DIC. When both the images were merged, the outlines of THP1 cells with intracellular amastigotes were seen more clearly **(Figure 2.3)**. The ImageJ software was used to analyze these images. ImageJ is public domain, Java-based, image-processing program developed at the National Institutes of Health (http://rsb.info.nih.gov/ij/download.html). ImageJ has been designed with an open architecture that provides extensibility via Java plugins and recordable macros. Custom acquisition, analysis, and processing plugins can be developed using ImageJ's built-in editor and a Java compiler. For differential counting of THP1 cells nuclei and parasite nuclei by ImageJ, the image was opened in ImageJ. Cell counter was found in Analyze option in a plugin of the Software. The image was initialized, and cell counter type 1 was selected for THP1 cell nuclei and cell counter type 2 was selected for parasite nuclei **(Figure 2.3)**. Differential counting was done for at least 200 THP1 cells nuclei and the intracellular amastigotes present in these THP1

cells nuclei. A comparison of the PRT assay and image analysis method was made for evaluating the infectivity of THP1 cells with different macrophage:promastigotes ratios **(Figure 2.4)**. **Figure 2.5** represents the differential infectivity in THP1 cells at different macrophage:promastigote ratios. Both the methods showed comparable results and the macrophage:promastigote ratio of 1:10 yielded optimum and reproducible infectivity.

Once the conditions for PRT assay and the digital image analysis were optimized, the utility of these assays was evaluated for anti-leishmanial drug screening. The Leishmania-infected THP1 cells were treated with different concentrations of standard antileishmanial drugs namely Amphotericin B, Pentamidine and Miltefosine for different time intervals ranging from 24 to 96 hr. The experiment for PRT assay was done in triplicate, and the experiment for direct cells counting method was done in duplicate. **Figure 2.6** shows microscopic images of the control uninfected, control infected untreated and Leishmania-infected, treated THP1 cells. The dose-response curves were prepared from the PRT assay (concentration of the drug vs. transformed parasites) and the image analysis assay (number of amastigotes/100 THP1 cells) **(Figure 2.7-2.9)**. The IC50 of the drugs were computed by ExcelFit and are presented in **Table 2.1**. Digital-Image-Analysis-Direct-Counting-Assay and PRT assay showed comparable results. Digital-Image-Analysis-Direct-Counting-Assay was less optimal during the early time points of 24 and 48 h drug treatments. While the PRT assay showed results more consistent with the reported values at all the time points during the 24-96 h after drug treatments. This difference in results with Digital-Image-Analysis-Direct-Counting-Assay and PRT assay may be due to the presence of non-viable amastigotes during early periods of drug treatment in Digital-Image-Analysis-Direct-Counting-Assay.

2.5.4. HTS OF NATURAL PRODUCTS FRACTIONS LIBRARY

Total 13584 plant extract fractions from 958 extracts were screened out in both *L. donovani* macrophage amastigote assay and cytotoxicity assay using differentiated THP1 cell lines at 10µg/mL concentration**.** Out of these 13584 fractions, only 243 plant extract fractions shows more than 50 percent inhibition of intracellular *L. donovani* amastigotes. The active 243 plant extract fractions were further screened for dose-response analysis. The selective antileishmanial activity of 64 plant extract fractions was re-confirmed with IC50 values less than ten µg/mL **(Supporting Table 2.1)**. 19 fractions with IC50s < 2µg/mL **(Table 2.2)**, 20 with IC50s between 2 and 5µg/mL and 25 with IC50s between 5 and 10µg/mL **(Figure 2.10)**. Only 13 plant fractions out of 13584 fractions show cytotoxicity on differentiated THP1 cells with % inhibition more than 50 %. Most active plant extract fractions with antileishmanial activity less than 2µg/mL were *Thuja occidentalis* c9 (0.25 µg/mL*), Asclepias asperula* c3 (0.33 µg/mL), *Inga laurina* c5 (0.86 µg/mL), *Gymnocladus dioica* c7 (1.69 µg/mL), *Rhodea japonica* c5 (1.08 µg/mL), *Rhodea japonica* c6 (0.70 µg/mL), *Rhodea japonica* c7 (0.39 µg/mL), *Rhodea japonica* c8 (0.41 µg/mL), *Nerium oleander* c3 (0.25 µg/mL), *Nerium oleander* c4 (0.53 µg/mL), *Nerium oleander* c6 (0.03 µg/mL), *Nerium oleander* c7 (0.54 µg/mL), *Marah macrocarpus* c8 (1.66 µg/mL), *Marah macrocarpus* c9 (1.07 µg/mL), *Juniperus californica* c5 (1.75 µg/mL), *Juniperus deppeana* c5 (1.85 µg/mL*), Eclipta prostrata* c5 (0.80 µg/mL), *Oplopanax horridus* c6 (1.98 µg/mL), *Falcataria moluccana* c7 (1.29 µg/mL) **(table 2.2)**.

Some fractions were further analyzed and compared with the QC-MS data of inactive fractions of the same plants. This most active fraction belongs to *Thuja occidentalis, Asclepias asperula, Rhodea japonica* and *Nerium oleander plant extracts*. QC-MS data of *Nerium oleander* active fractions suggest Oleandrin as an active chemical constituent. QC-MS data of *Thuja*

occidentalis active fractions suggest Deoxypodophylotoxin as an active chemical constituent.

2.5.5. QC-MS DATA OF FRACTIONS OF *N. OLEANDER* PLANT EXTRACT 80089

For *Nerium oleander* plant extract 80089, a total of four active plant factions 80089-c4, 80089-c5, 80089-c6, 80089-c7and 80089-c8 derived from AHTS fractionation of the ethanolic extract, shows antileishmanial activity against *Leishmania donovani* amastigote with IC50 values 8.31 μg/mL, 5.84 μg/mL, 0.03 μg/mL, 0.54 μg/mL and 7.72μg/mL respectively (**supporting table 2.1**). They were found to be devoid of cytotoxicity against differentiated THP1 cells. 80089 C6 is the most active fraction in all active fractions of *Nerium oleander* plant extract. Peaks were shown in fractions 80089-c6 at tR 1.17 to 1.19 min and tR 1.24 min in the ELSD chromatogram **(Figure 2.11).** These peaks were not detected in other inactive plant fractions for other *Nerium oleander* plant extract (plant extract number 80089). Therefore, peaks in QC-MS spectra at tR 1.17, 1.19, and 1.24 will be helpful in the prediction of active constituents of the plant fraction 80089-c6. The complete QC-MS analysis for the most active fraction 80089-c6 at tR 1.17, 1.19, and 1.24 minute is given in **figure 2.12**.

2.5.6. QC-MS DATA OF FRACTIONS OF *T. OCCIDENTALIS* PLANT EXTRACT 79863

In *Thuja occidentalis* plant extract 79863, only one active plant fraction 79863-c9 derived from AHTS fractionation of the ethanolic extract shows antileishmanial activity against *Leishmania donovani* amastigote with IC50 values 0.25 μg/mL. The fraction was found to be devoid of cytotoxicity against differentiated THP1 cells. Peaks were shown in fraction 79863-c9

at tR 1.18 and 1.24 min in the ELSD chromatogram **(Figure 2.13)**. This peak was not detected in other inactive plant fractions for other *Nerium oleander* plant extract (plant extract number 79863). Therefore, peaks in QC-MS spectra at tR 1.18 and 1.24 min will be helpful in the prediction of active constituents of the plant fraction 79863-c9. The complete QC-MS analysis for the most active fraction 79863-c9 at tR 1.18 and 1.24 minute is given in **Figure 2.14**.

2.5.7. QC-MS DATA OF FRACTIONS OF *A. ASPERULA* PLANT EXTRACT 78826

In *Asclepias asperula* plant extract 78826, only one active plant fraction 78826-c3 derived from AHTS fractionation of the ethanolic extract shows antileishmanial activity against *L. donovani* amastigote with IC50 values 0.33 μg/mL. The fraction was found to be devoid of cytotoxicity against differentiated THP1 cells. Peaks were shown in fraction 78826-c3 at tR 0.9 and 1.0 minute in the ELSD chromatogram **(Figure 2.15)**. This peak was not detected in other inactive plant fractions for other *Asclepias asperula* plant extract (plant extract number78826). Therefore, peaks in QC-MS spectra at tR 0.9 and 1.0 min will be helpful in the prediction of active constituents of the plant fraction 79863-c9. The complete QC-MS analysis for the most active fraction 78826-c3 at tR 0.9 and 1.0 minute is given in **Figure 2.16**.

2.5.8. QC-MS DATA OF FRACTIONS OF *R. JAPONICA* PLANT EXTRACT 81020

In 81020 *Rhodea japonica* plant extract 81020, a total of five fractions, 81020-c5, 81020-c6, 81020-c7, 81020-c8, and 81020-c9 derived from AHTS fractionation of the ethanolic extract, shows antileishmanial activity against *Leishmania donovani* amastigote with IC50 values 1.08

μg/mL, 0.70 μg/mL, 0.39 μg/mL, 0.41 μg/mL and 2.58 μg/mL respectively (**supporting table 2.1**). Fractions were found to be devoid of cytotoxicity against differentiated THP1 cells. 81020-c8 is one of the most active fractions in all active fractions of *Rhodea japonica* plant extract. Peaks were shown in fractions 81020-c8 at tR 2.10 and 2.21 minute in the ELSD chromatogram **(Figure 2.17)**. This peak was not detected in other inactive plant fractions for other *Rhodea japonica* plant extract (plant extract number 81020). Therefore, peaks in QC-MS spectra at tR 2.10 and 2.21 min will be helpful in the prediction of active constituents of the plant fraction 81020-c8. The complete QC-MS analysis for the most active fraction 81020-c8 at tR 2.10 and 2.21 minute is given in **Figure 2.18**.

2.5.9. RE-FRATIONATION OF *N. OLEANDER* AND *T. OCCIDENTALIS*

Nerium oleander plant extract was fractionated, and Oleandrin was confirmed as one of the active constituent in the active fraction (Unpublished data). The activity of Oleandrine was confirmed with PRT assay and as well as digital-image-analysis assay (**Figure 2.19**). *Thuja occidentalis* plant extract was fractionated, and Deoxypodophylotoxin was confirmed as one of the active constituent in the active fraction (Yang et al., 2014).

FIGURES AND TABLES

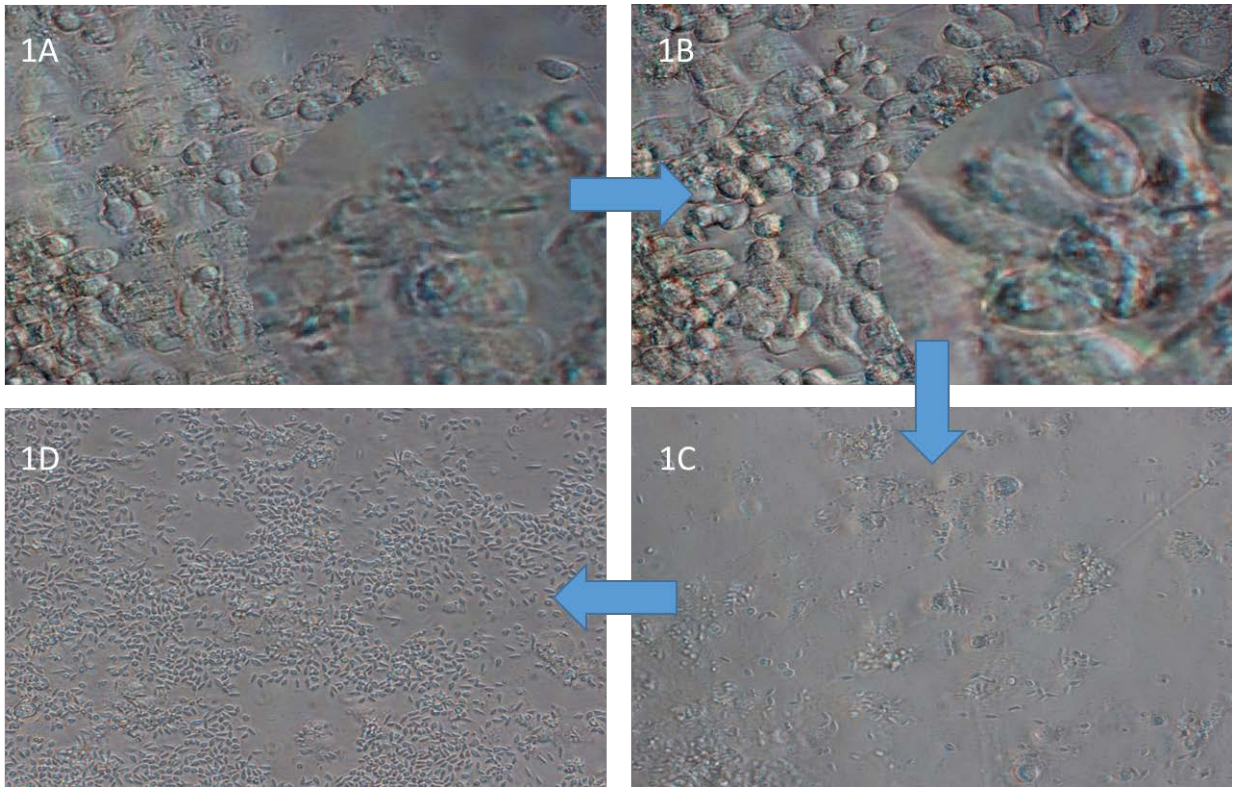

Figure 2.1: A microscopic view of the PRT assay. A - Adherent THP1cells infected with Leishmania amastigotes; B - Adherent, infected THP1 cells after controlled lysis with SDS C - *L. donovani* promastigotes transformed from the rescued live amastigotes D - Growth, and proliferation of transformed *L. donovani* promastigotes. Figure from Jain et al., JoVE, 2012 (Jain et al., 2012).

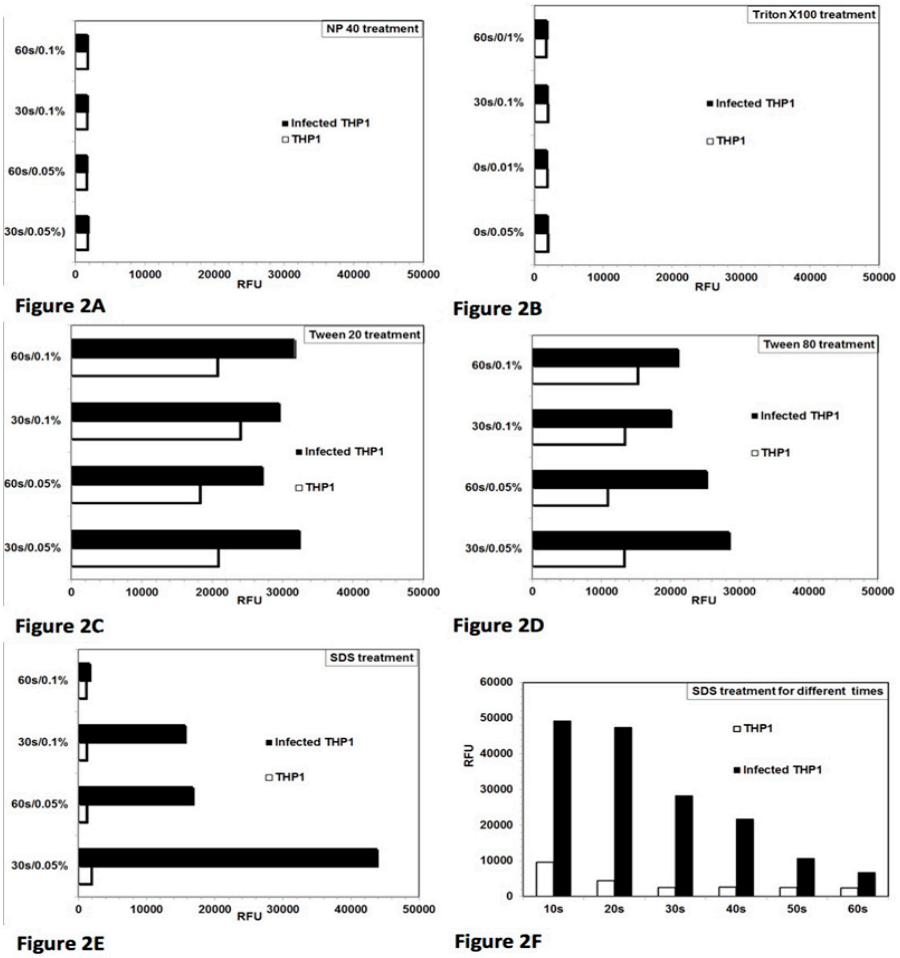

Figure 2.2: Optimization of controlled lysis of THP1 cells to achieve maximum rescue of live *L. donovani* amastigotes and their transformation to promastigotes with different detergents. Two concentrations (0.05% and 0.1%) of detergents and two time periods (30 sec and 60 sec) for treatment were tested. RFU (Relative fluorescence units). Each bar represents the mean of duplicate observations. [A] NP-40 [B] Triton X-100 [C] Tween 80 [D] Tween 80 and [E] SDS treatment caused almost complete lysis of THP1 cells and did not affect the viability of the rescued amastigotes at 0.05%/30 sec. [F] Treatment with 0.05% SDS for 20-30 sec caused almost complete lysis of THP1 cells and rescued viable parasite amastigotes to transform into promastigotes. Figure from Jain et al., JoVE, 2012 (Jain et al., 2012).

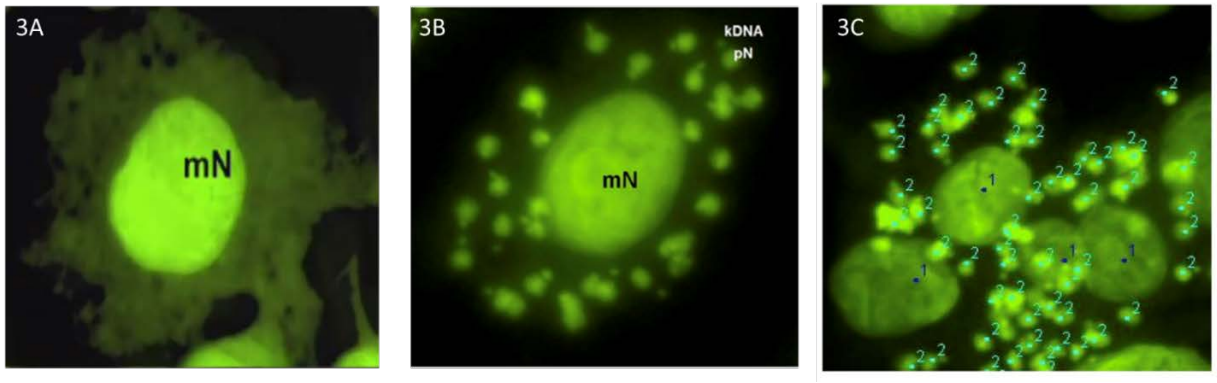

Figure 2.3: The fluorescent digital image of a differentiated THP1 cell infected *in vitro* with *L. donovani* amastigotes. A- Uninfected differentiated THP1 cells. B- L. donovani amastigote infected differentiated THP1 cells. The characteristic kDNA can also be seen with each parasite nucleus. The macrophage nucleus (mN) (1) and the parasite nuclei (pN) (2) can be differentially marked. C- Differentially counted by of macrophage nuclei and parasite nuclei with the help of ImageJ analysis software for quantitative evaluation of the infection. The quantification was done as a number of amastigotes/100 THP1 cells. Figure from Jain et al., JoVE, 2012 (Jain et al., 2012).

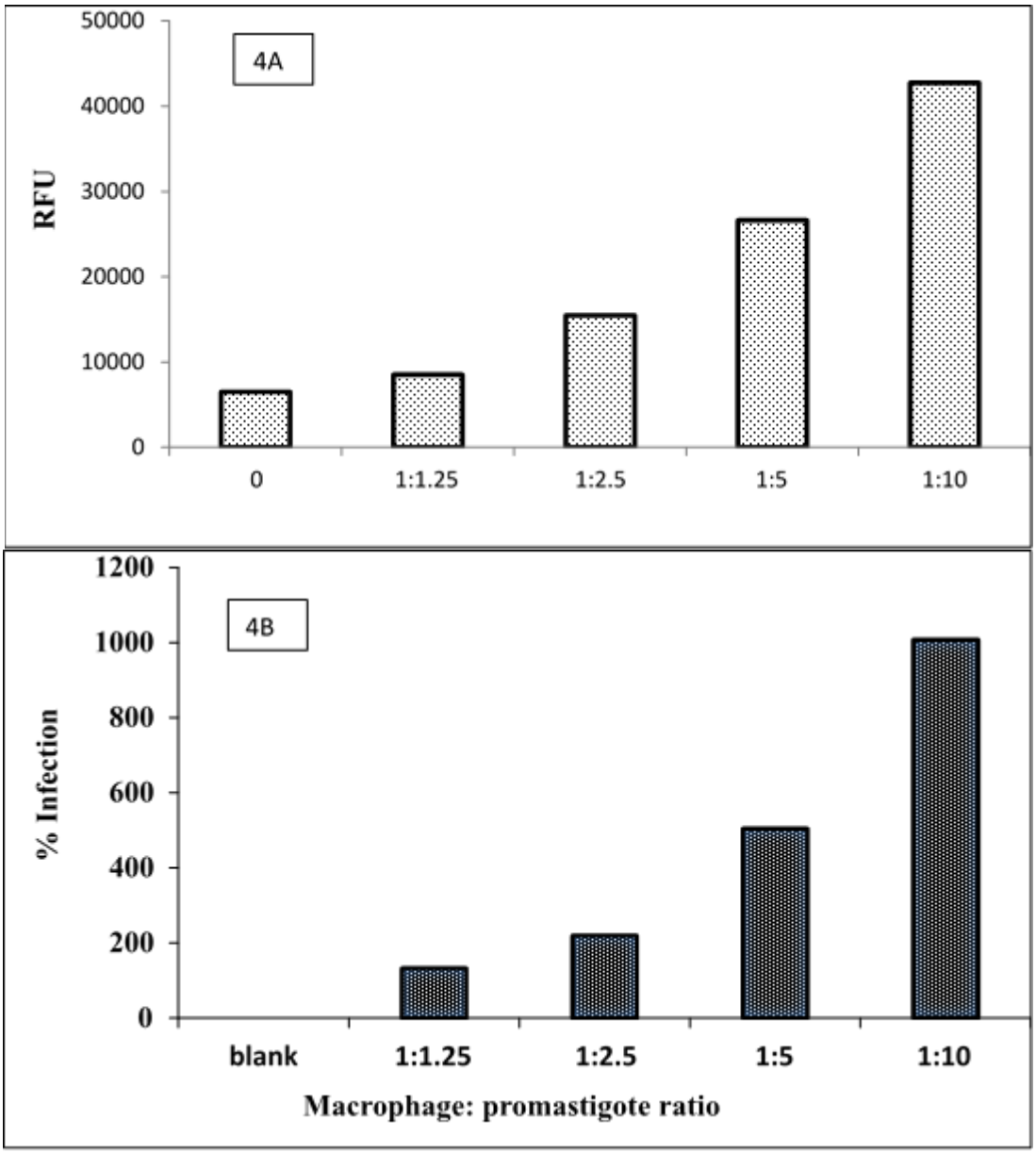

Figure 2.4: Different THP1 cells to parasite ratio in PRT assay (4A) and Digital-Image-Analysis-Direct-Counting-Assay (4B). The macrophage:promastigote ratio of 1:10 yielded optimal infection. Both showed comparable results. The PRT assay showed some background values. Each bar shows mean of duplicate values. Figure from Jain et al., JoVE, 2012 (Jain et al., 2012).

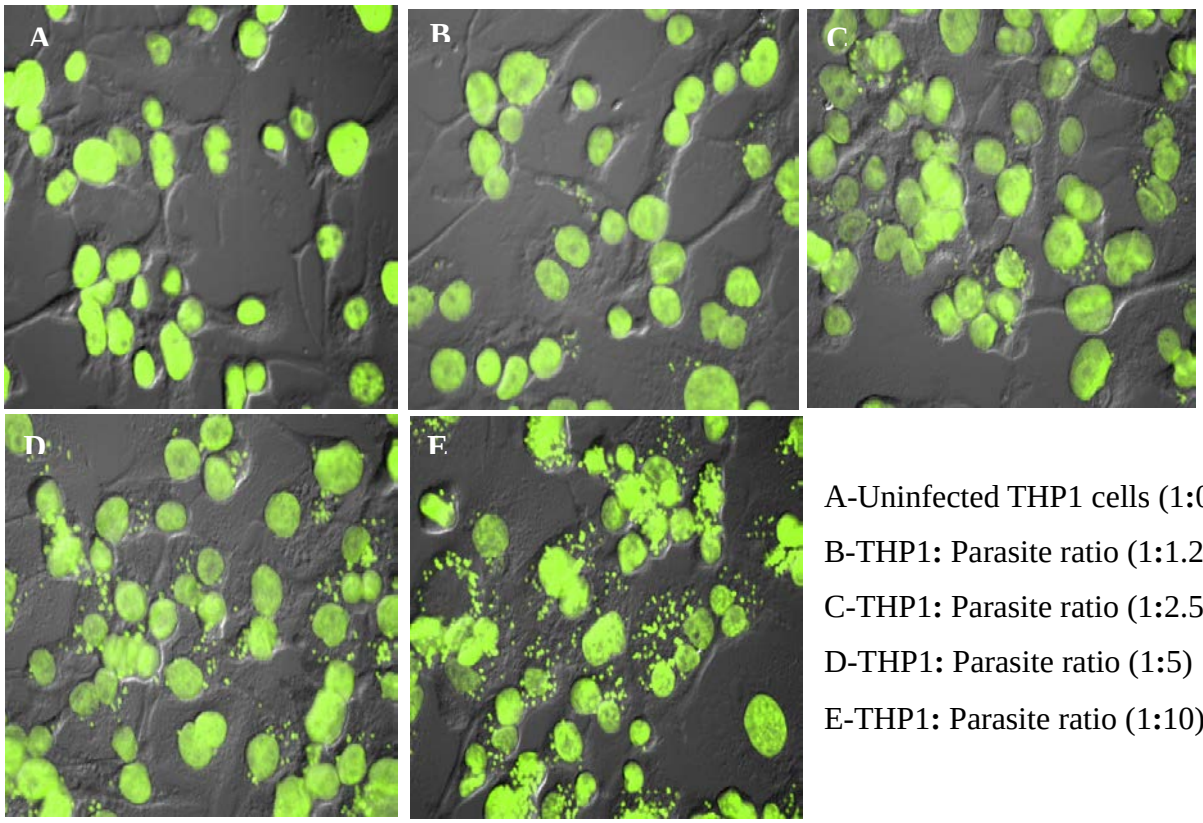

Figure 2.5: Comparative images of THP1 cells infected with different ratios of amastigotes. THP1 cells were infected by leishmania promastigotes by different THP1: Parasites ratio from uninfected THP1 cells (1:0, A) to maximum infected (1:10, E). Each different image was taken at 40 X magnification with 2X2 area. Images have taken by FITC filter with DIC. Figure from Jain et al., JoVE, 2012 (Jain et al., 2012).

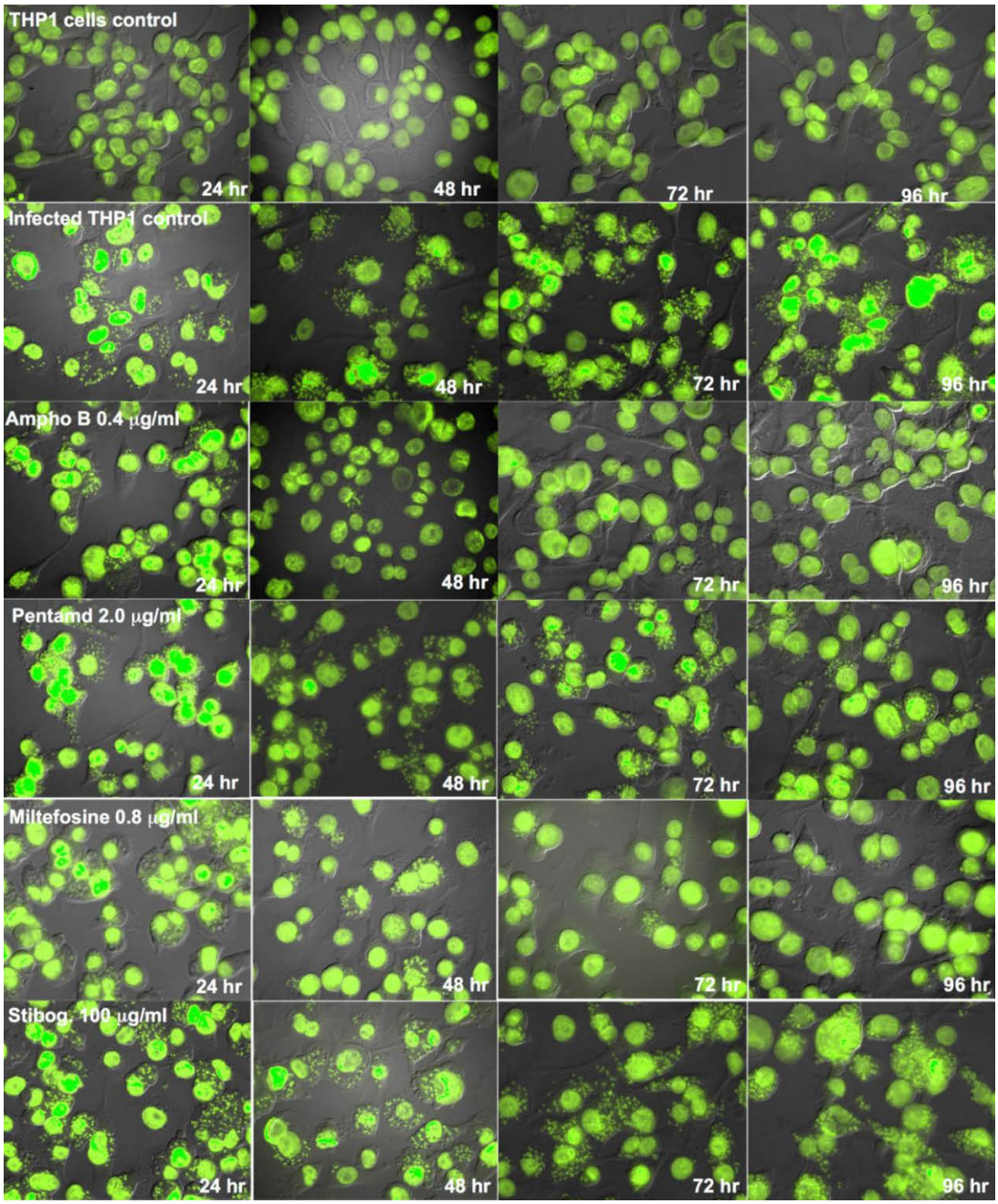

Figure 2.6: Digital images (FITC + DIC) of THP1 cells infected with *L. donovani* amastigotes after treatment with standard antileishmanial drugs for different time periods. Results were quantified as a number of amastigotes/100 THP1 cells and used to compute the percent growth compared to untreated controls and determine the IC50 values. Figure from Jain et al., JoVE, 2012 (Jain et al., 2012).

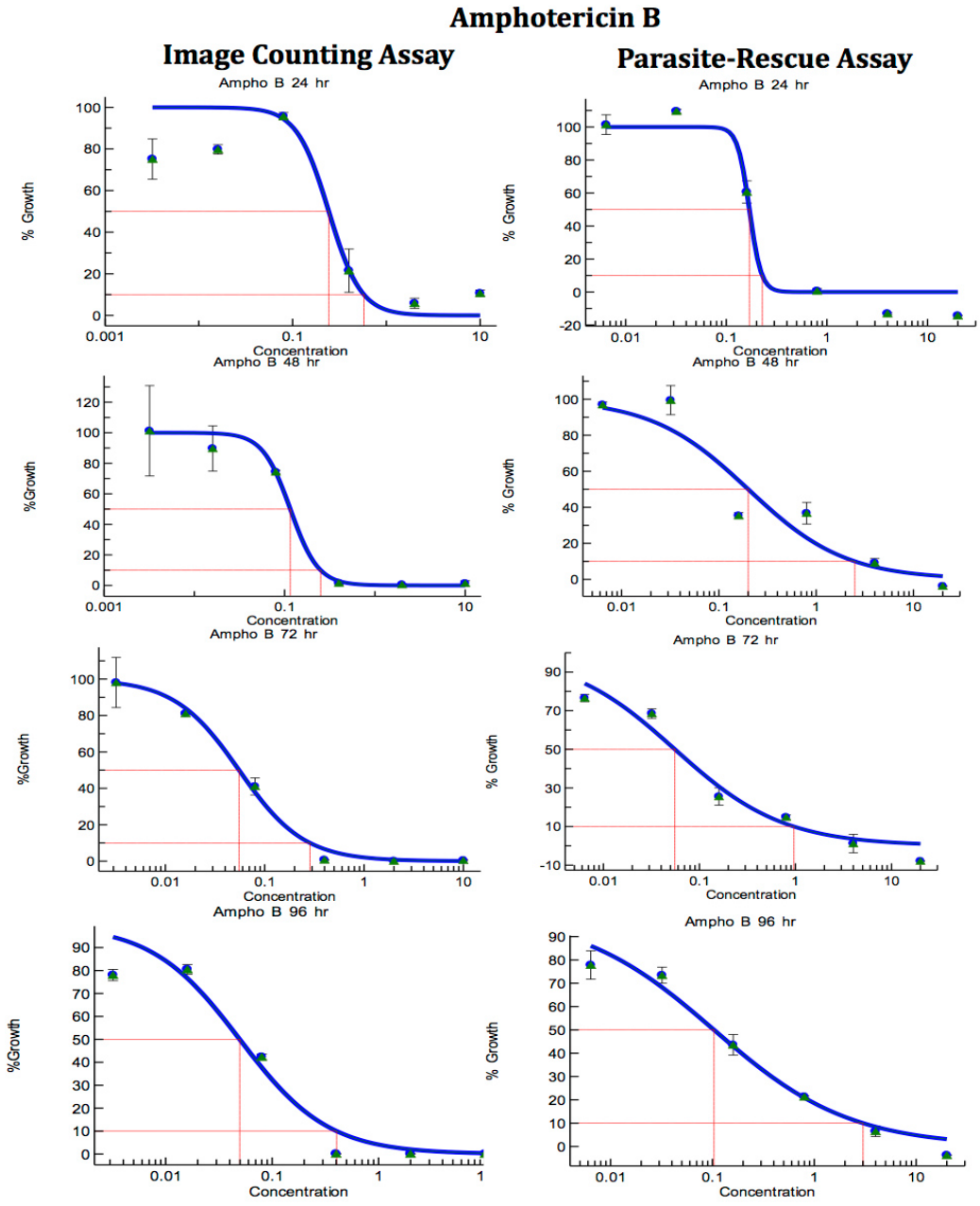

Figure 2.7: Comparison of Digital-Image-Analysis-Direct-Counting-Assay and PRT assay for anti-leishmanial drug screening (Amphotericin B). The infected macrophages were treated with different concentrations of standard anti-leishmanial drug for different periods. IC50 (µg/mL) values were computed from the dose-response curve by Excelfit. Figure from Jain et al., JoVE, 2012 (Jain et al., 2012).

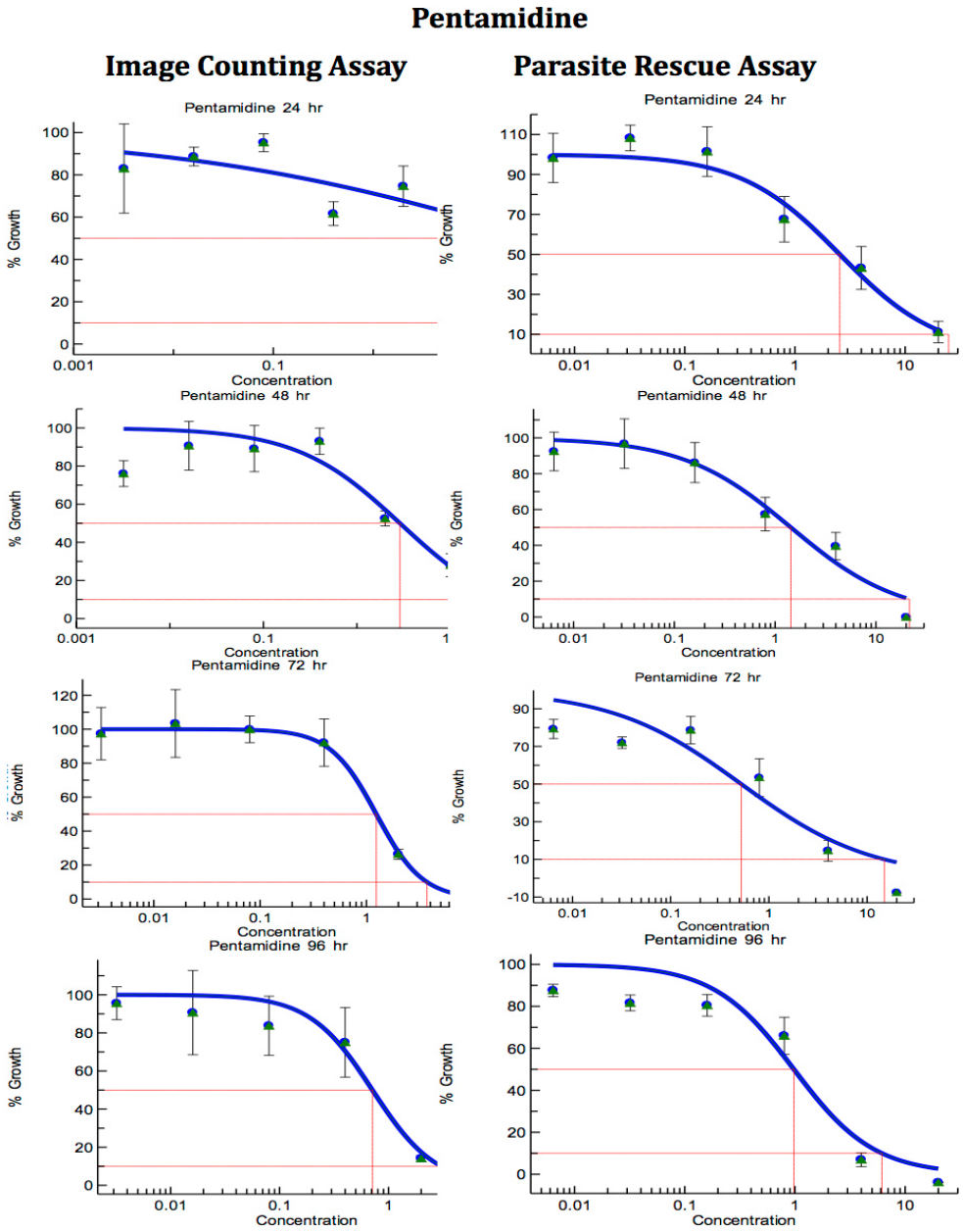

Figure 2.8: Comparison of Digital-Image-Analysis-Direct-Counting-Assay and PRT assay for anti-leishmanial drug screening (Pentamidine). The infected macrophages were treated with different concentrations of standard anti-leishmanial drug for different periods. IC50 (μg/mL) values were computed from the dose-response curves by Excelfit. Figure from Jain et al., JoVE, 2012 (Jain et al., 2012).

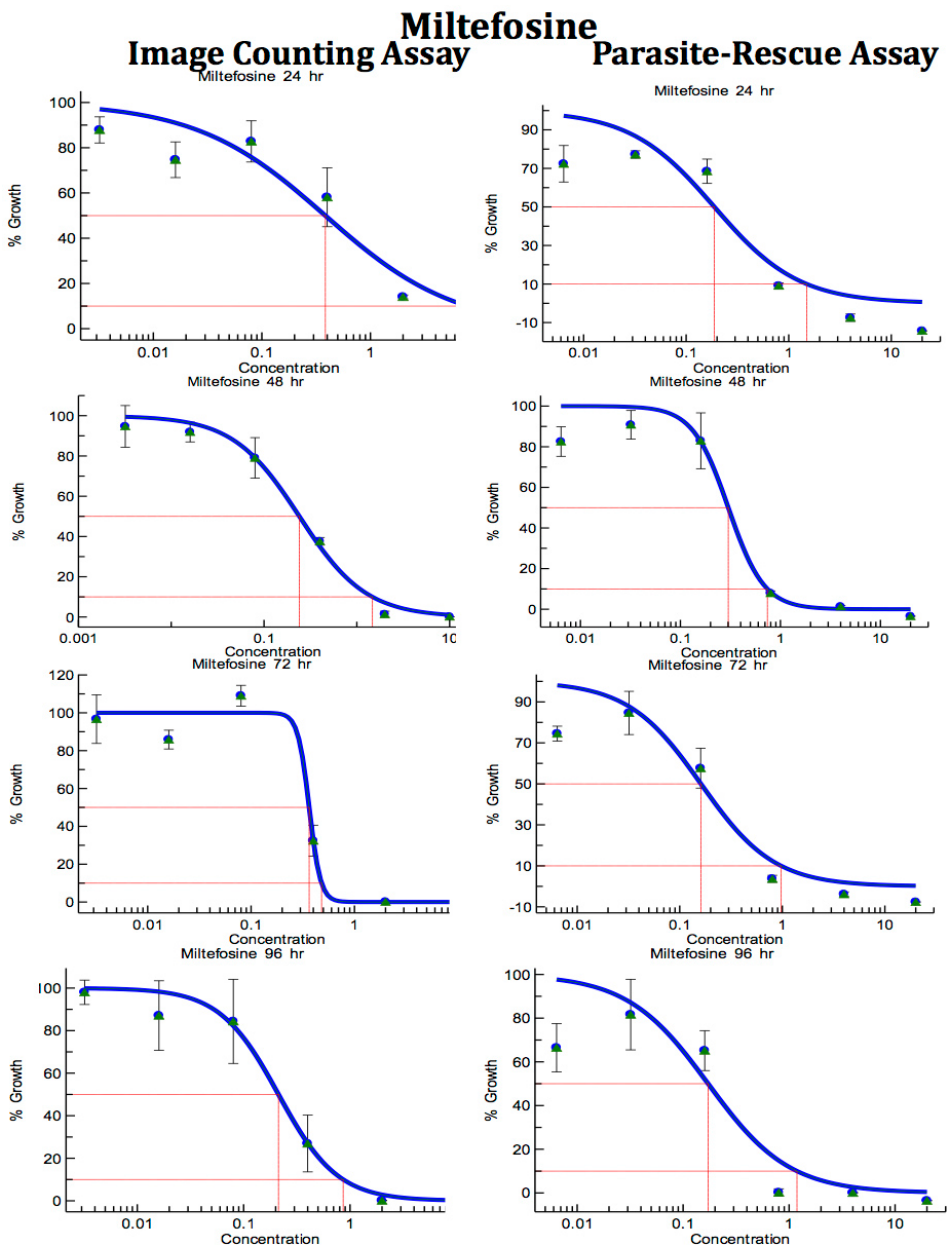

Figure 2.9: Comparison of Digital-Image-Analysis-Direct-Counting-Assay and PRT assay for anti-leishmanial drug screening (Miltefosine). The infected macrophages were treated with different concentrations of standard anti-leishmanial drug for different time periods. IC50 (μg/mL) values were computed from the dose-response curves by Excelfit. Figure from Jain et al., JoVE, 2012 (Jain et al., 2012).

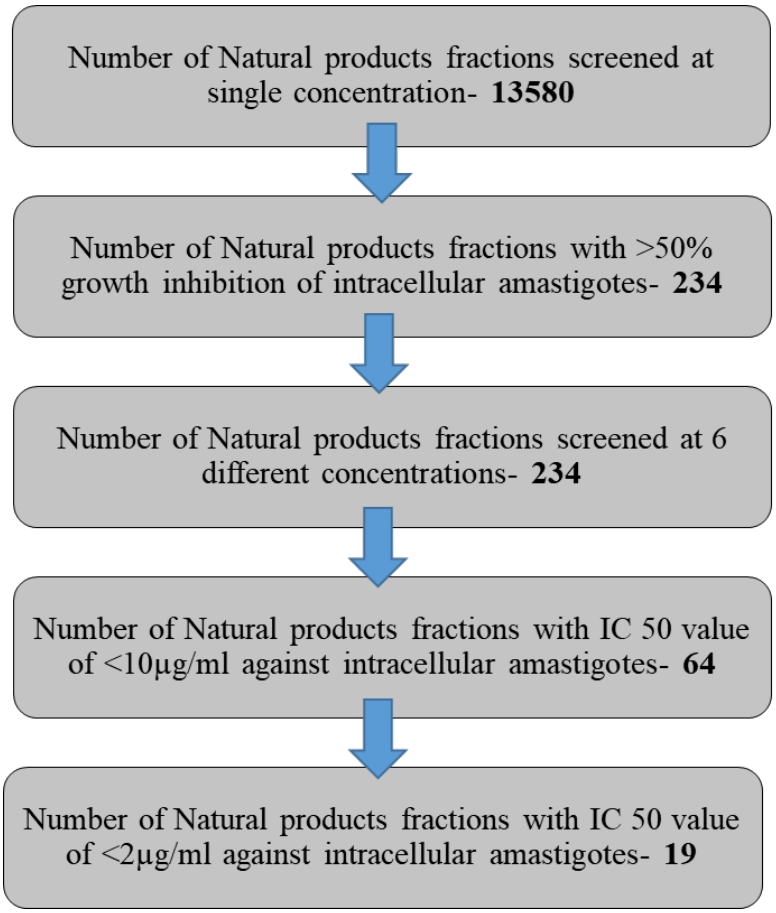

Figure 2.10. Flow diagram for the screening of natural products fractions library. Total of 13580 fractions was screened with PRT assay for intracellular amastigotes of *L. donovani at a* single concentration. 234 plant fractions have more than 50% inhibition for intracellular amastigotes. 234 active fraction was again screened at 6 different concentrations for concentration-response curve analysis. The 64 plant fraction was confirmed with an IC50 value of <10µg/ml. Total 19 plant fractions have potent activity with IC50 value <2µg/ml.

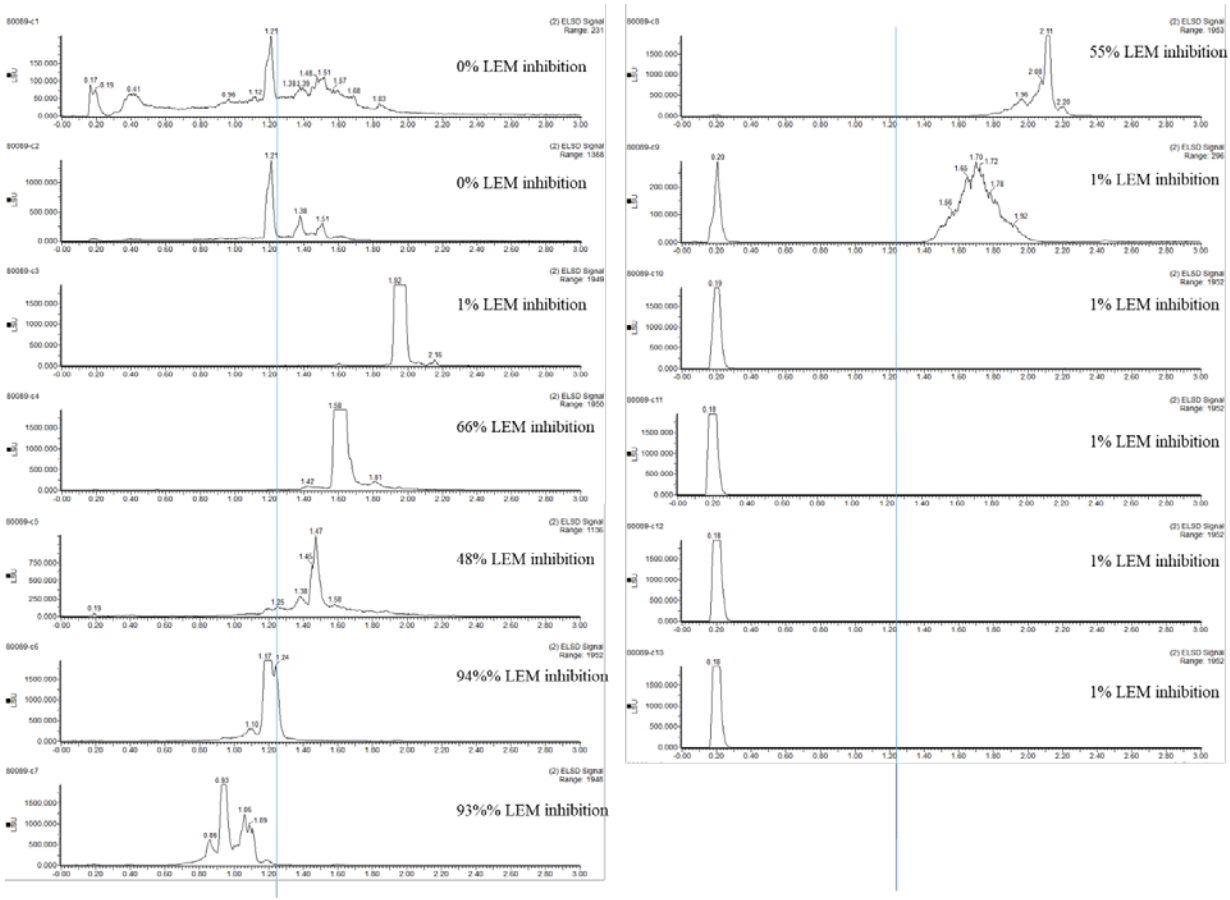

Figure 2.11: ELSD data for fractions of *Nerium oleander* plant extract 80089. % LEM inhibition- Inhibition of intracellular amastigotes growth in PRT assay. The ELSD data of all fractions of *Nerium oleander* plant extract 80089 are compared. The retention time of peaks in ELSD spectra of active fraction those are not present in inactive fractions was selected for further mass spectra analysis. The active fraction 80089-C6 have peaks with retention time 1.17 and 1.24 those are not present in other inactive fraction.

Panel A

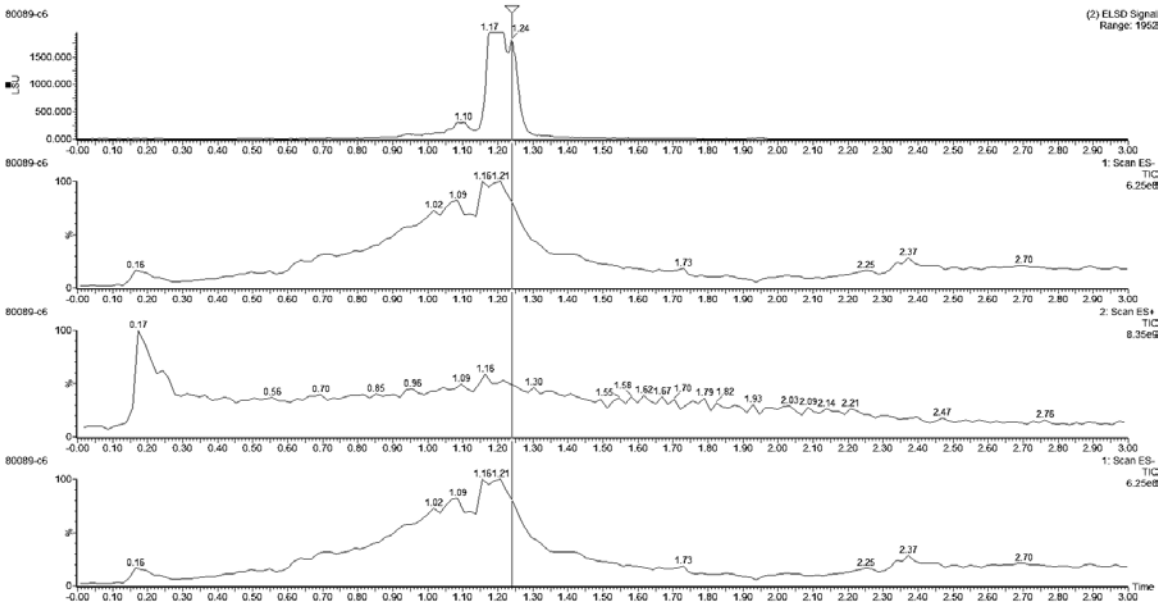

Panel B

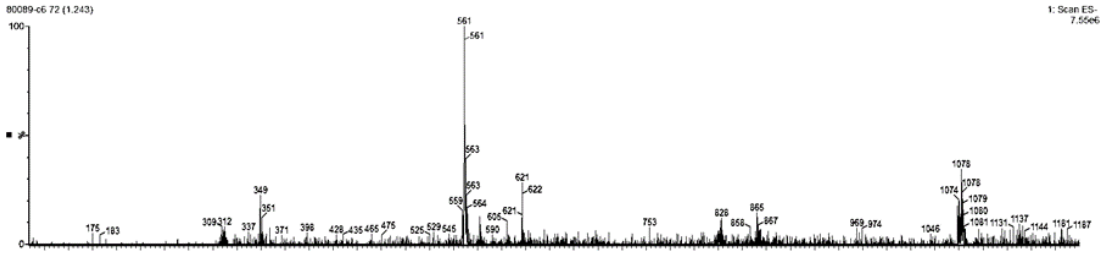

Panel C

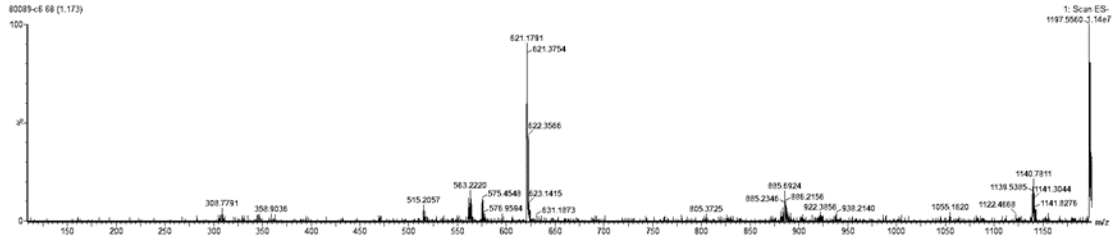

Figure 2.12: UPLC-MS-ELSD-PDA data for *Nerium oleander* plant extract fraction 80089-c6. Panel A have ELSD, PDA and ESI data of active fraction 80089-c6. Panel B and Panel C are the mass spectra at retention time 1.24 and 1.17 respectively.

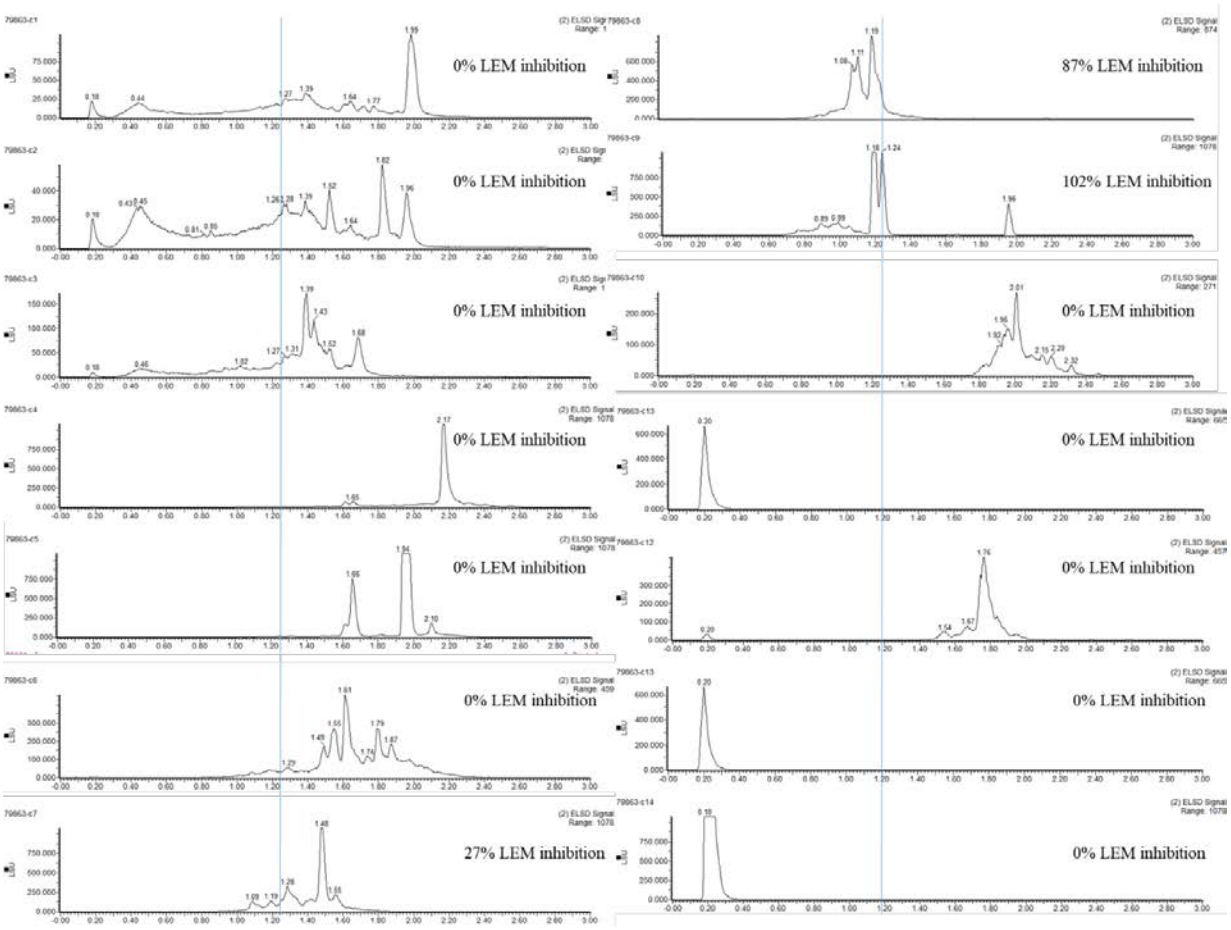

Figure 2.13: ELSD data for fractions of *Thuja occidentalis* plant extract 79863. % LEM inhibition - inhibition of intracellular amastigotes in PRT assay. The ELSD data of all fractions of *Thuja occidentalis* plant extract 79863 are compared. The retention time of peaks in ELSD spectra of active fraction those are not present in inactive fractions was selected for further mass spectra analysis. The active fraction 79863-C9 have peaks with retention time 1.18 and 1.24 those are not present in other inactive fraction.

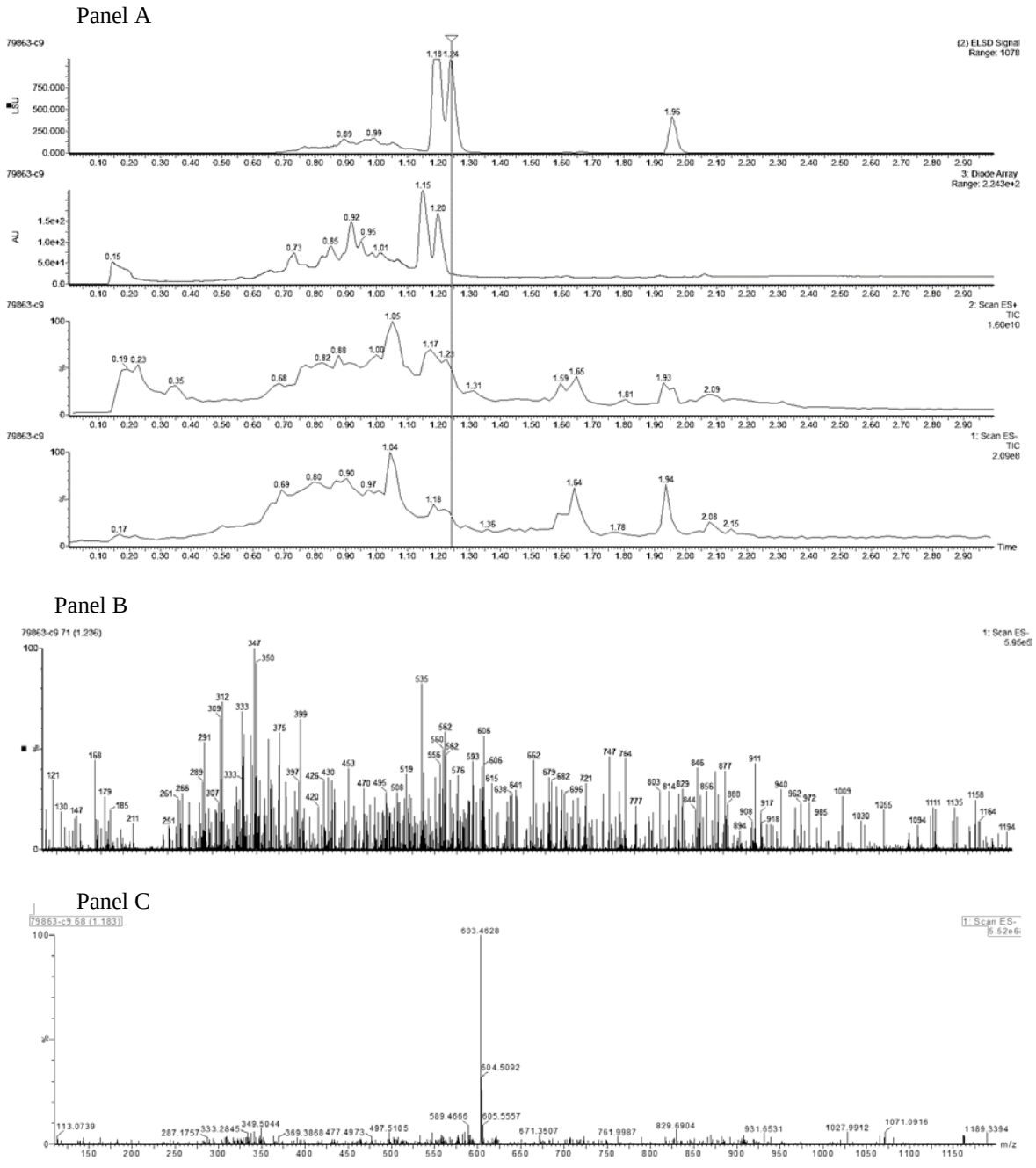

Figure 2.14: UPLC-MS-ELSD-PDA data for *Thuja occidentalis* plant extract fraction 79863-c9. Panel A have ELSD, PDA and ESI (Positive and negative) data of active fraction 79863-c9. Panel B and Panel C are the mass spectra at retention time 1.24 and 1.18 respectively.

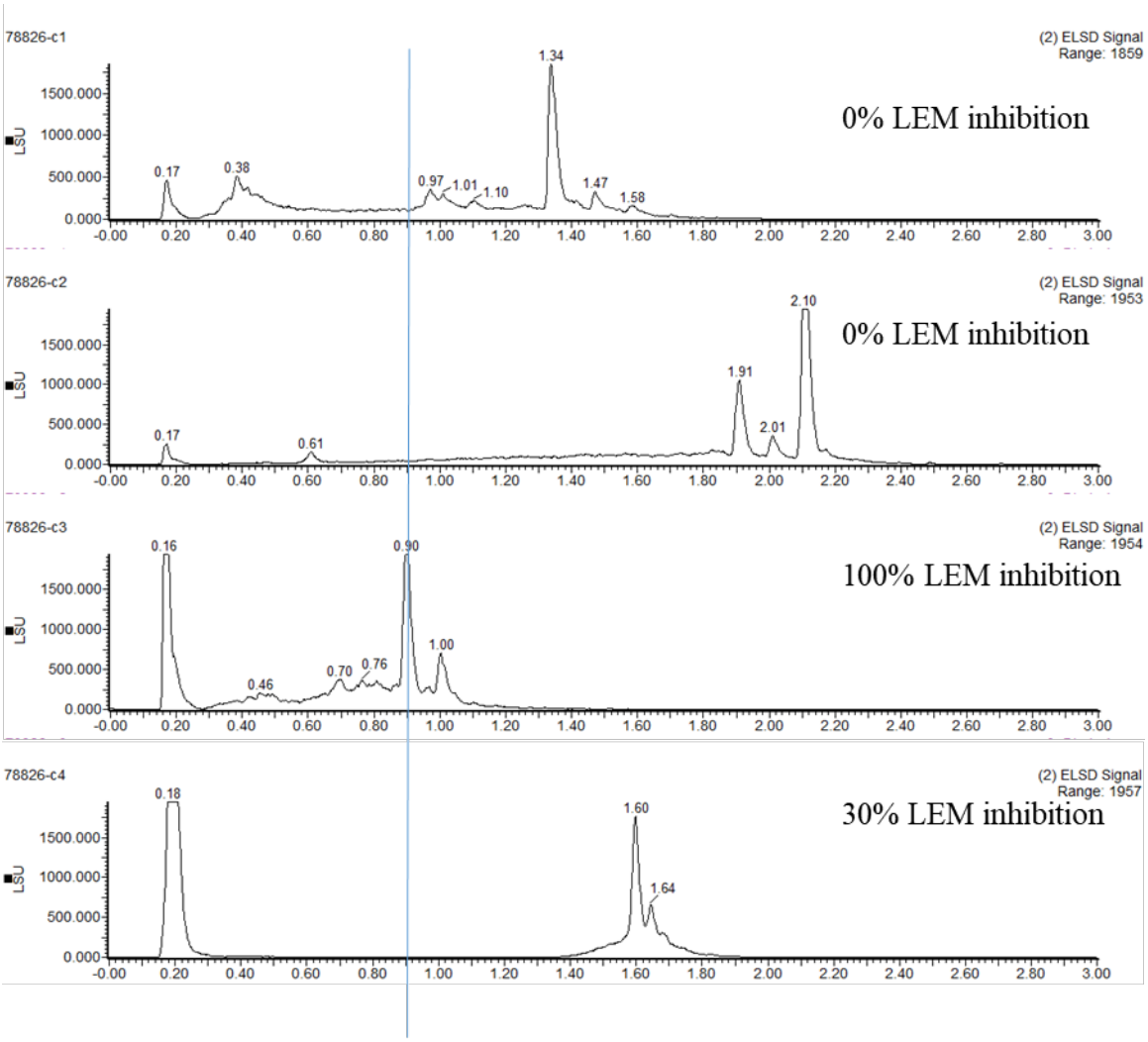

Figure 2.15: ELSD data for fractions of *Asclepias asperula* plant extract 78826. % LEM inhibition - Inhibition of intracellular amastigotes in PRT assay. The ELSD data of all fractions of *Asclepias asperula* plant extract 78826 are compared. The retention time of peaks in ELSD spectra of active fraction those are not present in inactive fractions was selected for further mass spectra analysis. The active fraction 78826-C3 have peaks with retention time 0.90 and 1.00 those are not present in other inactive fraction.

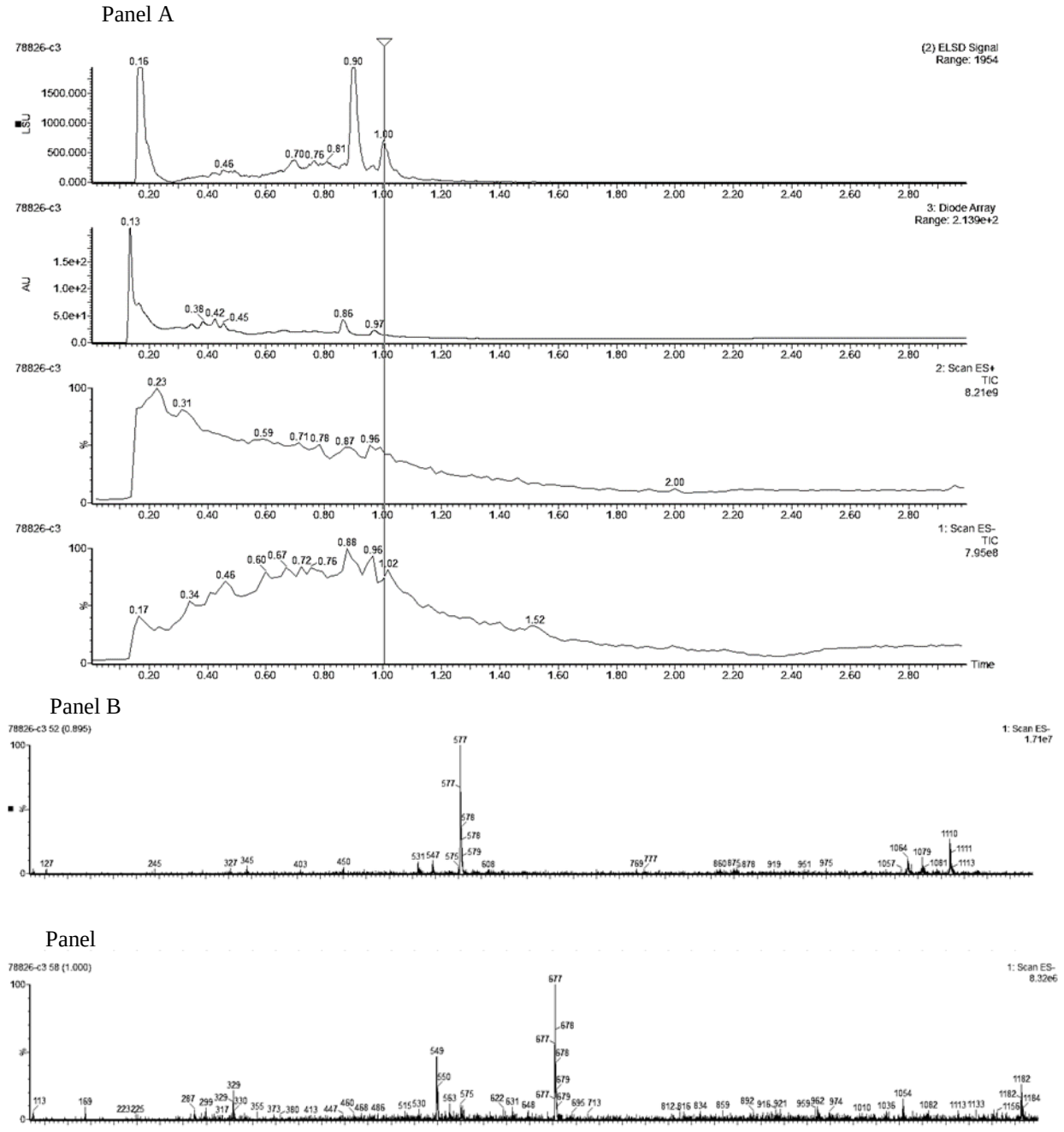

Figure 2.16: UPLC-MS-ELSD-PDA data for *Asclepias asperula* plant extract fraction 78826-c3. Panel A have ELSD, PDA and ESI (Positive and negative) data of active fraction 78826-c3. Panel B and Panel C are the mass spectra at retention time 0.089 and 1.00 respectively.

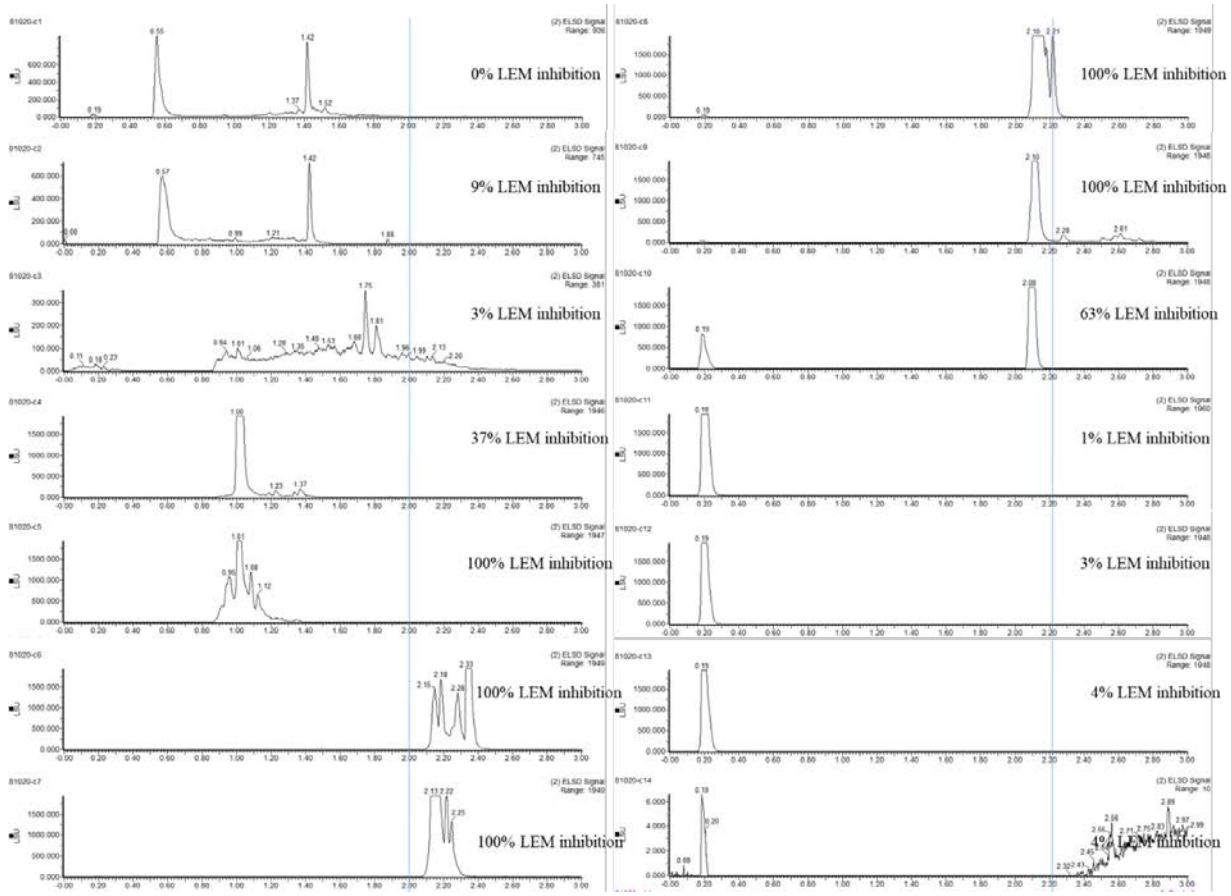

Figure 2.17: ELSD data for fractions of *Rhodea japonica* plant extract 81020. % LEM inhibition - inhibition of intracellular amastigotes in PRT assay. The ELSD data of all fractions of *Rhodea japonica* plant extract 81020 are compared. The retention time of peaks in ELSD spectra of active fraction those are not present in inactive fractions was selected for further mass spectra analysis. The active fraction 81020-C8 have peaks with retention time 2.216 and 2.095 those are not present in other inactive fraction.

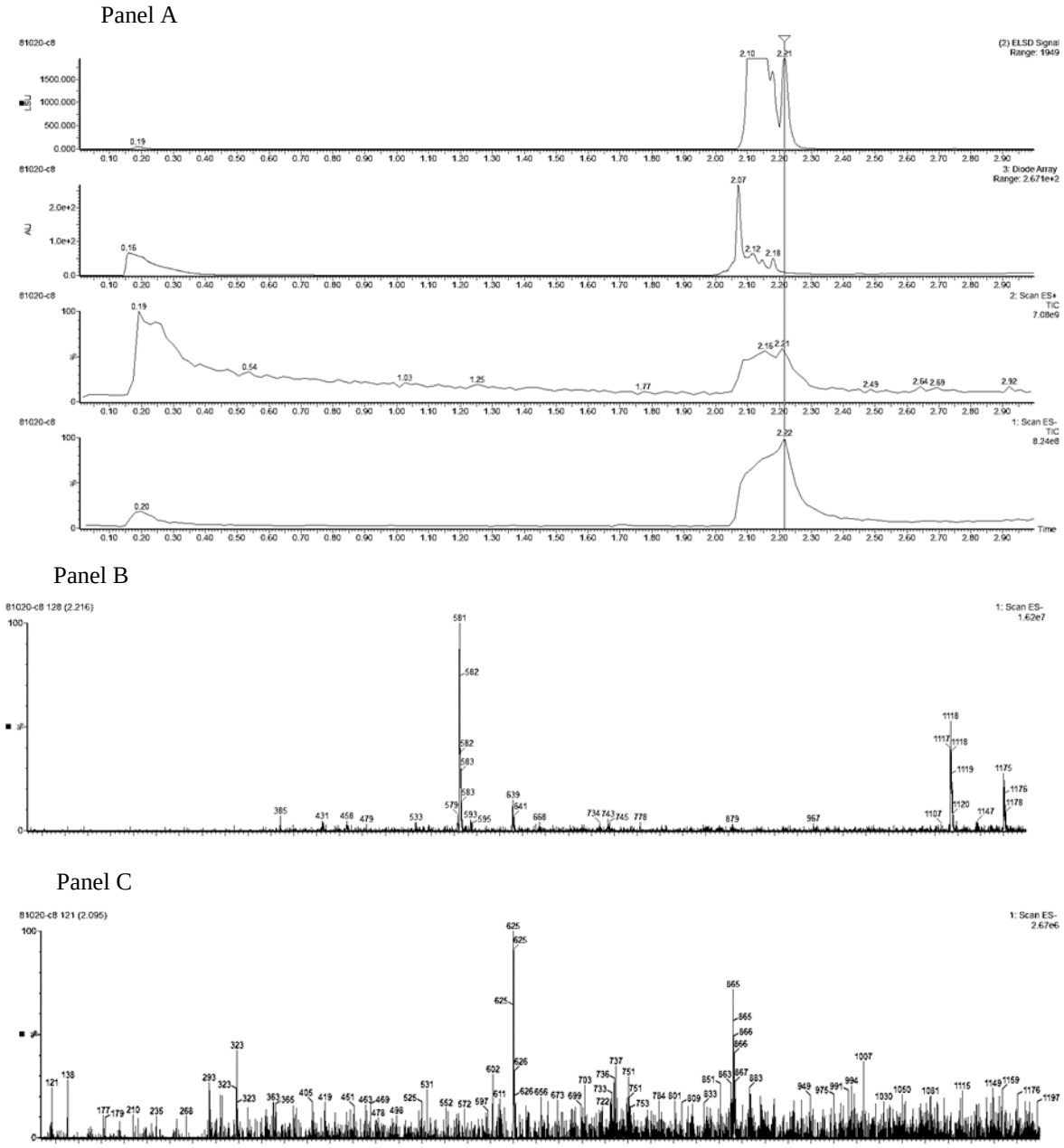

Figure 2.18: UPLC-MS-ELSD-PDA data for *Rhodea japonica* plant extract fraction 81020-c8. Panel A have ELSD, PDA and ESI (Positive and negative) data of active fraction 81020-c8. Panel B and Panel C are the mass spectra at retention time 2.216 and 2.095 respectively.

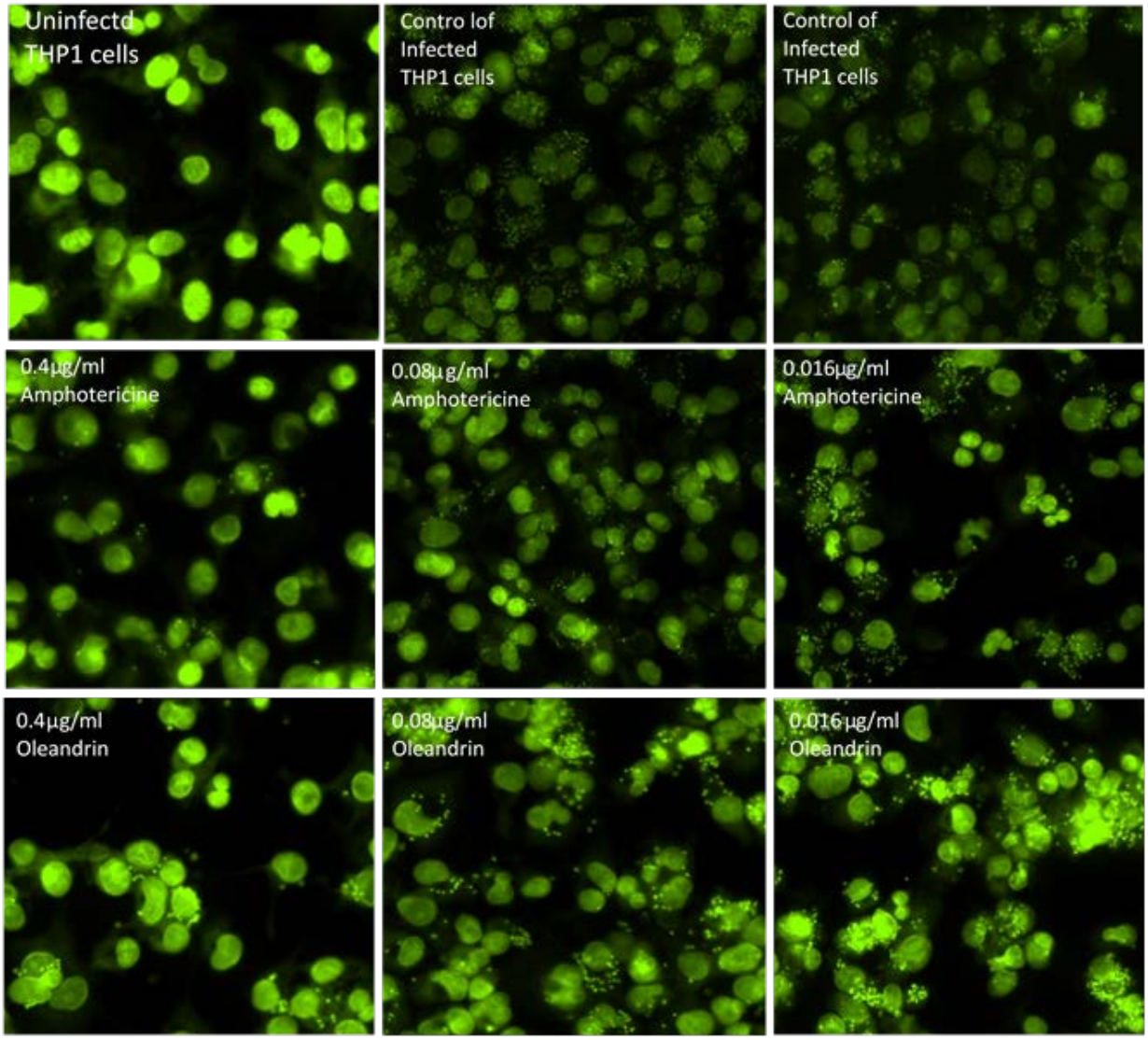

Figure 2.19: The antileishmanial activity of oleandrin by SYBR Green I nucleus DNA staining digital image analysis assay.

Table 2.1: Comparison of Digital-Image-Analysis-Direct-Counting-Assay and PRT assay for anti-leishmanial drug screening. The infected macrophages were treated with different concentrations of standard anti-leishmanial drug for different periods. IC50 (µg/mL) values were computed from the dose-response curves by Excelfit (Figures 7-9). [a]hours post drug treatment; [b]IAC = Image Analysis and Direct-Counting assay; [c]PRT = Parasite Rescue and Transformation assay. Values given are IC50 (concentration of the drug causing 50% inhibition of parasite growth) as µg/mL and are the mean ± S.D. of at least three experiments. * Statistically different (<0.05) compared to IC50 values with IAC assay. Table from Jain et al., JoVE, 2012 (Jain et al., 2012).

Test drug	24 hr[a] IC50 µg/ml		48 hr[a] IC50 µg/ml		72 hr[a] IC50 µg/ml		96 hr[a] IC50 µg/ml	
	IAC assay[b]	PRT assay[c]	IAC assay[b]	PRT assay[c]	IAC assay[b]	PRT assay[c]	IAC assay[b]	PRT assay[c]
Amphotericin B	0.24± 0.03	0.17± 0.01*	0.12± 0.04	0.20± 0.07	0.06± 0.01	0.06± 0.01	0.11± 0.03	0.10± 0.03
Pentamidine	>10	2.55± 1.16*	2.88± 0.58	1.43± 0.91	1.24± 0.35	1.52± 0.16	0.71± 0.63	0.98± 0.33
Miltefosine	0.38± 0.02	0.19± 0.08*	0.24± 0.06	0.30± 0.08	0.36± 0.02	0.16± 0.06	0.21± 0.15	0.17± 0.10

Table 2.2: Antileishmanial activity and THP1 toxicity of the most active plant extract fractions. NP=Natural Product number. Parent Extract= Original extract that was fractionated into several fractions. The ic50= inhibitory concentration at which 50 % parasite growth inhibited compared to the untreated positive control of parasite. IC90= inhibitory concentration at which 90 % parasite growth inhibited compared to the untreated positive control of parasite.

Sample information				THP1 cells internalized Amastigotes		THP1 Cytotoxicity	
NP number	Parent extract number	Sample Name	Sample Code	IC50 µg/mL	IC90 µg/mL	IC50 µg/mL	IC90 µg/mL
86064	79863	*Thuja occidentalis c9*	79863-c9	0.25	>10	>10	>10
85901	78826	*Asclepias asperula c3*	78826-c3	0.33	0.69	>10	>10
90057	81079	*Inga laurina c5*	81079-c5	0.86	4.00	>10	>10
89396	81004	*Gymnocladus dioica c7*	81004-c7	1.69	3.29	>10	>10
89480	81020	*Rhodea japonica c5*	81020-c5	1.08	2.56	>10	>10
89481	81020	*Rhodea japonica c6*	81020-c6	0.70	3.37	>10	>10
89482	81020	*Rhodea japonica c7*	81020-c7	0.39	1.13	>10	>10
89483	81020	*Rhodea japonica c8*	81020-c8	0.41	0.53	>10	>10
86328	80088	*Nerium oleander c3*	80088-c3	0.25	0.70	>10	>10
86329	80088	*Nerium oleander c4*	80088-c4	0.53	3.04	>10	>10
86344	80089	*Nerium oleander c6*	80089-c6	0.03	0.15	>10	>10
86345	80089	*Nerium oleander c7*	80089-c7	0.54	2.69	>10	>10
88490	80620	*Marah macrocarpus c8*	80620-c8	1.66	>10	>10	>10
88491	80620	*Marah macrocarpus c9*	80620-c9	1.07	>10	>10	>10
88571	80625	*Juniperus californica c5*	80625-c5	1.75	>10	>10	>10
88928	80650	*Juniperus deppeana c5*	80650-c5	1.85	>10	>10	>10
91657	79612	*Eclipta prostrata c5*	79612-c5	0.80	>10	9.34	>10
93627	81341	*Oplopanax horridus c6*	81341-c6	1.98	>10	>10	>10
97654	83352	*Falcataria moluccana c7*	83352-c7	1.29	4.75	>10	>10
103651		Amphotericin B	AmB	0.10	0.11	>10	>10
103650		Pentamidine	Pent	2.51	3.12	>10	>10

2.6. DISCUSSION

There are several methods available for anti-leishmanial drug screening based on macrophage-amastigote models. Assays can be done with the peritoneal exudate cells (PEC) collected from mice, peripheral blood monocyte cells (PBMC) (Seifert et al., 2010), bone marrow-derived macrophages (BMM), monocytic cell lines (J774 and RAW264.7) (Kolodziej and Kiderlen, 2005) and human monocytic cells (THP1, U937, HL-60) (Maia et al., 2007). The assays, which use dividing host cells, must ensure that the confounding effects of drug activity on both parasite and host cells number are considered. The differentiated primary macrophages collected from various sources such as mice and rats are non-dividing in nature. These cell preparations may not have homogeneous cell populations. Monocytic cells-derived cell lines are homogenous in nature and are a better model for the macrophage-amastigote-based screening. Differentiated THP1 cells (human acute monocytic leukemia cell line) can form a non-dividing monolayer and offer an attractive alternative to primary isolated macrophages.

To overcome the demerits and limitations of previous macrophage-amastigote-based screening assays (Gupta and Nishi, 2011), we have developed and optimized a parasite rescue and transformation (PRT) assay. This assay is based on the application of differentiated THP1 cells as the host macrophages. The differentiated THP1 cells have good homogeneity and are non-dividing in nature, as the host cells. The PRT assay described here is comparable to the assay based on Digital-Image-Analysis-Direct-Counting of the intracellular amastigotes. Fluorescent and DIC microscopy, digital image analyses by ImageJ for differential counting of the macrophage nuclei and the parasite nuclei has been further refined. Capturing the images under fluorescent light filters and differential interference contrast (DIC) filters have improved the quality of digital images for more accurate counting of the intracellular amastigotes. The

fluorescent and DIC images can be merged to obtain the digital images with clear macrophage cell outlines and fluorescent intracellular nuclei. The macrophage nuclei and the parasite nuclei can be differentially recognized with ImageJ. Therefore, both Digital Image Analysis (DIA) Assay and PRT Assay have the potential for automation and application to large-scale screening. Critical steps in the PRT Assay are: (a) repeated washings of THP1 cell cultures after exposure to Leishmania promastigotes, to ensure almost complete removal of the non-internalized promastigotes and (b) controlled lysis of the infected THP1 cells with SDS. Both the steps may also be controlled with automation and should not compromise with a throughput of the assay. The second step of washings, after exposure of the Leishmania-infected THP1 cells to the test drugs/compounds remove the remaining non-internalized parasites, if any. The PRT Assay offers significant advantages over existing microscopic, reporter gene and image analysis assays. The assay is simple, robust, and reproducible, can be automated for large-scale screening and therefore should have important application in screening of large compounds libraries for new anti-leishmanial drug discovery. Further, the assay can also be applied for evaluating infectivity of clinical, as well as, laboratory isolates of Leishmania *in vitro* (Hendrickx et al., 2015; Paape et al., 2014; Price et al., 2013).

The PRT assay and cytotoxicity assay against differentiated THP1 cells were applied for screening of a library of 13584 natural products fractions. A total of 243 fractions were identified with 50% or higher inhibition vs. leishmania intracellular amastigotes. The active 240 fractions were screened further for dose-response analysis, and 64 fractions were confirmed with IC_{50} <10µg/mL. Notably, the most active anti-leishmanial fractions originated from *Thuja occidentalis* (IC_{50}-0.25 µg/mL), *Asclepias asperula* (IC_{50}-0.33 µg/mL), *Rhodea japonica* (IC_{50}-0.41µg/mL) and *Nerium oleander* (IC_{50}-0.03 µg/mL). The active fractions from *Thuja occidentalis* and *Nerium*

oleander were selected for further analysis. Oleandrin was confirmed as an active constituent from the active fraction of *Nerium oleander* (Unpublished). Similarly, Deoxypodophylotoxin was confirmed as an active constituent from the active fraction of *Thuja occidentalis* (Yang et al., 2014). Oleandrin is an inhibitor of p-type ATPase (Jortani et al., 1996) and deoxypodophyllotoxin is a topoisomerase inhibitor (Wang et al., 1992).

Further original plant of active extract fractions was investigated in the literature. *Thuja occidentalis* is an evergreen coniferous ornamental tree, which is native to the eastern Canada and the Northeastern United States. Several anticancer activities have been reported in *Thuja occidentalis* (Biswas et al., 2011; Mazzio et al., 2014; Sunila and Kuttan, 2006). Even a protective action of *Thuja occidentalis* has been reported against the damage induced by gamma radiations (Sunila and Kuttan, 2005). Clinical efficacy of *Thuja occidentalis* has been reported in the treatment of upper respiratory tract infections (Naser et al., 2005). *Thuja occidentalis* and its active compound, thujone have an anticancer effect and promising effects in the treatment of polycystic ovary syndrome (Biswas et al., 2011; Kupeli Akkol et al., 2015). *Thuja occidentalis* also shows antioxidant potential (Yogesh and Ali, 2014) and ability to counteract oxidative-induced damage has been reported in isoquercitrin from *Thuja orientalis* (Jung et al., 2010). Anti-inflammatory activity is also reported in *Thuja orientalis*. *Asclepias asperula* is reported as an ingredient in Hispanic folk medicine preparations (Kelley et al., 1988). Desglucouzarin, a cardenolide reported in *Asclepias asperula* has Na^+, K^+-ATPase inhibition activity (Abbott et al., 1998). Antimicrobial and cytotoxic activities are reported in *Inga laurina* plant (Furtado et al., 2014). Cytotoxic activity has been reported in rhodexin A, which is a cardiotonic agent in *Rhodea japonica* (Masuda et al., 2003). Several cardenolides have been reported in *Nerium oleander,* which may be responsible for its toxicity and also pharmacological activity (Bai et al., 2010; Zhao et al., 2011). The anticancer

activities have been reported in isolated cardenolides particularly oleandrin from *N. oleander* which acts through inhibition of the plasma membrane-bound Na^+K^+-ATPase (Pan et al., 2015; Rashan et al., 2011). Bioactive pregnanes and triterpenes from *Nerium oleander* have shown the anti-inflammatory and cytotoxic activity (Bai et al., 2007; Fu et al., 2005; Zhao et al., 2006). Hepatoprotective and neuro protective activity have been reported in *Nerium oleander* (Dunn et al., 2011; Singhal and Gupta, 2012). Antifungal activity against plant fungal diseases has been reported in *Nerium oleander* (Hadizadeh *et al*., 2009). The anticancer activity has been reported in *Juniperus communis* (Van Slambrouck *et a*l., 2007). Leishmanicidal activity has already been reported in saponins isolated from the leaves of *Eclipta prostrate* (Khanna *et al*., 2009). *In vivo* Antiplasmodial activity has been reported in palladium nanoparticles of *Eclipta prostrata* extract (Rajakumar et al., 2015). *Eclipta prostrata has* shown anti-angiogenic and antitumor activity also (Kim et al., 2015; Lirdprapamongkol et al., 2008; Liu et al., 2012). Extract of *Eclipta prostrata* has been used for its anti-venom potential (Melo et al., 1994; Pithayanukul et al., 2004). *Eclipta prostrata* also found effective in reducing serum lipid levels (Dhandapani, 2007; Zhao et al., 2015). antibacterial and antifungal activities also reported in *Eclipta prostrata* (Wiart et al., 2004). Echinocystic acid, Thiophenes, polyacetylenes and terpenes from *Eclipta prostrate* has shown anti-inflammatory properties (Ryu et al., 2013; Xi et al., 2014). *Oplopanax horridus* is an ethnobotanical plant used by the indigenous people native to the Pacific Northwest of North America (Calway et al., 2012). Potential anticancer activity has been reported in compounds (falcarindiol and oplopantriol A) isolated from *Oplopanax horridus* (Jin et al., 2014; Wang et al., 2013; Zhang et al., 2014). Antimycobacterial effect has also been reported in *Oplopanax horridus* (Kobaisy et al., 1997; Qiu et al., 2013).

In conclusion, the *in vitro* screening of more than 13584 plant fractions, prepared from 958

plants extracts has been done against macrophage cells internalized *L. donovani* amastigotes. Macrophage cells internalized amastigote form of parasite represent the real pathophysiology of leishmaniasis disease. Most of the active plant fractions have good antileishmanial activity with no cytotoxicity to THP1 cells. The active fractions of plants extracts namely, *Thuja occidentalis, Asclepias asperula, Inga laurina, Rhodea japonica, Nerium oleander, Eclipta prostrata* represent new antileishmanial leads. Most of the leadplant fractions have very limited phytochemical and pharmacological data available. Further, follow up studies with these plant fractions are likely to provide novel compounds as potential antileishmanial drug leads.

CHAPTER III

DEVELOPMENT OF TRANSGENIC LEISHMANIA DONOVANI PARASITES WITH STABLE EXPRESSION OF CITRINE AND MCHERRY REPORTER PROTEINS AND THEIR UTILITY FOR *IN VITRO* ANTILEISHMANIAL DRUGS SCREENING.

3.1. INTRODUCTION

Phenotypic parasite culture-based *in vitro* screening and *in vivo* preclinical evaluation are the hallmark of new antileishmanial drug discovery (Gupta and Nishi, 2011; Reguera et al., 2014; Sereno et al., 2007). The reporter gene is a segment of DNA containing a gene sequence that has been isolated from one organism and is introduced into a different organism. This non-native segment of DNA has retained the ability to express the protein that has a readily measurable phenotype and is easily distinguishable over endogenous cellular background. Transgenic parasites expressing reporter proteins are valuable tools to perform robust high throughput screening (HTS) and to understand the underlying mechanisms of pathogenesis (Dube et al., 2009; Lang et al., 2009). The technologies based on genetically modified pathogens represent valuable complementary tools for *in vitro* screening as well as real-time *in vivo* imaging. As long as the transgenic parasite retains the virulence of the parent parasite, they can be used for studies of pathogenesis and therapy in several ways. Several attempts have been made to develop transgenic cell lines that express bioluminescent and/or fluorescent reporter proteins (Hutchens and Luker,

2007; Lang et al., 2009). Reporter transgenic parasite can be developed by episomal transfection or by stable transfection methods. The reporter gene retained in the transfected plasmid in the transgenic parasite. While, the reporter genes, which get integrated into the genome of the parasite, the stably transfected transgenic cells retain the genetic information of reporter gene for a longer duration. The transgenic parasite cell lines with fluorescent reporter genes offer several advantages. Fluorescent reporters do not require specific substrates to convert the reporter protein to a measurable phenotype. The fluorescence emitted is stable over the time and reliable for studies involving longer durations. This approach is also useful when studying the tissue harvested from infected animals since parasites can be individually identified (Shaner et al., 2005).

The first transgenic Leishmania species was developed with the green fluorescent protein (GFP) as a reporter protein (Ha et al., 1996) by episomal transfection. Several other researchers have developed GFP transgenic cell lines of *L. infantum* (Kamau et al., 2001), *L. donovani* (Singh and Dube, 2004) and *L. amazonensis* (Chan et al., 2003) by episomal transfection and further addressed the application of HTS methods. Significant research has been done for developing the HTS methods for amastigotes forms using transgenic GFP amastigotes of *L. donovani* (Dube et al., 2005), and *L. Major* (Kram et al., 2008). Automation for large compounds library screening may be possible using reporter genes. The majority of transgenic parasite cell lines requires drug selection for maintaining the episomal expression of the reporter genes. This may not be ideal for a drug screening experiments (Sereno et al., 2007). In case of episomal reporters, the relative expression of the reporter gene may depend on the number of copies of the transfected plasmid, rather than on the activity of the drug (Buckner and Wilson, 2005). The assays based on transgenic parasites with luciferase reporter gene required substrate and cell lysis buffer, which make the assays expensive for large-scale screening (Calvo-Alvarez et al., 2015; Roy et al., 2000). BALB/c

mice and Syrian golden hamsters are commonly used experimental animal models for evaluating antileishmanial effects and host-parasite interactions (Gupta and Nishi, 2011). For visceral leishmaniasis, most of the *in vivo* studies have been done by classical microscopic methods.

A stable transfection method in which the GFP gene was integrated downstream of the 18S ribosomal promoter region of Leishmania genome was developed (Misslitz et al., 2000). Different transgenic leishmania parasite (*L.donovani, L.major, and L. infantum*) have been developed by stable transfection method (Bolhassani et al., 2011; Singh et al., 2009). However, the stable transfection of the enhanced GFP (EGFP) reporter has been found suitable for both *in vitro* and *in vivo* leishmania parasite related studies (Pulido et al., 2012). Although native GFP produces bright fluorescence and is extremely stable, the excitation maximum is close to the ultraviolet range, which can damage the live cells.

Transgenic *Leishmania mexicana* expressing red fluorescence (RFP) has been used to determine the early stages of cutaneous leishmaniasis pathogenesis at the infection site (Millington et al., 2010). Transgenic *L. major* with RFP-1 has been used to identify the site of sand-fly bites *in vivo* in a mouse model. These studies reveal essential roles for both neutrophils and dendritic cells in early leishmania infections (Peters et al., 2008; Ribeiro-Gomes et al., 2012). Transgenic mCherry *L. infantum chagasi* a parasite of visceral leishmaniasis (VL) revealed the recruitment of neutrophils and role of dendritic cells in VL (De Trez et al., 2009; Lecoeur et al., 2010; Thalhofer et al., 2011). Transgenic *L. donovani* cells, stably expressing either EGFP or RFP, have been used to identify hybrid parasites produced during the early development of the sandfly (Sadlova et al., 2011). Similarly, transgenic *L. infantum* parasite stably expressing either citrine or mCherry have been used to show the intraclonal genetic exchange in Trypanosomatids (Calvo-Alvarez et al., 2014). A *L. major* strain, which episomally expressed the DsRed protein, was used for quantifying

the infectious dosage transmitted by a sandfly bite (Kimblin et al., 2008).

mCherry has improved photostability as well as suitability for intravital imaging (Graewe et al., 2009). mCherry is a protein derived from the coral *Discosoma striata* RFP. It has a maximum emission peak at 610 nm with a 587 nm excitation wavelength. Despite the fact that it is 50% less bright than EGFP, it is more photostable and has higher tissue penetration [12]. mCherry is a suitable choice for applications of single-molecule fluorescence or multicolor fluorescent imaging [34]. Transgenic mCherry *L. major* has been developed by stable transfection method and used for *in vitro* and *in vivo* screening for cutaneous leishmaniasis (Calvo-Alvarez et al., 2012). Recently transgenic mCherry *L. donovani* (stably transfected) based screening method was developed for promastigote forms of the parasite (Vacchina and Morales, 2014).

Intracellular amastigotes represent the real pathophysiology of leishmaniasis disease. Parasite resides in deep visceral organs particularly in liver and spleen in visceral leishmaniasis disease state. That warrants a need for the development of transgenic cells, which could be utilized for *in vitro*, *ex-vivo* well as *in vivo* intracellular amastigotes antileishmanial screening. Ideally, the fluorescent reporter gene model should be free of ultraviolet excitation range and should have good penetration. Considering these requirements, two different stably transfected transgenic *L. donovani* cell lines by integrating *mCherry* or *citrine* open reading frames (ORFs) into the 18S rRNA *ssu* locus of *L. donovani* parasite genome, which constitutively expresses Citrine or mCherry fluorophore-proteins. We selected Citrine, a green fluorescent protein derivative, derived from the jellyfish *Aequorea victoria* (Haas et al., 2012; Roura et al., 2013) and mCherry, a red fluorescent protein derived from the tetrameric Discosoma (Campbell et al., 2002) as the reporter genes. There are several advantages of these reporter genes. The excitation spectra of these fluorophores are free of ultraviolet region. The proteins expressed from

mCherry and Citrine genes have high photostability, resistance to photobleaching and bright fluorescence. Both proteins constitutively expressed in the leishmanial cytoplasm mature rapidly, allowing fluorescence detection shortly after the gene is expressed. This is appropriate for real-time analysis. Integration of *mCherry* and *citrine* ORFs was done using LEXSY plasmid. LEXSY has been constructed based on the protozoan host, which combines eukaryotic protein synthesis and modification with simplicity and ease of handling. This system promises protein synthesis with correct folding with a full range of post-translational modifications. This vector also gives high expression success rate (LeBowitz, 1994). LEXSY is a constitutive type of LEXSY plasmid, which has 3' and 5' end *ssu* regions. These regions direct the linearized DNA with target gene and marker gene for homologous recombination at *ssu* locus of Leishmania parasite genome.

3.2 HYPOTHESIS

The bright fluorescence of Citrine or mCherry fluorescent reporter proteins allows detection and quantification of stably transfected transgenic leishmania cells by different fluorescence-based techniques like fluorescence reading, fluorescent microscopy, and flow-cytometry.

3.3 OBJECTIVES

Stable transfection of mCherry and Citrine reporter genes was done using leishmania expression plasmid vector (LEXSY). A plasmid with mCherry reporter gene with blasticidin marker and another plasmid with Citrine reporter genes with hygromycin B marker were electroporated into wild-type of *L. donovani* cells. The strong fluorescent signal from mCherry and Citrine transgenic *L. donovani* parasite indicated the successful development of transgenic

parasites. Both mCherry and Citrine transgenic parasite could be analyzed by different fluorescence-based techniques. The fluorimetric measurements, fluorescent microscopy and flow cytometry were applied for growth analysis of promastigotes and macrophage-internalized transgenic *L. donovani* amastigotes.

3.4. MATERIALS AND METHODS

3.4.1. *LEISHMANIA DONOVANI* PROMASTIGOTE CULTURE

The cell cultures of promastigote forms of wild type *L. donovani* (WT-Ld) (S1 strain) were maintained in M199 medium supplemented with 25 mM HEPES pH 7.2, 0.1 mM adenine, 0.0005% (w/v) hemin, 2 mg/mL biopterin, 0.0001% (w/v) biotin, 10% (v/v) antibiotic cocktail (50 U/mL penicillin, 50 mg/mL streptomycin) and 10% fetal bovine serum.

3.4.2. THP1 CELLS CULTURE AND DIFFERENTIATION

THP1 cells are being grown in RPMI medium supplemented with 10% fetal bovine serum. The culture is maintained at 37^{o}C in 5% CO_2 incubator. Subculture is being done on every 3-4 days or cell growth of 0.8 million cells/mL. THP1 cells were differentiated using Phorbol 12-myristate 13-acetate (PMA) as described previously. After differentiation, the medium with PMA from each well was discarded, and adherent cells were gently washed at least twice with serum-free RPMI1640 medium (Jain et al., 2016b; Jain et al., 2012).

3.4.3. LEXSY PLASMID WITH *MCHERRY* AND *CITRINE* GENE INSERTS

The plasmids were adapted from a previous study (Calvo-Alvarez et al., 2014). In short, two fluorescent proteins namely, mCherry (excitation 587 nm; emission 610 nm) and Citrine (Excitation 516 nm; emission 529 nm), were selected to develop two different transgenic *L. donovani* cell lines. For the *CITRINE-HYGROMYCIN (CTN-HYG)* construct, the 720-bp *CTN* coding region was amplified by PCR. The amplified DNA fragment was cut with *BglII-NotI* and inserted into the pLEXSY-hyg2 vector (Jena Bioscience GmbH, Germany) to yield *pLEXSY-CTN-HYG* construct. For the *mCherry-BLASTICIDIN (CHR-BSD)* construct, the 711-bp *CHR* coding region was amplified by PCR. The resulting fragment was digested with BglII-NotI and inserted into the pLEXSY-hyg2 vector (Calvo-Alvarez et al., 2012). The *HYG* selection drug cassette was replaced by the *BSD* ORF, which confers resistance to the antibiotic blasticidin S (Goyard and Beverley, 2000) (**Figure 3.1**).

3.4.4. GENERATION OF MCHERRY AND CITRINE TRANSGENIC *L. DONOVANI* PARASITES

Plasmids *pLEXSY-CTN-HYG* and *pLEXSY-CHR-HSP70-BSD* with Citrine and mCherry gene respectively were transformed into XL10-Gold ultracompetent *Escherichia coli* cells. The *mCherry* and *citrine* gene inserts in the respective plasmids were confirmed by *BglII* and *NotI* double digestion and analysis by agarose gel electrophoresis. The isolated plasmids were digested with *SwaI* restriction enzyme to linearize the plasmid DNA with *mCherry* and *citrine* genes. Linearization of the plasmids was confirmed by agarose gel electrophoresis. The linearized DNA was electroporated into wild-type *L. donovani* promastigotes. 20 ml *L. donovani* promastigote

culture (~ $5X10^6$ parasites/mL) was centrifuged at 3000 rpm for 10min at 4°C in two 15 ml tubes. The cell pellets were re-suspended in a total of 10 mL of pre-chilled cytomix. (~ $10X10^6$ parasites/mL). The cells were centrifuged again at 3000 rpm for 10min at 4°C in two 15 ml tubes. Cell pellets were finally re-suspended in 0.5 mL of ice-cold cytomix (~ $200X10^6$ parasites/mL). The cell suspensions were chilled on ice for 10 min. BioRad gene pulser was set for electroporation of L. donovani with linearized DNA from *mCherry* and *citrine* constructs. The electroporation conditions used (450 μF, 900V) that require a capacitance extender module with the gene pulsar unit (For 4mm distance cuvette 2.25kV/cm). 0.5 ml of the cell suspension (1 x 10^8 parasites) was mixed with the DNA to be electroporated in the pre-chilled centrifuge tube by pipetting up and down and transferred to a pre-chilled (4°C) 4mm electroporation cuvette and electroporated at selected pulse settings. The cuvette was returned to the ice after electroporation. The cells electroporated with *CHR-BSD* and *CTN-HYG* reporters linked to their corresponding antibiotic-resistance cassettes were obtained after the electroporation of *L. donovani* promastigotes with the large SwaI fragment from *pLEXSY-CHR-BSD* and *pLEXSY-CTN-HYG* vectors and plated on semisolid M199 medium. Transgenic *L. donovani* promastigotes derived from the integration of reporter genes into the leishmanial 18S rRNA locus were selected on semisolid medium containing 200 μg/mL of hygromycin B or blasticidin S, respectively. The colonies appeared after 2-3 weeks on semisolid M199 medium with respective resistance antibiotic. The colonies were transferred to M199 liquid medium without selection drugs for 24 h and then transferred to M199 liquid medium with selection drugs. The transgenic parasites were grown in M199 medium with selection drug to 10 generations. After 10 generations both transgenic parasites were transferred to M199 medium without selection drugs.

3.4.5. THE CONFIRMATION OF GENE INTEGRATION AND EXPRESSION IN TRANSGENIC *L. DONOVANI* CELLS

The confirmation of the presence of reporter genes in *L. donovani*, as well as integration of these reporter genes in *L. donovani* genome, was done by primer Polymerase chain reaction (PCR) method. Forward mCherry primer (P1), reversed mCherry primer (P2), forward citrine primer (P4) reverse citrine primer (P5) and forward integration primer (P3) were selected according to previously published research (Calvo-Alvarez et al., 2014). The linearized DNA with 5' and 3' *ssu* region get integration in *ssu* locus of *L. donovani* genome. So forward integration primer was selected from *L. donovani* genome *ssu* region and integration reverse primer was selected from the reporter gene either *citrine* or *mCherry* in linearized DNA 5' and 3' *ssu* integrated region (**Figure 3.2**). The genomic DNA was isolated by citrine transgenic, mCherry transgenic and wild-type *L. donovani* parasites and PCR was done using given primers.

Confirmation of gene expression was done by a strong fluorescent signal from mCherry or Citrine by fluorescence microscopy. The microscopic images were collected under Nikon 90i Eclipse fluorescence microscope. Citrine transgenic *L. donovani* (Citrine-Ld) cells were analyzed under Differential Interference Contrast (DIC), and Fluorescein isothiocyanate (FITC) filter and mCherry transgenic *L. donovani* (mCherry-Ld) cells were analyzed under DIC and TEXAS-RED (TXR) filter in a fluorescent microscope. Both citrine and mCherry transgenic *L. donovani* promastigotes were also run underflow cytometric analysis. Thirty thousand promastigotes per sample were analyzed in a flow cytometer for all promastigote parasites types including both mCherry-Ld and citrine-Ld promastigotes and WT-Ld promastigotes. Citrine-Ld promastigotes were analyzed in FL-1 channel histogram plot, and transgenic mCherry-Ld promastigotes were analyzed in FL-3 channel histogram plot. BD FACS Calibur flow cytometer.

3.4.6. DIRECT FLUORESCENT ANALYSIS (DFA) BASED *IN VITRO* SCREENING FOR TRANSGENIC PROMASTIGOTES PARASITES

Both mCherry-Ld and citrine-Ld parasites were serially diluted in 1:1 ratio from 20 million/mL to 0.625 million/mL in the M199 medium in 96 wells plates. Plates were read by the fluorimeter. For citrine-Ld parasites, plates were read at excitation 486 nm and emission 535nm. For mCherry-Ld parasites, plates were read at excitation 544 nm and emission 590nm. Based on this DFA of transgenic parasites, an assay has been applied to assess the activity of control drugs amphotericin B and pentamidine for 96 h. Simultaneously, AlamarBlue assay was applied for WT-Ld, mCherry-Ld and Citrine-Ld promastigotes parasites. Three-day-old cultures of mCherry-Ld citrine-Ld and WT-Ld promastigote parasites were diluted to 1 million parasites/mL. 196 µl of diluted culture was added to each well of the 96 well plate. 4 µl of diluted amphotericin B and pentamidine samples were added in plate culture. Assay for control drugs was done in triplicates. The plates were incubated in 26^{o}C for 96 h. The plates with mCherry-Ld and citrine-Ld promastigotes parasites were analyzed directly by the fluorimeter. The other plates with wild-type and both transgenic promastigote parasites with AlamarBlue assay were read on a fluorimeter All the IC50, and IC90 values were computed, and dose-response curves were developed by XLfit 5.2.2 software.

3.7.7. INFECTIVITY OF TRANSGENIC *L. DONOVANI* CELLS IN DIFFERENTIATED THP1 CELLS

Fifty thousand cells/well of THP1 cells were differentiated in chamber slides. For infecting differentiated THP1 cells, a 5-6 day old culture of mCherry-Ld and citrine-Ld stationary promastigote parasite were diluted to $2.5x10^6$ parasite cells/mL. 200 µl of diluted cultures were dispensed on differentiated THP1 cells in separate chamber slide. All chamber slides were incubated at 37°C in a 5% CO_2 incubator for 24 h to allow parasites to infect differentiated THP1 cells. All chamber slides with THP1 cells infected with *L. donovani* promastigotes were washed with serum-free, RPMI-1640 medium to remove the external parasite. Chamber slides were incubated again at 37°C, 5% CO_2 for 48 hr. After a 48 h incubation, chamber slides were washed three times with serum-free RPMI-1640 medium and washed once with warm (37^oC) Dulbecco's phosphate-buffered saline (DPBS). Four percent formaldehyde (v/v) was prepared from 16% (v/v) formaldehyde (methanol free, Polysciences, Inc) by diluting 1 to 4 in warm 1X PBS to make a 4% formaldehyde solution. DPBS was aspirated, and 200 µl warm 4% formaldehyde was dispensed on differentiated THP1 cells. Cells were allowed to fix for 15 min at 37^oC. Fixed differentiated THP1 cells were washed again with warm (37^oC) DPBS. Digital images have been captured from slides in different filters (DIC + FITC filter for Citrine-Ld and DIC + Texas red filter mCherry-Ld parasites. The number of differentiated THP1 cells and number of amastigotes in all images was calculated with the help of ImageJ software and infectivity were calculated by the ratio of infected amastigote THP1 cells.

3.4.8. FLOW CYTOMETRIC ANALYSIS OF INTRACELLULAR *L. DONOVANI* AMASTIGOTES

Fifty thousand cells/well of THP1 cells were differentiated in 96 well plates. For infecting

differentiated THP1 cells, a five to six-day-old promastigote cultures of both transgenic (both citrine-Ld and mCherry-Ld) and wild-type *L. donovani* were diluted to $2.5x10^6$ cells/mL. The diluted culture of mCherry-Ld, citrine-Ld and WT-Ld parasites was added over differentiated THP1 cells in separate 96 well plates. All 96 well plates were incubated at 37^oC in 5% CO_2 incubator for 24 hr. External parasites were washed with incomplete RPMI medium, and infected THP1 cells were treated with control drugs for 96 hr. Plates were again washed to remove the external parasites. Infected differentiated THP1 cells were detached by treating them with 20µl of 1X trypsin solution (0.25% trypsin (w/v)) for 5 min. Cells were gated from middle regions of SSC/FSC (Side scatter/forward scatter) plot for analysis to avoid the cell clumps and debris, and 10,000 gated events were analyzed on relevant histogram plot for the fluorescent peak. Peak in FL1-H (Green fluorescence) histogram plot was observed for the citrine-Ld parasite. Peak in FL3-H (Red fluorescence) histogram plot was observed for the mCherry-Ld parasite. Assay for control drugs was done in triplicates.

A parasite rescue and transformation (PRT) assay for macrophage cells internalized amastigote (Jain et al. 2012) with 96 h of treatment with control drugs (amphotericin B and pentamidine) were also performed using wild-type, transgenic citrine, and transgenic *L. donovani* parasites. Assay for control drugs was done in triplicates. A comparative analysis is given between PRT assay and FACS analysis in **Table 3.3**.

3.4.9. MICROSCOPIC ANALYSIS OF INTRACELLULAR TRANSGENIC AMASTIGOTES

The microscopic method was followed as mentioned above in 3.2.6. Section. The assay

has been done in triplicate for control drugs amphotericin B and pentamidine. Effect of control drugs was observed for 96 h medium with drug dilutions was replaced daily. The assay has been applied for both mCherry-Ld and citrine-Ld parasites. After 96 h, chamber slides were fixed with 4% formaldehyde. Digital images have been captured from slides in different filters (DIC + FITC filter for Citrine and DIC + Texas red filter mCherry Leishmania Parasite). (Jain et al., 2012). The infectivity was calculated from the ratio of total infected amastigote count to total THP1 cells count.

3.4.10. *IN VITRO* MACROPHAGE AMASTIGOTE ASSAY

A recently developed promastigote rescue assay was applied for both mCherry and citrine *L. donovani* parasites and wild-type of *L. donovani* parasite (Jain et al., 2012). The plates with differentiated THP1 cells were washed with serum-free medium with the help of 384 well plate cell washing system (Molecular device AquaMax 4000). *L. donovani* promastigotes were harvested at the stationary phase (metacyclic infective stage) and suspended into RPMI1640 medium with 2% FBS at the density of $2.5X10^6$ cells/mL. After 24 h the non-adherent macrophages and external Leishmania promastigotes were washed off with the serum-free RPMI1640 medium. Control drugs amphotericin B and pentamidine (six different concentrations in triplicate) were diluted in separate plates and transferred to plates with infected THP1 cells. The plates were placed again in a CO_2 incubator at 37^oC for 96 hr. After 96 h, the plates were washed again with serum free RPMI medium. Infected differentiated THP1 cells subjected to control lysis by 0.05% (w/v) SDS solution in incomplete RPMI medium for 30 seconds. SDS solution was diluted with completed RPMI medium after control lysis. Control lysis confirm the lysis of THP1

cells membrane lysis without affecting the viability of amastigote. Plates with rescued amastigotes allowed to grow and transform to promastigotes for 48 h at 26^{o}C incubator. After 48 h AlamarBlue was added to the plates and again incubated at 26^{o}C for overnight. Plates were read on a fluorimeter (BMG Lab Technologies) at an excitation wavelength of 544 nm and an emission wavelength of 590 nm. IC50 and IC90 values were computed from the dose-response curves. Dose-response curves were developed by XLfit 5.2.2 software.

3.5. RESULTS

3.5.1. STABLE TRANSFECTION OF *L. DONOVANI* CELLS WITH MCHERRY AND CITRINE REPORTER GENES

The LEXSY plasmids were constructed, one with a *mCherry* reporter gene in a combination of blasticidin marker gene and another with a *citrine* reporter gene in a combination of hygromycin marker gene (**Figure 3.1**). The *mCherry* and *citrine* gene inserts in *pLEXSY* plasmids were confirmed by BglII and NotI double restriction enzyme digestion. The *mCherry* and *citrine* genes inserts were confirmed by agarose gel electrophoresis with a band of 711bp for *mCherry* and band of 717bp for the *citrine* gene (**Figure 3.1**). Both plasmid constructs were linearized by SwaI digestion, and the linearization of plasmid construct (with 5'SSU and 3'SSU region) was confirmed by agarose gel electrophoresis by bands of ~5700bp for both CHR-BSD and CTN-HYG LEXSY plasmid (**Figure 3.1**). The linearized plasmid DNA (with *5'ssu* and *3'ssu* regions) were electroporated in WT-Ld promastigotes. The confirmation of gene integration was done by primer PCR method. A band of 1790pb was observed for primers P2, and P3 and a band of 711 pb was observed for primers P1 and P2 for genomic DNA isolated from mCherry-Ld

parasites. Similarly, a band of 1790pb was observed for primers P5, and P3 and a band of 717 bp was observed for primers P4 and P3 for genomic DNA isolated from citrine-Ld parasites (**Table 3.1**).

3.5.2. EXPRESSION OF REPORTER GENES

Expression of the *mCherry* gene in mCherry-Ld parasites and *citrine* gene in citrine-Ld parasites was confirmed by both fluorescent microscopy and flow cytometry. The mCherry-Ld parasite was detected under DIC + TEX RED filter, and the citrine-Ld parasite was detected under DIC + FITC filter of Nikon 90i Eclipse fluorescent microscope (**Figure 3.3**) (**Supporting file 3.1**). The WT-Ld parasites have not shown any fluorescence either in FITC filter or in TEXAS RED filter. However, the citrine-Ld parasites have shown strong fluorescence in FITC filter (represent by Green color). Similarly, mCherry-Ld parasites have shown strong fluorescence in the TEXAS-RED filter (represented by red color). In flow cytometry, The mCherry-Ld parasites have shown two peaks in FL-3 (Red fluorescence) dot plot and histogram plot, one for auto fluorescence and another for the fluorescence signals from reporter protein from mCherry-Ld. Similarly, The citrine-Ld parasites have shown two peaks in FL-1 (green fluorescence) dot plot and histogram plot, one for auto fluorescence and another for the fluorescence signals from reporter protein from citrine-Ld. (**Figure 3.4**).

3.5.3. TRANSGENIC PROMASTIGOTES BASED *IN VITRO* SCREENING

Because of high expression of the reporter gene, the growth of both mCherry-Ld and citrine-Ld parasites could be analyzed by the fluorimeter. Relative fluorescence unit (RFU) increased with the increase in parasite number for both mCherry-Ld and citrine-Ld promastigote

parasites. A scatter plot between a number of mCherry-Ld promastigote parasites and RFU value. A linear trend line was drawn which has a correlation coefficient (R square) value 0.9983 (**Figure 3.5A**). Similarly, a scatter plot between a number of citrine-Ld promastigote parasites and RFU value. A linear trend line was drawn which has correlation coefficient (R square) value 0.9994 (**Figure 3.5B**). Here, >0.9900 of correlation coefficient proofs an excellent correlation in the manual counting of parasite and RFU value. Based on this fluorimetric growth analysis, a screening method was developed for *in vitro* promastigote screening using both transgenic mCherry-Ld and citrine-Ld parasites. The assay was validated using six different concentrations of control drugs amphotericin B and pentamidine in triplicates. A similar assay was done by AlamaBlue assay for both mCherry-Ld and citrine-Ld promastigote parasite and WT-Ld promastigote parasites. The IC50 values for amphotericin B against mCherry-Ld and citrine-Ld were 0.15 ± 0.02 µg/mL, 0.25 ± 0.06 µg/mL and 0.20 ± 0.06 µg/mL respectively in DFA method. The IC50 values for amphotericin B against WT-Ld, mCherry-Ld, and citrine-Ld were 0.16 ± 0.01 µg/mL and 0.34 ± 0.03 µg/mL respectively in AlamarBlue based method (**Table 3.2**). Similarities in IC50 values of control drugs amphotericin B and pentamidine in both DFA and AlamarBlue based method prove the validity of fluorimetry based *in vitro* promastigote screening assay.

3.5.4. INTRACELLULAR TRANSGENIC AMASTIGOTES BASED *IN VITRO* SCREENING

3.5.4.1. MICROSCOPIC EVALUATION

Infectivity of transgenic parasites was confirmed in differentiated THP1 cells. The images of differentiated THP1 cells infected with either mCherry-Ld amastigotes or by citrine-Ld amastigotes were collected by Nikon 90i Eclipse fluorescence microscope. The THP1 cells are

represented in DIC filter (Grey colored). The citrine-Ld intracellular amastigotes have shown strong fluorescence in FITC filter (represent by Yellow color) inside the THP1 cells. Similarly, mCherry-Ld parasites have shown strong fluorescence in the TEXAS-RED filter (represented by red color) inside the THP1 cells (**Figure 6**). Infectivity was calculated by the ratio of amastigote count to THP1 cells counts with the help of ImageJ software.

Based on above transgenic intracellular microscopic analysis, a microscopic assay for intracellular amastigote was developed for both mCherry-Ld and citrine-Ld amastigotes as parasites. Both transgenic intracellular amastigotes were treated with the standard antileishmanial drugs amphotericin B and pentamidine from 2µg/mL to 0.016µg/mL concentration. The images of both mCherry-Ld and citrine-Ld intracellular amastigotes treated with different concentration of standard antileishmanial drugs were collected by Nikon 90i Eclipse fluorescent microscope (**Figure 3.8**). The infectivity was calculated for each treated samples and compared with uninfected THP1 cells (Negative control) and untreated infected THP1 cells (Positive control). Infectivity of untreated infected THP1 cells was considered as 100%, and the infectivity of other treated samples was compared to calculate the IC50 values using the XLfit software. The IC 50 values of amphotericin B against mCherry-Ld amastigotes and citrine-Ld amastigotes were 0.08± 0.05µg/mL and 0.06± 0.012 µg/mL respectively (**Table 3.3**). The IC 50 values of pentamidine against mCherry-Ld amastigotes and citrine-Ld amastigotes were 0.45± 0.12 µg/mL and 0.34± 0.15 µg/mL respectively (**Table 3.3**).

3.5.4.2. FLOW CYTOMETRIC EVALUATION

Macrophage internalized amastigote growth can be analyzed with the help of flow cytometry (**Figure 3.7**). The differentiated THP1 cells infected with mCherry-Ld amastigotes

come with shift the peak toward the right side in FL3 channel histogram plot in flow cytometry compared to the peak for uninfected differentiated THP1 cells (**Figure 3.7 A**). Similarly, the differentiated THP1 cells infected with citrine-Ld amastigotes come with shift the peak toward the right side in FL1 channel histogram plot in flow cytometry compared to the peak for uninfected differentiated THP1 cells (**Figure 3.7 B**). The mean fluorescence of the pick area M1 was utilized to compare the infectivity of the parasites. Based on this flow cytometric analysis, a macrophage-internalized amastigote screening method was developed. The differentiated THP1 cells infected with either mCherry or citrine transgenic *L. donovani* parasites were treated with control drug amphotericin B and pentamidine in 6 different concentrations from 10µg/mL to 0.0032µg/mL. The IC 50 values of amphotericin B against mCherry-Ld amastigotes and citrine-Ld amastigotes were 0.08± 0.05µg/mL and The IC 50 values of amphotericin B against mCherry-Ld amastigotes and citrine-Ld amastigotes were 0.08± 0.05µg/mL and 0.06± 0.012 µg/mL respectively **(Table 3.3)**. The IC 50 values of pentamidine against mCherry-Ld amastigotes and citrine-Ld amastigotes were 0.13 ± 0.015 µg/mL and 0.12 ± 0.02 µg/mL respectively (**Table 3.3**). The IC 50 values of pentamidine against mCherry-Ld amastigotes and citrine-Ld amastigotes were 1.3 ± 0.05 µg/mL and 1.1 ± 0.02 µg/mL respectively (**Table 3.3**).

3.5.4.3. EVALUATION BY PARASITE RESCUED AND TRANSFORMATION ASSAY

The control drugs amphotericin B and pentamidine activity was also analyzed against WT-Ld, mCherry-Ld and citrine-Ld intracellular amastigotes by PRT assay (Jain et al., 2012). The IC 50 values of amphotericin B were 0.039 ± 0.028µg/mL, 0.044 ± 0.027µg/mL and 0.061 ± 0.025µg/mL against WT-Ld, mCherry-Ld and citrine-Ld intracellular amastigotes respectively. The IC 50 values of pentamidine were 0.389 ± 0.012 µg/mL, 0.360 ± 0.010 µg/mL and 0.332 ±

0.008 µg/mL against WT-Ld, mCherry-Ld and citrine-Ld intracellular amastigotes respectively.

The activities of control drugs by fluorescent microscopy and flow cytometry for both mCherry and citrine internalized amastigotes, and PRT assay for wild-type of internalized amastigotes of *L. donovani* was evaluated and compared in **Table 3.3**. The comparative IC50 values of control drugs Amphotericin B and Pentamidine validated the screening assay for transgenic internalized amastigotes.

FIGURES AND TABLES

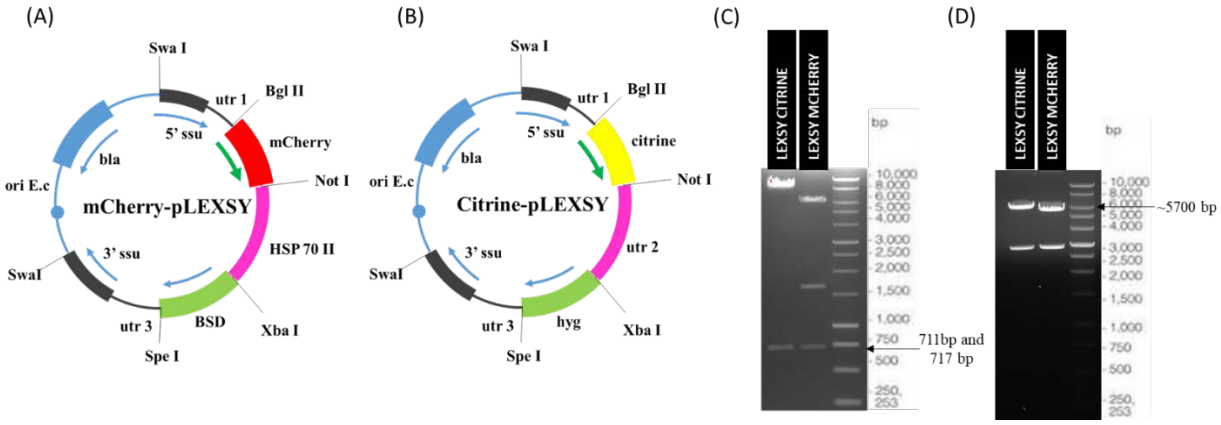

Figure 3.1: (A) LEXSY plasmid with a mCherry reporter gene and blasticidin (BSD) resistance marker gene. **(B)** LEXSY plasmid with a citrine reporter gene and hygromycin *(hyg*) resistance marker gene. **(C)** Confirmation of mCherry and Citrine gene in plasmids isolated from XL10 gold ultra-competent E.coli cells. The plasmids were digested with *bgl II* and *Not I* double restriction enzyme digestion. **(D)** Linearization of 5'*ssu* to 3'*ssu* fragment of the plasmid by *Swa I* restriction enzyme digestion.

Table 3.1: Primer sequence used for PCR method to confirm the reporter genes and their integration in *L. donovani* genome.

Primer	**Purpose**	**Sequence**
P1	mCherry Forward	CCGCTCGAGGAAGATCTCCACCATGGTGAGCAAGGGCG
P2	mCherry Reverse	ATAAGAATGCGGCCGCTTACTTGTACAGCTCGTCCATGC
P3	Citrine Forward	CCGCTCGAGGAAGATCTCCACCATGGTGAGCAAGGGCGAGG
P4	Citrine Reverse	ATAAGAATGCGGCCGCTTACTTGTACAGCTCGTCCATG
P5	Integration Forward	CTTGTTTCAAGGACTTAGCCATG

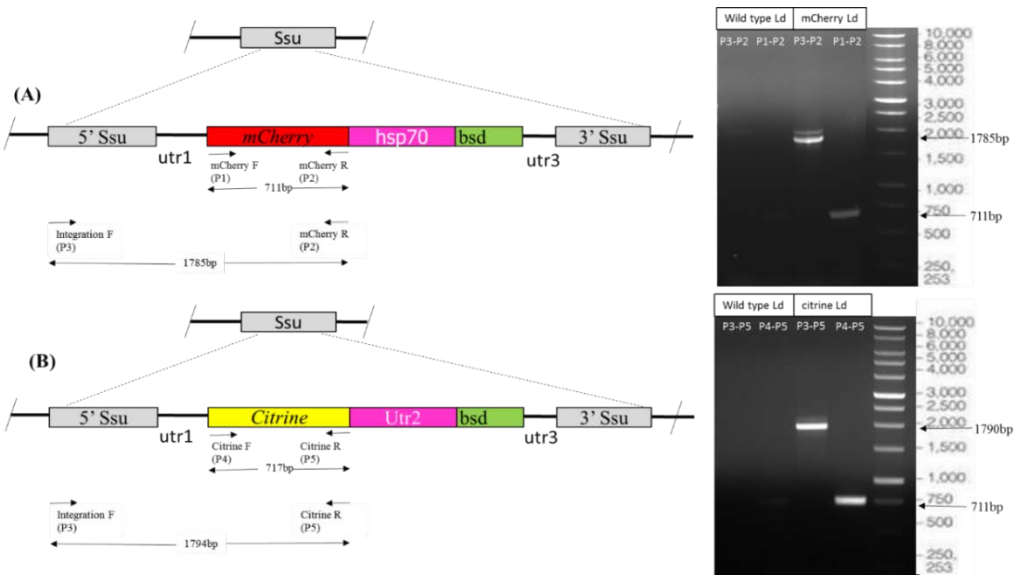

Figure 3.2: (A) Schematic view of the integration of the DNA fragment with the 5'*ssu* end and 3'*ssu* end with a *mCherry* reporter gene and a BSD resistance marker gene (previously linearized with *SwaI LEXSY-MCHERRY* plasmid) into the 18S rRNA locus of wild-type *L. donovani* genome. The confirmation of *mCherry* gene in leishmania genomic DNA was done by PCR using *mCherry* forward (P1) and *mCherry* Reverse (P2) primers (711bp band). The confirmation of integration of linear DNA with 5'*ssu* end and 3'*ssu* end was done by PCR using integration forward (P3, primers of Leishmania genomic region) and *mCherry* reverse (P2) primers (Band of 1785bp). **(B)** Schematic view of the integration of the DNA fragment with the 5'*ssu* end and 3'*ssu* end with a *citrine* reporter gene and *hyg* resistance marker gene (previously linearized with *SwaI LEXSY-CITRINE* plasmid) into the 18S rRNA locus of wild-type *L. donovani* genome. The confirmation of *citrine* gene in leishmania genomic DNA was done by PCR using *citrine* forward (P4) and citrine Reverse (P5) primers (717 bp band). The confirmation of integration of linear DNA with 5'*ssu* end and 3'*ssu* end was done by PCR using integration forward (P3) and *citrine* reverse (P5) primers (Band of 1794 bp).

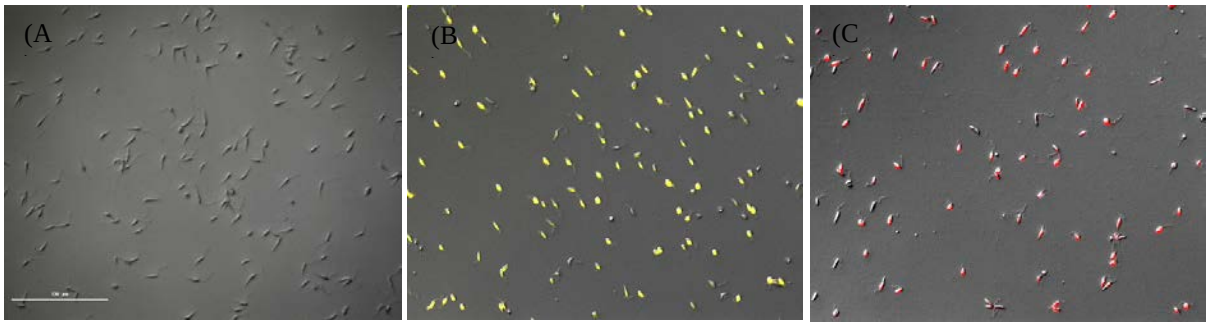

Figure 3.3: (A) Image of WT-Ld promastigote parasites. The image has been taken in DIC+FITC+TXR filters. **(B)** Image of Citrine-Ld promastigote parasites. The image has been taken in DIC+FITC filters. **(C)** Image of mCherry-Ld promastigote parasites. The image has been taken in DIC+TXR filters. All images collected by Nikon 90i Eclipse fluorescent microscope.

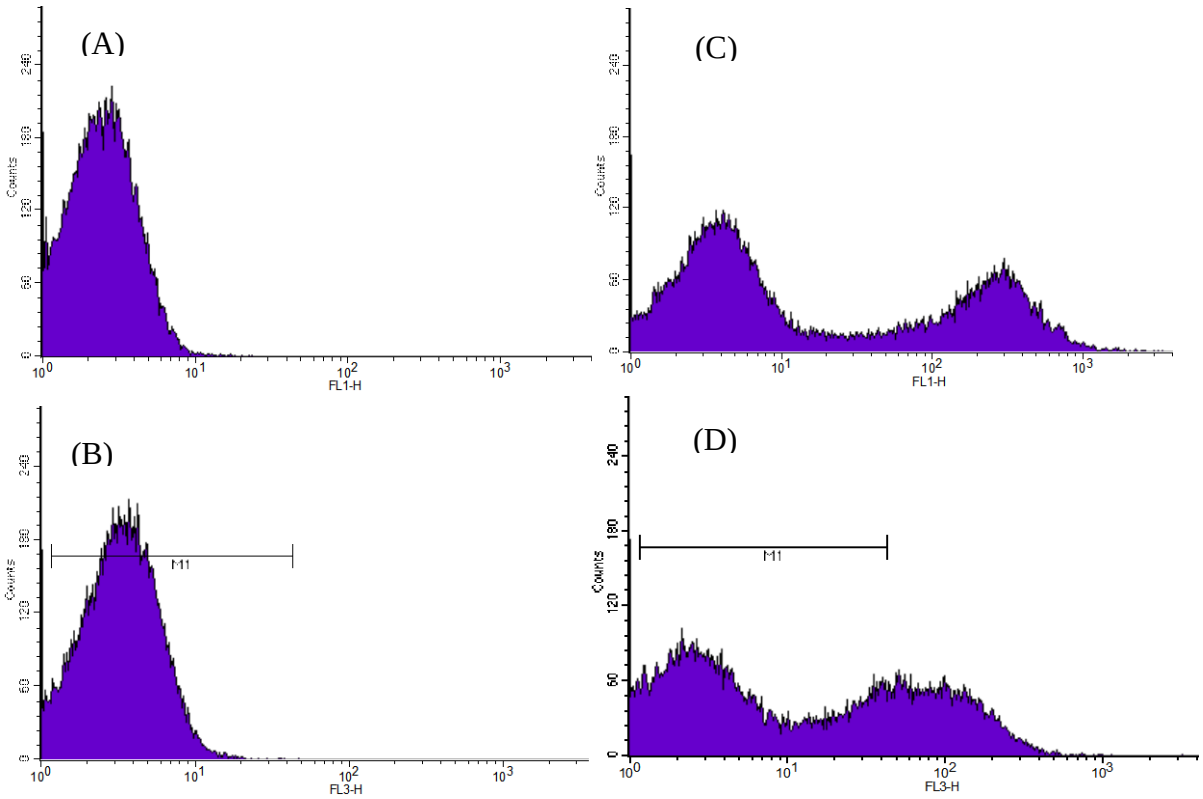

Figure 3.4: (A) FL3 Histogram plot with no fluorescent signal peak in flow cytometry for WT-Ld promastigote parasites. (B) FL1 Histogram plot with no fluorescent signal peak in flow cytometry for WT-Ld promastigote parasites. (C) FL3 Histogram plot with a prominent fluorescent signal peak in flow cytometry for mCherry-Ld promastigote parasites. (D) FL1 Histogram plot with a prominent fluorescent signal peak in flow cytometry for citrine-Ld promastigote parasites.

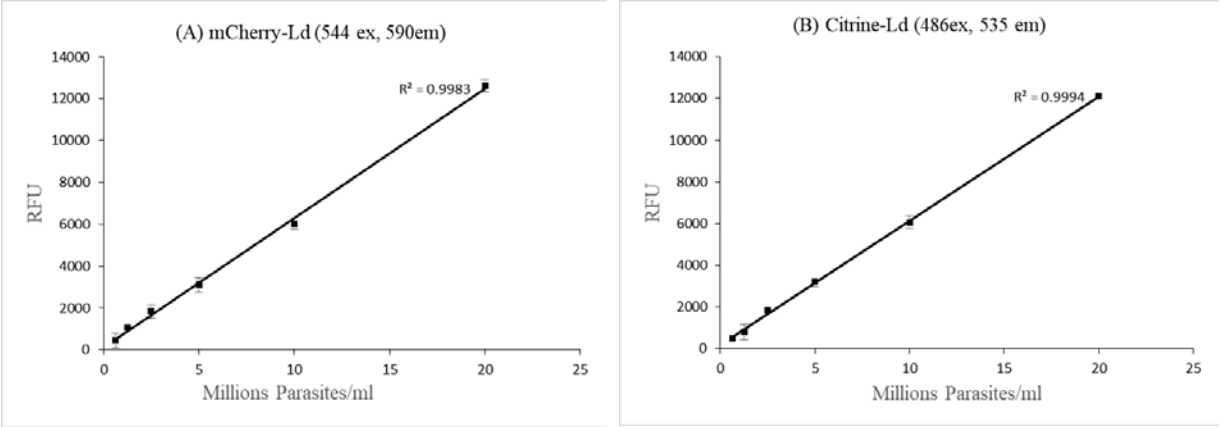

Figure 3.5: (A) Scatter plot between a number of mCherry-Ld promastigote parasites and Relative fluorescent unit (RFU). A linear trend line was drawn which has a correlation coefficient (R square) value 0.9983. **(B)** Scatter plot between a number of citrine-Ld promastigote parasites and Relative fluorescent unit (RFU). A linear trend line was drawn which has a correlation coefficient (R square) value 0.9994.

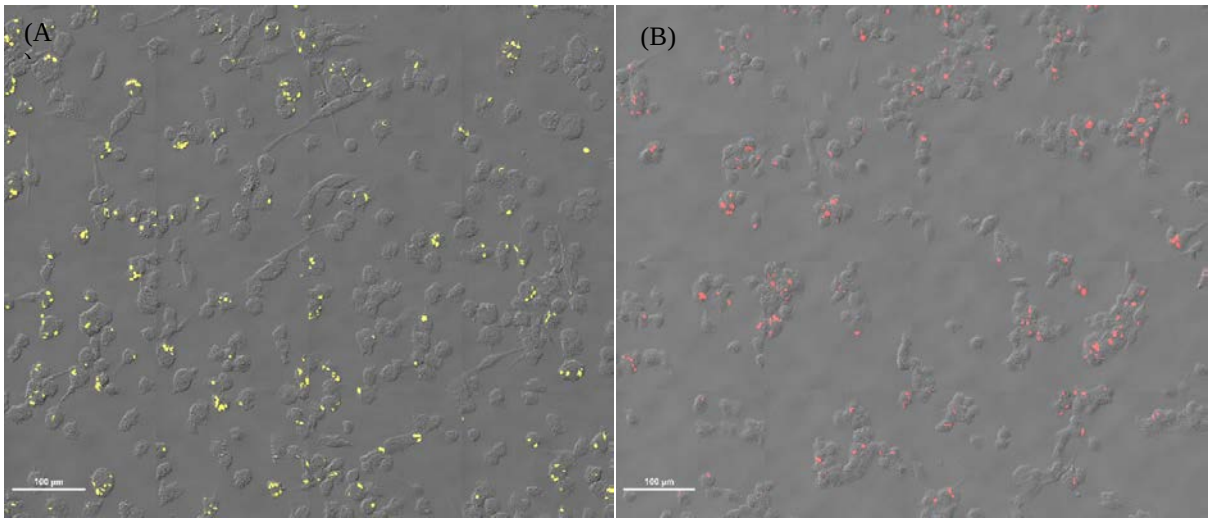

Figure 3.6: (A) Differentiated THP1 cells infected with citrine-Ld amastigotes. The image has been taken in DIC+FITC filter. **(B)** Differentiated THP1 cells infected with mCherry-Ld amastigotes. Image has been taken in DIC+TXR filter. A single image here is a montage of 4X4 area. The images have been taken at 400X magnification.

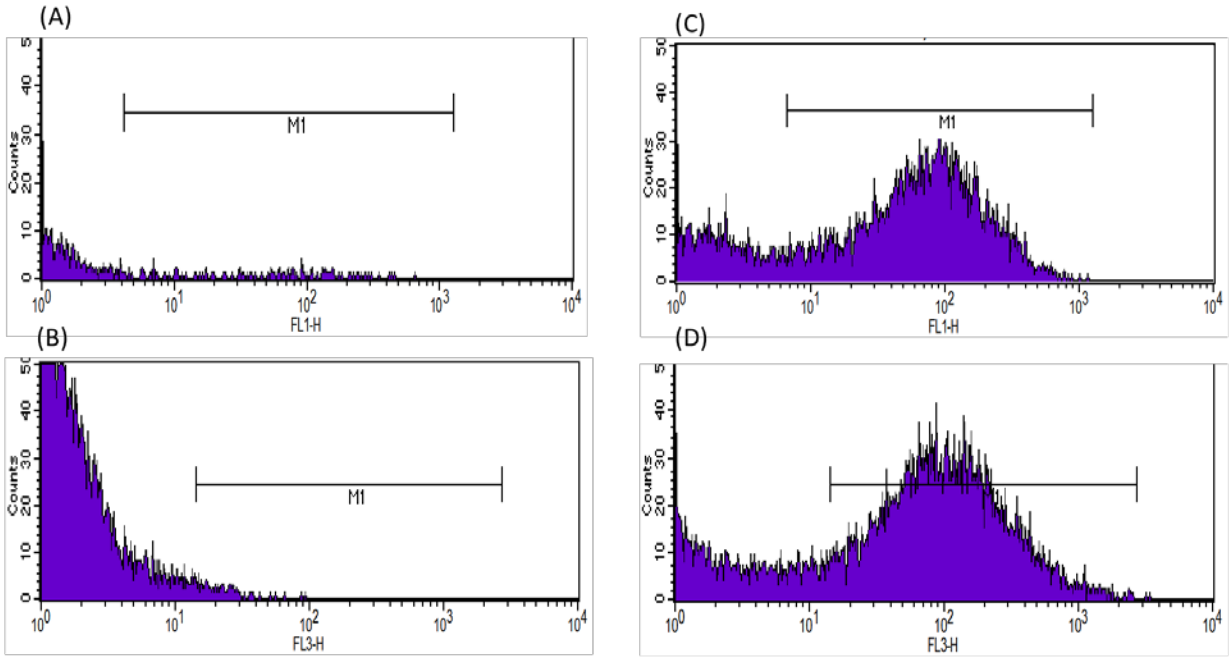

Figure 3.7: (A) FL1 Histogram plot with no fluorescent signal peak in M1 area flow cytometry for uninfected differentiated THP1 cells (B) FL3 Histogram plot with no fluorescent signal peak in M1 area flow cytometry for uninfected differentiated THP1 cells (C) FL1 Histogram plot with prominent fluorescent signal peak in M1 area flow cytometry for differentiated THP1 cells infected with citrine-Ld amastigotes. (D) FL3 Histogram plot with a prominent fluorescent signal peak in M1 area flow cytometry for differentiated THP1 cells infected with mCherry-Ld amastigotes.

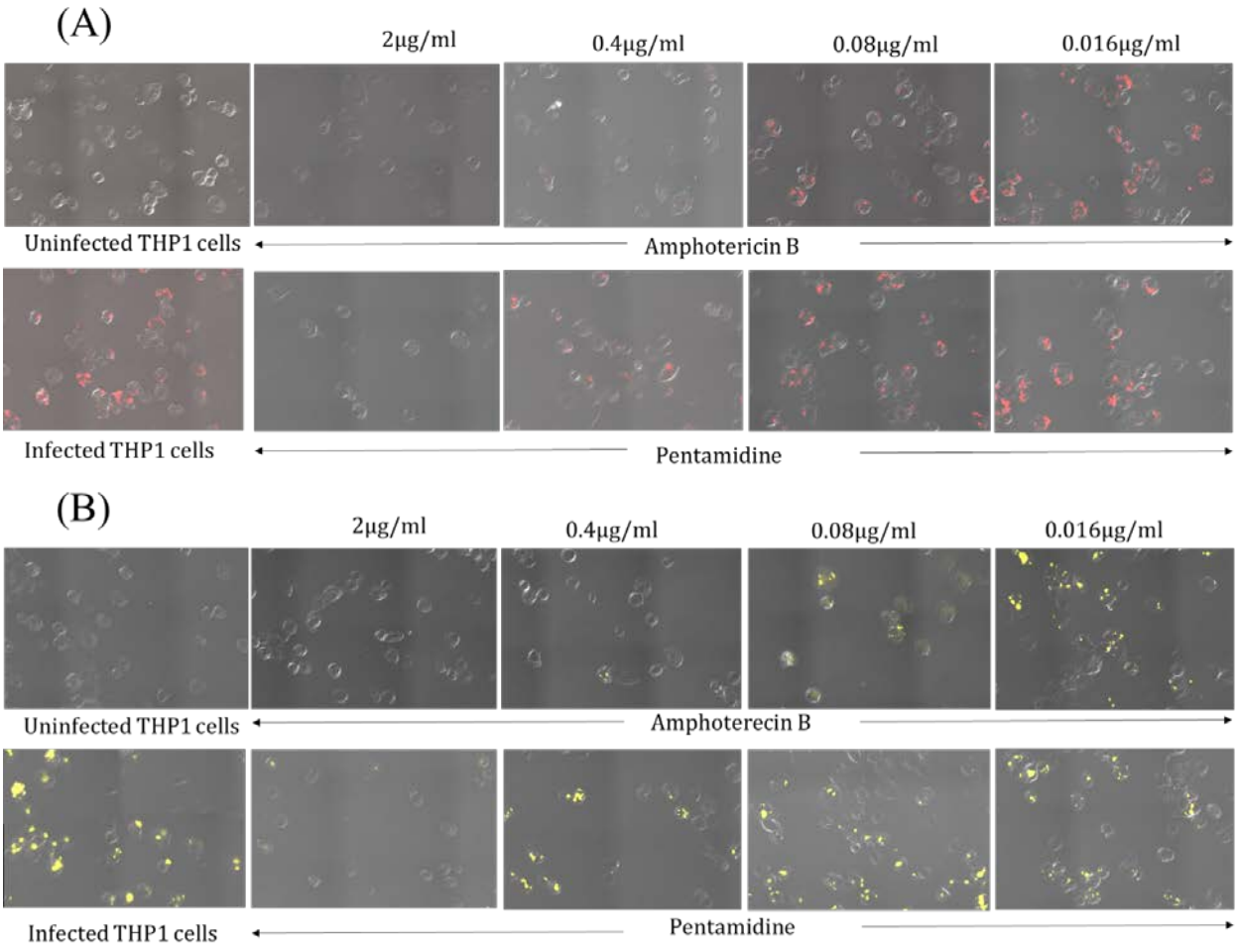

Figure 3.8: (A) Images of transgenic *L. donovani* infected differentiated THP1 cells treated with different concentrations of control drugs Amphotericin B and Pentamidine and compared with infected THP1 cells without treatment (Positive control) and uninfected THP1 cells (Negative control). In panel (A) differentiated THP1 cells infected with mCherry-Ld parasites and in panel (B) differentiated THP1 cells infected with citrine-Ld parasites. Images were collected in DIC+TXR filter for mCherry transgenic leishmania infected Cells and images were collected in DIC+FITC filter for citrine transgenic leishmania infected Cells.

Table 3.2: Promastigote assay for WT-Ld, citrine-Ld, and mCherry-Ld. Direct Florescence analysis based activity assessment for Amphotericin B and pentamidine was done on both citrine-Ld and mCherry-Ld promastigote parasites which was based on expression of citrine and mCherry fluorophore protein. Activity assessment of Amphotericin B and pentamidine was also done by alamarBlue assay for WT-Ld, and both citrine-Ld and mCherry-Ld promastigote parasites.

	Direct Florescence analysis		**AlamarBlue assay**		
Compounds	Citrine-Ld	mCherry-Ld	Wild-Type Ld	Citrine-Ld	mCherry-Ld
	IC 50 µg/mL	IC 50 µg/mL	IC 50 µg/mL	IC 50 µg/mL	IC 50 µg/mL
Amphotericin B	0.34 ± 0.03	0.16 ± 0.01	0.15 ± 0.02	0.20 ± 0.06	0.25 ± 0.06
Pentamidine	1.73 ± 0.11	1.63 ± 0.05	1.30 ± 0.27	1.76 ± 0.05	1.73 ± 0.09

Table 3.3: *L. donovani* intracellular amastigote assay using WT-Ld, citrine-Ld, and mCherry-Ld. Activity assessment for Amphotericin B and pentamidine was done on both citrine-Ld, and mCherry-Ld amastigote parasites infected in differentiated THP1 cells was done by flow cytometry and fluorescent microscopy. Activity assessment of Amphotericin B and pentamidine was also done by PRT assay for WT-Ld, and both citrine-Ld and mCherry-Ld amastigote parasites infected in differentiated THP1 cells.

Compounds	**PRT assay**			**FACS analysis assay**		**microscopic analysis assay**	
	WT- Ld	Citrine-Ld	mCherry-Ld	Citrine-Ld	mCherry-Ld	Citrine-Ld	mCherry - Ld
	IC 50 µg/mL	IC 50 µg/mL	IC 50 µg/mL	IC 50 µg/mL	IC 50 µg/mL	IC 50 µg/mL	IC 50 µg/mL
Amphotericin B	0.04 ± 0.03	0.06 ± 0.02	0.04 ± 0.03	0.12 ± 0.02	0.13 ± 0.01	0.06 ± 0.01	0.08 ± 0.05
Pentamidine	0.39 ± 0.01	0.33 ± 0.01	0.36 ± 0.01	1.10 ± 0.02	1.30 ± 0.05	0.34 ± 0.15	0.45 ± 0.12

3.6. DISCUSSION

In this study transgenic, *L. donovani* parasites were developed with mCherry and citrine fluorophore gene by stable transfection approaches. The leishmania cells developed through stable transfection method do not require the selection drug to maintain the expression level (Roy et al., 2000). Stable integration of reporter genes into the ribosomal locus represents a valuable tool for assessing phenotypes related to parasite intracellular infectivity in *ex-vivo* or *in vivo* models when a long period of growth without selection is required (Misslitz et al., 2000). The reporter gene is integrated into the parasite genome, so the relative output of expression of reporter gene does not depend on the number of copy of transfected plasmid (Misslitz et al., 2000). This increases the advantages for application of these transgenic cell lines for complex macrophage amastigote infection model. Citrine, a yellow fluorescent protein (a derivative of green fluorescent protein), and mCherry, a red fluorescent protein, are suitable due to better photo-stability, sensitivity, resistant to photo-bleaching and bright fluorescence of these reporter proteins. These fluorescent Proteins can be constitutively expressed in the leishmanial cytoplasm and mature rapidly. These properties are appropriate for the real-time analysis of the reporter proteins. Stable transfection of both mCherry and Citrine reporter genes was done using leishmania expression system (LEXSY) plasmid vector. LEXSY plasmid is based on the protozoan host that combined the eukaryotic protein synthesis with correct folding and Full range of post-translational modifications. LEXSY plasmid has a high expression-success rate with higher yield. The transgenic cells developed by LEXSY based stable transfection does not require selection drug in medium to maintain the expression level. The Linear DNA with reporter and marker gene integrated into to leishmanial genome at 18S ssu locus by recombination. Here, LEXSY plasmid with mCherry reporter gene with blasticidin marker and another LEXSY plasmid with Citrine reporter genes with hygromycin

B marker will be electroporated separately into wild-type of *L. donovani* cells. The reporter gene and its integration were confirmed by PCR. The expression of the reporter gene was confirmed by the strong fluorescent signal from both mCherry and Citrine transgenic *L. donovani* parasites. Both mCherry and Citrine transgenic parasite can be analyzed by different fluorescence-based techniques. A fluorimetry, fluorescent microscopy, and flow cytometry were applied for growth analysis of promastigotes and macrophage-internalized transgenic *L. donovani* amastigotes. Screening methods were developed for both transgenic mCherry and citrine *L. donovani* promastigotes, and internalized amastigotes using these fluorescence-based techniques and screening methods were validated by the activity of control drugs Amphotericin B and Pentamidine and compared the activity of these drugs in previously available older screening methods.

In conclusion, two transgenic cell lines of *L. donovani* have been developed with mCherry and Citrine fluorophore genes by stable transfection approach using LEXSY plasmid vector. Both the transgenic cell lines have a stable and constitutive expression of fluorescentent reporter proteins. Further, the screening methods have been developed with promastigotes, and THP1 cells internalized amastigote forms of the transgenic parasites cell lines employing flowcytometric analysis and fluorescent microscopy. Furthermore, these transgenic parasites have the potential for other applications that include understanding the parasite biology, host-parasite interactions and *in vitro/in vivo* screening for new drug discovery.

CHAPTER IV

FLUORESCENCE-BASED ASSAYS FOR MONITORING INTRA-ERYTHROCYTIC MALARIA PARASITES USING LDS-751, A NUCLEIC ACID STAIN

4.1. INTRODUCTION

There are many challenges in malaria control, particularly diagnosis and treatment of malaria. The current conditions of emerging resistance against available antimalarials alarm the further possibility of an increase in malaria fatalities. There is an urgent need of better alternative treatment for malaria and necessitate the discovery of new drugs and drug leads. The majority of malaria cases worldwide rely on clinical diagnosis to define the type of treatment (Landier et al., 2016). Diagnosis of malaria is primarily based on the confirmation of malaria parasites in RBCs of patients. New antimalarial drug discovery approaches primarily rely on *in vitro* screening of compound libraries against malaria parasite culture and further activity assessment of lead compounds in preclinical *in vivo* animal models. *In vitro* and *in vivo* antimalarial screening methods were initially based on analysis of parasitemia, which is the ratio of the malaria parasite-infected RBCs to total RBCs. The method for analysis of parasitemia based on microscopic examination of Giemsa stained blood smears was developed in 1904 (Shute and Maryon, 1963). Since that time it has remained as the official gold standard for malaria diagnosis (Makler et al., 1998). Most of the laboratories in the field still depend on microscopy for confirmation of malaria in blood and also identification of the parasite species. Microscopy is the major method for malaria

diagnosis in the clinical laboratories as well as malaria parasitemia analysis in antimalarial screenings (Makler et al., 1998). However, microscopic analysis has potentials problem with clinical diagnosis as well as laboratory parasitemia analysis. Significant misdiagnoses namely, false positives (7–36%), false negatives (5–18%), and wrong identification of species (13–15%) have been reported in the microscopic diagnosis of malaria in the United Kingdom (Milne et al., 1994) and Thailand (Beadle et al., 1994; Fix et al., 1988). A high frequency of technical errors (e.g., wrong pH of the staining solution or a poor quality the smears) has also been reported. Therefore, microscopy is an imperfect 'Gold Standard' method for diagnosis as well as parasitemia analysis in antimalarial drug screenings (Collier and Longmore, 1983; Makler et al., 1998).

The parasitemia analysis method based on incorporation of radioactive hypoxanthine was developed as an alternative to laborious and time-consuming microscopic assays (Desjardins et al., 1979). Although this method could be used for high-throughput screenings, there are several challenges in this assay. The assay requires specific needs for a radioactive lab. Incorporation of radioactive hypoxanthine by other proliferative cells in blood may cause high background. The hypoxanthine uptake assay does not measure parasitemia directly, as its incorporation is dependent on DNA synthesis which only occurs in the later stages of the parasite life cycle (Yayon et al., 1983). This assay measures the further growth of the malaria parasite.

Additional methods have been developed for monitoring malaria growth based on the enzymatic activity of parasites lactate dehydrogenase (pLDH) (Knobloch and Henk, 1995) or ELISA assay for malarial histidine-rich protein 2 (HRP2) (Beadle et al., 1994). The pLDH assay is based on selective utilization of 3-acetyl pyridine NAD (APAD) as co-factor by the malaria LDH. The colorimetric methods have been developed based on the pLDH assay(Makler and Hinrichs, 1993). These assays may be performed in microplates and can be used for high-

throughput screening. However, there is a low degree of concordance between LDH based assay and standard microscopy based determinations of parasitemia (Jelinek et al., 1996; Knobloch and Henk, 1995). The parasite's histidine-rich protein 2 (HRP2)-based ELISA assay has a good correlation with the hypoxanthine uptake (Desakorn et al., 1997). However, these assays are not cost-effective, especially for large-scale screening.

The methods based on flow cytometric analysis (FCA) of the malaria parasite have been developed for diagnosis and the parasitemia analysis. These methods can be applied to automation and high throughput parasitemia analysis (Woodrow et al., 2015). However, application of FCA methods for routine clinical diagnosis of malaria has not been reported for automated screening (Grimberg, 2011). The FCA methods take advantage of the absence of DNA in uninfected RBCs and presence of parasite DNA in malaria-infected RBCs. The intraerythrocytic malaria parasite could be detected by flow cytometry by staining with an appropriate DNA-binding fluorescent dye. Different fluorescent dyes namely, Hoechst 33258 (van Vianen et al., 1990), SYTO-9 (Izumiyama et al., 2009), SYTO-61 (Fu et al., 2010), ethidium bromide (Staalsoe et al., 1999), propidium iodide (Pattanapanyasat et al., 1997), acridine orange (Hare, 1986), 4,6-diamidino-2-phenylindole (Baniecki et al., 2007), YOYO-1 (Campo et al., 2011; Xie et al., 2007) and SYBR Green I (Izumiyama et al., 2009) have been used for analysis of parasitemia in *in vitro* cultures of *Plasmodium falciparum* by FCA. YOYO-1 (Xie et al., 2007), SYTO-16 (Jimenez-Diaz et al., 2009) and SYBR Green I (Somsak et al., 2012) have also been employed for the determination of parasitemia in *in vivo* blood samples from the *Plasmodium berghei* infected mice. The parasitemia analysis directly from the human or mice blood sample is particularly difficult because blood samples have a mixed population of erythrocytes, neutrophils, lymphocytes, monocytes, and reticulocytes. The currently used FCA methods for parasitemia analysis show high background

values due to the mixed cell populations in the blood. The blood cell populations may be analyzed by gating in the FSC/SSC dot plots in FCA. However, separation of reticulocyte and erythrocyte populations in FSC/SSC dot plot is challenging (Terstappen and Levin, 1992; Wiczling and Krzyzanski, 2008). Therefore, the varing population of circulating reticulocytes pose may result in high background and false signals for parasitemia analysis by FCA. This problem occurs due to significant levels of RNA in the reticulocytes. The fluorescent probes YOYO-1, SYTO-16 and SYBR Green I bind with RNA, even though less prominently compared to binding to DNA. This problem may be solved by treatment of blood cells samples with RNase. In case of a nonpermeant fluorescent nucleic acid dye, an additional processing for permeabilization the cells are required. Current FCA methods require cells fixation, permeabilization, RNase treatments, nucleic acid dye staining and complex flow cytometric analysis (Jimenez-Diaz et al., 2009; Xie et al., 2007).

Laser dye styryl–751 (LDS-751) **(Fig 4.1)** is a cell-permeant nucleic acid stain that has been used to discriminate intact nucleated cells from nonnucleated and damaged nucleated cells, as well as to identify distinct cell types in mixed populations of neutrophils, leukocytes and monocytes by flow cytometry (Nicholson et al., 2007). LDS-751 in combination with other nucleic acid stains has been used for accurate enumeration of erythrocytes, reticulocytes, platelets, neutrophils, eosinophils, monocytes, lymphocytes, nucleated erythrocytes, and immature nucleated cells by flow cytometry (Terstappen and Levin, 1992). LDS-751 binds to RNA (excitation/emission maxima approx 590/607 nm) and to DNA (excitation/emission maxima approx 543/approx 712 nm) with an approx 20-fold increase in fluorescence on binding to double-stranded DNA (Terstappen and Loken, 1988). Due to its differential excitation/emission spectra, LDS-751 permit its use to discriminate DNA and RNA in cells. This advantage of LDS-751 allows differentiation of reticulocyte populations from nucleated cells as well infected erythrocytes

(Wiczling and Krzyzanski, 2008). The LDS-751 is a cell-permeable stain, which produces differential fluorescence signals on binding with RNA (ex/em 590/607 nm) and DNA (ex/em 543/712 nm). Due to the differential excitation/emission spectra, LDS-751 permits its use to discriminate DNA and RNA in cells. LDS-751 can be utilized in the flow cytometric analysis of the malaria-infected blood samples. The LDS-751 based parasitemia analysis will be-be quick and simple because the staining of erythrocytes with LDS-751 may not require fixation, permeabilization, and RNase pre-treatment to remove background due to reticulocytes.

4.2. HYPOTHESIS

Staining of malaria-infected blood cells with LDS-751 (a cell-permeant nucleic acid stain) allows differential detection of malaria parasite-infected and uninfected erythrocytes, which may be implemented for malaria parasitemia analysis in *in vitro* and *in vivo* settings without misleading reticulocytes background signals.

4.3. APPROACH

We have developed the FCA and fluorescent microscopy methods with LDS-751, a fluorescent cell-permeant DNA binding probe, for determination of parasitemia in the blood from malaria-infected mice and *in vitro* P. falciparum culture. The FCA method was implemented for in vivo antimalarial screening assays. The classical Giemsa-staining based microscopic method was standardized with digital images analysis of parasitemia with ImageJ software.

4.4. MATERIALS AND METHODS

4.4.1. ANIMAL HOST AND *P. BERGHEI* PARASITE

Most the in vivo work has been done under the protocol for in vivo antimalarial evaluation. This protocol was approved by the University of Mississippi Institutional Animal Care and Use Committee (IACUC). Male mice (Swiss Webster strain) with 18-20g body weight were obtained from ENVIGO.inc. All animals were quarantined for at least seven days before infection. Mice were divided into different groups with five mice in each group and were housed in top filter cages with food and water supplied ad libitum. *P. berghei* parasite was maintained in malaria mice model. To initiate the malaria infection in new mice, 0.5ml of highly parasitized blood (>20% parasitemia) of infected mouse stored in liquid nitrogen was thawed and injected intraperitoneally. Blood with high parasitemia level (18-20%) was collected from an infected donor mouse at 14^{th} post-infection day by cardiac puncture method in Acid citrate dextrose (ACD) buffer. A new group of mice was intraperitoneally inoculated with 4×10^7 parasitized RBCs from infected blood. All group of infected mice was regularly observed for change in weight, change in appearance and change in behavior.

4.4.2. MICROSCOPIC CONFIRMATION OF LDS-751 FLUORESCENCE

The blood samples were collected on the slides from uninfected mice and highly infected mice by tail snipping method. Thin smears were prepared from collected blood samples. The slides were fixed with the help of methanol for 30 sec and dried for 30 min. The fixed slides were stained with LDS-751 at 2µg/mL concentration in DPBS for 20 min. Slides were washed and dried and observed under Nikon 90i Eclipse fluorescent microscope at 1000X magnification with the help of emergen oil. The images were collected in TEXAS-RED (TXR) and Differential interference contrast (DIC) filter. The TXR filter was used to collect the fluorescence of LDS-751 and DIC to collect the sample surface image. Differential interference contrast microscopy is similar to phase contrast microscopy but without the bright diffraction halo in images.

4.4.3. DIGITAL IMAGES ANALYSIS METHOD (DIAM) IN *P. BERGHEI* BLOOD SAMPLES

This is microscopic parasitemia analysis method based on the counting of infected RBCs and total RBCs in thin smears of blood samples on glass slides. The blood samples were collected on the slides from infected mice by tail snipping method. Thin smears were prepared from collected blood samples. Slides were fixed with the help of methanol for 30 sec and dried for 30 min. All dried slides were stained with 1X Giemsa stain for 45 min. Slides were washed and dried. All blood smears images were collected by Nikon i90 light microscope at 1000X magnification with the help of emergency oil. In digital images based parasitemia analysis, the images were analyzed with ImageJ software. Parasitemia is the ratio of malaria-infected RBCs to total RBCs. Images were opened in ImageJ software. Infected RBCs were counted by manual cells counter in image J software. The total RBC were counted by automated counting protocol in ImageJ software. The ImageJ software protocol for manual and automatic counting is given in **figure 4.8**.

4.4.4. FCA of PARASITEMIA IN *P. BERGHEI* INFECTED MOUSE BLOOD SAMPLES

Most the in vivo work has been done under the protocol for in vivo antimalarial evaluation. The whole blood was collected from a 14-day post infection mice and uninfected normal mice in ACD buffer. The blood samples were washed with Dulbecco's phosphate-buffered saline (DPBS). RBCs counting of both kinds of the sample was done by Bio-Rad TC 10 Automated cell counter. The uninfected samples RBCs counting was adjusted to equal to infected samples RBCs counting. The infected blood sample was serially diluted in 1:1 ratio by uninfected blood samples with same RBCs

counting. The slides were prepared for undiluted an infected blood samples for microscopic parasitemia analysis. 5µl of serially diluted samples were stained for 20 min with LDS-751 1.0 µg/mL in DPBS that was diluted from its stock solution of 1mg/mL in DMSO. All samples were centrifuged and resuspended in DPBS. All the blood samples were run in a flow cytometer in FSC/SSC dot plot. RBCs population was gated in FSC/SSC dot plot. 100,000 gated population was analyzed on SSC/FL4 dot plot and as well as FL4 channel histogram plot. Parasitemia is the ratio of malaria-infected RBCs to total RBCs. So parasitemia was calculated based on the percent gated population in the upper right region of SSC/FL4 dot plot or by a percent gated population change in the second peak in FL4 channel histogram. Thin smears were also prepared from uninfected, and *P. berghei* infected mice blood sample samples. Slides were fixed and stained with Giemsa. The images were collected by Nikon 90i eclipse light microscope at 600X magnification.

4.4.5. MODIFIED PETER'S TEST BASED ANTIMALARIAL ASSAY

Most the in vivo work has been done under the University of Mississippi IACUC approved the protocol for in vivo antimalarial evaluation. The four days' Peter's test has been modified for this study. Mice were divided into different groups with five mice in each group. Blood with high parasitemia level (18-20%) was collected from infected donor mice at 14^{th} post-infection day by cardiac puncture method in ACD buffer. The slide was prepared, and parasitemia level was calculated by Giemsa staining method. The high parasitemia blood was diluted in PBS to $8X10^7$ parasitized RBCs per ml. All the mice in all groups were inoculated with 4×10^7 parasitized RBCs (0.5ml) intraperitoneally at day 0. One group of 5 infected mice were treated with vehicle control. Separate groups of mice were treated with Chloroquine and amodiaquine at three different doses (33mg/kg, 11mg/kg, and 3.7mg/kg). For each dose, one group of 5 mice are treated once daily from day 0 to 2

post infection. Blood samples from mice of control and treated groups were collected on slides (~10µl) as well as tubes (~2µl) with 500 µl of ACD buffer by tail snipping method on day 5, 7, 10, 14, 21, and 28 post-infection. Timeline for infection, dosing and blood sample collections are given in **Figure 4.2**. All mice were observed for the change in appearance, behavior, and weight of the mice. Mice those lost equal or more than 25% of their weight were euthanized by CO2 gas euthanization method.

4.4.6. DIA AND FCA BASED PARASITEMIA ANALYSIS IN BLOOD SAMPLES IN ANTIMALARIAL ASSAY

Slides were prepared from all blood samples. Slides were fixed with methanol for 30 sec and stained with Giemsa 1X for 45 min. Slides were washed and dried. For digital analysis of parasitemia, all blood smears images were collected by Nikon i90 eclipse light microscope at 600X magnification with Emerson oil, and parasitemia was calculated with the help of ImageJ software as mentioned earlier. For Flow cytometric analysis of parasitemia, all blood samples were collected in 500 µl of ACD buffer. All samples were centrifuged at 2000rpm, and blood sample pellets were re-suspended in 500µl of DPBS. All the samples were stained with LDS-751 stain in 1.0 µg/mL concentration for 20 min at room temperature. After staining, all samples were again centrifuged and resuspended in DPBS and run on flow-cytometer. All the samples were run in FSC/SSC dot plot. RBCs population was gated in FSC/SSC dot plot. 100,000 gated population was analyzed on SSC/FL4 dot plot and FL4 channel histogram. Here parasitemia was calculated based on percent gated population in the upper-right region in SSC/FL4 quadrangle dot plot or by percent gated population under the second peak in FL4 channel histogram. Parasitemia and mean survival time of mice in untreated control and treated groups are determined.

4.4.7. RETICULOCYTES RICH BLOOD SAMPLES PARASITEMIA ANALYSIS

A high number of reticulocyte appeared in the blood of Chloroquine (33.3mg/kg) Treated mice at 28 days of post-infection. Blood samples were collected on the slide as well as a tube with ACD solution. Slides were prepared and stained with Giemsa, and the images were collected by NIKON 90i Eclipse microscope. The Giemsa-stained images of blood smears with high reticulocytes are given in **Figure 4.10**. The blood samples collected in the tube in ACD buffer were stained with LDS-751 and run in a flow cytometer for parasitemia analysis (similar to section 4.2.4.).

4.4.8. *P. FALCIPARUM* CULTURE MAINTAINANCE

The continuous culture of a chloroquine-susceptible *P. falciparum* strain (D6, Sierra Leone) was routinely maintained in the $25cm^2$ flask. The parasite was grown in RPMI 1640 medium supplemented with 0.23% sodium bicarbonate, 0.006% Amikacin, 10% A+ human serum and A+ human erythrocytes (6% hematocrit). Culture flasks were incubated in a 37^oC incubator with 5% O_2, 5% CO_2, and 90% N_2. A fresh subculture waw initiated with an initial parasitemia of ~1% and 6% hematocrit. The medium was changed every 48 h, and the parasite was subcultured with fresh RBCs after every 6 to 7 days. Slides were prepared before every subculture. Slides were fixed and stained by a quick stain to evaluate the parasitemia level.

4.4.9. PARASITEMIA ANALYSIS IN *P. FALCIPARUM* INFECTED CULTURES BY LDS-751

For microscopic parasitemia analysis, thin smear slides were prepared from infected RBCs of *P. falciparum* culture. The slides were fixed with the help of methanol for 30 sec and dried for 30 min. The fixed slides were stained with LDS-751 at 2µg/mL concentration in DPBS for 20 min. Slides were washed and dried and observed under Nikon 90i Eclipse microscope in TXR and DIC filter (similar to section 4.2.2.). For flow cytometric analysis, 10µl of infected RBCs diluted to 500µl with PBS and stained with LDS-751 at 1.0 µg/mL concentration. The stained sample run through Flow cytometer (similar to section 4.2.4.). Thin smears were also prepared from uninfected and *P. falciparum*-infected human RBCs samples. Slides were fixed and stained with Giemsa. The images were collected by Nikon 90i eclipse light microscope at 600X magnification.

4.4.10. DIA AND FCA BASED PARASITEMIA IN *P. FALCIPARUM* INFECTED RBCs

An assay was set up with standard antimalarial drugs chloroquine (CQ) and artemisinin (ART). Stock solutions of the drugs or compounds were prepared in water (CQ) or DMSO (ART) and diluted further with serum-free RPMI to achieve appropriate concentrations. The parasite cultures (mainly with ring stage) were diluted with fresh human erythrocytes to achieve 2% hematocrit and 2% parasitemia. The assays were performed in clear flat-bottom 96-well plates. Each well-received 190µl of the parasite culture and 10µl of the test compound. Each compound was tested at 6 different concentrations (238-1 ng/mL). The plates were placed in an incubator with a gas mixture containing 90% N2, 5% O2, and 5% at 37 °C for 72 h. 10µl of RBCs were collected from each well including all well of treated infected RBCs, untreated infected RBCs and uninfected RBCs. These samples were stained with LDS-751 (see section 4.2.4.) and run in a flow cytometer. 3µl of RBCs were collected from each well including all well of treated infected RBCs, untreated infected RBCs and uninfected RBCs on slides. I thin smears were prepared and fixed with methanol. These fixed slides were stained

with Giemsa (Blue colored nucleic acid stain). Images of Giemsa stained RBCs were collected by Nikon 90i eclipse light microscope in 600X magnification.

4.5. RESULTS

4.5.1. MICROSCOPIC CONFIRMATION OF LDS-751 FLUORESCENCE

The blood samples were collected, and thin smear slides were prepared from infected and uninfected mice. The LDS-751 have excitation wavelength 543nm and an emission wavelength of 712nm. So, the LDS-751 stained slides of *P. berghei* infected blood samples were observed under the fluorescent microscope under TXR and DIC filters. The TXR filter was used to collect the fluorescence of LDS-751 (**Red colored in Figure 4.3**) and DIC to collect the sample surface image (**Grey colored in figure 4.3**). Both TXR and DIC images were merged. Fluorescence of LDS-751 could be seen inside RBCs. Images of different stages of *P. berghei* parasite in peripheral blood sample slide could be seen in red color inside the RBCs (**Figure 4.3**.

4.5.2. FCA OF PARASITEMIA IN *P. BERGHEI* BLOOD SAMPLES

The LDS-751 stained *P. berghei* infected blood samples, and uninfected blood samples were run in a flow cytometer. RBCs population was gated in FSC/SSC dot plot, and 100,000 gated population was analyzed further in SSC/FL4 dot plot as well as FL4 channel histogram plot. The SSC/FL4 dot plot was converted in the quadrangle. Panel (A) of **Figure 4.4** represents the flow cytometric analysis of uninfected blood samples. The Most of the gated population located in the upper-left area of the quadrangle of SSC/FL4 plot and only one peak observed for uninfected RBCs population in FL4 channel histogram. Panel (B) of **Figure 4.4** represents the flow cytometric analysis

for *P. berghei* infected blood samples. When the gated population was analyzed in quadrangle dot plot, the population appeared partly in both upper-left and upper-right region of the quadrangle. The uninfected RBCs appeared in the upper-left region of the quadrangle and the *P. berghei* infected RBCs appeared in in the upper-right area of the quadrangle in SSC/FL4 dot plot. Similarly, there were two peaks appear in FL4 channel histogram plot. The first peak appeared for the uninfected RBCs population while the other peak appeared for infected RBCs population. The percent Gated population in the upper-right region of quadrangle dot plot show the level of parasitemia. The percent gated population under peak area under M1 region in FL4 histogram plot also represent the level of parasitemia. Parasitemia analysis of *P berghei* infected serially diluted blood samples was done by LDS-751 flow cytometric analysis method. Parasitemia was calculated for the highly infected blood sample without dilution by microscopy. Two separate area in thin smear slide were counted separately for infected and uninfected RBCs (**Figure 4.5**). The average parasitemia (ratio of *P.berghei* infected RBCs to total RBCs) was found 30.02 percent by microscopy. So expected parasitemia for with microscopic analysis was 30.02, 15.01, 7.51, 3.75, 1.88, 0.94, 0.47, 0.23, and 0.12 in up to 9 serially dilutions of the sample including the first sample. The parasitemia was analyzed for these samples were 30.55, 15.85, 8.28, 4.22, 2.26, 1.19, 0.67, 0.28, 0.18 and 0.12 **(Table 4.1**) The accuracy of the flow cytometric parasitemia analysis was calculated by comparing with microscopic parasitemia analysis. A correlation graph was prepared between flow cytometric parasitemia and microscopic parasitemia. The correlation coefficient (R^2) of the linear regression line was 0.9995 proof the validity of the flow cytometric method of parasitemia analysis (**Figure 4.6**). The microscopic comparative images of uninfected and P. *berghei* infected mice blood samples is given in **Figure 4.5**.

4.5.3. DIA AND FCA BASED PARASITEMIA ANALYSIS IN MICE BLOOD SAMPLES

The microscopic digital images based parasitemia analysis was developed using ImageJ software. **Figure 4.7** represents the *P. berghei* infected blood smear image, manual counting of parasite-infected RBCs and automatic counting of total RBCs. A whole Rodent in vivo antimalarial assay was done using *P. berghei* parasite in 3 different doses of chloroquine and amodiaquine in separate groups of mice. The blood samples were collected by tail snipping method simultaneously on glass slides (~10µl) and in tubes (~2µl) ACD buffer. The parasitemia in slides was calculated using a digital images analysis method (DIAM) using ImageJ software. The average parasitemia in blood samples collected from different groups of mice for different dose treatment at different days (day 5, 7, 10, 14, 21 and 28) is given in **Figure 4.9.A**. The parasitemia was calculated using LDS-751 based FCA. The average parasitemia in blood samples collected from different groups of mice for different dose at different days (day 5, 7, 10, 14, 21 and 28) is given in **Figure 4.9.B**. The correlation scatters plot was prepared to compare the flow cytometric parasitemia and microscopic parasitemia for all different treatment groups of mice. The parasitemia by FCA and microscopic method for samples of all days for particular treatment groups were analyzed on the scattered plot. There were total seven treatment groups namely, Vehicle control group, Chloroquine 33.3 mg/kg treatment group, Chloroquine 11.1 mg/kg treatment group, Chloroquine 3.7 mg/kg treatment group, Amodiaquine 33.3 mg/kg treatment group, Amodiaquine 11.1 mg/kg treatment group and Amodiaquine 3.7 mg/kg treatment group. The correlation scattered plot for six groups is given in **Figure 4.10.** There were maximum 30 parasitemia samples were compared. Some group may have lesser samples because few mice were died before day 28 due to high parasitemia. The correlation plot for amodiaquine 33.3 mg/kg treatment group is not provided in **Figure 4.10** as no parasitemia appeared in any mice of this treatment group. The average correlation coefficient (R-square) of all scattered plots is 0.9230. That show good correlation in both flow cytometric and microscopic method of parasitemia analysis.

4.5.4. RETICULOCYTES RICH BLOOD SAMPLES PARASITEMIA ANALYSIS

Giemsa-stained images of blood smears with high reticulocytes are given in **Figure 4.11**. The high reticulocyte population could be misdiagnosed as false positive in microscopy for malaria parasitemia analysis. The microscopic image looks like high parasitemia, but most of the blues cells are reticulocytes. The parasitemia was analyzed by both DIAM and LDS-751 based FCAM. SSC/FL4 quadrangle dot plot of gated RBCs population of same blood sample do not have a high percent of gated populations in upper right regions which represent the parasitemia level in blood samples. So the real parasitemia is less than 1 and flows cytometric assay counted accurately here. So Even though blood sample may have high reticulocytes but the LDS-751 can differentiate the infected RBCs from reticulocyte in flow cytometric analysis.

4.5.5. MICROSCOPIC CONFIRMATION OF LDS-751 FLUORESCENCE IN *P. FALCIPARUM* INFECTED RBCS

The human infected RBCs samples were collected from *in vitro P. falciparum* culture. The thin smear slides were prepared for infected as well as uninfected human RBCs. The slides were fixed with methanol. The fixed slides were stained with LDS-751. The slides were observed under the fluorescent microscope under TXR and DIC filters. The TXR filter was used to collect the fluorescence of LDS-751 (Red colored) and DIC to collect the sample surface image (Gray colored). Both TXR and DIC images were merged. Fluorescence of LDS-751 could be seen inside RBCs. Images of different stages of *P. falciparum* parasite in peripheral blood sample slide could be seen in red color inside the RBCs (**Figure 4.12**).

4.5.6. FLOW CYTOMETRIC ANALYSIS OF LDS-751 STAINED *P. FALCIPARUM* INFECTED RBCS

The human uninfected and infected RBCs samples stained with LDS-751 were run through a flow cytometer. RBC population was gated in FSC/SSC plot, and 100,000 gated RBCs population was analyzed in SSC/FL-4 quadrangle dot plot. Panel (A) of **Figure 4.13** represents the flow cytometric analysis of uninfected blood samples. The Most of the gated population located in the upper-left area of the quadrangle of SSC/FL4 plot. Panel (B) of **Figure 4.13** represents the flow cytometric analysis for *P. falciparum*-infected blood samples. When the gated population was analyzed in quadrangle dot plot, the population appeared partly in both upper-left and upper-right region of the quadrangle. The uninfected RBCs appeared in the upper-left region of the quadrangle and the *P. falciparum*-infected RBCs appeared in in the upper-right area of the quadrangle in SSC/FL4 dot plot. The percent Gated population in the upper-right region of quadrangle dot plot show the level of parasitemia. The microscopic comparative images of uninfected and P. *berghei* infected mice blood samples is given in **Figure 4.14**. The uninfected RBCs presented in pink colored cells and infection *P. falciparum* presented blue/purple dot inside pink RBCs.

4.5.7. LDS-751 STAINING BASED *IN VITRO P. FALCIPARUM* ANTIMALARIAL ASSAY

The *in vitro* antimalarial assay was set up using standard antimalarial drugs chloroquine and artemisinin at six different concentrations in triplicate against *P. falciparum.* Treated infected RBCs samples were stained with LDS-751 and analyzed by flow cytometer. Blood smears also prepared from the same treated infected RBCs samples and analyzed by microscopy after Giemsa staining. The

parasitemia by both flow cytometry and microscopy of treated infected RBCs was compared with untreated infected RBCs to calculate the IC50 values. IC 50s for chloroquine were 1.71µg/mL and 1.67µg/mL by microscopic and flow cytometric assay respectively **(Table 4.2)**. IC 50s for chloroquine were 10.08µg/mL and 9.90µg/mL by microscopic and flow cytometric assay respectively **(Table 4.2)**. The similarity in IC50 values proof the utility of the LDS-751 based flow cytometric assay.

FIGURES AND TABLES

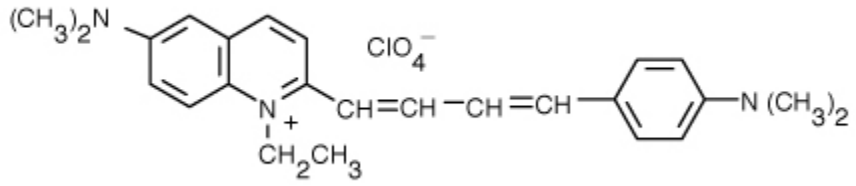

Figure 4.1: Chemical Structures of Laser dye styryl–751 (LDS-751).

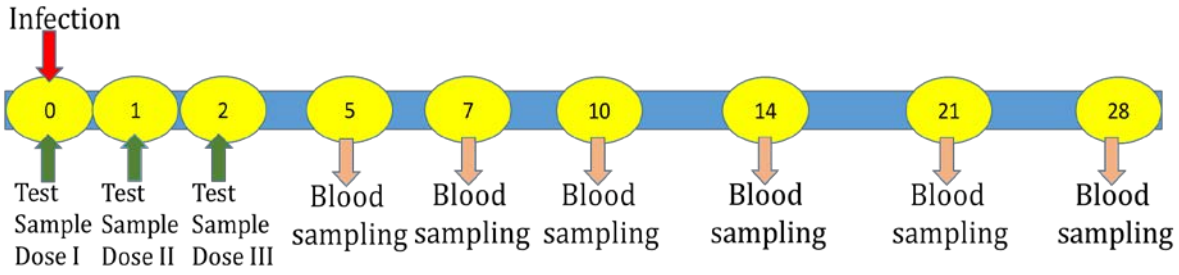

Figure 4.2. Modified Peter's test timeline of infection, test sample dosing and blood sampling in each group of mice. Yellow is marked as the day post infection (from 0 to 28), Infection ($4X10^7$ *P. berghei* infected RBCs inoculated intraperitoneally) was given on day 0. The doses of the test samples were given orally once daily on day 0, day1, and day 2. Blood samples were collected on day 5, 7, 10, 14, 21 and 28 for parasitemia analysis.

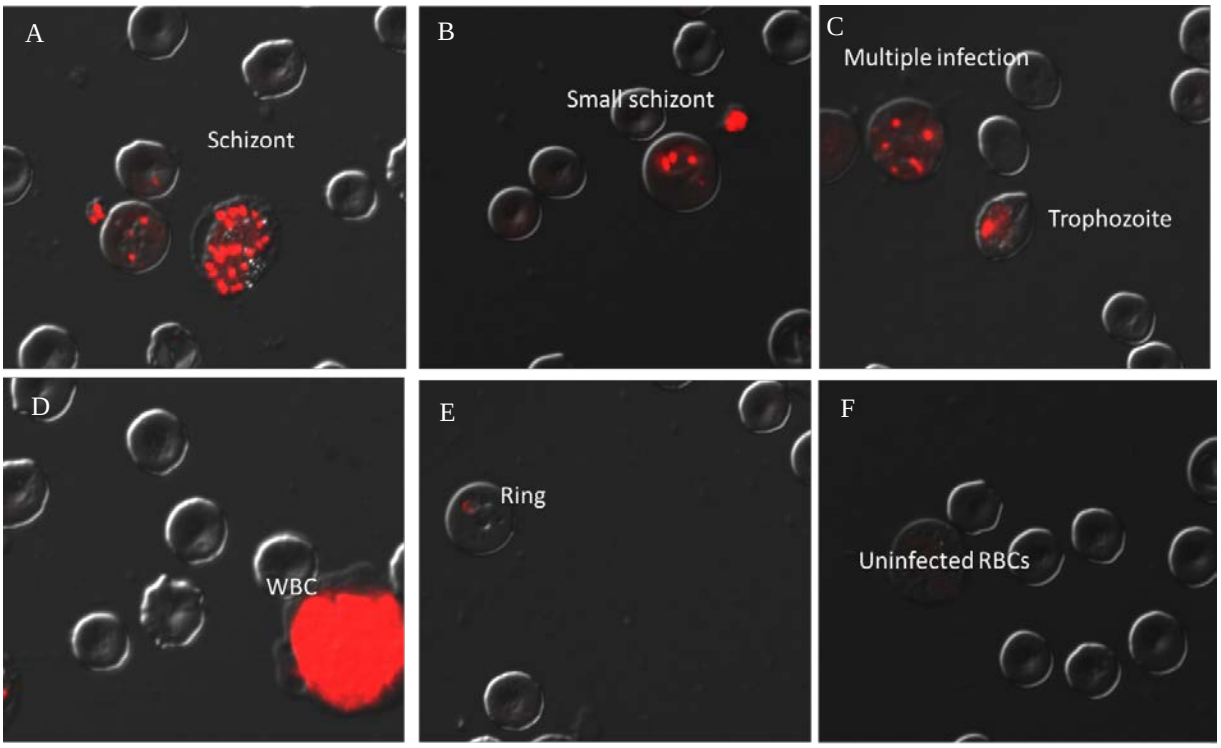

Figure 4.3: *P. berghei* infected RBCs. Images were collected under TXR and DIC filter. LDS-751 fluorescence (Red) enables the detection of different stages of *P. berghei* parasite inside the RBCs (Gray). A and B= Schizont (multiple parasites), C= Trophozoite and multiple infection in an RBC, D= White blood cell, E =Ring stage, F=uninfected RBCs.

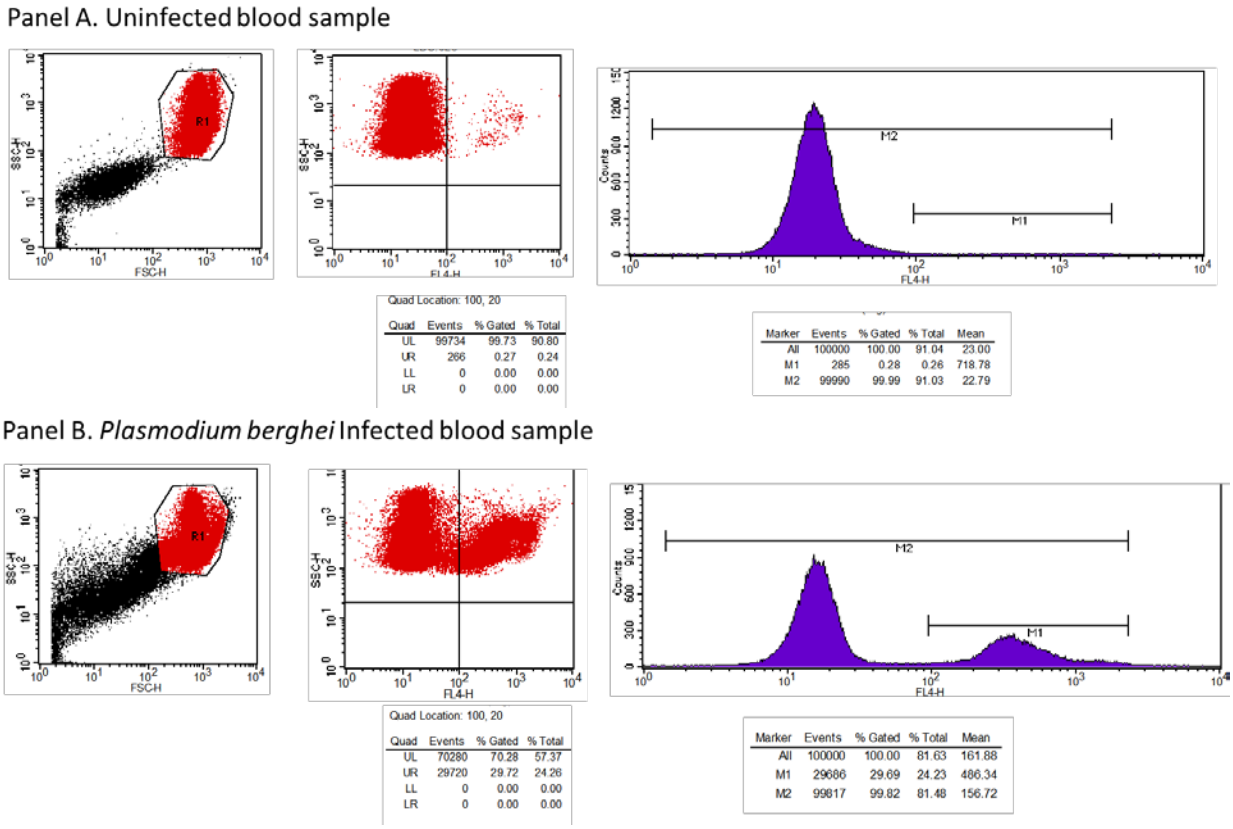

Figure 4.4: Flow cytometric analysis of *P. berghei* infected mice blood samples. A. uninfected mice blood samples run in FSC/SSC plot. B. *P. berghei* infected mice blood samples run in FSC/SSC plot. Gated RBCs population analyzed on an SSC/FL4 quadrangle dot plot and FL4 channel histogram plot. The percent gated population in the upper-right SSC/FL4 quadrangle and the percent population under M1 region in FL4 histogram plot show the parasitemia in the running sample.

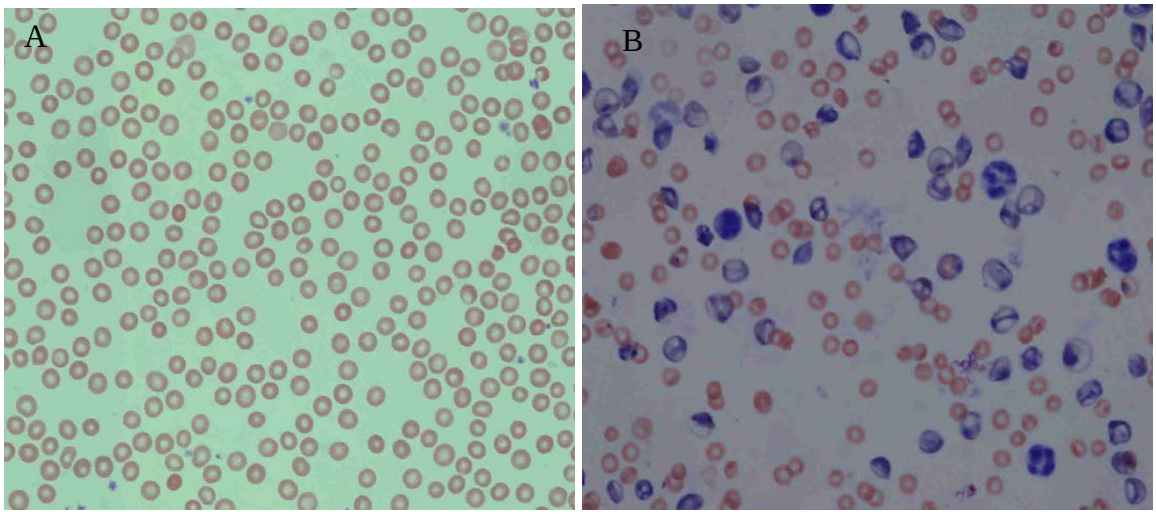

Figure 4.5: Microscopic analysis of *P. berghei* infected mice blood samples. A. Smear of uninfected mice blood sample. B. Smear of *P. berghei* infected mice blood sample.

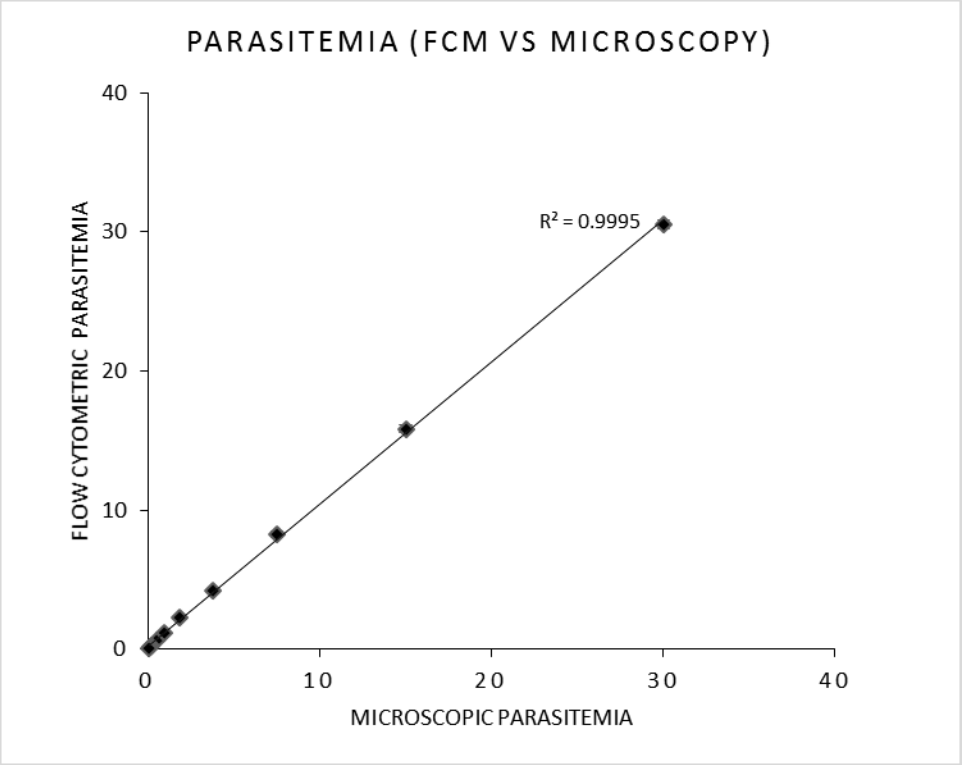

Figure 4.6: Comparison of parasitemia analysis my microscopy and LDS-751-based flow cytometry. The high parasitemia mice blood was serially diluted with uninfected mice blood in 1:1 ratio. A linear trend line was drawn in the scattered plot. (Correlation coefficient R^2 is 0.9995).

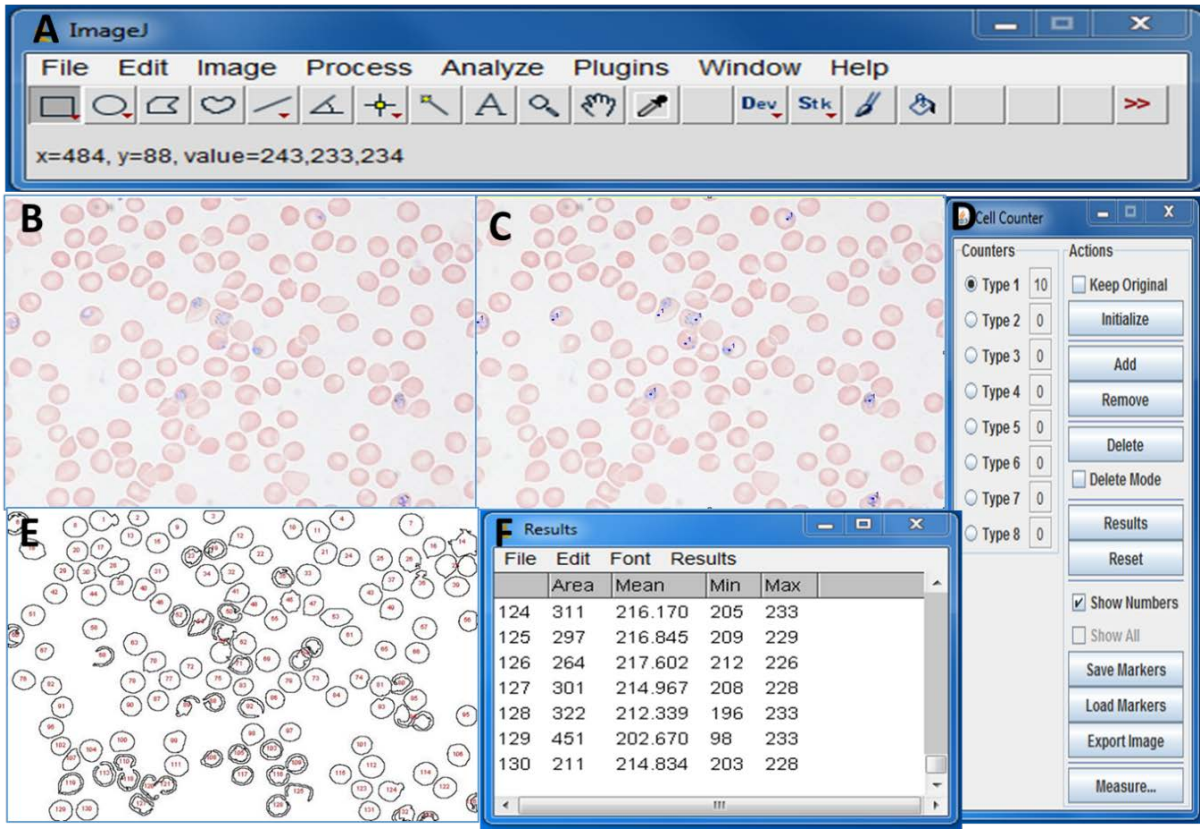

Figure 4.7: Parasitemia analysis by ImageJ software. The infected RBCs were counted by the manual cell counting tool, and the total RBCs were counted by automated total cell counting tool of ImageJ software. **A.** ImageJ software interface. **B.** Digital image of infected RBCs. **C.** Manual counting on image B. **D.** Manual cell counting module of ImageJ software. E Outline of total RBCs. F. Result of automated counting module in ImageJ software

ImageJ software step by step protocol for infected and uninfected RBC Counting

1) Images opening protocol
ImageJ>file>open>select image>open

2) Infected RBCs manual counting protocol
Plugins>Analyze>Cell counter
Cell counter>Initialize> Select counter type> click on infected RBCs on images.

3) The total RBCs automated counting protocol
process>binary>make binary
process>bindary>fill holes
process>bindary>watershade
Analyze>analyze particles
analyze particles> Size ($Pixel^2$)= 500-Infinity (Depend on quality of image).
Circularity=0.25-1.00.
Show=outline
Display results>Ok

Figure 4.8: ImageJ software step by step protocol for infected and uninfected RBC Counting.

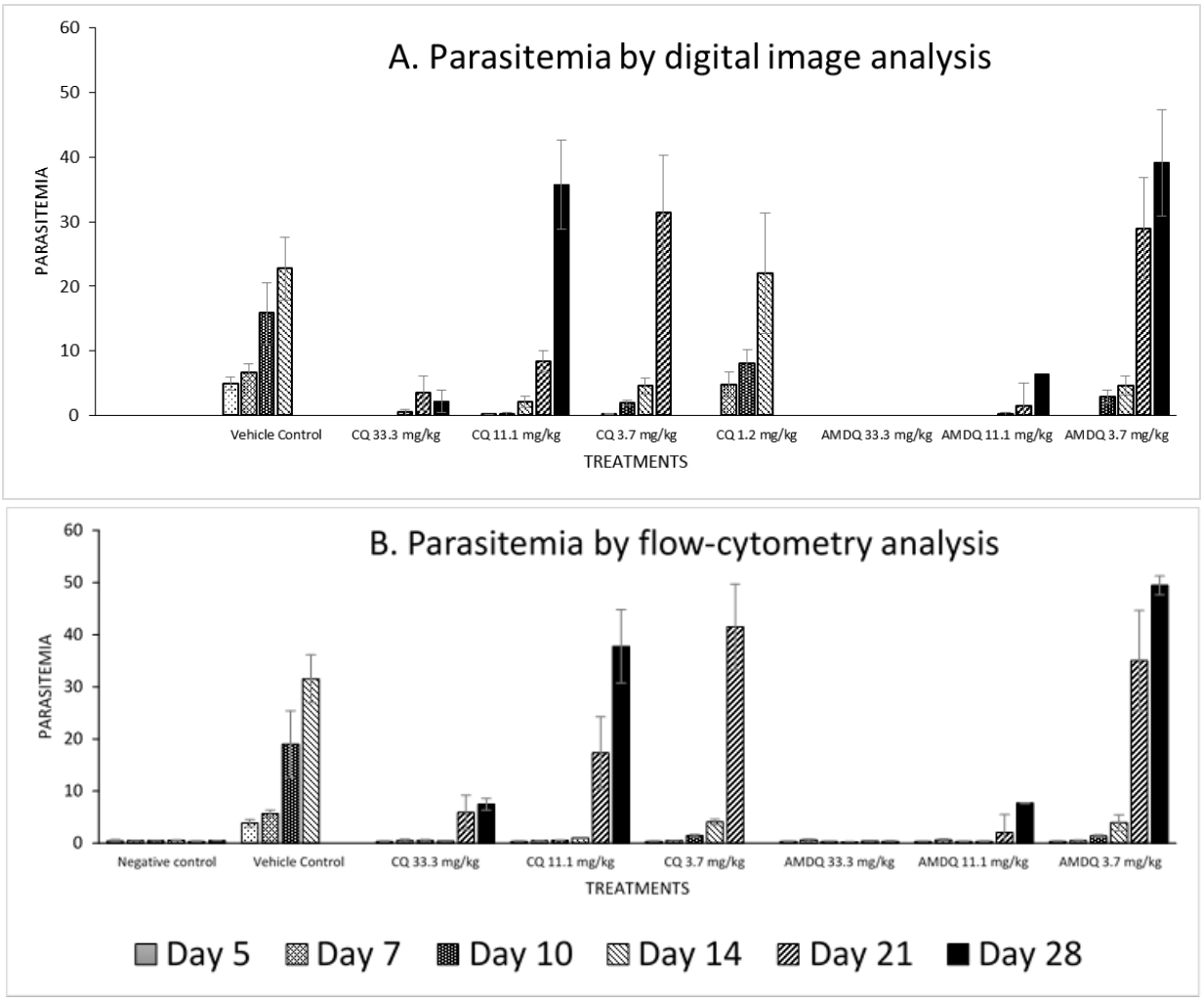

Figure 4.9: The parasitemia analysis in samples collected from different treatment group of *P. berghei* infected mice on day 5, 7, 10, 14, 21 and 28 of post-infection. A. Parasitemia analysis by ImageJ software-based digital image analysis method. B. Parasitemia analysis by LDS-751-based flow cytometric analysis method.

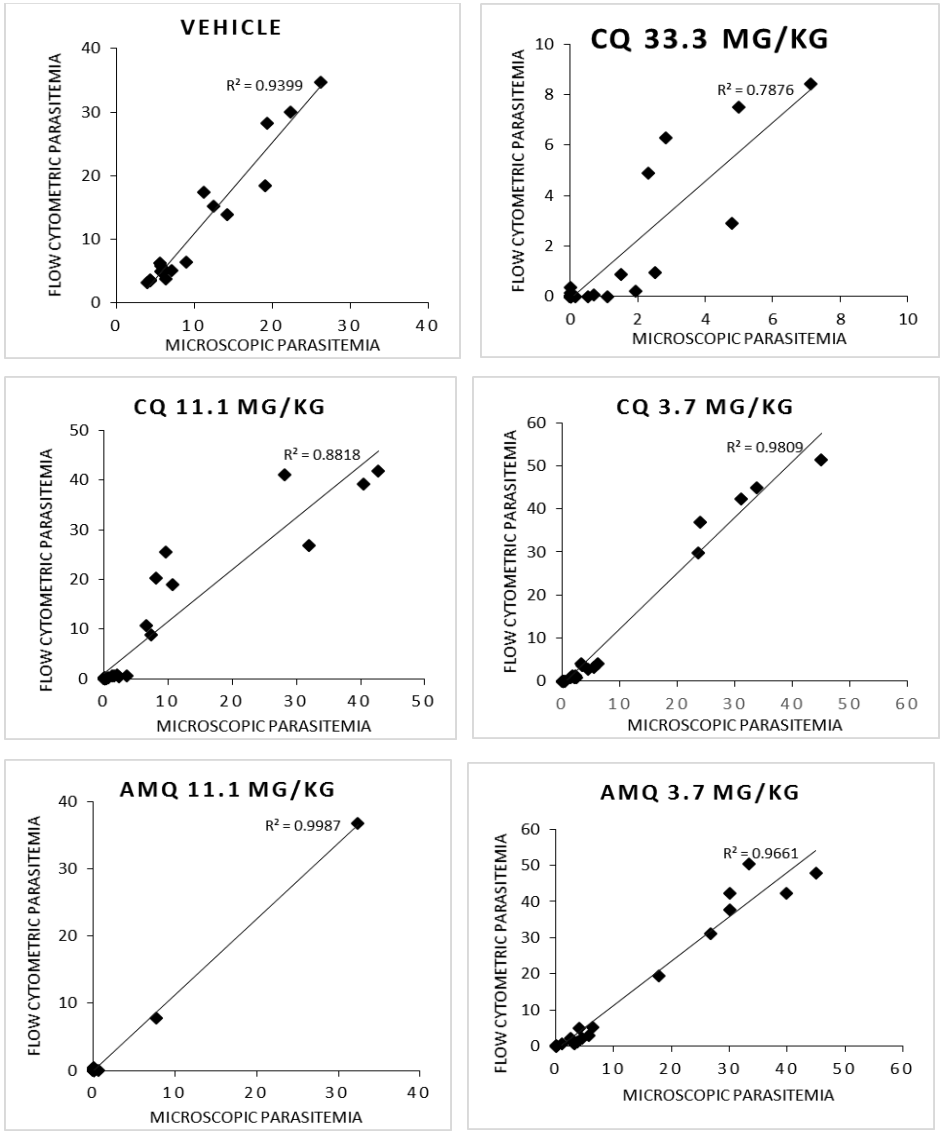

Figure 4.10: Scattered plot for parasitemia on day 5,7, 10, 14, 21 and 28 samples from all five mice for a particular treatment group. A maximum number of samples are 30. Some treatment groups have lesser samples because of earlier death due to parasitemia. The average correlation coefficient (R2) is 0.9230 that proof a good correlation between flow cytometric and microscopic data in real in vivo antimalarial assay. AMQ 33.3 mg/kg treatment group is not presented here as no parasitemia appears in all five mice till day 28. CQ = Chloroquine. AMQ = Amodiaquine.

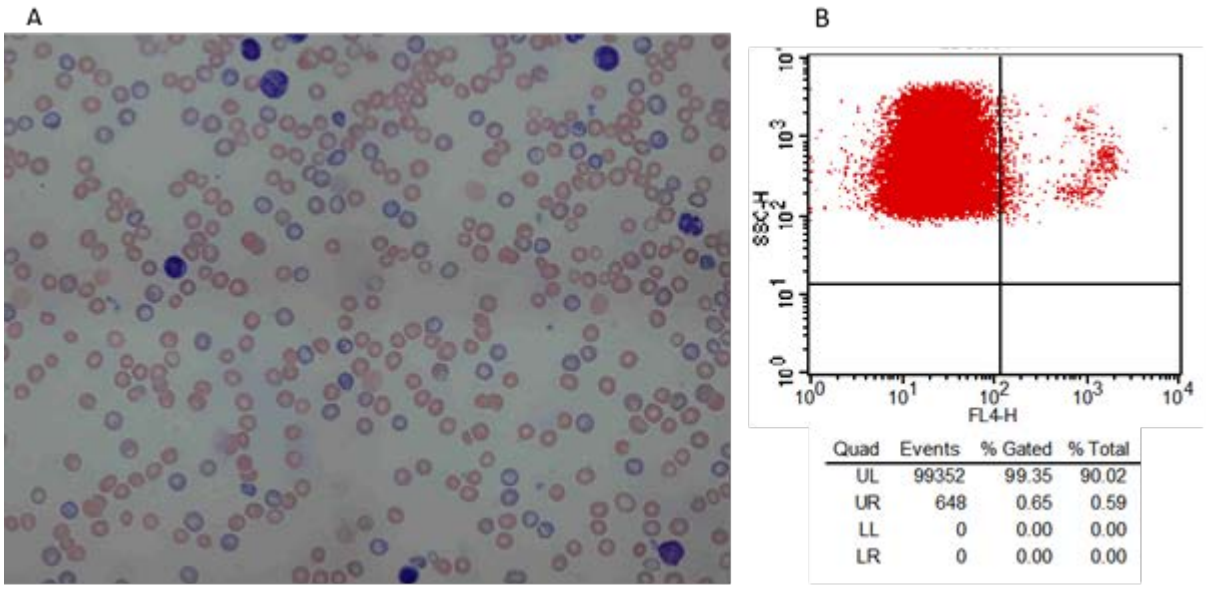

Figure 4.11: A- Blood smears of mice blood sample with high reticulocyte population which could be considered as false positive in microscopy for malaria parasitemia analysis. **B-** Dot plot of gated RBCs population of same blood sample does not have a high percent of gated populations in upper right regions which represent the parasitemia level in blood samples.

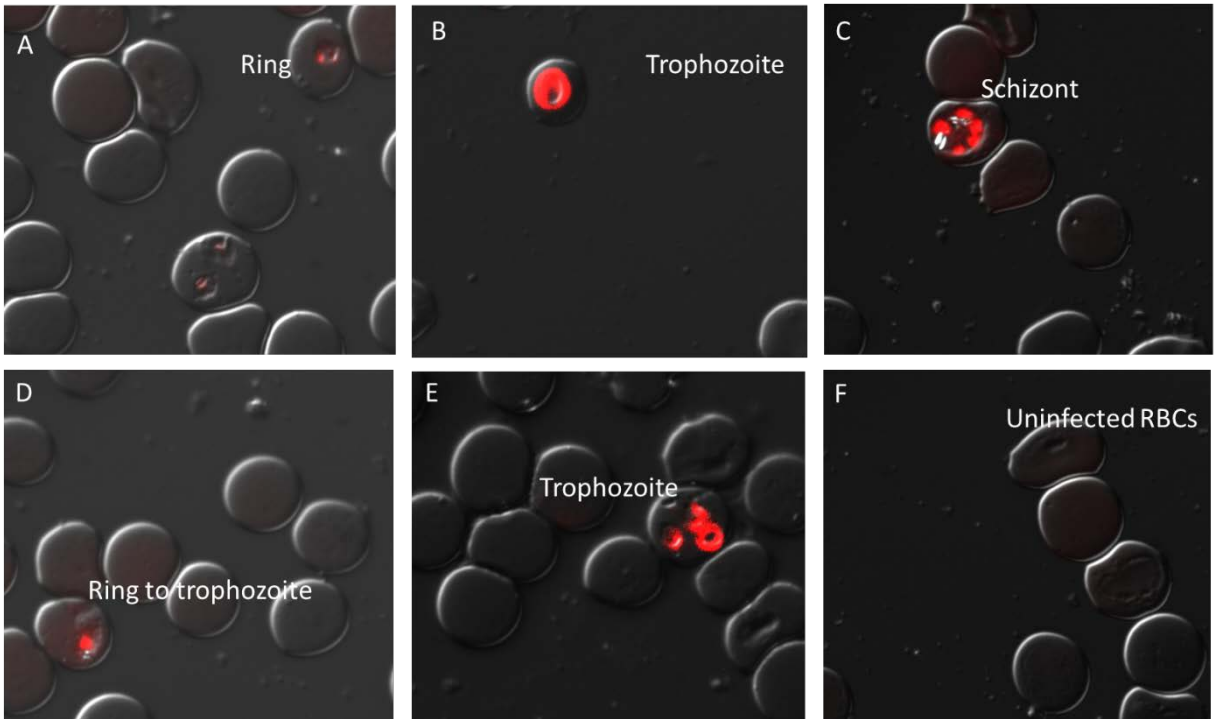

Figure 4.12: *P. falciparum*-infected RBCs. Images were collected in TEXAS-RED and DIC filter. LDS-751 fluorescence (Red) enables the detection of different stages of *P. falciparum* parasite inside the RBCs (Gray). A- Ring stage (multiple parasites), B- missing C-schizont, D- Ring to trophozoite stage E – Trophozoite, F-uninfected RBCs.

Panel A. Uninfected RBCs

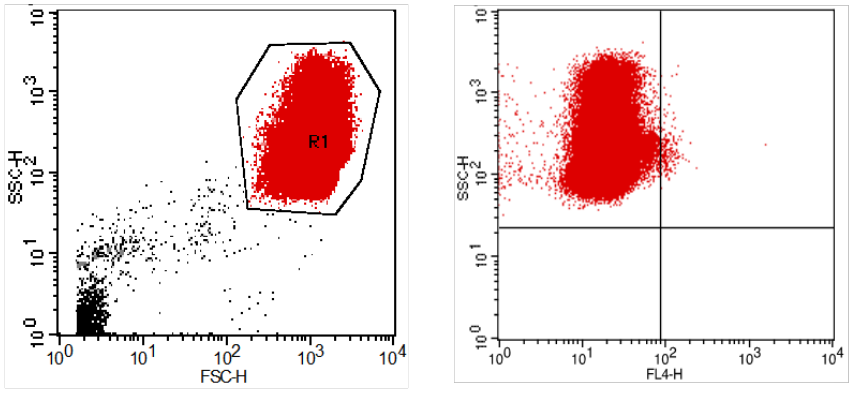

Quad	Events	% Gated	% Total
UL	99773	99.77	95.47
UR	227	0.23	0.22
LL	0	0.00	0.00
LR	0	0.00	0.00

Panel B. *Plasmodium falciparum* infected RBCs

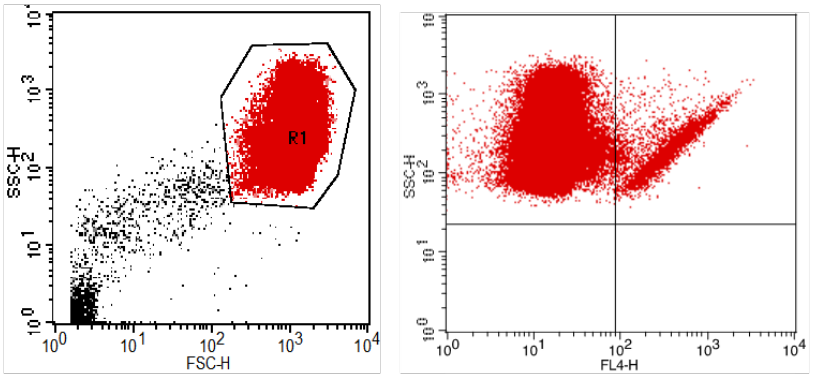

Quad	Events	% Gated	% Total
UL	95888	95.89	91.55
UR	4112	4.11	3.93
LL	0	0.00	0.00
LR	0	0.00	0.00

Figure 4.13: Flow cytometric analysis of *P. falciparum*-infected mice blood samples. The Panel A. uninfected human RBCs samples run in FSC/SSC plot. The Panel B. *P. falciparum*-infected human RBCs samples run in FSC/SSC dot plot. Gated RBCs population analyzed on SSC/FL4 quadrangle FL4 channel histogram plot. The percent gated population in the upper-right area in SSC/FL4 quadrangle plot shows the parasitemia.

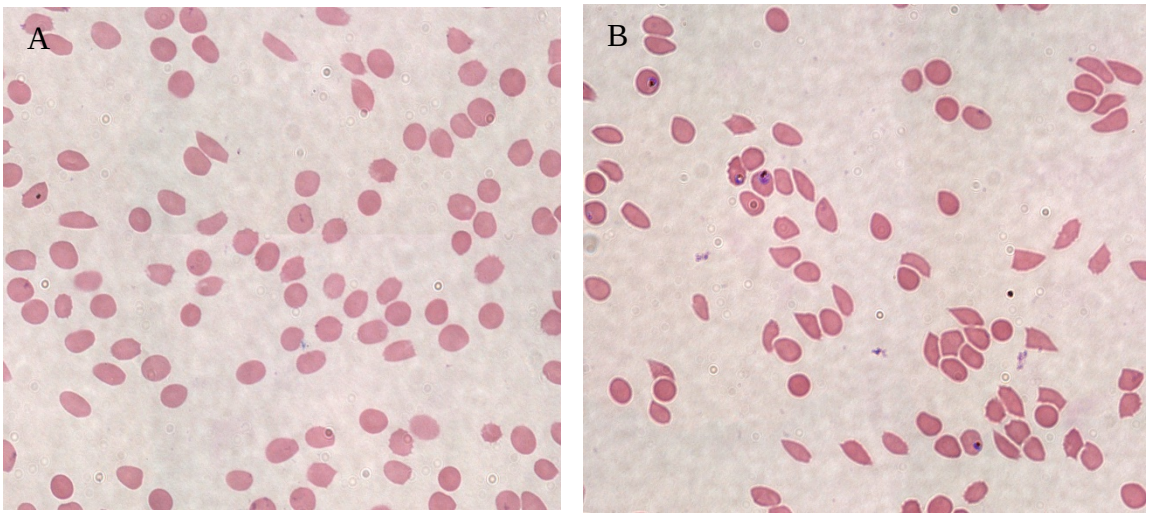

Figure 4.14: Microscopic analysis of *P. falciparum*-infected human RBCs samples. The Image A and B are stained with Giemsa nucleic acid stain. The Image A is uninfected human RBCs samples. The Panel B. is *P. falciparum*-infected human RBCs sample.

Table 4.1. Comparison of Parasitemia by flow cytometric method (FCA) and microscopic method for blood samples from *P. berghei* infected mice. Accuracy was calculated by comparing average parasitemia by flow cytometric analysis with microscopic analysis. The mean accuracy is above 100% Proof the accuracy of Flow cytometric assay.

Parasitemia by FCA	Parasitemia by Microscopy	FCA vs Microscopy Accuracy
30.55 ± 0.32	30.02 ± 1.70	101.84
15.85 ± 0.25	15.01 ± 0.85	105.66
8.28 ± 0.22	7.51 ± 0.42	110.36
4.22 ± 0.08	3.75 ± 0.21	112.54
2.26 ± 0.07	1.88 ± 0.11	120.75
1.19 ± 0.10	0.94 ± 0.05	126.46
0.67 ± 0.03	0.47 ± 0.03	143.24
0.28 ± 0.06	0.23 ± 0.01	117.66
0.18 ± 0.07	0.12 ± 0.01	151.59

Table 4.2. *In vitro* activity comparison of control antimalarial drugs chloroquine and Artemisinin against *P. Falciparum* D6 strain. Microscopic parasitemia analysis is based on Giemsa staining. Flow cytometric analysis is based on LDS-751 staining.

Compound Name	Microscopic data	Flow cytometry data
	IC 50 Average STD	IC 50 Average STD
Chloroquine	1.71 ± 0.94	1.67 ± 0.67
Artemisinin	10.08 ± 2.93	9.90 ± 2.93

4.6. DISCUSSION

There are two flow cytometric based parasitemia analysis methods developed in the past those have utility in both in vivo antimalarial screening and clinical diagnosis. Flow cytometric method was developed in 2007 using YOYO-1 stain for parasitemia analysis (Xie et al., 2007). Similar other flow cytometric methods developed using SYTO-16 (Cell-permeant stain) (Jimenez-Diaz et al., 2009). Both methods have very complex analysis in which blood samples with different cells population like erythrocytes, reticulocytes, white blood cells, and lymphocytes. The YOYO-1 based parasitemia analysis method requires large volume of the blood sample (10µl in 1% heparinized buffer). The blood samples pass through several steps in YOYO-1 based parasitemia analysis method. The blood cells are fixed with glutaraldehyde. And treated with 0.25% Triton X for permeabilization. The fixed and permeabilized blood samples are treated with RNase (1mg/mL) for two hours to minimize the background effect of the reticulocytes (RNA-containing cells). The RNase treated samples are stained with YOYO-1 (0.5 µg/mL). The analysis was also very complex in YOYO-1 based assay using FL2/FL-1 compensation. The flow cytometric assay for parasitemia analysis based on SYTO-16 also follow similar protocol except for permeabilization, since SYTO-16 is a cell-permeable stain. The complex processing causes loss of samples, increase the duration for the parasitemia analysis, high cost of analysis and increased labor (Jimenez-Diaz et al., 2009; Xie et al., 2007).

We have developed a new FCA method based on the LDS-751 stain that has utility in both *in vivo* and *in vitro* antimalarial screening. This novel method addresses the important challenges as pointed above. LDS-751 is a cell-permeable stain and does not require cell fixation and permeabilization for binding with the DNA of intra-erythrocytic malaria parasites. LDS-751 binds with RNA (excitation/emission maxima approx. 590/607 nm) and DNA (excitation/emission

maxima approx. 543/ 712 nm) with an approx 20-fold increase in fluorescence on binding with double-stranded DNA. Due to its differential excitation/emission spectra, LDS-751 differentiates between reticulocyte (RNA-containing cells) and malaria-infected erythrocytes populations. The RNase treatment is not required in LDS-751 based parasitemia analysis. The complete protocol requires single-step staining with LDS-751. Previously, the YOYO-1 methods did the flow cytometric analysis by a flow cytometer in FL2 and FL1 dot plot for whole blood population. However, here we gated the RBCs population only in FSC/SSC dot plot.100,000 RBCs were analyzed in SSC/FL4 dot plot or FL4 channel histogram plot. The LDS-751 FCA method requires simple flow cytometric analysis, in which parasitemia are directly calculated from percent gated population in the upper-right area of the quadrangle of SSC/FL4 dot plot or percent gated population under M1 region of FL4 channel histogram plot **(Figure 4.3**). The LDS-751 based FCA method is the simple, fast, and requires a low volume of the blood (≤2µl) with good sensitivity (till 0.2 percent of parasitemia, **Table 4.1**). The correlation coefficient (R-square) for linear line in scattered plot between flow cytometric parasitemia and microscopic parasitemia is 0.9995. That shows a good correlation between the two new assays. To further prove the utility of this method, it was applied for in vivo assay using different doses of standard antimalarial drugs chloroquine and amodiaquine. Chloroquine and amodiaquine are primary antimalarial drugs used solely in clinics for complete treatment of malaria. So these drugs are the most suitable control antimalarial drugs for in vivo antimalarial screening with wide therapeutic window. The average correlation coefficient for different blood samples from mice of the different treatment group was 0.9230 that further validate the flow cytometric parasitemia analysis method. A digital images analysis assay was also developed with the help of ImageJ software. This assay could be useful in a clinical setting that will help in reducing human biases and error in parasitemia calculation. The similarity

in parasitemia level calculated in both digital image analysis and flow cytometric analysis method proove the validity and utility of the assay. This LDS-751 based flow cytometric parasitemia analysis method has the potential for diagnosis of malaria in clinical isolates.

CHAPTER 5

FUTURE STUDIES

Presently, The PRT assay was successfully developed, and the assay was successfully applied to high throughput screening. There are several other applications are possible based on PRT assay.

The concept of control lysis of PRT assay could be applied for collecting the amastigotes and evaluating infectivity of clinical as well as, laboratory isolates. Molecular level of studied in amastigote is possible in axenic amastigotes, but these amastigotes are artificially created by providing optimal physiological condition like pH 5.5 and temperature 37ºC. These axenic amastigotes have several molecular level differences from amastigote growing inside the phago-lysosomal vacuoles in macrophages cells. To collect these intracellular amastigotes, a control lysis can be applied to rescue the amastigote from macrophages cells and separate the amastigotes by centrifugation. The PRT assay can use to evaluate the infectivity of clinical isolates. Here, the differentiated THP1 cells were infected with of promastigote parasites in different ratio cells to parasites. Infectivity was calculated with PRT assay and microscopic assay (**Figure 2.6**). Similarly, the PRT assay can be applied for evaluating the level of infection in clinical samples collected from VL patients.

A leishmania promastigote culture has mixed populations of promastigotes with high virulence, low virulence, and no virulence. So the overall population comes with reduced

infectivity in macrophages cells. The parasite with high virulence power can infect the macrophages and transform to amastigote. In PRT assay, macrophage cells infected with amastigotes are subjected to control lysis to rescue amastigote. Infected amastigotes have high virulence power. So the promastigotes transformed from rescued amastigote have high virulence power. Thus promastigote parasites with low infectivity can be run in PRT assay, and the rescued parasite comes with better infectivity. Thus PRT assay can be useful in increasing infectivity of leishmania parasite.

In the screening of natural product fractions library, the Oleandrin was confirmed as an active constituent from the active fraction of *Nerium oleander*. Similarly, Deoxypodophylotoxin was confirmed as an active constituent from the active fraction of *Thuja occidentalis*. Oleandrin is an inhibitor of P-type ATPase and deoxypodophyllotoxin is a topoisomerase inhibitor. Oleandrin is a cardiac glycoside and is known for its cardiac toxicity. So oleandrin as such cannot be further study in *in vivo* antileishmanial screening. However, a library of similar compounds can be further screen against intracellular amastigotes, and structure-activity analysis (SAR) can be done to search compounds with less cardiac effect and better antileishmanial efficacy. The compounds with less cardiac effect and potent antileishmanial effect on intracellular amastigote *in vitro* screening could be further evaluated in *in vivo* rodent models for leishmaniasis. Similarly, Deoxypodophylotoxin induced G2/M Cell Cycle Arrest and known for its severe gastrointestinal side effects and bone marrow depression. However similar compounds with less side effect and potent antileishmanial effect on intracellular amastigote *in vitro* screening could be further evaluated in *in vivo* rodent models for leishmaniasis.

The developed mcherry-Ld and citrine-Ld parasite have been successfully implemented in the *in vitro* screening methods promastigotes and intracellular amastigotes. Both developed

parasites have bright fluorescence which enables to real-time monitoring of the parasite in complex *in vivo* settings. Leishmania parasites reside in visceral organs (e.g., liver, spleen) during a disease state. Every time animal has to secrecy to access the parasite load in liver or spleen at any time point for wild-type of leishmania parasite. So large number of animals has to sacrifice for a small *in vivo* study. *In vivo* studies with non-human primate are more problematic due to less availability of such type of animals. Even several IACUC does not allow such type of studies those involve the sacrifice of a large number of animals. Here, these transgenic parasites can be helpful in *in vivo* studies. Parasite load can be monitor directly with the help of *in vivo* imaging systems. Previously one attempt was made to develop *in vivo* screening method for VL using transgenic infrared fluorescent *L. infantum* parasite (Calvo-Alvarez et al., 2015). Still, the animals have to shave to reduce the background signal due to the fur. The developed mcherry-Ld and citrine-Ld with bright fluorescence can be implemented for *in vivo* rodent based antileishmanial screening method. Furthermore, these transgenic parasites have the potential for other applications that include understanding the parasite biology and host-parasite interactions with the help of real-time cell fluorescent imager systems.

In this research project, a new FCA method based on the LDS-751 stain that has utility in both *in vivo* and *in vitro* antimalarial screening has been developed. This novel method addresses the important challenges as pointed above. The methods based on flow cytometric analysis (FCA) of the malaria parasite have been developed for diagnosis and the parasitemia analysis. These methods can be applied to automation and high throughput parasitemia analysis (Woodrow et al., 2015). However, application of FCA methods for routine clinical diagnosis of malaria has not been reported for automated screening (Grimberg, 2011). Recently, a miniaturized flow cytometer has been developed by Millipore company for the diagnosis of malaria. The work has been presented

in American Society of Tropical Medicine and Hygiene (ASTMH) in November 2016, at Atlant, GA, USA (Chromy, 2016). This miniaturized flow worked based on malaria antigen detection with the help of monoclonal antibody which may not be cost effective especially for the poor population of tropical areas. LDS-751 based FCA method can be further extended to the diagnosis of clinical samples, and a miniaturized flow cytometer can be developed that can be implanted for diagnostic purpose in malaria clinics in the tropical area.

REFERENCES

Abamor, E.S., 2017. Antileishmanial activities of caffeic acid phenethyl ester loaded PLGA nanoparticles against Leishmania infantum promastigotes and amastigotes in vitro. Asian Pac J Trop Med 10, 25-34.

Abbott, A.J., Holoubek, C.G., Martin, R.A., 1998. Inhibition of Na+,K+-ATPase by the cardenolide 6'-O-(E-4-hydroxycinnamoyl) desglucouzarin. Biochem Biophys Res Commun 251, 256-259.

Abdullah, S.M., Flath, B., Presber, H.W., 1999. Comparison of different staining procedures for the flow cytometric analysis of U-937 cells infected with different Leishmania-species. J Microbiol Methods 37, 123-138.

Ager, A.L., 1984. Rodent malaria models. . Handbook of Experimental Pharmacology. Germany: Springer-Verlag; 1984., 225-227.

Albuquerque, A., Campino, L., Cardoso, L., Cortes, S., 2017. Evaluation of four molecular methods to detect Leishmania infection in dogs. Parasit Vectors 10, 57.

Alexander, J., Satoskar, A.R., Russell, D.G., 1999. Leishmania species: models of intracellular parasitism. J Cell Sci 112 Pt 18, 2993-3002.

Alvar, J., Canavate, C., Molina, R., Moreno, J., Nieto, J., 2004. Canine leishmaniasis. Adv Parasitol 57, 1-88.

Amino, R., Thiberge, S., Martin, B., Celli, S., Shorte, S., Frischknecht, F., Menard, R., 2006. Quantitative imaging of Plasmodium transmission from mosquito to mammal. Nat Med 12, 220-224.

Amit, A., Vijayamahantesh, Dikhit, M.R., Singh, A.K., Kumar, V., Suman, S.S., Singh, A., Kumar, A., Thakur, A.K., Das, V.R., Das, P., Bimal, S., 2017. Immunization with Leishmania donovani protein disulfide isomerase DNA construct induces Th1 and Th17 dependent immune response and protection against experimental visceral leishmaniasis in Balb/c mice. Mol Immunol 82, 104-113.

Angulo-Barturen, I., Jimenez-Diaz, M.B., Mulet, T., Rullas, J., Herreros, E., Ferrer, S., Jimenez, E., Mendoza, A., Regadera, J., Rosenthal, P.J., Bathurst, I., Pompliano, D.L., Gomez de las Heras, F., Gargallo-Viola, D., 2008. A murine model of falciparum-malaria by in vivo selection of competent strains in non-myelodepleted mice engrafted with human erythrocytes. PLoS One 3, e2252.

Antony, H.A., Parija, S.C., 2016. Antimalarial drug resistance: An overview. Trop Parasitol 6, 30-41.

Ashutosh, Gupta, S., Ramesh, Sundar, S., Goyal, N., 2005. Use of Leishmania donovani field isolates expressing the luciferase reporter gene in in vitro drug screening. Antimicrob Agents Chemother 49, 3776-3783.

Aslan, H., Dey, R., Meneses, C., Castrovinci, P., Jeronimo, S.M., Oliva, G., Fischer, L., Duncan, R.C., Nakhasi, H.L., Valenzuela, J.G., Kamhawi, S., 2013. A new model of progressive visceral

leishmaniasis in hamsters by natural transmission via bites of vector sand flies. J Infect Dis 207, 1328-1338.

Aulner, N., Danckaert, A., Rouault-Hardoin, E., Desrivot, J., Helynck, O., Commere, P.H., Munier-Lehmann, H., Spath, G.F., Shorte, S.L., Milon, G., Prina, E., 2013. High content analysis of primary macrophages hosting proliferating Leishmania amastigotes: application to anti-leishmanial drug discovery. PLoS Negl Trop Dis 7, e2154.

Bai, L., Wang, L., Zhao, M., Toki, A., Hasegawa, T., Ogura, H., Kataoka, T., Hirose, K., Sakai, J., Bai, J., Ando, M., 2007. Bioactive pregnanes from Nerium oleander. J Nat Prod 70, 14-18.

Bai, L., Zhao, M., Toki, A., Sakai, J., Yang, X.Y., Bai, Y., Ando, M., Hirose, K., Ando, M., 2010. Three new cardenolides from methanol extract of stems and twigs of Nerium oleander. Chem Pharm Bull (Tokyo) 58, 1088-1092.

Baneth, G., Koutinas, A.F., Solano-Gallego, L., Bourdeau, P., Ferrer, L., 2008. Canine leishmaniosis - new concepts and insights on an expanding zoonosis: part one. Trends Parasitol 24, 324-330.

Baniecki, M.L., Wirth, D.F., Clardy, J., 2007. High-throughput Plasmodium falciparum growth assay for malaria drug discovery. Antimicrob Agents Chemother 51, 716-723.

Barbosa Junior, A.A., Andrade, Z.A., Reed, S.G., 1987. The pathology of experimental visceral leishmaniasis in resistant and susceptible lines of inbred mice. Braz J Med Biol Res 20, 63-72.

Beadle, C., Long, G.W., Weiss, W.R., McElroy, P.D., Maret, S.M., Oloo, A.J., Hoffman, S.L., 1994. Diagnosis of malaria by detection of Plasmodium falciparum HRP-2 antigen with a rapid dipstick antigen-capture assay. Lancet 343, 564-568.

Beck-Johnson, L.M., Nelson, W.A., Paaijmans, K.P., Read, A.F., Thomas, M.B., Bjornstad, O.N., 2013. The effect of temperature on Anopheles mosquito population dynamics and the potential for malaria transmission. PLoS One 8, e79276.

Beignon, A.S., Le Grand, R., Chapon, C., 2014. In vivo imaging in NHP models of malaria: challenges, progress and outlooks. Parasitol Int 63, 206-215.

Bhattacharjee, A.K., Nichols, D.A., Gerena, L., Roncal, N., Gutteridge, C.E., 2007. An in silico 3D pharmacophore model of chalcones useful in the design of novel antimalarial agents. Med Chem 3, 317-326.

Billerbeck, E., de Jong, Y., Dorner, M., de la Fuente, C., Ploss, A., 2013. Animal Models for Hepatitis C, in: Bartenschlager, R. (Ed.), Hepatitis C Virus: From Molecular Virology to Antiviral Therapy. Springer Berlin Heidelberg, Berlin, Heidelberg, pp. 49-86.

Biswas, R., Mandal, S.K., Dutta, S., Bhattacharyya, S.S., Boujedaini, N., Khuda-Bukhsh, A.R., 2011. Thujone-Rich Fraction of Thuja occidentalis Demonstrates Major Anti-Cancer Potentials: Evidences from In Vitro Studies on A375 Cells. Evid Based Complement Alternat Med 2011, 568148.

Bolhassani, A., Taheri, T., Taslimi, Y., Zamanilui, S., Zahedifard, F., Seyed, N., Torkashvand, F., Vaziri, B., Rafati, S., 2011. Fluorescent Leishmania species: development of stable GFP expression and its application for in vitro and in vivo studies. Exp Parasitol 127, 637-645.

Bruce-Chwatt, L.J., 1982. Qinghaosu: a new antimalarial. Br Med J (Clin Res Ed) 284, 767-768.

Buckner, F.S., Wilson, A.J., 2005. Colorimetric assay for screening compounds against Leishmania amastigotes grown in macrophages. Am J Trop Med Hyg 72, 600-605.

Cajueiro, A.P.B., Goma, E.P., Dos Santos, H.A.M., Almeida Rodrigues, I., Toma, H.K., Araujo, S.M., Bonamin, L.V., Gomes, N.B.N., Castelo-Branco, M.T.L., de Souza Dias, E.P., Dos Santos

Pyrrho, A., Holandino, C., 2017. Homeopathic medicines cause Th1 predominance and induce spleen and megakaryocytes changes in BALB/c mice infected with Leishmania infantum. Cytokine 95, 97-101.

Callahan, H.L., Portal, A.C., Devereaux, R., Grogl, M., 1997. An axenic amastigote system for drug screening. Antimicrob Agents Chemother 41, 818-822.

Calvo-Alvarez, E., Alvarez-Velilla, R., Jimenez, M., Molina, R., Perez-Pertejo, Y., Balana-Fouce, R., Reguera, R.M., 2014. First evidence of intraclonal genetic exchange in trypanosomatids using two Leishmania infantum fluorescent transgenic clones. PLoS Negl Trop Dis 8, e3075.

Calvo-Alvarez, E., Guerrero, N.A., Alvarez-Velilla, R., Prada, C.F., Requena, J.M., Punzon, C., Llamas, M.A., Arevalo, F.J., Rivas, L., Fresno, M., Perez-Pertejo, Y., Balana-Fouce, R., Reguera, R.M., 2012. Appraisal of a Leishmania major strain stably expressing mCherry fluorescent protein for both in vitro and in vivo studies of potential drugs and vaccine against cutaneous leishmaniasis. PLoS Negl Trop Dis 6, e1927.

Calvo-Alvarez, E., Stamatakis, K., Punzon, C., Alvarez-Velilla, R., Tejeria, A., Escudero-Martinez, J.M., Perez-Pertejo, Y., Fresno, M., Balana-Fouce, R., Reguera, R.M., 2015. Infrared fluorescent imaging as a potent tool for in vitro, ex vivo and in vivo models of visceral leishmaniasis. PLoS Negl Trop Dis 9, e0003666.

Calway, T., Du, G.J., Wang, C.Z., Huang, W.H., Zhao, J., Li, S.P., Yuan, C.S., 2012. Chemical and pharmacological studies of Oplopanax horridus, a North American botanical. J Nat Med 66, 249-256.

Campbell, R.E., 2004. Realization of beta-lactamase as a versatile fluorogenic reporter. Trends Biotechnol 22, 208-211.

Campbell, R.E., Tour, O., Palmer, A.E., Steinbach, P.A., Baird, G.S., Zacharias, D.A., Tsien, R.Y., 2002. A monomeric red fluorescent protein. Proc Natl Acad Sci U S A 99, 7877-7882.

Campo, J.J., Aponte, J.J., Nhabomba, A.J., Sacarlal, J., Angulo-Barturen, I., Jimenez-Diaz, M.B., Alonso, P.L., Dobano, C., 2011. Feasibility of flow cytometry for measurements of Plasmodium falciparum parasite burden in studies in areas of malaria endemicity by use of bidimensional assessment of YOYO-1 and autofluorescence. J Clin Microbiol 49, 968-974.

Chan, M.M., Bulinski, J.C., Chang, K.P., Fong, D., 2003. A microplate assay for Leishmania amazonensis promastigotes expressing multimeric green fluorescent protein. Parasitol Res 89, 266-271.

Chang, K.P., Fong, D., 1983. Cell biology of host-parasite membrane interactions in leishmaniasis. Ciba Found Symp 99, 113-137.

Chapman, W.L., Jr., Hanson, W.L., 1981. Visceral leishmaniasis in the squirrel monkey (Saimiri sciurea). J Parasitol 67, 740-741.

Chapman, W.L., Jr., Hanson, W.L., Hendricks, L.D., 1983. Toxicity and efficacy of the antileishmanial drug meglumine antimoniate in the owl monkey (Aotus trivirgatus). J Parasitol 69, 1176-1177.

Chen, A., Yu, J., Zhang, L., Sun, Y., Zhang, Y., Guo, H., Zhou, Y., Mitchelson, K., Cheng, J., 2009. Microarray and biochemical analysis of bufalin-induced apoptosis of HL-60 Cells. Biotechnol Lett 31, 487-494.

Chernov, K.G., Redchuk, T.A., Omelina, E.S., Verkhusha, V.V., 2017. Near-Infrared Fluorescent Proteins, Biosensors, and Optogenetic Tools Engineered from Phytochromes. Chem Rev 117, 6423-6446.

Chong, C.R., Chen, X., Shi, L., Liu, J.O., Sullivan, D.J., Jr., 2006. A clinical drug library screen identifies astemizole as an antimalarial agent. Nat Chem Biol 2, 415-416.

Chromy, B.T., K. Clor, J. Mcdonald, J. Greco, B. Mulry, J. Ambroziak, J. Tyagarajan, K., 2016. A miniaturized flow cytometry platform for malaria diagnostics. AJTMH 95, 1.

Ciaramella, P., Oliva, G., Luna, R.D., Gradoni, L., Ambrosio, R., Cortese, L., Scalone, A., Persechino, A., 1997. A retrospective clinical study of canine leishmaniasis in 150 dogs naturally infected by Leishmania infantum. Vet Rec 141, 539-543.

ClinicalTrial, 2012. Multiple Dose Study to Evaluate Security, Tolerance and Pharmacokinetic of Fexinidazole (Drug Candidate for Human African Trypanosomiasis) Administered With a Loading Dose and With Food. http://clinicaltrials.gov/show/NCT01483170.

ClinicalTrial, 2013. Trial to Determine Efficacy of Fexinidazole in Visceral Leihmaniasis Patients in Sudan. http://clinicaltrials.gov/show/NCT01980199.

ClinicalTrial, 2014. First in Man Clinical Trial of a New Medicinal Product, the Fexinidazole. http://clinicaltrials.gov/show/NCT00982904.

Coatney, G.R., 1971. The simian malarias: zoonoses, anthroponoses, or both? Am J Trop Med Hyg 20, 795-803.

Coatney, G.R., Elder, H.A., Contacos, P.G., Getz, M.E., Greenland, R., Rossan, R.N., Schmidt, L.H., 1961. Transmission of the M strain of Plasmodium cynomolgi to man. Am J Trop Med Hyg 10, 673-678.

Collier, J.A., Longmore, J.M., 1983. The reliability of the microscopic diagnosis of malaria in the field and in the laboratory. Ann Trop Med Parasitol 77, 113-117.

Collins, W.E., 2002a. Nonhuman primate models. I. Nonhuman primate host-parasite combinations. Methods Mol Med 72, 77-84.

Collins, W.E., 2002b. Nonhuman primate models. II. Infection of Saimiri and Aotus monkeys with Plasmodium vivax. Methods Mol Med 72, 85-92.

Cosledan, F., Fraisse, L., Pellet, A., Guillou, F., Mordmuller, B., Kremsner, P.G., Moreno, A., Mazier, D., Maffrand, J.P., Meunier, B., 2008. Selection of a trioxaquine as an antimalarial drug candidate. Proc Natl Acad Sci U S A 105, 17579-17584.

Cragg, G.M., Newman, D.J., 2013. Natural products: a continuing source of novel drug leads. Biochim Biophys Acta 1830, 3670-3695.

Croft, S.L., Davidson, R.N., Thornton, E.A., 1991. Liposomal amphotericin B in the treatment of visceral leishmaniasis. J Antimicrob Chemother 28 Suppl B, 111-118.

Croft, S.L., Olliaro, P., 2011. Leishmaniasis chemotherapy--challenges and opportunities. Clin Microbiol Infect 17, 1478-1483.

Croft, S.L., Seifert, K., Yardley, V., 2006a. Current scenario of drug development for leishmaniasis. Indian J Med Res 123, 399-410.

Croft, S.L., Sundar, S., Fairlamb, A.H., 2006b. Drug resistance in leishmaniasis. Clin Microbiol Rev 19, 111-126.

Da Silva, J.R., Lopes, P.F., 1964. Chloroquine Resistance in Plasmodium Falciparum in Brazil. Rev Bras Malariol Doencas Trop 16, 301-310.

de Almeida, L., Passalacqua, T.G., Dutra, L.A., Fonseca, J., Nascimento, R.F.Q., Imamura, K.B., de Andrade, C.R., Dos Santos, J.L., Graminha, M.A.S., 2017. In vivo antileishmanial activity and histopathological evaluation in Leishmania infantum infected hamsters after treatment with a furoxan derivative. Biomed Pharmacother 95, 536-547.

de Koning-Ward, T.F., Janse, C.J., Waters, A.P., 2000. The development of genetic tools for dissecting the biology of malaria parasites. Annu Rev Microbiol 54, 157-185.

de Koning-Ward, T.F., Thomas, A.W., Waters, A.P., Janse, C.J., 1998. Stable expression of green fluorescent protein in blood and mosquito stages of Plasmodium berghei. Mol Biochem Parasitol 97, 247-252.

De Lima, H., De Guglielmo, Z., Rodriguez, A., Convit, J., Rodriguez, N., 2002. Cotton rats (Sigmodon hispidus) and black rats (Rattus rattus) as possible reservoirs of Leishmania spp. in Lara State, Venezuela. Mem Inst Oswaldo Cruz 97, 169-174.

De Rycker, M., Hallyburton, I., Thomas, J., Campbell, L., Wyllie, S., Joshi, D., Cameron, S., Gilbert, I.H., Wyatt, P.G., Frearson, J.A., Fairlamb, A.H., Gray, D.W., 2013. Comparison of a high-throughput high-content intracellular Leishmania donovani assay with an axenic amastigote assay. Antimicrob Agents Chemother 57, 2913-2922.

De Trez, C., Magez, S., Akira, S., Ryffel, B., Carlier, Y., Muraille, E., 2009. iNOS-producing inflammatory dendritic cells constitute the major infected cell type during the chronic Leishmania major infection phase of C57BL/6 resistant mice. PLoS Pathog 5, e1000494.

Delves, M., Plouffe, D., Scheurer, C., Meister, S., Wittlin, S., Winzeler, E.A., Sinden, R.E., Leroy, D., 2012. The activities of current antimalarial drugs on the life cycle stages of Plasmodium: a comparative study with human and rodent parasites. PLoS Med 9, e1001169.

Desakorn, V., Silamut, K., Angus, B., Sahassananda, D., Chotivanich, K., Suntharasamai, P., Simpson, J., White, N.J., 1997. Semi-quantitative measurement of Plasmodium falciparum antigen PfHRP2 in blood and plasma. Trans R Soc Trop Med Hyg 91, 479-483.

Desjardins, R.E., Canfield, C.J., Haynes, J.D., Chulay, J.D., 1979. Quantitative assessment of antimalarial activity in vitro by a semiautomated microdilution technique. Antimicrob Agents Chemother 16, 710-718.

Deye, G.A., Gettayacamin, M., Hansukjariya, P., Im-erbsin, R., Sattabongkot, J., Rothstein, Y., Macareo, L., Fracisco, S., Bennett, K., Magill, A.J., Ohrt, C., 2012. Use of a rhesus Plasmodium cynomolgi model to screen for anti-hypnozoite activity of pharmaceutical substances. Am J Trop Med Hyg 86, 931-935.

Dhandapani, R., 2007. Hypolipidemic activity of Eclipta prostrata (L.) L. leaf extract in atherogenic diet induced hyperlipidemic rats. Indian J Exp Biol 45, 617-619.

Di Giorgio, C., Ridoux, O., Delmas, F., Azas, N., Gasquet, M., Timon-David, P., 2000. Flow cytometric detection of Leishmania parasites in human monocyte-derived macrophages: application to antileishmanial-drug testing. Antimicrob Agents Chemother 44, 3074-3078.

Dorlo, T.P., Balasegaram, M., Beijnen, J.H., de Vries, P.J., 2012. Miltefosine: a review of its pharmacology and therapeutic efficacy in the treatment of leishmaniasis. J Antimicrob Chemother 67, 2576-2597.

Dow, G.S., Gettayacamin, M., Hansukjariya, P., Imerbsin, R., Komcharoen, S., Sattabongkot, J., Kyle, D., Milhous, W., Cozens, S., Kenworthy, D., Miller, A., Veazey, J., Ohrt, C., 2011. Radical curative efficacy of tafenoquine combination regimens in Plasmodium cynomolgi-infected Rhesus monkeys (Macaca mulatta). Malar J 10, 212.

Doyle, P.S., Engel, J.C., Pimenta, P.F., da Silva, P.P., Dwyer, D.M., 1991. Leishmania donovani: long-term culture of axenic amastigotes at 37 degrees C. Exp Parasitol 73, 326-334.

Dube, A., Gupta, R., Singh, N., 2009. Reporter genes facilitating discovery of drugs targeting protozoan parasites. Trends Parasitol 25, 432-439.

Dube, A., Singh, N., Sundar, S., Singh, N., 2005. Refractoriness to the treatment of sodium stibogluconate in Indian kala-azar field isolates persist in in vitro and in vivo experimental models. Parasitol Res 96, 216-223.

Dunn, D.E., He, D.N., Yang, P., Johansen, M., Newman, R.A., Lo, D.C., 2011. In vitro and in vivo neuroprotective activity of the cardiac glycoside oleandrin from Nerium oleander in brain slice-based stroke models. J Neurochem 119, 805-814.

Dupouy-Camet, J., 2004. [New drugs for the treatment of human parasitic protozoa]. Parassitologia 46, 81-84.

Dutta, A., Bandyopadhyay, S., Mandal, C., Chatterjee, M., 2005. Development of a modified MTT assay for screening antimonial resistant field isolates of Indian visceral leishmaniasis. Parasitol Int 54, 119-122.

Farrell, J.P., 1976. Leishmania donovani: acquired resistance to visceral leishmaniasis in the golden hamster. Exp Parasitol 40, 89-94.

Fidock, D.A., Rosenthal, P.J., Croft, S.L., Brun, R., Nwaka, S., 2004. Antimalarial drug discovery: efficacy models for compound screening. Nat Rev Drug Discov 3, 509-520.

Fix, A.S., Waterhouse, C., Greiner, E.C., Stoskopf, M.K., 1988. Plasmodium relictum as a cause of avian malaria in wild-caught magellanic penguins (Spheniscus magellanicus). J Wildl Dis 24, 610-619.

Fonseca, L.L., Alezi, H.S., Moreno, A., Barnwell, J.W., Galinski, M.R., Voit, E.O., 2016. Quantifying the removal of red blood cells in Macaca mulatta during a Plasmodium coatneyi infection. Malar J 15, 410.

Forestier, C.L., Spath, G.F., Prina, E., Dasari, S., 2015. Simultaneous multi-parametric analysis of Leishmania and of its hosting mammal cells: A high content imaging-based method enabling sound drug discovery process. Microb Pathog 88, 103-108.

Franke-Fayard, B., Trueman, H., Ramesar, J., Mendoza, J., van der Keur, M., van der Linden, R., Sinden, R.E., Waters, A.P., Janse, C.J., 2004. A Plasmodium berghei reference line that

constitutively expresses GFP at a high level throughout the complete life cycle. Mol Biochem Parasitol 137, 23-33.

Franke-Fayard, B., Waters, A.P., Janse, C.J., 2006. Real-time in vivo imaging of transgenic bioluminescent blood stages of rodent malaria parasites in mice. Nat Protoc 1, 476-485.

Frischknecht, F., Baldacci, P., Martin, B., Zimmer, C., Thiberge, S., Olivo-Marin, J.C., Shorte, S.L., Menard, R., 2004. Imaging movement of malaria parasites during transmission by Anopheles mosquitoes. Cell Microbiol 6, 687-694.

Fu, L., Zhang, S., Li, N., Wang, J., Zhao, M., Sakai, J., Hasegawa, T., Mitsui, T., Kataoka, T., Oka, S., Kiuchi, M., Hirose, K., Ando, M., 2005. Three new triterpenes from Nerium oleander and biological activity of the isolated compounds. J Nat Prod 68, 198-206.

Fu, Y., Tilley, L., Kenny, S., Klonis, N., 2010. Dual labeling with a far red probe permits analysis of growth and oxidative stress in P. falciparum-infected erythrocytes. Cytometry A 77, 253-263.

Furtado, F.B., de Aquino, F.J., Nascimento, E.A., de, M.M.C., de Morais, S.A., Chang, R., Cunha, L.C., Leandro, L.F., Martins, C.H., Martins, M.M., da Silva, C.V., Machado, F.C., de Oliveira, A., 2014. Seasonal variation of the chemical composition and antimicrobial and cytotoxic activities of the essential oils from Inga laurina (Sw.) Willd. Molecules 19, 4560-4577.

Galinski, M.R., Barnwell, J.W., 2012. Nonhuman primatemodels for humanmalaria research. Nonhuman primates in biomedical research:diseases. Elsevier, editor. 2rd ed.

Academic Press, 299–323.

Galinski, M.R., Lapp, S.A., Peterson, M.S., Ay, F., Joyner, C.J., KG, L.E.R., Fonseca, L.L., Voit, E.O., Mahpic, C., 2017. Plasmodium knowlesi: a superb in vivo nonhuman primate model of antigenic variation in malaria. Parasitology, 1-16.

Ganguly, S., Bandyopadhyay, S., Sarkar, A., Chatterjee, M., 2006. Development of a semi-automated colorimetric assay for screening anti-leishmanial agents. J Microbiol Methods 66, 79-86.

Garg, R., Dube, A., 2006. Animal models for vaccine studies for visceral leishmaniasis. Indian J Med Res 123, 439-454.

Gifawesen, C., Farrell, J.P., 1989. Comparison of T-cell responses in self-limiting versus progressive visceral Leishmania donovani infections in golden hamsters. Infect Immun 57, 3091-3096.

Ginsberg, A.M., Laurenzi, M.W., Rouse, D.J., Whitney, K.D., Spigelman, M.K., 2009. Safety, tolerability, and pharmacokinetics of PA-824 in healthy subjects. Antimicrob Agents Chemother 53, 3720-3725.

Goldsmith, K., 1946. A controlled field trial of SN 7618-5 (chloroquine) for the suppression of malaria. J Malar Inst India 6, 311-316.

Goyard, S., Beverley, S.M., 2000. Blasticidin resistance: a new independent marker for stable transfection of Leishmania. Mol Biochem Parasitol 108, 249-252.

Graewe, S., Retzlaff, S., Struck, N., Janse, C.J., Heussler, V.T., 2009. Going live: a comparative analysis of the suitability of the RFP derivatives RedStar, mCherry and tdTomato for intravital and in vitro live imaging of Plasmodium parasites. Biotechnol J 4, 895-902.

Grimberg, B.T., 2011. Methodology and application of flow cytometry for investigation of human malaria parasites. J Immunol Methods 367, 1-16.

Guinet, F., Louise, A., Jouin, H., Antoine, J.C., Roth, C.W., 2000. Accurate quantitation of Leishmania infection in cultured cells by flow cytometry. Cytometry 39, 235-240.

Gupta, S., Nishi, 2011. Visceral leishmaniasis: experimental models for drug discovery. Indian J Med Res 133, 27-39.

Ha, D.S., Schwarz, J.K., Turco, S.J., Beverley, S.M., 1996. Use of the green fluorescent protein as a marker in transfected Leishmania. Mol Biochem Parasitol 77, 57-64.

Haas, A.K., Mayer, K., Brinkmann, U., 2012. Generation of fluorescent IgG fusion proteins in mammalian cells. Methods Mol Biol 901, 265-276.

Hadizadeh, I., Peivastegan, B., Kolahi, M., 2009. Antifungal activity of nettle (Urtica dioica L.), colocynth (Citrullus colocynthis L. Schrad), oleander (Nerium oleander L.) and konar (Ziziphus spina-christi L.) extracts on plants pathogenic fungi. Pak J Biol Sci 12, 58-63.

Handman, E., 1999. Cell biology of Leishmania. Adv Parasitol 44, 1-39.

Hare, J.D., 1986. Two-color flow-cytometric analysis of the growth cycle of Plasmodium falciparum in vitro: identification of cell cycle compartments. J Histochem Cytochem 34, 1651-1658.

Hendrickx, S., Eberhardt, E., Mondelaers, A., Rijal, S., Bhattarai, N.R., Dujardin, J.C., Delputte, P., Cos, P., Maes, L., 2015. Lack of correlation between the promastigote back-transformation assay and miltefosine treatment outcome. J Antimicrob Chemother 70, 3023-3026.

Herwaldt, B.L., 1999. Leishmaniasis. Lancet 354, 1191-1199.

Hobbs, C.V., Neal, J., Conteh, S., Donnelly, L., Chen, J., Marsh, K., Lambert, L., Orr-Gonzalez, S., Hinderer, J., Healy, S., Borkowsky, W., Penzak, S.R., Chakravarty, S., Hoffman, S.L., Duffy, P.E., 2014. HIV treatments reduce malaria liver stage burden in a non-human primate model of malaria infection at clinically relevant concentrations in vivo. PLoS One 9, e100138.

Hoekenga, M.T., 1952. Treatment of malaria with a single dose of amodiaquine or chloroquine. J Am Med Assoc 149, 1369-1371.

Hurwitz, E.S., Johnson, D., Campbell, C.C., 1981. Resistance of Plasmodium falciparum malaria to sulfadoxine-pyrimethamine ('Fansidar') in a refugee camp in Thailand. Lancet 1, 1068-1070.

Hutchens, M., Luker, G.D., 2007. Applications of bioluminescence imaging to the study of infectious diseases. Cell Microbiol 9, 2315-2322.

Imani, M., Dehkharghani, A.D., Ghelman, M., Mohammadloo, M., 2014. Molecular technique for detection of Leishmania infantum isolates in Iran. Trop Parasitol 4, 35-37.

Izumiyama, S., Omura, M., Takasaki, T., Ohmae, H., Asahi, H., 2009. Plasmodium falciparum: development and validation of a measure of intraerythrocytic growth using SYBR Green I in a flow cytometer. Exp Parasitol 121, 144-150.

Jain, M., Vangapandu, S., Sachdeva, S., Singh, S., Singh, P.P., Jena, G.B., Tikoo, K., Ramarao, P., Kaul, C.L., Jain, R., 2004. Discovery of a bulky 2-tert-butyl group containing primaquine analogue that exhibits potent blood-schizontocidal antimalarial activities and complete elimination of methemoglobin toxicity. J Med Chem 47, 285-287.

Jain, S., Jacob, M., Walker, L., Tekwani, B., 2016a. Screening North American plant extracts in vitro against Trypanosoma brucei for discovery of new antitrypanosomal drug leads. BMC Complement Altern Med 16, 131.

Jain, S., Jacob, M., Walker, L., Tekwani, B., 2016b. Screening North American plant extracts in vitro against Trypanosoma brucei for discovery of new antitrypanosomal drug leads. BMC Complementary and Alternative Medicine 16, 1-6.

Jain, S.K., Sahu, R., Walker, L.A., Tekwani, B.L., 2012. A parasite rescue and transformation assay for antileishmanial screening against intracellular Leishmania donovani amastigotes in THP1 human acute monocytic leukemia cell line. J Vis Exp.

Jambulingam, P., Pradeep Kumar, N., Nandakumar, S., Paily, K.P., Srinivasan, R., 2017. Domestic dogs as reservoir hosts for Leishmania donovani in the southernmost Western Ghats in India. Acta Trop 171, 64-67.

Jelinek, T., Kilian, A.H., Henk, M., Mughusu, E.B., Nothdurft, H.D., Loscher, T., Knobloch, J., Van Sonnenburg, F., 1996. Parasite-specific lactate dehydrogenase for the diagnosis of Plasmodium falciparum infection in an endemic area in west Uganda. Trop Med Int Health 1, 227-230.

Jha, T.K., Sundar, S., Thakur, C.P., Felton, J.M., Sabin, A.J., Horton, J., 2005. A phase II dose-ranging study of sitamaquine for the treatment of visceral leishmaniasis in India. Am J Trop Med Hyg 73, 1005-1011.

Jimenez-Diaz, M.B., Mulet, T., Gomez, V., Viera, S., Alvarez, A., Garuti, H., Vazquez, Y., Fernandez, A., Ibanez, J., Jimenez, M., Gargallo-Viola, D., Angulo-Barturen, I., 2009. Quantitative measurement of Plasmodium-infected erythrocytes in murine models of malaria by flow cytometry using bidimensional assessment of SYTO-16 fluorescence. Cytometry A 75, 225-235.

Jimenez-Diaz, M.B., Viera, S., Fernandez-Alvaro, E., Angulo-Barturen, I., 2014. Animal models of efficacy to accelerate drug discovery in malaria. Parasitology 141, 93-103.

Jin, H.R., Liao, Y., Li, X., Zhang, Z., Zhao, J., Wang, C.Z., Huang, W.H., Li, S.P., Yuan, C.S., Du, W., 2014. Anticancer compound Oplopantriol A kills cancer cells through inducing ER stress and BH3 proteins Bim and Noxa. Cell Death Dis 5, e1190.

Jin, Y., Kebaier, C., Vanderberg, J., 2007. Direct microscopic quantification of dynamics of Plasmodium berghei sporozoite transmission from mosquitoes to mice. Infect Immun 75, 5532-5539.

Jortani, S.A., Helm, R.A., Valdes, R., Jr., 1996. Inhibition of Na,K-ATPase by oleandrin and oleandrigenin, and their detection by digoxin immunoassays. Clin Chem 42, 1654-1658.

Judith Recht, E.A.a.N.W., 2014. Safety of 8-aminoquinoline antimalarial medicines. World Health Organisation, p. 224.

Jung, S.H., Kim, B.J., Lee, E.H., Osborne, N.N., 2010. Isoquercitrin is the most effective antioxidant in the plant Thuja orientalis and able to counteract oxidative-induced damage to a transformed cell line (RGC-5 cells). Neurochem Int 57, 713-721.

Kalra, B.S., Chawla, S., Gupta, P., Valecha, N.,, 2006. screening of antimalarial drugs: an overview. Indian Journal of Pharmacology 38, 5-12.

Kamau, S.W., Grimm, F., Hehl, A.B., 2001. Expression of green fluorescent protein as a marker for effects of antileishmanial compounds in vitro. Antimicrob Agents Chemother 45, 3654-3656.

Kaushansky, A., Mikolajczak, S.A., Vignali, M., Kappe, S.H., 2014. Of men in mice: the success and promise of humanized mouse models for human malaria parasite infections. Cell Microbiol 16, 602-611.

Kelley, B.D., Appelt, G.D., Appelt, J.M., 1988. Pharmacological aspects of selected herbs employed in hispanic folk medicine in the San Luis Valley of Colorado, USA: II. Asclepias asperula (inmortal) and Achillea lanulosa (plumajillo). J Ethnopharmacol 22, 1-9.

Kelly, J.X., Smilkstein, M.J., Brun, R., Wittlin, S., Cooper, R.A., Lane, K.D., Janowsky, A., Johnson, R.A., Dodean, R.A., Winter, R., Hinrichs, D.J., Riscoe, M.K., 2009. Discovery of dual function acridones as a new antimalarial chemotype. Nature 459, 270-273.

Khan, Z.M., Vanderberg, J.P., 1991. Role of host cellular response in differential susceptibility of nonimmunized BALB/c mice to Plasmodium berghei and Plasmodium yoelii sporozoites. Infect Immun 59, 2529-2534.

Khanna, V.G., Kannabiran, K., Getti, G., 2009. Leishmanicidal activity of saponins isolated from the leaves of Eclipta prostrata and Gymnema sylvestre. Indian J Pharmacol 41, 32-35.

Kim, H.Y., Kim, H.M., Ryu, B., Lee, J.S., Choi, J.H., Jang, D.S., 2015. Constituents of the aerial parts of Eclipta prostrata and their cytotoxicity on human ovarian cancer cells in vitro. Arch Pharm Res.

Kimblin, N., Peters, N., Debrabant, A., Secundino, N., Egen, J., Lawyer, P., Fay, M.P., Kamhawi, S., Sacks, D., 2008. Quantification of the infectious dose of Leishmania major transmitted to the skin by single sand flies. Proc Natl Acad Sci U S A 105, 10125-10130.

Kinnamon, K.E., Steck, E.A., Loizeaux, P.S., Hanson, W.L., Chapman, W.L., Jr., Waits, V.B., 1978. The antileishmanial activity of lepidines. Am J Trop Med Hyg 27, 751-757.

Knobloch, J., Henk, M., 1995. Screening for malaria by determination of parasite-specific lactate dehydrogenase. Trans R Soc Trop Med Hyg 89, 269-270.

Kobaisy, M., Abramowski, Z., Lermer, L., Saxena, G., Hancock, R.E., Towers, G.H., Doxsee, D., Stokes, R.W., 1997. Antimycobacterial polyynes of Devil's Club (Oplopanax horridus), a North American native medicinal plant. J Nat Prod 60, 1210-1213.

Kocken, C.H., Remarque, E.J., Dubbeld, M.A., Wein, S., van der Wel, A., Verburgh, R.J., Vial, H.J., Thomas, A.W., 2009. Statistical model to evaluate in vivo activities of antimalarial drugs in a Plasmodium cynomolgi-macaque model for Plasmodium vivax malaria. Antimicrob Agents Chemother 53, 421-427.

Kolodziej, H., Kiderlen, A.F., 2005. Antileishmanial activity and immune modulatory effects of tannins and related compounds on Leishmania parasitised RAW 264.7 cells. Phytochemistry 66, 2056-2071.

Kram, D., Thale, C., Kolodziej, H., Kiderlen, A.F., 2008. Intracellular parasite kill: flow cytometry and NO detection for rapid discrimination between anti-leishmanial activity and macrophage activation. J Immunol Methods 333, 79-88.

Kulshrestha, A., Bhandari, V., Mukhopadhyay, R., Ramesh, V., Sundar, S., Maes, L., Dujardin, J.C., Roy, S., Salotra, P., 2013. Validation of a simple resazurin-based promastigote assay for the routine monitoring of miltefosine susceptibility in clinical isolates of Leishmania donovani. Parasitol Res 112, 825-828.

Kupeli Akkol, E., Ilhan, M., Ayse Demirel, M., Keles, H., Tumen, I., Suntar, I., 2015. Thuja occidentalis L. and its active compound, alpha-thujone: Promising effects in the treatment of polycystic ovary syndrome without inducing osteoporosis. J Ethnopharmacol 168, 25-30.

Landier, J., Parker, D.M., Thu, A.M., Carrara, V.I., Lwin, K.M., Bonnington, C.A., Pukrittayakamee, S., Delmas, G., Nosten, F.H., 2016. The role of early detection and treatment in malaria elimination. Malar J 15, 363.

Lang, T., Lecoeur, H., Prina, E., 2009. Imaging Leishmania development in their host cells. Trends Parasitol 25, 464-473.

LeBowitz, J.H., 1994. Transfection experiments with Leishmania. Methods Cell Biol 45, 65-78.

Lecoeur, H., de La Llave, E., Osorio, Y.F.J., Goyard, S., Kiefer-Biasizzo, H., Balazuc, A.M., Milon, G., Prina, E., Lang, T., 2010. Sorting of Leishmania-bearing dendritic cells reveals subtle parasite-induced modulation of host-cell gene expression. Microbes Infect 12, 46-54.

Lirdprapamongkol, K., Kramb, J.P., Chokchaichamnankit, D., Srisomsap, C., Surarit, R., Sila-Asna, M., Bunyaratvej, A., Dannhardt, G., Svasti, J., 2008. Juice of eclipta prostrata inhibits cell migration in vitro and exhibits anti-angiogenic activity in vivo. In Vivo 22, 363-368.

Liu, Q.M., Zhao, H.Y., Zhong, X.K., Jiang, J.G., 2012. Eclipta prostrata L. phytochemicals: isolation, structure elucidation, and their antitumor activity. Food Chem Toxicol 50, 4016-4022.

Loiseau, P.M., Cojean, S., Schrevel, J., 2011. Sitamaquine as a putative antileishmanial drug candidate: from the mechanism of action to the risk of drug resistance. Parasite 18, 115-119.

Lopez-Martin, C., Perez-Victoria, J.M., Carvalho, L., Castanys, S., Gamarro, F., 2008. Sitamaquine sensitivity in Leishmania species is not mediated by drug accumulation in acidocalcisomes. Antimicrob Agents Chemother 52, 4030-4036.

Loria-Cervera, E.N., Andrade-Narvaez, F.J., 2014. Animal models for the study of leishmaniasis immunology. Rev Inst Med Trop Sao Paulo 56, 1-11.

Maia, C., Rolao, N., Nunes, M., Goncalves, L., Campino, L., 2007. Infectivity of five different types of macrophages by Leishmania infantum. Acta Trop 103, 150-155.

Makler, M.T., Hinrichs, D.J., 1993. Measurement of the lactate dehydrogenase activity of Plasmodium falciparum as an assessment of parasitemia. Am J Trop Med Hyg 48, 205-210.

Makler, M.T., Palmer, C.J., Ager, A.L., 1998. A review of practical techniques for the diagnosis of malaria. Ann Trop Med Parasitol 92, 419-433.

Manda, S., Khan, S.I., Jain, S.K., Mohammed, S., Tekwani, B.L., Khan, I.A., Vishwakarma, R.A., Bharate, S.B., 2014. Synthesis, antileishmanial and antitrypanosomal activities of N-substituted tetrahydro-beta-carbolines. Bioorg Med Chem Lett 24, 3247-3250.

Masuda, T., Oyama, Y., Yamamoto, N., Umebayashi, C., Nakao, H., Toi, Y., Takeda, Y., Nakamoto, K., Kuninaga, H., Nishizato, Y., Nonaka, A., 2003. Cytotoxic screening of medicinal and edible plants in Okinawa, Japan, and identification of the main toxic constituent of Rhodea japonica (Omoto). Biosci Biotechnol Biochem 67, 1401-1404.

Mazzio, E., Badisa, R., Mack, N., Deiab, S., Soliman, K.F., 2014. High throughput screening of natural products for anti-mitotic effects in MDA-MB-231 human breast carcinoma cells. Phytother Res 28, 856-867.

Melby, P.C., Chandrasekar, B., Zhao, W., Coe, J.E., 2001. The hamster as a model of human visceral leishmaniasis: progressive disease and impaired generation of nitric oxide in the face of a prominent Th1-like cytokine response. J Immunol 166, 1912-1920.

Melby, P.C., Yang, Y.Z., Cheng, J., Zhao, W., 1998. Regional differences in the cellular immune response to experimental cutaneous or visceral infection with Leishmania donovani. Infect Immun 66, 18-27.

Melo, P.A., do Nascimento, M.C., Mors, W.B., Suarez-Kurtz, G., 1994. Inhibition of the myotoxic and hemorrhagic activities of crotalid venoms by Eclipta prostrata (Asteraceae) extracts and constituents. Toxicon 32, 595-603.

Meshnick, S.R., 1998. Artemisinin antimalarials: mechanisms of action and resistance. Med Trop (Mars) 58, 13-17.

Mikhail, J.W., Mansour, N.S., 1973. Mystromys albicaudatus, the African white-tailed rat, as an experimental host for Leishmania donovani. J Parasitol 59, 1085-1087.

Mikus, J., Steverding, D., 2000. A simple colorimetric method to screen drug cytotoxicity against Leishmania using the dye Alamar Blue. Parasitol Int 48, 265-269.

Miller, J.L., Murray, S., Vaughan, A.M., Harupa, A., Sack, B., Baldwin, M., Crispe, I.N., Kappe, S.H., 2013. Quantitative bioluminescent imaging of pre-erythrocytic malaria parasite infection using luciferase-expressing Plasmodium yoelii. PLoS One 8, e60820.

Millington, O.R., Myburgh, E., Mottram, J.C., Alexander, J., 2010. Imaging of the host/parasite interplay in cutaneous leishmaniasis. Exp Parasitol 126, 310-317.

Milne, L.M., Kyi, M.S., Chiodini, P.L., Warhurst, D.C., 1994. Accuracy of routine laboratory diagnosis of malaria in the United Kingdom. J Clin Pathol 47, 740-742.

Misslitz, A., Mottram, J.C., Overath, P., Aebischer, T., 2000. Targeted integration into a rRNA locus results in uniform and high level expression of transgenes in Leishmania amastigotes. Mol Biochem Parasitol 107, 251-261.

Montgomery, R., 1964. Chloroquine-Resistant Falciparum Malaria in South-East Asia, with a Report of a Case from Thailand. J R Army Med Corps 110, 172-174.

Moreno, A., Cabrera-Mora, M., Garcia, A., Orkin, J., Strobert, E., Barnwell, J.W., Galinski, M.R., 2013. Plasmodium coatneyi in rhesus macaques replicates the multisystemic dysfunction of severe malaria in humans. Infect Immun 81, 1889-1904.

Mwakingwe, A., Ting, L.M., Hochman, S., Chen, J., Sinnis, P., Kim, K., 2009. Noninvasive real-time monitoring of liver-stage development of bioluminescent Plasmodium parasites. J Infect Dis 200, 1470-1478.

Naser, B., Lund, B., Henneicke-von Zepelin, H.H., Kohler, G., Lehmacher, W., Scaglione, F., 2005. A randomized, double-blind, placebo-controlled, clinical dose-response trial of an extract of Baptisia, Echinacea and Thuja for the treatment of patients with common cold. Phytomedicine 12, 715-722.

Neal, R.A., Croft, S.L., 1984. An in-vitro system for determining the activity of compounds against the intracellular amastigote form of Leishmania donovani. J Antimicrob Chemother 14, 463-475.

Newman, D.J., Cragg, G.M., 2012. Natural products as sources of new drugs over the 30 years from 1981 to 2010. J Nat Prod 75, 311-335.

Nicholson, G.C., Tennant, R.C., Carpenter, D.C., Sarau, H.M., Kon, O.M., Barnes, P.J., Salmon, M., Vessey, R.S., Tal-Singer, R., Hansel, T.T., 2007. A novel flow cytometric assay of human whole blood neutrophil and monocyte CD11b levels: upregulation by chemokines is related to receptor expression, comparison with neutrophil shape change, and effects of a chemokine receptor (CXCR2) antagonist. Pulm Pharmacol Ther 20, 52-59.

Nolan, T.J., Farrell, J.P., 1987. Experimental infections of the multimammate rat (Mastomys natalensis) with Leishmania donovani and Leishmania major. Am J Trop Med Hyg 36, 264-269.

Okuno, T., Goto, Y., Matsumoto, Y., Otsuka, H., Matsumoto, Y., 2003. Applications of recombinant Leishmania amazonensis expressing egfp or the beta-galactosidase gene for drug screening and histopathological analysis. Exp Anim 52, 109-118.

Oliveira, C.I.D., Teixeira, M.J.,, Gomes, R., Barral, A., Brodskyn, C., 2004. Animal models for infectious diseases caused by parasites: Leishmaniasis. Drug Discovery Today: Disease Models 1, 81-86.

Osorio, Y., Rodriguez, L.D., Bonilla, D.L., Peniche, A.G., Henao, H., Saldarriaga, O., Travi, B.L., 2012. Congenital transmission of experimental leishmaniasis in a hamster model. Am J Trop Med Hyg 86, 812-820.

Paape, D., Bell, A.S., Heal, W.P., Hutton, J.A., Leatherbarrow, R.J., Tate, E.W., Smith, D.F., 2014. Using a non-image-based medium-throughput assay for screening compounds targeting N-myristoylation in intracellular Leishmania amastigotes. PLoS Negl Trop Dis 8, e3363.

Pan, Y., Rhea, P., Tan, L., Cartwright, C., Lee, H.J., Ravoori, M.K., Addington, C., Gagea, M., Kundra, V., Kim, S.J., Newman, R.A., Yang, P., 2015. PBI-05204, a supercritical CO(2) extract of Nerium oleander, inhibits growth of human pancreatic cancer via targeting the PI3K/mTOR pathway. Invest New Drugs 33, 271-279.

Pasini, E.M., Zeeman, A.M., Voorberg, V.A.N.D.E.R.W.A., Kocken, C.H., 2016. Plasmodium knowlesi: a relevant, versatile experimental malaria model. Parasitology, 1-15.

Pattanapanyasat, K., Thaithong, S., Kyle, D.E., Udomsangpetch, R., Yongvanitchit, K., Hider, R.C., Webster, H.K., 1997. Flow cytometric assessment of hydroxypyridinone iron chelators on in vitro growth of drug-resistant malaria. Cytometry 27, 84-91.

Patterson, S., Wyllie, S., Stojanovski, L., Perry, M.R., Simeons, F.R., Norval, S., Osuna-Cabello, M., De Rycker, M., Read, K.D., Fairlamb, A.H., 2013. The R enantiomer of the antitubercular drug PA-824 as a potential oral treatment for visceral Leishmaniasis. Antimicrob Agents Chemother 57, 4699-4706.

Peters, N.C., Egen, J.G., Secundino, N., Debrabant, A., Kimblin, N., Kamhawi, S., Lawyer, P., Fay, M.P., Germain, R.N., Sacks, D., 2008. In vivo imaging reveals an essential role for neutrophils in leishmaniasis transmitted by sand flies. Science 321, 970-974.

Peters, W., 1987. Techniques of drug evaluation 1: primary screening. In: Chemotherapy and drug resistance in Malaria. Florida: Academic Press.

Peters, W., Robinson, B.L., 1999. The chemotherapy of rodent malaria. LVI. Studies on the development of resistance to natural and synthetic endoperoxides. Ann Trop Med Parasitol 93, 325-329.

Pithayanukul, P., Laovachirasuwan, S., Bavovada, R., Pakmanee, N., Suttisri, R., 2004. Anti-venom potential of butanolic extract of Eclipta prostrata against Malayan pit viper venom. J Ethnopharmacol 90, 347-352.

Ploemen, I.H., Prudencio, M., Douradinha, B.G., Ramesar, J., Fonager, J., van Gemert, G.J., Luty, A.J., Hermsen, C.C., Sauerwein, R.W., Baptista, F.G., Mota, M.M., Waters, A.P., Que, I.,

Lowik, C.W., Khan, S.M., Janse, C.J., Franke-Fayard, B.M., 2009. Visualisation and quantitative analysis of the rodent malaria liver stage by real time imaging. PLoS One 4, e7881.

Price, H.P., Paape, D., Hodgkinson, M.R., Farrant, K., Doehl, J., Stark, M., Smith, D.F., 2013. The Leishmania major BBSome subunit BBS1 is essential for parasite virulence in the mammalian host. Mol Microbiol 90, 597-611.

Prugnolle, F., McGee, K., Keebler, J., Awadalla, P., 2008. Selection shapes malaria genomes and drives divergence between pathogens infecting hominids versus rodents. BMC Evol Biol 8, 223.

Pulido, S.A., Munoz, D.L., Restrepo, A.M., Mesa, C.V., Alzate, J.F., Velez, I.D., Robledo, S.M., 2012. Improvement of the green fluorescent protein reporter system in Leishmania spp. for the in vitro and in vivo screening of antileishmanial drugs. Acta Trop 122, 36-45.

Qiu, F., Cai, G., Jaki, B.U., Lankin, D.C., Franzblau, S.G., Pauli, G.F., 2013. Quantitative purity-activity relationships of natural products: the case of anti-tuberculosis active triterpenes from Oplopanax horridus. J Nat Prod 76, 413-419.

Raether, W., Hanel, H., 2003. Nitroheterocyclic drugs with broad spectrum activity. Parasitol Res 90 Supp 1, S19-39.

Rahman, A.A., Samoylenko, V., Jain, S.K., Tekwani, B.L., Khan, S.I., Jacob, M.R., Midiwo, J.O., Hester, J.P., Walker, L.A., Muhammad, I., 2011. Antiparasitic and antimicrobial isoflavanquinones from Abrus schimperi. Nat Prod Commun 6, 1645-1650.

Rajakumar, G., Rahuman, A.A., Chung, I.M., Kirthi, A.V., Marimuthu, S., Anbarasan, K., 2015. Antiplasmodial activity of eco-friendly synthesized palladium nanoparticles using Eclipta prostrata extract against Plasmodium berghei in Swiss albino mice. Parasitol Res 114, 1397-1406.

Rashan, L.J., Franke, K., Khine, M.M., Kelter, G., Fiebig, H.H., Neumann, J., Wessjohann, L.A., 2011. Characterization of the anticancer properties of monoglycosidic cardenolides isolated from Nerium oleander and Streptocaulon tomentosum. J Ethnopharmacol 134, 781-788.

Reguera, R.M., Calvo-Alvarez, E., Alvarez-Velilla, R., Balana-Fouce, R., 2014. Target-based vs. phenotypic screenings in Leishmania drug discovery: A marriage of convenience or a dialogue of the deaf? Int J Parasitol Drugs Drug Resist 4, 355-357.

Ribeiro-Gomes, F.L., Peters, N.C., Debrabant, A., Sacks, D.L., 2012. Efficient capture of infected neutrophils by dendritic cells in the skin inhibits the early anti-leishmania response. PLoS Pathog 8, e1002536.

Rocha, L.G., Almeida, J.R., Macedo, R.O., Barbosa-Filho, J.M., 2005. A review of natural products with antileishmanial activity. Phytomedicine 12, 514-535.

Rongvaux, A., Takizawa, H., Strowig, T., Willinger, T., Eynon, E.E., Flavell, R.A., Manz, M.G., 2013. Human hemato-lymphoid system mice: current use and future potential for medicine. Annu Rev Immunol 31, 635-674.

Rouault, E., Lecoeur, H., Meriem, A.B., Minoprio, P., Goyard, S., Lang, T., 2017. Imaging visceral leishmaniasis in real time with golden hamster model: Monitoring the parasite burden and hamster transcripts to further characterize the immunological responses of the host. Parasitol Int 66, 933-939.

Roura, S., Galvez-Monton, C., Bayes-Genis, A., 2013. Bioluminescence imaging: a shining future for cardiac regeneration. J Cell Mol Med 17, 693-703.

Roy, G., Dumas, C., Sereno, D., Wu, Y., Singh, A.K., Tremblay, M.J., Ouellette, M., Olivier, M., Papadopoulou, B., 2000. Episomal and stable expression of the luciferase reporter gene for

quantifying Leishmania spp. infections in macrophages and in animal models. Mol Biochem Parasitol 110, 195-206.

Ryu, S., Shin, J.S., Jung, J.Y., Cho, Y.W., Kim, S.J., Jang, D.S., Lee, K.T., 2013. Echinocystic acid isolated from Eclipta prostrata suppresses lipopolysaccharide-induced iNOS, TNF-alpha, and IL-6 expressions via NF-kappaB inactivation in RAW 264.7 macrophages. Planta Med 79, 1031-1037.

Sacci, J.B., Jr., Alam, U., Douglas, D., Lewis, J., Tyrrell, D.L., Azad, A.F., Kneteman, N.M., 2006. Plasmodium falciparum infection and exoerythrocytic development in mice with chimeric human livers. Int J Parasitol 36, 353-360.

Sadlova, J., Yeo, M., Seblova, V., Lewis, M.D., Mauricio, I., Volf, P., Miles, M.A., 2011. Visualisation of Leishmania donovani fluorescent hybrids during early stage development in the sand fly vector. PLoS One 6, e19851.

Sahu, R., Walker, L.A., Tekwani, B.L., 2014. In vitro and in vivo anti-malarial activity of tigecycline, a glycylcycline antibiotic, in combination with chloroquine. Malar J 13, 414.

Sanchez, B.A., Mota, M.M., Sultan, A.A., Carvalho, L.H., 2004. Plasmodium berghei parasite transformed with green fluorescent protein for screening blood schizontocidal agents. Int J Parasitol 34, 485-490.

Sandgren, E.P., Palmiter, R.D., Heckel, J.L., Daugherty, C.C., Brinster, R.L., Degen, J.L., 1991. Complete hepatic regeneration after somatic deletion of an albumin-plasminogen activator transgene. Cell 66, 245-256.

Sandosham, A.A., 1963. Chloroquine-Resistant Falciparum Malaria in Malaya. Singapore Med J 3, 3-5.

Sanni, L.A., Fonseca, L.F., Langhorne, J., 2002. Mouse models for erythrocytic-stage malaria. Methods Mol Med 72, 57-76.

Scheller, L.F., Wirtz, R.A., Azad, A.F., 1994. Susceptibility of different strains of mice to hepatic infection with Plasmodium berghei. Infect Immun 62, 4844-4847.

Seifert, K., Escobar, P., Croft, S.L., 2010. In vitro activity of anti-leishmanial drugs against Leishmania donovani is host cell dependent. J Antimicrob Chemother 65, 508-511.

Sen, R., Chatterjee, M., 2011. Plant derived therapeutics for the treatment of Leishmaniasis. Phytomedicine 18, 1056-1069.

Sereno, D., Alegre, A.M., Silvestre, R., Vergnes, B., Ouaissi, A., 2005. In vitro antileishmanial activity of nicotinamide. Antimicrob Agents Chemother 49, 808-812.

Sereno, D., Cordeiro da Silva, A., Mathieu-Daude, F., Ouaissi, A., 2007. Advances and perspectives in Leishmania cell based drug-screening procedures. Parasitol Int 56, 3-7.

Sereno, D., Lemesre, J.L., 1997. Use of an enzymatic micromethod to quantify amastigote stage of Leishmania amazonensis in vitro. Parasitol Res 83, 401-403.

Sereno, D., Roy, G., Lemesre, J.L., Papadopoulou, B., Ouellette, M., 2001. DNA transformation of Leishmania infantum axenic amastigotes and their use in drug screening. Antimicrob Agents Chemother 45, 1168-1173.

Shaner, N.C., Steinbach, P.A., Tsien, R.Y., 2005. A guide to choosing fluorescent proteins. Nat Methods 2, 905-909.

Shcherbakova, D.M., Baloban, M., Verkhusha, V.V., 2015. Near-infrared fluorescent proteins engineered from bacterial phytochromes. Curr Opin Chem Biol 27, 52-63.

Shcherbo, D., Merzlyak, E.M., Chepurnykh, T.V., Fradkov, A.F., Ermakova, G.V., Solovieva, E.A., Lukyanov, K.A., Bogdanova, E.A., Zaraisky, A.G., Lukyanov, S., Chudakov, D.M., 2007. Bright far-red fluorescent protein for whole-body imaging. Nat Methods 4, 741-746.

Sherwood, J.A., Gachihi, G.S., Muigai, R.K., Skillman, D.R., Mugo, M., Rashid, J.R., Wasunna, K.M., Were, J.B., Kasili, S.K., Mbugua, J.M., et al., 1994. Phase 2 efficacy trial of an oral 8-aminoquinoline (WR6026) for treatment of visceral leishmaniasis. Clin Infect Dis 19, 1034-1039.

Shimony, O., Jaffe, C.L., 2008. Rapid fluorescent assay for screening drugs on Leishmania amastigotes. J Microbiol Methods 75, 196-200.

Shu, X., Royant, A., Lin, M.Z., Aguilera, T.A., Lev-Ram, V., Steinbach, P.A., Tsien, R.Y., 2009. Mammalian expression of infrared fluorescent proteins engineered from a bacterial phytochrome. Science 324, 804-807.

Shute, P.G., Maryon, M., 1963. An Improved Technique for Staining Malaria Parasites with Giemsa Stain. Arch Roum Pathol Exp Microbiol 22, 887-894.

Simon, G.G., 2016. Impacts of neglected tropical disease on incidence and progression of HIV/AIDS, tuberculosis, and malaria: scientific links. Int J Infect Dis 42, 54-57.

Simpson, B., Jamieson, W.S., Dimond, A.H., 1972. Sulphadoxine and pyrimethamine as treatment for acute Plasmodium falciparum malaria. Trans R Soc Trop Med Hyg 66, 222-224.

Singh, B., Daneshvar, C., 2013. Human infections and detection of Plasmodium knowlesi. Clin Microbiol Rev 26, 165-184.

Singh, K., Agarwal, A., Khan, S.I., Walker, L.A., Tekwani, B.L., 2007. Growth, drug susceptibility, and gene expression profiling of Plasmodium falciparum cultured in medium

supplemented with human serum or lipid-rich bovine serum albumin [corrected]. J Biomol Screen 12, 1109-1114.

Singh, N., Dube, A., 2004. Short report: fluorescent Leishmania: application to anti-leishmanial drug testing. Am J Trop Med Hyg 71, 400-402.

Singh, N., Gupta, R., Jaiswal, A.K., Sundar, S., Dube, A., 2009. Transgenic Leishmania donovani clinical isolates expressing green fluorescent protein constitutively for rapid and reliable ex vivo drug screening. J Antimicrob Chemother 64, 370-374.

Singhal, K.G., Gupta, G.D., 2012. Hepatoprotective and antioxidant activity of methanolic extract of flowers of Nerium oleander against CCl4-induced liver injury in rats. Asian Pac J Trop Med 5, 677-685.

Siqueira-Neto, J.L., Moon, S., Jang, J., Yang, G., Lee, C., Moon, H.K., Chatelain, E., Genovesio, A., Cechetto, J., Freitas-Junior, L.H., 2012. An image-based high-content screening assay for compounds targeting intracellular Leishmania donovani amastigotes in human macrophages. PLoS Negl Trop Dis 6, e1671.

Siu, E., Ploss, A., 2015. Modeling malaria in humanized mice: opportunities and challenges. Ann N Y Acad Sci 1342, 29-36.

Sodji, Q., Patil, V., Jain, S., Kornacki, J.R., Mrksich, M., Tekwani, B.L., Oyelere, A.K., 2014. The antileishmanial activity of isoforms 6- and 8-selective histone deacetylase inhibitors. Bioorg Med Chem Lett 24, 4826-4830.

Somsak, V., Srichairatanakool, S., Yuthavong, Y., Kamchonwongpaisan, S., Uthaipibull, C., 2012. Flow cytometric enumeration of Plasmodium berghei-infected red blood cells stained with SYBR Green I. Acta Trop 122, 113-118.

Staalsoe, T., Giha, H.A., Dodoo, D., Theander, T.G., Hviid, L., 1999. Detection of antibodies to variant antigens on Plasmodium falciparum-infected erythrocytes by flow cytometry. Cytometry 35, 329-336.

Stewart, V.A., 2003. Plasmodium vivax under the microscope: the Aotus model. Trends Parasitol 19, 589-594.

Strowig, T., Rongvaux, A., Rathinam, C., Takizawa, H., Borsotti, C., Philbrick, W., Eynon, E.E., Manz, M.G., Flavell, R.A., 2011. Transgenic expression of human signal regulatory protein alpha in Rag2-/-gamma(c)-/- mice improves engraftment of human hematopoietic cells in humanized mice. Proc Natl Acad Sci U S A 108, 13218-13223.

Sundar, S., Jha, T.K., Thakur, C.P., Sinha, P.K., Bhattacharya, S.K., 2007. Injectable paromomycin for Visceral leishmaniasis in India. N Engl J Med 356, 2571-2581.

Sunila, E.S., Kuttan, G., 2005. Protective effect of Thuja occidentalis against radiation-induced toxicity in mice. Integr Cancer Ther 4, 322-328.

Sunila, E.S., Kuttan, G., 2006. A preliminary study on antimetastatic activity of Thuja occidentalis L. in mice model. Immunopharmacol Immunotoxicol 28, 269-280.

Tarun, A.S., Baer, K., Dumpit, R.F., Gray, S., Lejarcegui, N., Frevert, U., Kappe, S.H., 2006. Quantitative isolation and in vivo imaging of malaria parasite liver stages. Int J Parasitol 36, 1283-1293.

Teja-Isavadharm, P., Siriyanonda, D., Rasameesoraj, M., Limsalakpeth, A., Chanarat, N., Komcharoen, N., Weina, P.J., Saunders, D.L., Gettayacamin, M., Scott Miller, R., 2016. Comparative pharmacokinetics and pharmacodynamics of intravenous artelinate versus artesunate in uncomplicated Plasmodium coatneyi-infected rhesus monkey model. Malar J 15, 453.

Tekwani, B.L., Walker, L.A., 2006. 8-Aminoquinolines: future role as antiprotozoal drugs. Curr Opin Infect Dis 19, 623-631.

Terstappen, L.W., Levin, J., 1992. Bone marrow cell differential counts obtained by multidimensional flow cytometry. Blood Cells 18, 311-330; discussion 331-312.

Terstappen, L.W., Loken, M.R., 1988. Five-dimensional flow cytometry as a new approach for blood and bone marrow differentials. Cytometry 9, 548-556.

Thalhofer, C.J., Chen, Y., Sudan, B., Love-Homan, L., Wilson, M.E., 2011. Leukocytes infiltrate the skin and draining lymph nodes in response to the protozoan Leishmania infantum chagasi. Infect Immun 79, 108-117.

Tiuman, T.S., Santos, A.O., Ueda-Nakamura, T., Filho, B.P., Nakamura, C.V., 2011. Recent advances in leishmaniasis treatment. Int J Infect Dis 15, e525-532.

Trape, J.F., 2001. The public health impact of chloroquine resistance in Africa. Am J Trop Med Hyg 64, 12-17.

Tsuji, M., Ishihara, C., Arai, S., Hiratai, R., Azuma, I., 1995. Establishment of a SCID mouse model having circulating human red blood cells and a possible growth of Plasmodium falciparum in the mouse. Vaccine 13, 1389-1392.

Tu, Y., Jeffries, C., Ruan, H., Nelson, C., Smithson, D., Shelat, A.A., Brown, K.M., Li, X.C., Hester, J.P., Smillie, T., Khan, I.A., Walker, L., Guy, K., Yan, B., 2010. Automated high-throughput system to fractionate plant natural products for drug discovery. J Nat Prod 73, 751-754.

Tu, Y., Yan, B., 2012. High-throughput fractionation of natural products for drug discovery. Methods Mol Biol 918, 117-126.

Vacchina, P., Morales, M.A., 2014. In vitro screening test using Leishmania promastigotes stably expressing mCherry protein. Antimicrob Agents Chemother 58, 1825-1828.

Van Slambrouck, S., Daniels, A.L., Hooten, C.J., Brock, S.L., Jenkins, A.R., Ogasawara, M.A., Baker, J.M., Adkins, G., Elias, E.M., Agustin, V.J., Constantine, S.R., Pullin, M.J., Shors, S.T., Kornienko, A., Steelant, W.F., 2007. Effects of crude aqueous medicinal plant extracts on growth and invasion of breast cancer cells. Oncol Rep 17, 1487-1492.

van Spaendonk, R.M., Ramesar, J., van Wigcheren, A., Eling, W., Beetsma, A.L., van Gemert, G.J., Hooghof, J., Janse, C.J., Waters, A.P., 2001. Functional equivalence of structurally distinct ribosomes in the malaria parasite, Plasmodium berghei. J Biol Chem 276, 22638-22647.

van Vianen, P.H., Thaithong, S., Reinders, P.P., van Engen, A., van der Keur, M., Tanke, H.J., van der Kaay, H.J., Mons, B., 1990. Automated flow cytometric analysis of drug susceptibility of malaria parasites. Am J Trop Med Hyg 43, 602-607.

Vargas-Serrato, E., Corredor, V., Galinski, M.R., 2003. Phylogenetic analysis of CSP and MSP-9 gene sequences demonstrates the close relationship of Plasmodium coatneyi to Plasmodium knowlesi. Infect Genet Evol 3, 67-73.

Vaughan, A.M., Kappe, S.H., Ploss, A., Mikolajczak, S.A., 2012. Development of humanized mouse models to study human malaria parasite infection. Future Microbiol 7, 657-665.

Vergnes, B., Vanhille, L., Ouaissi, A., Sereno, D., 2005. Stage-specific antileishmanial activity of an inhibitor of SIR2 histone deacetylase. Acta Trop 94, 107-115.

Vermeersch, M., da Luz, R.I., Tote, K., Timmermans, J.P., Cos, P., Maes, L., 2009. In vitro susceptibilities of Leishmania donovani promastigote and amastigote stages to antileishmanial reference drugs: practical relevance of stage-specific differences. Antimicrob Agents Chemother 53, 3855-3859.

Wang, C.Z., Zhang, Z., Huang, W.H., Du, G.J., Wen, X.D., Calway, T., Yu, C., Nass, R., Zhao, J., Du, W., Li, S.P., Yuan, C.S., 2013. Identification of potential anticancer compounds from Oplopanax horridus. Phytomedicine 20, 999-1006.

Wang, Z.Q., Hu, H., Chen, H.X., Cheng, Y.C., Lee, K.H., 1992. Antitumor agents. 124. New 4 beta-substituted aniline derivatives of 6,7-O,O-demethylene-4'-O-demethylpodophyllotoxin and related compounds as potent inhibitors of human DNA topoisomerase II. J Med Chem 35, 871-877.

Wengelnik, K., Vidal, V., Ancelin, M.L., Cathiard, A.M., Morgat, J.L., Kocken, C.H., Calas, M., Herrera, S., Thomas, A.W., Vial, H.J., 2002. A class of potent antimalarials and their specific accumulation in infected erythrocytes. Science 295, 1311-1314.

WHO, 2016. World Malaria Report 2016. World health organization, p. 186.

WHO Expert Committee on the Control of the Leishmaniases. Meeting (2010 : Geneva), World Health Organization., 2010. Control of the leishmaniases : report of a meeting of the WHO Expert Committee on the Control of Leishmaniases, Geneva, 22-26 March 2010. World Health Organization, Geneva.

Wiart, C., Mogana, S., Khalifah, S., Mahan, M., Ismail, S., Buckle, M., Narayana, A.K., Sulaiman, M., 2004. Antimicrobial screening of plants used for traditional medicine in the state of Perak, Peninsular Malaysia. Fitoterapia 75, 68-73.

Wiczling, P., Krzyzanski, W., 2008. Flow cytometric assessment of homeostatic aging of reticulocytes in rats. Exp Hematol 36, 119-127.

Woodrow, C.J., Wangsing, C., Sriprawat, K., Christensen, P.R., Nosten, F., Renia, L., Russell, B., Malleret, B., 2015. Comparison between Flow Cytometry, Microscopy, and Lactate

Dehydrogenase-Based Enzyme-Linked Immunosorbent Assay for Plasmodium falciparum Drug Susceptibility Testing under Field Conditions. J Clin Microbiol 53, 3296-3303.

Wyllie, S., Patterson, S., Stojanovski, L., Simeons, F.R., Norval, S., Kime, R., Read, K.D., Fairlamb, A.H., 2012. The anti-trypanosome drug fexinidazole shows potential for treating visceral leishmaniasis. Sci Transl Med 4, 119re111.

Xi, F.M., Li, C.T., Han, J., Yu, S.S., Wu, Z.J., Chen, W.S., 2014. Thiophenes, polyacetylenes and terpenes from the aerial parts of Eclipata prostrate. Bioorg Med Chem 22, 6515-6522.

Xie, L., Li, Q., Johnson, J., Zhang, J., Milhous, W., Kyle, D., 2007. Development and validation of flow cytometric measurement for parasitaemia using autofluorescence and YOYO-1 in rodent malaria. Parasitology 134, 1151-1162.

Yang, J., Liang, Q., Wang, M., Jeffries, C., Smithson, D., Tu, Y., Boulos, N., Jacob, M.R., Shelat, A.A., Wu, Y., Ravu, R.R., Gilbertson, R., Avery, M.A., Khan, I.A., Walker, L.A., Guy, R.K., Li, X.C., 2014. UPLC-MS-ELSD-PDA as a powerful dereplication tool to facilitate compound identification from small-molecule natural product libraries. J Nat Prod 77, 902-909.

Yayon, A., Vande Waa, J.A., Yayon, M., Geary, T.G., Jensen, J.B., 1983. Stage-dependent effects of chloroquine on Plasmodium falciparum in vitro. J Protozool 30, 642-647.

Yeates, C.L., Batchelor, J.F., Capon, E.C., Cheesman, N.J., Fry, M., Hudson, A.T., Pudney, M., Trimming, H., Woolven, J., Bueno, J.M., Chicharro, J., Fernandez, E., Fiandor, J.M., Gargallo-Viola, D., Gomez de las Heras, F., Herreros, E., Leon, M.L., 2008. Synthesis and structure-activity relationships of 4-pyridones as potential antimalarials. J Med Chem 51, 2845-2852.

Yogesh, K., Ali, J., 2014. Antioxidant potential of thuja (Thuja occidentalis) cones and peach (Prunus persia) seeds in raw chicken ground meat during refrigerated (4 +/- 1 degrees C) storage. J Food Sci Technol 51, 1547-1553.

Zakai, H.A., Chance, M.L., Bates, P.A., 1999. The axenic cultivation of Leishmania donovani amastigotes. Saudi Med J 20, 334-340.

Zhang, Z., Yu, C., Zhang, C.F., Wu, X.H., Wen, X.D., Anderson, S., Du, W., Huang, W.H., Li, S.P., Wang, C.Z., Yuan, C.S., 2014. Chemopreventive effects of oplopantriol A, a novel compound isolated from Oplopanax horridus, on colorectal cancer. Nutrients 6, 2668-2680.

Zhao, M., Bai, L., Toki, A., Hasegawa, R., Sakai, J., Hasegawa, T., Ogura, H., Kataoka, T., Bai, Y., Ando, M., Hirose, K., Ando, M., 2011. The structure of a new cardenolide diglycoside and the biological activities of eleven cardenolide diglycosides from Nerium oleander. Chem Pharm Bull (Tokyo) 59, 371-377.

Zhao, M., Zhang, S., Fu, L., Li, N., Bai, J., Sakai, J., Wang, L., Tang, W., Hasegawa, T., Ogura, H., Kataoka, T., Oka, S., Kiuch, M., Hirose, K., Ando, M., 2006. Taraxasterane- and ursane-type triterpenes from Nerium oleander and their biological activities. J Nat Prod 69, 1164-1167.

Zhao, Y., Peng, L., Lu, W., Wang, Y., Huang, X., Gong, C., He, L., Hong, J., Wu, S., Jin, X., 2015. Effect of Eclipta prostrata on lipid metabolism in hyperlipidemic animals. Exp Gerontol 62, 37-44.

Zlokarnik, G., Negulescu, P.A., Knapp, T.E., Mere, L., Burres, N., Feng, L., Whitney, M., Roemer, K., Tsien, R.Y., 1998. Quantitation of transcription and clonal selection of single living cells with beta-lactamase as reporter. Science 279, 84-88.

VITA

Surendra Kumar Jain [M.S. (Pharm.)]
Senior Research and Development Biologist
National Center for Natural Products Research
School of Pharmacy, University of Mississippi,
University, MS-38677, USA.
Phone Office: 662-915-1364

EMPLOYMENT HISTORY:

Year	Employee title	Employer
2014 to till date	Senior Research and Development Biologist	University of Mississippi, USA.
2010 to 2014	Research and Development Biologist	University of Mississippi, USA.
2009 to 2010	Research trainee	RMRIMS, Indian Council of Medical Research, India.

EDUCATIONAL QUALIFICATION:

Year	Degree/Exam Passed	School/College/University
2013-Dec 2017	Ph.D. in Pharmaceutical Sciences: (Pharmacology)	Department of Biomolecular Sciences, Division of Pharmacology, University of Mississippi, USA (Current GPA 3.93)
2007-09	M.S. (Pharm.) Biotechnology	National Institute of Pharmaceutical Education and Research, Hajipur, India
2007	Graduate Aptitude Test in Engineering (Pharmaceutical sciences) 2007	IIT Kanpur, India (Percentile 99.15)
2003-07	B. Pharm (Bachelor of Pharmacy)	Dr. H. S. Gour university sagar, India

PROFESSIONAL MEMBERSHIPS:

2017 Member of Rho Chi (International honor society for pharmaceutical sciences)
2017 Member of Sigma Xi (The Scientific Research Honor Society)
2016 Member of Phi Kappa Phi honor society.
2015 Member of American Society of Pharmacognosy.
2015 Member of American Society of Tropical Medicine and Hygiene.
2015 Member of Gamma Beta Phi Society.
2014 Member of Golden Key Honors Society.

LEADERSHIP QUALITIES:

- Treasurer, Graduate Student Council, University of Mississippi. (May 2016 to May 2017)
- Member, Institutional Biosafety Committee (IBC), University of Mississippi, USA. (Since June 2016)
- Member in the National Editorial and Reviewer Board of the "International Journal of Comprehensive and Advanced Pharmacology". (Since December 2016)
- Representative for the Information, Resources and Computing Committee, Graduate Student Body, School of Pharmacy, University of Mississippi. (November 2015 to 2017).
- Member of Indian Student Association, University of Mississippi. (Since October 2015)

WORKSHOPS PARTICIPATION:

- 3rd Annual Workshop on Metabolomics; Sunday, June 14th - Thursday June 18th, 2015. University of Alabama at Birmingham, AL, USA.
- EuPathDB Workshop 2012 database workshop and training, June 17-20, 2012. University of Georgia, Athens, GA, USA.
- Workshop on "Advance separation techniques". 20-22 February, 2009. NIPER Hajipur and RMRIMS (ICMR) India.

FELLOWSHIPS AND AWARDS:

2016 Marvin Davis Graduate Student Award, University of Mississippi, 2016.
2015 2nd Podium presentation award, Graduate Student Council, University of Mississippi.
2015 Paratryp travel award 2015
2015 Podium presentation in Drug Discovery and Development colloquium, 2015.

INVITED LECTURES:

Scopes and Hopes in Pharmacy Profession; Bhagyodaya Tirth Pharmacy College; Shastri Nagar, Sagar, Madhya Pradesh 470002, India; August 2015.

PEER REVIWED PUBLICATIONS:

(https://scholar.google.com/citations?user=xghx92gAAAAJ&hl=en)

Jain J, **Jain SK**, Walker LA, Tekwani BL. Inhibitors of ubiquitin E3 ligase as potential new antimalarial drug leads. BMC Pharmacol Toxicol. 2017 Jun 2; 18(1):40.

Jain S, Jacob M, Walker L, Tekwani B. Screening North American plant extracts in vitro against *Trypanosoma brucei* for discovery of new antitrypanosomal drug leads. **BMC Complement**

Altern Med. 2016 May 18;16 (1):131.

Mohamed NM, Makboul MA, Farag SF, **Jain S**, Jacob MR, Tekwani BL, Ross SA; Triterpenes from the roots of *Lantana montevidensis* with antiprotozoal activity; **Phytochemistry Letters**. 2016 March; 15: 30-36.

Mohamed SM, Bachkeet EY, Bayoumi SA**, Jain S**, Cutler SJ, Tekwani BL, Ross SA. Potent antitrypanosomal triterpenoid saponins from *Mussaenda luteola*. **Fitoterapia**. 2015 Dec; 107:114-21.

Tekwani BL, Avula B, Sahu R, Chaurasiya ND, Khan SI, **Jain S**, Fasinu PS, Herath HM, Stanford D, Nanayakkara NP, McChesney JD, Yates TW, ElSohly MA, Khan IA, Walker LA. Enantioselective pharmacokinetics of primaquine in healthy human volunteers. **Drug Metab Dispos**. 2015 Apr; 43(4):571-7.

Donega MA, Mello SC, Moraes RM, **Jain SK**, Tekwani BL, Cantrell CL. Pharmacological activities of cilantro's aliphatic aldehydes against *Leishmania donovani*. **Planta Med**. 2014 Dec; 80(18):1706-11.

Sodji Q, Patil V, **Jain S**, Kornacki JR, Mrksich M, Tekwani BL, Oyelere AK. The antileishmanial activity of isoforms 6- and 8-selective histone deacetylase inhibitors. **Bioorg Med Chem Lett.** 2014 Oct 15; 24(20):4826-30.

Manda S, Khan SI, **Jain SK**, Mohammed S, Tekwani BL, Khan IA, Vishwakarma RA, Bharate SB. Synthesis, antileishmanial and antitrypanosomal activities of N-substituted tetrahydro-β-carbolines. Bioorg Med Chem Lett. 2014 Aug 1;24(15):3247-50.

Avolio F, Rimando AM, Cimmino A, Andolfi A, **Jain S**, Tekwani BL, Evidente A. Inuloxins A-D and derivatives as antileishmanial agents: structure-activity relationship study. **J Antibiot (Tokyo)**. 2014 Aug; 67(8):597-601. doi: 10.1038/ja.2014.47. Nature.com/JA

Jain SK, Sahu R, Walker LA, Tekwani BL. A parasite rescue and transformation assay for antileishmanial screening against intracellular *Leishmania donovani* amastigotes in THP1 human acute monocytic leukemia cell line. J Vis Exp. 2012 Dec 30; (70). pii: 4054.

Rahman AA, Samoylenko V, Jacob MR, Sahu R, **Jain SK**, Khan SI, Tekwani BL, Muhammad I. Antiparasitic and antimicrobial indolizidines from the leaves of *Prosopis glandulosa var. glandulosa*. **Planta Med**. 2011 Sep;77 (14):1639-43.

Rahman AA, Samoylenko V, **Jain SK**, Tekwani BL, Khan SI, Jacob MR, Midiwo JO, Hester JP, Walker LA, Muhammad I. Antiparasitic and antimicrobial isoflavanquinones from *Abrus schimperi*. **Nat Prod Commun**. 2011 Nov; 6 (11):1645-50.

Rahman AA, **Jain S**, Jacob MR, Khan SI, Tekwani BL, Ilias M. Antimicrobial and antiparasitic abietane diterpenoids from *Cupressus sempervirens*. **Research and Reports in Medicinal Chemistry.** 2012 April; 2: 1 – 6.

MANUSCRIPTS IN PROCESS:

A novel flow cytometric method of malaria parasitemia analysis using LDS-751 stain Jain SK, Chaurasiya ND, Walker LA, and Tekwani BL. Scientific Reports, 2017 (Under review)

Development of transgenic *Leishmania donovani* cells (mCherry and citrine) by stable transfection and their applications in drug discovery. (Under review)

Epley B, **Jain S**, Archibald S, Walker A, Davilla D, Hubin T, Tekwani B, Amoyaw P, Carder T, Hasley T, Khan F. Tetraazamacrocyclic derivatives and their metal complexes as antileishmanial leads; Monocyclic polyamine derivatives. **Bioorganic & Medicinal Chemistry** 2017 (in communication).

Wang M, Zulfiqar F, Khan S, Abu-Darwish M, Tekwani BL, **Jain SK**, Cabral C, Salgueiro L, Khan I, zulfiqar A, Jacob MR, Efferth T. Salvia ceratophylla L. from South of Jordan: new insights on chemical composition and biological activities; **Journal of Ethnopharmacology** 2017 (in communication,).

PUBLISHED ABSTRACTS:

Jain SK, Gul W, Elsohly MA, Tekwani BL.The antileishmanial artemisinin dimer analogs induce apoptosis in *Leishmania donovani* promastigotes. (International Conference of Science and Botanicals 2017)

Jain SK, Gul W, Elsohly MA, Tekwani BL. Artemisinin dimers as promising new drug leads for visceral leishmaniasis. (American Society of Tropical Medicine and Hygiene 2016, Abstract 1748)

Jain S, Fouce RB, Reguera RM, Tekwani B. Transgenic *Leishmania donovani* cells with stable of expression of Citrine and mCherry fluorescent reporter proteins: Applications in phenotypic screening and parasite biology. (International conference on "Global Challenges In Neglected Tropical Diseases" León (Spain) July 2016)

Jain S, Chaurasiya ND, Walker LA, Tekwani BL. Flow cytometry based analysis of parasitemia in *Plasmodium berghei* rodent malaria model using LDS-751. (International conference on "Global Challenges In Neglected Tropical Diseases" León (Spain) July 2016)

Jain SK, Chaurasiya ND, Walker LA, Tekwani BL. *Plasmodium berghei*-Mouse Malaria Model for Preclinical Evaluation of Antimalarial Leads: Parasitemia Monitoring with Digital Image Analysis. (4th University of Mississippi Malaria Symposium, April 2016)

Jain SK, Fouce RB, Reguera RM, Tekwani BL. Transgenic *Leishmania donovani* cells and their applications in parasite biology and drug discovery. (Graduate Student Council, University of Mississippi, April 2016)

Jain SK, Jacob MR, Tekwani B. Screening North American Plants In Vitro Against *Leishmania*

Donovani, The Causative Agent For Visceral Leishmaniasis. Planta Med 2016; 82 - PB18. (International Conference of Science and Botanicals 2016)

Zaki AA, Ali Z, El-Amier YA, Ashour A, Oluwasesan BM, **Jain S**, Tekwani B, Khan AI. Antiprotozoal Activity Of Some Egyptian Plants. Planta Med 2016; 82 - PC85. (International Conference of Science and Botanicals 2016)

Oluwasesan BM, Fasinu PS, **Jain S**, Tekwani B, Ali Z, Khan IA, Ajao UL, Olubunmi OS. In Vitro Antileishmanial Activity of Selected Medicinal Plants from Nigeria. Planta Med 2016; 82 - PC18. (International Conference of Science and Botanicals 2016)

Imieje VO, Fasinu PS, **Jain S**, Tekwani B, Khan S, Ali Z, Khan IA, A Falodun. In Vitro Antiprotozoal Activity Of *Enantia Chlorantha* Oliv Stem Bark Used In Nigeria Ethnomedicine. **Planta Med** 2016; 82 - PC33. (International Conference of Science and Botanicals 2016)

Jain SK, Muhammad I, Walker LA, Tekwani BL. Inhibitors of Na+, K+-ATPase and related ion anti-porter functions as new antileishmanial drug leads. **American Journal of Tropical Medicine and Hygiene.** 2015 Oct; 93: 332. (American Society of Tropical Medicine and Hygiene 2015, Abstract 1087)

Jain SK, Jacob MR, Walker LA, BL Tekwani. Screening natural product extracts against kinetoplastid parasites. **Planta Med** 2015; 81 (5): PP5. (International Conference of Science and Botanicals 2015)

Jain SK, Fouce RB, Reguera RM, Tekwani BL. Transgenic *Leishmania donovani* cells with constitutive expression of Citrine and mCherry fluorescent proteins: Applications in biology, screening and new drug discovery. (Graduate Student Council, University of Mississippi, 2015).

Jain SK, Chaurasiya ND, Walker LA, Tekwani BL. *Plasmodium berghei*-Mouse Malaria Model for Preclinical Evaluation of Antimalarial Leads: Parasitemia Monitoring with Digital Image Analysis. (3rd University of Mississippi Malaria Symposium, April 2015)

Dharmaratne HRW, **Jain S**, Tekwani BL, Jacob MR, NPD Nanayakkara. Antifungal and antiparasitic activities of *Laurus nobilis* (bay leaves). **Planta Med** 2015; 81 - PK17. (American Society of Pharmacognosy July 2015)

Jain S, Ilias M, Walker L, Tekwani B. Selective antileishmanial activity of Bufalin and Proscillaridin A against intracellular amastigotes of *leishmania donovani*. (Drug Discovery and Development Colloquium AAPS student chapter 2015)

Cantrell CL, Donega MA, Mello SC, Moraes RM, **Jain SK**, Tekwani BL. Pharmacological Activities of Cilantro's Aliphatic Aldehydes against *Leishmania donovani*; (GA 2014)

Jain SK, Jacob MR, Jeffries C, Shelat A, Bryan J, Tu Y, Walker LA, Ilias M, Tekwani BL. Natural products drug discovery for treatment of human African trypanosomiasis: new drug leads from a natural products fractions library. **American Journal of Tropical Medicine and**

Hygiene. 2014 Nov; 91: 332-33. (American Society of Tropical Medicine and Hygiene 2014, Abstract 1096).

Jain SK, Ilias M, Larry A. Walker LA, Tekwani BL. Na+, K+-ATPase and related ion antiporters as potential molecular targets for new antileishmanial drug discovery. (MALTO 2014)

Jain SK, Jacob MR, Ilias M, Walker LA, Tekwani BL. Screening North American plant extracts for discovery of new drug leads for visceral leishmaniasis. (American Society of Pharmacognosy 2014)

Sahu R, **Jain S**, Walker LA, Tekwani BL. A fluorescence-DIC digital image analysis technique for quantitative analysis of *Leishmania donovani* infection in thp1 cells. (American Society of Cell Biology 2013)

Zhang J, **Jain SK**, Jacob MR, Tekwani BL, Hufford CD, Ilias M. Antileishmanial and Antimicrobial Clerodane Diterpenes from *Polyalthia longifolia.* Planta Med 2013; 79 - P88 (American Society of Pharmacognosy 2013)

Jain SK, Zhang J, Jacob M, Li X, Shelat A, Bryan J, Tu Y, Guy K, Walker L, Ilias M, Babu Tekwani B. Molecular targets and antileishmanial drug leads identified through screening a library of natural products prepared by high throughput fractionation paradigm. **American Journal of Tropical Medicine and Hygiene.** 2013 Nov; 89: 91. (American Society of Tropical Medicine and Hygiene meeting 2013, Abstract 293).

Tekwani BL**, Jain S**, Sahu R, Khan SI, Ilias M, Nanayakkara NPD, Walker LA. Antiparasitic Drug Discovery from the Natural Products Resources: A Molecular Targets-Based Approach. (Academic Drug Discovery Conference Nashville 2013)

Jain SK, Sahu R, Ilias M, LA Walker , Tekwani BL. Appraisal of Na+, K+-ATPase and Related Ion Antiporter Functions as Potential Molecular Targets for New Antileishmanial Drug Discovery. **Planta Med** 2013; 79 - P89. (International Conference of Science and Botanicals 2013).

Tekwani B, **Jain S**, Zhang J, Sahu R, Jacob M, Li X, Jeffries C, Shelat A, Bryan J, Tu Y, Guy K, Walker L, Ilias M. New antileishmanial drug leads identified from a library of natural product fractions prepared by high throughput fractionation. (American Society of Pharmacognosy 2012)

Jain SK, Sahu R, Zhang J, Jacob MR, Li XC, Ilias M, Jeffries C, Shelat A, Bryan J, Tu Y, Guy RK, Walker L, Tekwani BL. New antileishmanial drug leads from a library of natural product fractions prepared by a high throughput fractionation paradigm**. Planta Med** 2012; 78 - P_105. (International Conference of Science and Botanicals 2012).

Zhang J, Rahman AA, **Jain SK**, Tekwani BL, Khan SI, Jacob MR, Ilias M. Antimicrobial and Antiparastic Abietane Diterpenoids from *Cupressus sempervirens.* **Planta Med** 2012; 78 - P_76. (International Conference of Science and Botanicals 2012)

Jain SK, Sahu R, Walker LA, Tekwani BL. Screening different fractions of plant extracts occurs worldwide, against *Trypanosoma brucei*, a causative agent for sleeping sickness. (Zing drug discovery conference 2012)

Jain SK, Sahu R, Tekwani BL. A promastigotes rescue assay for antileishmanial screening of compounds against intracellular *Leishmania donovani* amastigotes in THP1 Human Acute Monocytic Leukemia cell line**. American Journal of Tropical Medicine and Hygiene.** 2011 Dec; 85: 97. (American Society of Tropical Medicine and Hygiene meeting 2011, Abstract 321).

Jain SK, Sahu R, Ilias M, Walker LA, Tekwani BL. Natural products drug discovery for treatment of human african trypanosomiasis: screening north american plant extracts in vitro against *trypanosoma brucei*. (American Society of Pharmacognosy 2011)

Jain SK, Sahu R, Samoylenko V, Ilias M, Walker LA, Tekwani BL. Screening North American plant extracts against *Trypanosoma brucei*, a causative agent for sleeping sickness**. Planta Med** 2011; 77 - P_147. (International Conference of Science and Botanicals 2011)

ACKNOWLEDGEMENT IN FOLLOWING PUBLISHED RESEARCH:

Antiprotozoal and antimicrobial compounds from the plant pathogen *Septoria pistaciarum*. Kumarihamy M, Khan SI, Jacob M, Tekwani BL, Duke SO, Ferreira D, Nanayakkara NP. J Nat Prod. 2012 May 25;75(5):883-9.

Synthesis and antikinetoplastid activity of a series of N,N'-substituted diamines. Caminos AP, Panozzo-Zenere EA, Wilkinson SR, Tekwani BL, Labadie GR. Bioorg Med Chem Lett. 2012 Feb 15;22(4):1712-5.

Synthesis and structure-activity relationships of lansine analogues as antileishmanial agents. Pieroni M, Girmay S, Sun D, Sahu R, Tekwani BL, Tan GT. ChemMedChem. 2012Nov;7(11):1895-900.

Discovery of 3,3'-diindolylmethanes as potent antileishmanial agents. Bharate SB, Bharate JB, Khan SI, Tekwani BL, Jacob MR, Mudududdla R, Yadav RR, Singh B, Sharma PR, Maity S, Singh B, Khan IA, Vishwakarma RA. Eur J Med Chem. 2013 May;63:435-43.

Synthesis and biological evaluation of tricyclic guanidine analogues of batzelladine K for antimalarial, antileishmanial, antibacterial, antifungal, and anti-HIV activities. Ahmed N, Brahmbhatt KG, Khan SI, Jacob M, Tekwani BL, Sabde S, Mitra D, Singh IP, Khan IA, Bhutani KK. Chem Biol Drug Des. 2013 Apr;81(4):491-8.

Antimicrobial and Antileishmanial Activities of Diterpenoids Isolated from the Roots of *Salvia deserta*. Búfalo J, Cantrell CL, Jacob MR, Schrader KK, Tekwani BL, Kustova TS, Ali A, Boaro CS. Planta Med. 2016 Jan;82(1-2):131-7.

Bio-pesticidal and Antimicrobial Coumarins from Angelica dahurica (Fisch. Ex Hoffm). Qian Xie; Shun-Xiang Li; Duan-Fang Liao; Wei Wang; Babu Tekwani; Hui-Yong Huang; Abbas Ali; Junaid ur Rehman; Kevin K. Schrader; Stephen O. Duke; Charles L. Cantrell; David E. Wedge Records of Natural Products . 2016, Vol. 10 Issue 3, p294-306. 13p.

Structure Identification And Biological Evaluation Of Compounds Isolated From *Polygonum Hydropiper*. H Xiao, RR Ravu, MR Jacob , S Khan , B Tekwani, IA Khan, W Wang, XC Li, Planta Med 2016; 82 - PC65.